UNIVERSITAT DE BARCELONA

Early signals in *Drosophila* imaginal disc regeneration: from ROS to Cytokines

Señales tempranas en la regeneración de discos imaginales de *Drosophila*: desde las ROS hasta las Citoquinas

Paula Santa Bárbara Ruiz

Departamento de Genética, Microbiología y Estadística

Programa de Doctorado en Genética

Facultad de Biología

Universidad de Barcelona

Early signals in *Drosophila* imaginal disc regeneration: From ROS to Cytokines

(Señales tempranas en la regeneración de discos imaginales de *Drosophila:* Desde las ROS hasta las Citoquinas)

Memoria presentada por

Paula Santa Bárbara Ruiz

Para optar al grado de

Doctora

por la Universidad de Barcelona

Tesis doctoral realizada bajo la dirección del Dr. Florenci Serras i Rigalt.

Realizada en el Departamento de Genética, Microbiología y Estadística de la Facultad de Biología de la Universidad de Barcelona.

Barcelona, Mayo 2017

Departamento de Genética, Microbiología y Estadística

Programa de Doctorado en Genética

Facultad de Biología

Universidad de Barcelona

Early signals in *Drosophila* imaginal disc regeneration: From ROS to Cytokines

(Señales tempranas en la regeneración de discos imaginales de *Drosophila:* Desde las ROS hasta las Citoquinas)

Memoria presentada por

Paula Santa Bárbara Ruiz

Para optar al grado de

Doctora

por la Universidad de Barcelona

Tesis doctoral realizada bajo la dirección del Dr. Florenci Serras i Rigalt.

Realizada en el Departamento de Genética, Microbiología y Estadística de la Facultad de Biología de la Universidad de Barcelona.

El director y tutor, La autora,

Dr. Florenci Serras i Rigalt Paula Santa Bárbara Ruiz

Barcelona, Mayo 2017

Front and back covers

On the cover, injured wing imaginal discs in which Reactive Oxygen Species (ROS) are displayed in green, a JNK reporter is represented in cyan, the P-p38 is labelled in purple and the mRNA of *upd* is shown in red. On the back cover, a wing imaginal disc shape fill in with the most commonly-used words in the discussion of this thesis. The larger the word, the higher word frequency.

Portada y contraportada

En la portada hay varios discos imaginales de ala cortados, en los cuales las Especies Reactivas de Oxígeno (ROS) se muestran en verde, la activación de un reportero de la vía de la JNK en cian, la fosforilación de la proteína p38 en morado y el ARN mensajero de *upd* en rojo. En la contraportada, la forma de un disco imaginal de ala está rellena con las palabras más usadas en la discusión de esta tesis. Cuanto más grande aparece la palabra, más veces se ha repetido.

I was taught that the way of progress was neither swift nor easy.

Marie Curie

ACKNOWLEDGMENTS

Gracias Florenci por haberme dado la oportunidad de hacer la tesis en este laboratorio, y sobretodo, por haberme enseñado a hacer ciencia de la buena. Gracias también Montse y Marta por todos los buenos consejos en estos años.

Gracias a todos mis amigos por estar siempre ahí, a las de Soria, las de Salamanca y a los de Barcelona, porque me habéis demostrado que la distancia no separa a los verdaderos amigos.

Millones de gracias a mis compañeros de laboratorio, aunque en este caso no sólo han sido compañeros, sino grandes amigos. A Qi, Haritz, Elena y Sandra, por haberme hecho disfrutar tanto de mi estancia en Barcelona. Por las eternas horas umpa-lumpa, los jueves de cerves (que eran de gimnasio), las canciones del flyroom, los viajes, las noches en los congresos, las charlas arreglando el mundo con Haritz, la inmersión en la cultura china con Qi, las protestas y suspiros de Sandra y 'los Elenas'. Por todos estos momentos y muchos más, estos años han sido geniales gracias a vosotros.

Por supuesto gracias a mis padres, mi hermana y mi abuela, que son las personas que más quiero en el mundo. Porque tener una familia así no tiene precio.

Y, por último, gracias a ti, Isma, ¡porque eres un santo! Creo que el mundo se nos va a quedar pequeño para recorrerlo juntos, ¡a ver si no se nos escapa ningún gamusino!

¡Ah! Y gracias también por aguantarme toda la tesis, ¡que no es moco de pavo!

ABSTRACT

Countless environmental aggressors could damage the integrity of tissues and organs. In humans, the limited regenerative ability prevents often the recovery of injured tissues, but this is not the case of the fruit fly *Drosophila melanogaster*.

Drosophila imaginal discs are larval tissues that can regenerate after fragmentation or massive cell death. That is the reason why in our laboratory, we focused towards the understanding of the genetic basis of imaginal disc repair.

We concentrated on the initiation of regeneration, and we found that one of the earliest responses to damage consist in the production of Reactive Oxygen Species (**ROS**), which propagate from the dying to the nearby living cells, which will drive tissue repair. We revealed that the burst of ROS is essential, because the reduction of those molecules impairs repair. Within the cells, the protein **Ask1** (Apoptotic signal-regulating kinase 1) sense ROS and activates both Jun kinase (**JNK**) and **p38** signalling pathways, which are critical for regenerative growth. Although Ask1 was previously associated to apoptosis, we unravelled a novel function related to survival and proliferation. Ask1 inhibition reduces life span after oxidative stress, as well as regenerative ability after cell death. To assume this function, **Insulin** signalling must attenuate Ask1 activity in living cells. Simultaneously with Ask1, the **TNF/Egr** signalling acts upstream of JNK after damage, indicating an accurate control of this pathway to promote repair. Finally, we described that both JNK and p38 pathways are necessaries for the transcriptional activation of the cytokines **Unpaired**, which will promote JAK/STAT signalling to drive regenerative growth and recover the missing tissue.

Altogether, we demonstrated a new stress-responsive module composed by many signalling pathways conserved through evolution. Hopefully, in the near future, those findings will help scientists to improve wound healing and regeneration in human tissues and organs.

RESUMEN

Los humanos no somos capaces de superar muchas adversidades que pueden dañar nuestra integridad celular, ya que nuestra capacidad regenerativa es realmente limitada. Sin embargo, en el reino animal hay una gran variedad de organismos que sí son capaces de regenerar estructuras completas, y este es el caso de la mosca de la fruta *Drosophila melanogaster*.

Los discos imaginales de *Drosophila* pueden dar lugar a estructuras adultas perfectas, aunque hayan sido fragmentados o sometidos a una gran muerte celular. Es por eso, que en nuestro laboratorio nos hemos focalizado en entender las increíbles habilidades regenerativas de este tejido epitelial, y así poder mejorar en un futuro la respuesta humana en el mismo proceso.

En concreto, decidimos estudiar el inicio del proceso regenerativo, y descubrimos que, al menos, una de las primeras respuestas del tejido dañado es producir una gran cantidad de Especies Reactivas de Oxígeno (**ROS**), que se propagan desde las células que están muriendo hacia el tejido vivo, responsable de regenerar. Comprobamos que esta explosión de ROS es necesaria para la reparación tisular, ya que su ausencia impide la recuperación total después del daño. Vimos que esto se debía a que las ROS son capaces de activar dos vías de señalización esenciales para el crecimiento regenerativo, que son la vía de la Jun kinasa (**JNK**) y la vía de la **p38**. Esto es gracias a la proteína **Ask1** (kinasa que regula la respuesta apoptótica 1), que detecta oxidación tisular y activa ambas. Aunque Ask1 fue descrita previamente como una proteína asociada a muerte celular, nosotros descubrimos una nueva función relacionada con supervivencia, ya que la ausencia de Ask1 provoca una menor esperanza de vida en moscas adultas tratadas con agentes oxidativos, así como una menor capacidad regenerativa de los discos imaginales. Para llevar a cabo esta función, es necesario que la vía de la Insulina atenúe la activación de Ask1 en el tejido vivo. Además de Ask1, comprobamos que la vía de la JNK necesita del factor de necrosis tumoral **TNF/Eiger** para ser activada, lo que revela un control exhaustivo de esta vía durante la regeneración. Para finalizar, describimos que tanto la vía de la JNK como de la p38 son necesarias para la activación transcripcional de las citoquinas **Unpaired**, que activan la vía de JAK/STAT y estimulan el crecimiento regenerativo para recomponer el tejido dañado.

TABLE OF CONTENTS

FIGURE INDEX

Introduction

Materials and Methods

Results

Discussion

TABLE INDEX

Introduction

Material and Methods

ABBREVIATIONS & ACRONYMS

% → Proliferation or Percentage
3-PPIs → 3-phosphoinositides
A → Anterior
AKT → Protein kinase B
AP → Antero-posterior
ap → *apterous*
AP1 → Activator protein 1 (Jun + Fos)
Aqp → Aquaporin
ara → *araucan*
Ark → Death-associated APAF1-related killer
ash2 → *absent, small or homeotic discs 2*
Ask1 → Apoptosis signal regulating kinase1
Atf1-3 → Activating transcription factor 1-3
BMMSCs → Bone marrow-derived mesenchymal stem cells
brk → *brinker*
BS → Blocking Serum
BSA → Blocking Serum Albumin
bsk → *basket*
BX-C → Bithorax complex
Ca^{2+} → Calcium
cap → *capicúa*
Casp → Caspase
Cat → Catalase
cbt → *cabut*
ccc → coiled-coil domain
Cdc → Cyclin-Dependent Kinase
CDX1 → caudal type homeobox-1
ci → *cubitus interruptus*
Cka → Connector of kinase to AP-1
CMs → Cardiomyocytes
CNS → Central Nervous system
crb → *crumbs*
CRISPR → clustered regularly interspaced short palindromic repeats
CTE → electron transport chain
CTRL → Control
CYLD → Cylindromatosis
Cys → Cysteine
D → Dorsal
DCF → 2',7'-dichlorofluorescein
Dcp-1 → Death Caspase-1, Caspase-7-like
DEDIF → Dedifferentiation
DiAP1 → *Drosophila* inhibitor of apoptosis protein 1
DIF → Differentiation
Dilp1-8 → *Drosophila* insulin-like peptide 1-8
dlg → *discs large 1*
DLK1 → Dual-leucine zipper-bearing kinase 1
dll → *distalless*
DMSO → Dimethyl sulfoxide
DNA → Deoxyribonucleic acid
DNMTs → DNA methyltransferases
dNTP → Deoxynucleotide triphosphate
dome → *domeless*
DP → Disc Proper

dp110 → same as PI3K
dpp → *decapentaplegic*
DrICE → *Drosophila* Interleukin-1 Converting Enzyme, Caspase-3-like
DRONC → *Drosophila* Nedd2-like caspase, Caspase-9-like
Dsrf/bs → *Drosophila Serum response factor/blistered*
DUOX → NADPH Dual Oxidase
dUTP → 2´-Deoxyuridine, 5´-Triphosphate
DV → Dorso-ventral
ECM → Extracellular Matrix
EDTA → Ethylene diaminetetraacetic acid
EdU → 5-ethynyl-2'-deoxyuridine
EGFR → Epidermal growth factor receptor
egr → *eiger*
en → *engrailed*
ER → Endoplasmic reticulum
ERK → Extracellular regulated kinase
ESC → Embryonic stem cells
esg → *escargot*
FA → Formaldehyde
FISH → Fluorescence In Situ Hybridization
Flp → Flipase (recombinase)
Fos → kayak
FRT → Flipase recombination target
ft → *fat*
G → Glutathione
Gal4 → Galactose-induced gene 4
GFP → Green Fluorescence protein
Gly → Glycine
GPx → Glutathione Peroxidase
G-rich → Guanine-rich region
grnd → *grindelwald*
GSH → Glutathione
h → hours
H2DCFDA → 2',7'- dichlorodihydrofluorescein diacetate
HDAC → Histone deacetylase
hep → *hemipterous*
HFSCs → Hair follicle epidermal stem cell
hh → *hedgehog*
hid → *head involution defective*
hml → *hemolectin*
hop → *hopscotch*
Hox → homeotic genes
HSCs → Hematopoietic stem cells
hth → *homothorax*
inv → *invected*
inx → *innexin*
ISS → Insulin signalling
JAK/STAT → Janus kinase/signal transducer and activator of transcription
JNK → c-Jun-NH_2-terminal kinase
Jun → Jun-related antigen
KO → Knock-out
L1, L2 and L3 → First, second and third instar larvae
L1 to L5 → Vein 1 to vein 5 in the wing
LacZ → bacterial beta-galactosidase gene
LexO → LexA Operator
lgl → *lethal giant larvae*
LHG → LexA- hinge- Gal4 activation domain

lic → *licorne*
Lgr3 → Leucine-rich repeat-containing G protein-coupled receptor 3
MAPK → Mitogen-activated protein kinase
MAPKK → Mitogen-activated protein kinase kinase
MAPKKK → Mitogen-activated protein kinase kinase kinase
MASCs → Multipotent adult stem cells
MEKK1-4 → MAP kinase kinase kinase 1-4
mirr → *mirror*
MLK3 → mixed lineage kinase 3
mmp1 → *matrix metalloprotease 1*
mRNA → messenger RNA
MSCs → Mesenchymal stem cells
Myrtom → myristillated tomato fluorescence protein
n → notum
n= → number
N → Notch
NAC → *N*-Acetyl-L-cysteine
NADPH → Nicotinamide adenine dinucleotide phosphate
NOS → Nitric oxide synthetase
NOX → NADPH Oxidases
n.s. → non-significant
NSCs → Neural stem cells
nub → *nubbin*
omb → *optomotor-blind*
P → Posterior
P- → phospho-
PcG → Polycomb group
PCP → Planar cell polarity
PCR → Polymerase chain reaction
PD → Proximo-distal
PG → Prothoracic gland
PGN → Peptidoglycan
PH3 → phospho-histone 3
PI3K → Phosphoinositol-3 kinase
PlexA → Plexin A
PM → Peripodial membrane
P-p38 → phospho-P38
POD → Peroxidase
pnr → *pannier*
pnt → *pointed*
Prx → Perioxidase
ptc → *patch*
PTEN → phosphatase and tensin homolog
PTTH → Prothoracicotropic hormone
puc → *puckered*
PVR/PVF → Drosophila homologues of the mammalian VEGF/PDGF growth factors
RHG → *reaper-hid-grim*
rho → *rhomboid*
rl → *rolled*
RNA → Ribonucleic acid
RNAi → interference RNA
ROI → Region of interest
ROS → Reactive Oxygen Species
RUNX3 → Runt-related transcription factor 3
rpr → *reaper*
sal$^{E/Pv}$ → *salt$^{E/Pv}$*
sal/salm → *spalt major*

SAPKs → Stress-activated protein kinases
scrib → *scribble*
SD → Standard Deviation
ser → *serrate*
Ser → Serine
Ser/Thr → Serine/Threonine
SH → Thiol or Sulphydryl group
Slpr → Slipper
sna → *snail*
smo → *smoothened*
Socs36E → Suppressor of cytokine signalling 36 E
SOD → Superoxide Dismutase
STAT92E → Signal transducer and activator of transcription 92
Std → Standard
TAB2 → TAK1-associated binding protein 2
TAO → Thousand-and-one amino acid
TAK1 → TGF-β activated kinase 1
tara → *taranis*
TD → Transdifferentiation
TdT → Terminal deoxyribonucleotidyl transferase
Thr → Threonine
TNF → Tumour Necrosis factor
TNT → 2,4,6-Trinitrotoluene
top → *torpedo*
TP-3 → TO-PRO-3
TPL-2 → Tumour progression loci 2
TRAF → TNF-receptor-associated factor
TRE → tetradecanoylphorbol acetate response element
Trr → Trithorax related
Trx → Thioredoxin (-SH reduced, -S oxidized)
TrxG → Trithorax Group
TS → thermosensitive
tsh → *teashirt*
tub → tubulin
UAS → Upstream Activation Sequences
UCSC → University of California Santa Cruz
ubx → *ultrabithorax*
upd → *unpaired*
UV → ultraviolet
V → Ventral
VEGF → Vascular endothelial growth factor
vg → *vestigial*
w → *white*
wg → *wingless*
wgn → *wengen*
WP → Wing pouch
wt → wild type
yki → *yorkie*
YP-1 → YO-PRO-1
ZAK1 → Leucine zipper and sterile-a motif kinase 1

INTRODUCTION

[…] Zeus was infuriated and decided to hide fire from mortals as punishment. Prometheus, to help humanity again, managed to steal fire back and give it to humans. Zeus punished Prometheus by having him chained to a rock, where an eagle ate his liver during the day, and the liver was regenerated during the night due to Prometheus' immortality […]

Greek Mythology

Human beings have started to conquer the world since they discovered the fire in the Early Stone Age over 2 million years ago. Fire allowed the expansion of human activity and provided a source of light, warmth and protection. These cultural advancements enabled for human geographic dispersal, cultural innovations, and changes in diet and behaviour. In response to consuming cooked foods, all our organs adapted to that new situation, particularly teeth, which were reduced in size, and all the digestive system.

Besides the brain, other organs in the human body started to demand an important level of metabolism and therefore the body mass portion of different organs changed throughout the process of evolution as a means for brain expansion. All those changes created what we currently are. But let there be no mistake, we are not perfect machines. Although our design is so accurately regulated, environmental changes could trigger from small failures to the death.

To maintain its integrity, animals have developed a series of strategies to replace and regenerate cells eliminated by the continuous cell renewal in physiological processes, as well as after partial or complete loss of tissues and organs caused by damage and injuries. Whereas certain species have an extraordinary ability to replace the missing tissues, humans cannot grow back their own arms and legs.

How these processes occur in different organisms, what are the necessary signals required for tissue repair and how to improve regenerative abilities in human tissues is detailed in the following introduction.

Regeneration

The phenomenon of **regeneration** consists in the replacement of damaged or lost tissues and organs to restore homeostasis. The ability to regenerate complex structures exists in some lower vertebrates and invertebrates and, to a limited extent, in the mammal foetus (Brockes et al. 2001). The early-gestation foetus can heal wounds by regenerating normal epidermis and dermis with restoration of the extracellular matrix (ECM) architecture, strength and function, rapidly and scarlessly (Ferguson et al. 1996). This phenomenon appears to be intrinsic to foetal skin and independent of the intrauterine environment. In contrast, as intrauterine development progresses, this ability is progressively missing. Indeed, adult wounds heal with fibrosis and scar (reviewed in Bullard et al. 2003). Adult mammals possess only a modest capacity for regeneration, exemplified by the renewal of tissues such as the haematopoietic system, epidermis and intestinal mucosa (Table 1). All these tissues contain stem cells that are capable of self-renewal and can give rise to differentiated adult cells of multiple lineages. Once activated, resident stem cells acted through the production of progenitor cells (Moore & Lemischka 2006), fusion with differentiated adult cells (Ishikawa et al. 2006) and induction of nuclear reprogramming in fated cells (Pomerantz & Blau 2004). Although stem cells could contribute after injuries, regenerative ability is limited in adult mammals. Examples of complex tissue regeneration are less common, but can be seen in the seasonal regrowth of deer antlers (Price et al. 2005), ear tissue in rabbits (Williams-Boyce & Daniel 1986) and distal fingertip regeneration in juvenile mammals (Han et al. 2005).

We are particularly interested on **epithelial tissues**, because they are the main barriers which protect us from every kind of insult. One example is the skin, that covers the body externally and gives us the perception of information from the environment, the control of body temperature and the secretion of substances. Besides, epithelial tissues shield the internal surfaces of hollow organs, such as the organs of the digestive tract, the airway, the renal tubules, the bladder, the ureters, the urethra, the blood vessels and the glands and serous membranes. Accordingly, epithelial tissues can be used as a layer for protection against the environment.

Epithelial cells are compactly positioned side-by-side with the help of structures specialized in cell adhesion, thus are characterized by the absence or the almost absence of space between cells. This property is related to the fact that these tissues are generally exposed to an exterior environment and, thus, need more resistance against the entrance of foreign materials into the body. Since epithelium is not vascularized (It exchanges substances by diffusion with the connective tissue located under it), the tiny skin injuries or scratches that happen all the time do not cause bleeding and do not expose the blood to contamination from foreign agents. This is an important protective strategy of evolution.

The **repair of wounds** in mammals is a complex biological process that occurs throughout the entire life. Upon damage, numerous biological pathways become activated and are synchronized to answer. Wound healing is a dynamic process which corresponds to the full or partial functional restoration of the tissue, that is often replaced by fibrotic scarring.

ORGAN	REGENERATIVE CAPACITY
Thymus	Only in young animals. It loses its structure, function and regenerative capacity with age, resulting in atrophy (Cannizzo et al. 2010).
Adrenal gland	The cortex regenerates, but not the medulla. This is achieved by the dedifferentiation, proliferation, and re-differentiation of the remaining cells in the cortex and/or from the stem cells present in the zone glumerolosa (Taki & Nickerson 1985; Engeland et al. 1996; Mitani et al. 2003).
Thyroid gland	Limited regeneration because the contribution of stem cells, embryonic stem cells (ESC) and bone marrow-derived mesenchymal stem cells (BMMSC) (Thomas et al. 2006; Hoshi et al. 2007; Lan et al. 2007).
Intestine	A high turnover rate, which aids in the organ's regenerative capability following injury. Stem cells can rapidly proliferate and differentiate into all the cell types of the intestine wall (epithelial cells and myofibroblasts, Podolsky 1999).
Lungs	Limited regeneration achieved by the presence of Progenitor cells in specific sites in the lungs (Evans et al. 1976).
Heart	Mammalian hearts respond to injury by scarring, whereby the damaged cardiac muscle is replaced by fibrotic scar tissue (Mummery & Passier 2011). Cardiomyocytes (CMs) rapidly proliferate during foetal life, as well as in one-day-old neonatal mice (Porrello et al. 2011). Only limited to very slow CMs replacement has been reported in human hearts after birth (Macmahon 1937; Beltrami et al. 2001).
Liver	The liver can regenerate even when 70% of the organ has been removed. In rodents, following hepatectomy, the liver is regenerated by compensatory growth of the remaining liver tissue. Progenitor cells are present in the liver (Farber, 1956) and in the Canals of Hering (Theise et al. 1999; Zhang et al. 2008) and they can contribute to the regeneration if the proliferation of the hepatocytes is blocked.
Blood vessels	To maintain a balance in blood delivery, endothelial cells respond to certain signals (VEGF, oxygen, low blood flow) by creating more blood vessels or by decreasing the branching in already existing blood vessels (Potente et al. 2011). The vascular endothelium can be repaired by endothelial cells that migrate to the injured area. Platelets, hematopoietic cells and progenitor cells play a role in blood vessel repair (Becher et al. 2010).
Germ cells	Only in males, high self-renewal capability of spermatogonia thanks to pluripotent stem cell-like. In females, oogenesis is completed upon birth, so that the starting number of oocytes cannot be increased throughout life.
Nervous system	Injuries in the axons of the Central Nervous System (CNS) are followed by inflammation and glial scar formation, both of which inhibit the regenerative response. But neurogenesis is possible in several regions of the CNS, such as hypothalamus, neocortex, cerebellum, striatum, amygdala, and substantia nigra (reviewed in Gould 2007; Martino et al. 2011), thanks to Neural stem cells (NSCs) residing in the CNS.
Kidney - bladder	Following injury, mammalian kidneys restore filtrate flow and repair the tubular epithelium by the action of renal residual epithelial cells, progenitor cells, and/or extra-renal cells (Sabbahy & Vaidya 2011). But the capability to regenerate is reduced, as well as in the bladder.
Skin	Following skin injury, platelets, blood cells, and other matrices form a clot. Macrophages, neutrophils, T-cells and platelets populate the area, and finally, re-epithelialization occurs. Endothelial cell, fibroblasts, BMDSCs, MSCs and myofibroblasts participate in skin repair (Delavary et al. 2011; Chesney & Bucala 2000). Complete regeneration is not achieved at the end of the process, and often scarring substitutes the previous tissue.
Lens - retina	Mammalian lens and retina cannot regenerate.
Hair follicles	Cells in the dermal sheath have been shown to regenerate the dermal papilla (Horne & Jahoda 1992). Hair follicles can also be regenerated from extra hair follicle epithelial progenitor cells (Taylor et al. 2000).
Pancreas	Pancreatic acinar cells can regenerate (Jensen et al. 2005; Desai et al. 2007). In contrast, islets have limited regeneration ability following injury or other conditions that promote diabetes.
Bone - cartilage	Throughout adult life, bone possesses the intrinsic ability to regenerate during skeletal development and to promote normal fracture healing (Einhorn 1998; Ferguson et al. 1999; Dimitriou et al. 2011). Natural bone remodelling involves osteoblasts and osteoclasts, both of which are responsible for maintaining a dynamic equilibrium between bone formation and bone resorption (Dalle Carbonare et al. 2012). However, many diseases due to the loss of large bone quantities compromise the regenerative process.

Table 1. Overview of organ regeneration in mammals. In the left column are summarized the organs and in the right one the regenerative skills of each one.

It can be divided into three phases, inflammation, proliferation and remodelling (Figure 1). These steps are not linear and wounds can often progress both forwards and back through the phases depending upon intrinsic and extrinsic forces at work within the patient (Leaper & Harding 1998; Kumar & Babu 2014; Harding et al. 2002).

Some evidences pointed to that scarring, with often occurs at the end of healing in mammals, impedes regeneration. However, amazingly, a certain immunological defective mutant mouse regenerated the hole in the ears after injury. This mutant mouse shows the defects of scar formation, suggesting that scarring may interfere with regeneration by blocking initiation signals for regeneration (Heber-Katz & Gourevitch 2009). A scar is the price we pay for evolutionary survival after wounding. Wound healing has been optimized for speed of healing under dirty conditions, where an extremely quick inflammatory response to overlapping cytokines and inflammatory cascades prevent infection and future wound breakdown (Bayat et al. 2003).

Currently, the main goals of **Regenerative medicine** are identifying the molecular and cellular signals that guide regeneration in regeneration-competent organisms, as well as those that prevent it in regeneration-incompetent organisms, including humans, to understand the biology for diagnosis, prevention and treatment of human damaged organs and tissues as soon as possible. Today we have the tools for the understanding of regeneration.

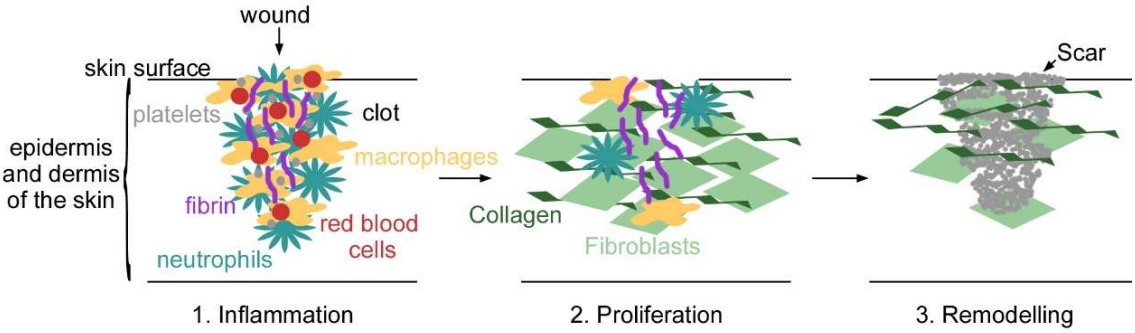

Figure 1. The phases of wound healing in mammals. 1. The **inflammatory phase** is the body's natural response to injury. After initial wounding, the blood vessels in the wound bed contract and platelet aggregation lead to the formation of the fibrin-rich clot. Once *haemostasis* has been achieved to stop the bleeding, blood vessels then dilate to allow neutrophils, macrophages, white blood cells, growth factors, enzymes and nutrients to reach the wounded area. Bleeding and inflammation, prevent infections and accelerate wound healing. 2. During **proliferation,** the wound is rebuilt with new granulation tissue, which is comprised of collagen and extracellular matrix. A new network of blood vessels develop (angiogenesis). Healthy granulation tissue is dependent upon the fibroblast receiving enough levels of oxygen and nutrients supplied by the blood vessels. 3.. The **Remodelling** is the final phase and occurs once the wound has closed. Epithelial cells finally resurface the wound. This phase involves remodelling of collagen from type III to type I. As collagen accumulates in the granulation tissue to produce scars, the density of blood vessels diminishes (Tonnesen et al. 2000).

How to regenerate?

Although a few examples of regeneration were discussed by Aristotle and Pliny, it was Abraham **Trembley** in the 18th century who did remarkable observations about regeneration of the freshwater polyp *Hydra*. He wanted to find animals that could be cut into pieces and regenerate a whole new organism. Some years later, René-Antoine Ferchault de **Réaumur**, found equivalent results in *Hydra* as well as in crustaceans, freshwater and terrestrial worms. Then, Charles **Bonnet**, decided to fragment annelids besides polyps. Afterwards, Lazzaro **Spallanzani**, discovered the regenerative potential of tadpoles, salamanders, snails, slugs and lizards. Together with Trembley, Réaumur and Bonnet, they established the mainstays of regenerative biology. Thomas Hunt **Morgan** studied the capacity of regeneration of crustaceans, worms, amphibians and fishes among others, and theorized about how growth and proliferation are controlled during regeneration (Morgan 1901).

Since then, regenerative biology has fascinated many hundred scientists in the 20th century. Today, we are aware that regeneration is widespread through the animal kingdom, with representatives from most animal phyla. The regenerative capacity of organisms varies according to the species, developmental stage and tissue involved (Brockes et al. 2001; Sánchez Alvarado 2000). It is an outstanding feature that closely related species show differences in regenerative capacity (Brockes et al. 2001). Thus, the understanding of how regeneration occurs in regeneration-competent species can be of interest in biomedical research. Many animals are being used as model systems in laboratories worldwide. The most commonly utilized as well for their regenerative skills are summarized in table 2.

Regeneration phenomena across the animal kingdom can occur at **multiple levels** of biological organization. This includes variation in the number of cell types to be made, ranging from restoring a single cell type, a tissue, an organ, a structure to the whole body (Bely & Nyberg 2010). The molecular mechanisms underlying tissue repair are conserved across phyla. For example, **local responses** in the wound are known to be critical for the initiation of regeneration. Wound healing (Gurtner et al. 2008), bioelectric signalling (Levin 2009), remodelling of the ECM (Quiñones et al. 2002; Yokoyama 2008), immune response (Katsuyama et al. 2015; Kimura et al. 2003; Ramírez-Gómez et al. 2008) and interactions between the wound epidermis and the underlying tissue are essential for regenerative growth.

In all instances, replacing an injured structure requires the production of **new cells.** Therefore, one of the main functions of early signalling events after the injury is to stimulate the production of additional cells to re-build lost structures. The new cells can be generated in a wide variety of strategies, depending on the tissues and the species. This includes the proliferation of stem cells, division of differentiated cells, dedifferentiation and/or transdifferentiation of mature cells to a stem cell–like precursor or another cell type (Figure 2; reviewed in King & Newmark 2012; Tanaka & Reddien 2011). Multiple of these candidate sources of new cells could act in concert to allow regeneration of a complex tissue.

Regeneration **stem cell-dependent** has been extensively described in *Hydra* and planarians. *Hydra* can regenerate whole individuals from small fragments, and this is because the existence of three distinct stem cell populations: ectodermal, interstitial, and endodermal stem cells (Galliot et al. 2006). Also, planarians display an extraordinary regenerative capacity, although they possess a unique well-characterized stem cell type, the neoblasts (Baguñà et al. 1989). In vertebrates, the source of stem cells and progenitors varies between tissues and organs. For example, in mammals, after mechanical injury, epidermal stem cells migrate toward the epithelium (Fuchs et al. 2004; Christiano 2004). In addition, cells deriving from different tissues may respond to different signals (Nacu & Tanaka 2011) and show lineage restriction not only in their tissue fates, but also on the positional identity they can adopt (Kragl et al. 2009). This lineage restriction has also been observed during fin regeneration in zebrafish (Tu & Johnson 2011).

MODEL ORGANISM	REGENERATIVE CAPACITY
Hydra	Small fragments of *Hydra* tissue can regenerate a complete organism; even dissociated single cells can reaggregate, re-establish polarity, and form a new animal (Noda 1971; Gierer et al. 1972). Stem cells and transdifferentiatiated cells, both contribute to the regenerative abilities of *Hydra* (Galliot et al. 2006).
C. elegans	*C. elegans* flatworms regenerate their axons (Ghosh-Roy & Chisholm 2010).
Drosophila	Larval Imaginal discs regenerate and embryonic epidermal wounds (Bryant 1975a; Strub 1979; Martin & Parkhurst 2004) Ovaries, testes and midgut are used to study homeostatic regeneration (reviewed in (Belacortu & Paricio 2011).
Planarian	Planarians are capable of re-growing new heads, tails, sides or even entire organisms from tiny body fragments (Morgan 1898). They owe their regenerative abilities to neoblasts, a population of mesenchymal stem cells (Baguñà et al. 1989).
Starfish	They can regenerate amputated arms (Achituv & Sher 1991; Alves et al. 2002; Rubilar et al. 2005; Shibata et al. 2010).
Zebrafish	*Zebrafish* can fully regenerate its heart after amputation of up to 20% of the ventricle. Cardiomyocytes dedifferentiate and proliferate after injury without scar formation and regenerate electrically coupled cardiac muscle (Kikuchi et al. 2010; Jopling et al. 2010). They also regrow amputated fins, jaw, hair cells, brain, retina, spinal cord, pancreas, liver and kidney (reviewed in Gemberling et al. 2013).
Axolotl	Axolotls are capable of complete and faithful regeneration of missing body parts through life (Carlson 2007), because they do not complete metamorphosis and their cells retain embryonic-like characteristics (Galliot & Ghila 2010). They can regenerate lens, spinal cord, appendage limbs, tail, ovaries and brain (reviewed in McCusker et al. 2015).
Salamander and newt	Salamanders and newts can regenerate limbs, tail, jaws (Maden 2008; Kurosaka et al. 2008), a part of their heart, spinal cord, eyes and brain (Reyer 1954; Oberpriller & Oberpriller 1974; Mitashov 1996; Okamoto et al. 2007).
Xenopus	Tadpole tail and limb buds can regenerate, but after metamorphosis lose this ability (Dent 1962; Muneoka et al. 1986). the epithelium of the gut regenerates during metamorphosis (Shi & Ishizuya-Oka 1996). In some frogs lens regeneration is observed from the cornea (Freeman 1963).
Chick	Chick embryos can regenerate its retina (Belecky-Adams et al. 2008) and its spinal cord well up to a certain stage. Glia do not scar (Whalley et al. 2006).
Mouse	See table 1 for mammal regenerative capacities. Mammal foetus experiment scar-free healing (Brockes et al. 2001). Neonatal and adult mice can only regenerate the distal part of the finger when amputated from the first joint (Borgens 1982; Muneoka et al. 2008). Following 70% hepatectomy the liver regenerates (Farber 1956).

Table 2. Main model organisms used in the laboratories to study regeneration. In the left column are summarized the model organisms and in the right the regenerative skills of each one.

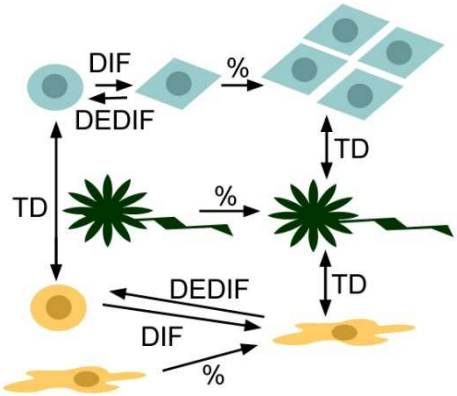

Figure 2. Different cell types could contribute to replace damaged tissue. After injury, many cells could re-build the missing part. Stem cells can proliferate (%) and differentiate (DIF). These differentiated cells divide as well. Cells also dedifferentiate (DEDIF) and transdifferentiate (TD) to other cell types.

The new cells can also be generated by the **division of differentiated** cells close to the wound. After partial hepatectomy or mild injuries, restoration of liver mass is accomplished through the proliferation of remaining hepatocytes (Riehle et al. 2011). In axolotl and *Xenopus* multiple cell types contribute to the regeneration of the missing tissues (Slack et al. 2004; Kragl et al. 2009). Nevertheless, in newts and axolotls, **dedifferentiation** also contributes during appendage regeneration. Near the site of amputation, skeletal and cardiac muscle cells can dedifferentiate and become proliferative during regeneration (Lo et al. 1993; Echeverri et al. 2001; Kumar et al. 2004; Laube et al. 2006). Similarly, studies in zebrafish established that cardiomyocytes and mature osteoblast cells do dedifferentiate and proliferate to produce heart muscle cells and new bone, respectively, during heart and fin regeneration (Jopling et al. 2010; Kikuchi et al. 2010; Knopf et al. 2011). **Transdifferentiation** has been reported in lens regeneration in newts. Cells from the dorsal iris dedifferentiate, re-enter into the cell cycle and differentiate to produce new lens cells (Henry & Tsonis 2010). In *Drosophila* imaginal discs, cells respecificate their fate to replace lost tissue (Repiso et al. 2013).

Traditionally, there were described two major ways by which regeneration can arise, according to the presence or the absence of a blastema formed upon wound healing. The first type was called **epimorphosis**, and involves the dedifferentiation of adult structures to form the blastema, which is a mass of morphologically undifferentiated and pluripotent cells that then conduct the regeneration of lost structures by proliferation.

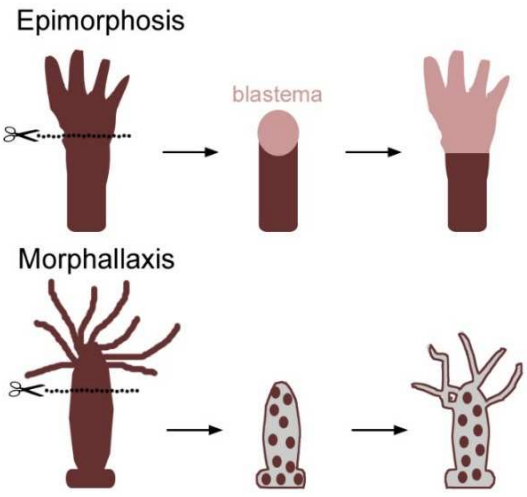

Figure 3. Classical classification of mechanisms of regeneration. A representative example of epimorphosis is the limb regeneration in amphibians; It consists on blastema formation upon wound healing. This undifferentiated mass of cells proliferates and differentiate to re-build missing tissue. *Hydra* regeneration is considered as morphallaxis. In this organism, there is no blastema formation, and regeneration occurs from the rearrangement of pre-existing cells.

Epimorphic regeneration has also been seen in a wide range of situations such as heart and fin regeneration in zebrafish (Johnson & Weston 1995; Poss et al. 2002), regeneration of digit tips in mammals (Muller et al. 1999), as well as appendage regeneration in hemimetabolous insects (French et al. 1976). The second mechanism was named **morphallaxis**, where regeneration occurs through the remodelling of pre-existing tissue, and there is little new growth (Figure 3). This classification, however, cannot reflect a mechanistic view of regeneration and suggest that this process in diverse animals may be controlled by different principles (Agata et al. 2007).

The **intercalation model** came up based on the work of grafting experiments of limbs in urodeles and cockroaches (Iten & Bryant 1975; French et al. 1976). It is because the regeneration of an appendage according to the **positional information** of the amputation level is well evidenced by intercalation. During amphibian limb regeneration as well as in the leg of cockroaches, the distal part is first formed and then the intermediate region to fill up the gaps of the missing positional values between the distal and proximal parts. *Drosophila* imaginal discs also regenerate by intercalation. When two opposite peripheral pieces of imaginal tissue are cultured together, they reconstruct the missing central part (Haynie & Bryant 1976). After genetically induced cell death intercalary regeneration occurs in the same way (Repiso et al. 2013). That rearrangement of positional information by intercalary events may occur both in morphallactic and epimorphic regeneration, and is evolutionarily conserved from insects to urodeles (Iten & Bryant 1975; Nye et al. 2003).

Given the wide spreading of the regenerative abilities throughout the animal kingdom, it has been hypothesized that some regenerative mechanisms have been conserved throughout evolution (Sánchez Alvarado & Tsonis 2006; Brockes & Kumar 2008; Bely & Nyberg 2010; Poss 2010). Thus, from this point of view, the lack of regenerative skills reflects evolutionary loss. Nevertheless, there are examples of molecules which have apparently evolved within a specific evolutionary lineage, the urodele amphibians (Garza-Garcia et al. 2010). Consequently, it will also be important to consider the roles of such taxon-specific genes in regeneration in diverse organisms and not only focus on canonical signalling pathways.

To understand the regenerative responses to injury and to develop therapeutic approaches, it will be crucial to appreciate how injured tissues initiate the regeneration program by triggering an immune response, changes in cell plasticity as well as specific cellular responses. To this date, many signalling pathways and factors are known to work in tissue regeneration, but often this information is unconnected. This can be assessed with genetic analysis, and particularly with *Drosophila* genetics. The use of sensitized genetic backgrounds, large-scale screenings, high-throughput techniques and the conditional activation or repression of transgenes will allow us to unravel the genetic interactions underlying cellular behaviour and morphogenesis, and will give us an integrative view of regeneration. For this reason, we have used *Drosophila melanogaster* to study regeneration in this thesis.

Drosophila imaginal discs

Drosophila has emerged as a valuable model for studying **wound healing** and **regeneration** because the genetic networks involved in epithelial movements occurring during embryonic dorsal closure, imaginal disc regeneration and embryonic repair are closely related to vertebrates (Martin & Parkhurst 2004). In this work, we used *Drosophila* imaginal discs to study epithelial regeneration, mainly due to their accessibility and the development of ingenious methods to manipulate the genetic content of cell populations within the discs. Its short generation times, a considerable number of progeny, easy-to-handle, suitability for genetic manipulations and well-described developmental biology (Figure 4) have converted the fruit fly in an awesome model organism to answer countless biological questions raised during more than two centuries.

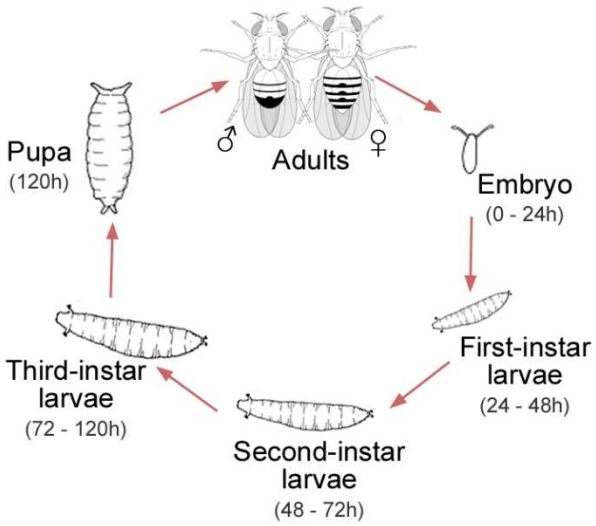

Figure 4. The life cycle of *Drosophila melanogaster*. The cycle starts with a 24-hour **embryogenesis**, where the polarity of the embryo and imaginal discs is determined. It is followed by four days of larval development (L1, L2 and L3), where most growth takes place, particularly in the imaginal tissues. After that, the pupal stage takes five days, when metamorphosis occurs and the imaginal tissues differentiate and give rise to the adult structures. At the end of the pupal stage, the adults emerge and complete the cycle. The length from the embryo to the adult stage ranges about ten days at 25°C.

The fruit fly is a simpler organism compared to vertebrates, with low genetic redundancy and simplify forms of the main signalling pathways, which have allowed scientists to identify the core functional elements and their function in an easier way. Indeed, the *Drosophila* genome was sequenced in 2000 (Adams et al. 2000), and it was found that about 75% of human disease-related genes have a recognisable orthologue in this organism (Reiter et al. 2001). That is why *Drosophila* is really useful in biomedical research being a model for human metabolic genetic disorders and making possible to test a wide variety of drugs in a simplified system (Padmanabha & Baker 2014; Wangler et al. 2015; Yamamoto et al. 2014; Zirin & Perrimon 2010).

Imaginal discs are well-characterized epithelial sacs determined in early embryogenesis capable of regenerating when parts are removed, as in the case of the appendages of amphibians and immature arthropods. After an injury or cell death, wound healing is followed by regeneration, whereas in mammals is accompanied by scar formation. There are nineteen imaginal discs in the larva, with nine bilateral pairs, that will form the head, thorax and appendages, and a genital medial disc (Figure 5; Held 2005). Imaginal discs grow and proliferate throughout larval stages and they differentiate and fuse during metamorphosis to form adult structures. In this thesis, we concentrated our experiments in the wing imaginal disc, which will give rise to the adult wing.

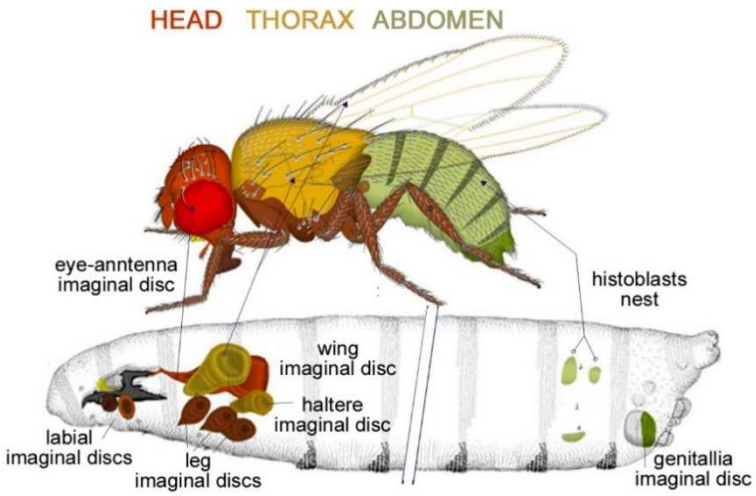

Figure 5. *Drosophila* imaginal discs and their derivatives in the adult. Imaginal discs in the mature larva (bottom) and the derived adult appendix (top). The head capsule, eyes and antennae derive from the eye-antennae imaginal discs (red) while the thorax and wings originate from the wing imaginal discs (yellow). The epidermis of the adult abdomen derives from the imaginal tissues called histoblast nests, which proliferate during metamorphosis (green).

Wing development starts from clusters of few epidermal cells that invaginate and develop into the imaginal tissues (Figure 6; Bate & Arias 1991; Cohen et al. 1993). Embryonic wing primordia originate from a cluster of cells of 20-70 cells from polyclonal origin (Mandaravally Madhavan & Schneiderman 1977) that isolate by invagination from the parasegments 4 and 5 of the embryonic ectoderm, which contribute to the second thoracic segment (T2) (Cohen et al. 1993).

Each wing imaginal disc gives rise to both a wing and the surrounding notum (body wall) (Figure 7 B). Throughout development, cells gradually become committed to different cell populations that will give rise to specific adult structures (Figure 7 A). The wing primordia starts to proliferate by the end of the first instar (Mandaravally Madhavan & Schneiderman 1977). After that, it divides exponentially up during second and third instar stages (Cohen et al. 1993). Prior to pupariation, each disc contains about 50.000 cells (Garcia-Bellido & Merriam 1971). The division rate is constant (about 8 h 30 min per each cell cycle) (Garcia-Bellido & Merriam 1971), although quick and slow dividing cells are detected (Milán et al. 1996). Apoptosis is scarce in the columnar epithelium, from which the proper wing will emerge of the wing of larval and pupal stages (Milán et al. 1997). Therefore, the final size and shape is controlled by proliferation, which depends both on the growth rate and the duration of growth during the feeding period. Both parameters are influenced by genetics and fitness variables, such as diet, mate selection, predation, temperature, crowding, tissue damage and infections (Bryant & Simpson 1984; Edgar 2006).

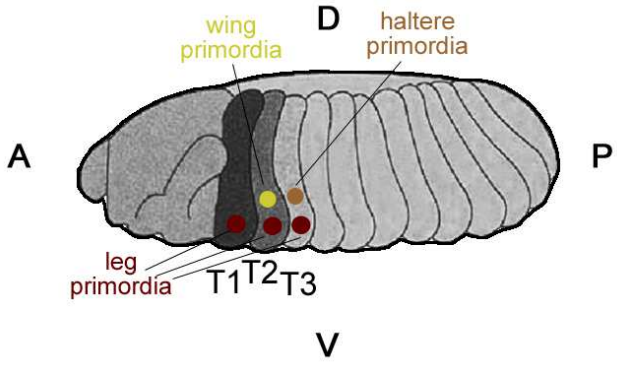

Figure 6. Embryonic origin of imaginal discs. Origin of the wing (yellow), haltere (sepia) and leg (brown) primordia in the embryo. Note that wing and haltere imaginal discs arise from the second and third thoracic segment (T2 and T3, respectively), and are located dorsally to the three ventral leg primordia. A (anterior), P (posterior), D (dorsal) and V (ventral) are the axis of the embryo.

At the end of the larval period most wing imaginal discs' cells stop at G_2, and there are two more divisions in the first 24 hours of the pupal stage. Subsequently, cells are progressively arrested at G_0 phase, when they differentiate (Milán et al. 1996). Mature discs undergo a major morphogenetic event during metamorphosis, as they evert in a process triggered by the ecdysone hormonal cascade (Fristrom and Fristrom 1993; Poodry 1980). The dynamics of such morphogenetic movements have been described and include a 90° folding of the disc followed by a rapprochement with the pupal epidermis and finally the disintegration of the peripodial membrane by apoptosis (Aldaz et al. 2010).

Proliferation of the wing disc is **intercalary**, because the progeny of ancestor cells becomes gradually separated, and **exponential,** since clones related in size can grow in any position throughout the whole disc (Resino et al. 2002). The elongation takes place through the proximal-distal (PD) axis in the wing blade, whereas in the notum appear more isodiametric, which is controlled by mitotic spindle orientation (Garcia-Bellido & Merriam 1971; Baena-López et al. 2005).

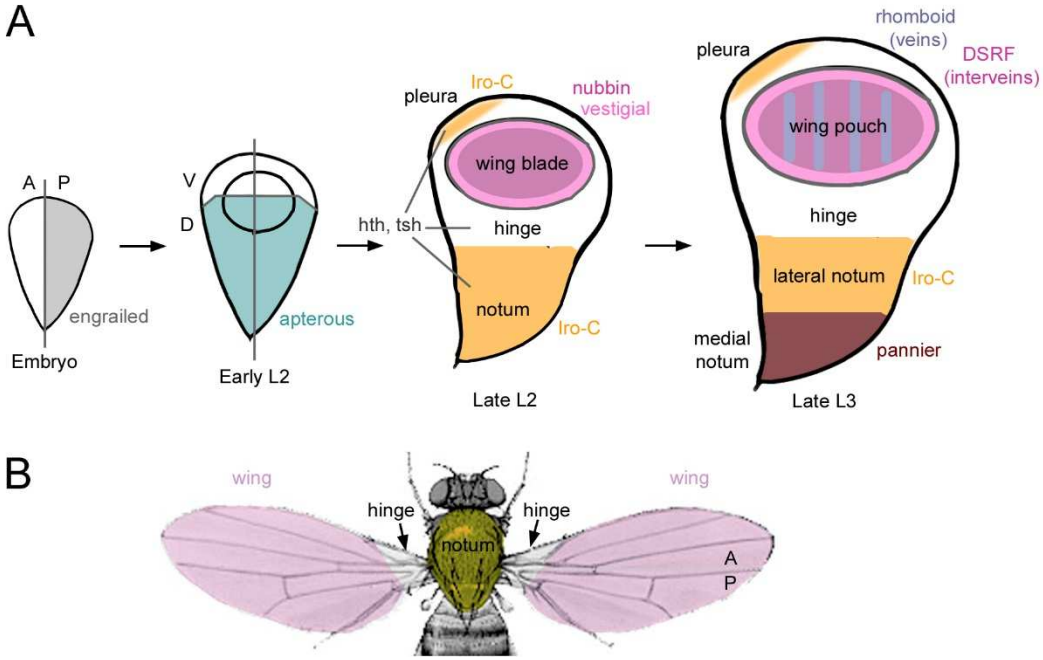

Figure 7. Specification of wing imaginal disc through development. (A) The AP axis is defined in early embryogenesis thanks to the expression of of the selector gene *engrailed* (*en*) and its partner *invected* (*inv*) in posterior cells (Garcia-Bellido & Santamaria 1972; Kornberg 1981; Kornberg et al. 1985; Simmonds et al. 1995; Morata & Lawrence 1975; Tabata et al. 1995; Lawrence & Morata 1976). The DV axis is defined in early L2 when dorsal cells express *apterous* (*ap*), (Cohen et al. 1992; Milán & Cohen 1999; Williams et al. 1993; Diaz-Benjumea & Cohen 1993), and the PD axis in mid-late L2 when future wing cells express *nubbin (nub)* and *vestigial (vg)* and downregulate *homothorax (hth)* and *teashirt (tsh),* limiting their expression to the hinge and notum (body wall) (Cifuentes & García-Bellido 1997; Williams et al. 1993; Azpiazu & Morata 2000; Wu & Cohen 2002; Casares & Mann 2000). Prospective notum cells upregulate genes of the Iroquis complex (Iro-C genes: *araucan (ara), caupolican (cap)* and *mirror (mirr)* (Diez del Corral et al. 1999). Later, during L3 lateral notum cells upregulate *pannier* (*pnr*) and downregulate Iro-C genes, distinguishing the medial from the lateral notum (Calleja et al. 2000). Finally, in late L3 prospective veins activate *rhomboid (rho) and* downregulating *Serum Responding Factor/Blistered (dsrf/Bs)* distinguishing presumptive vein and intervein territories (Sturtevant et al. 1993; Fristrom et al. 1994; Montagne et al. 1996; Roch et al. 1998; Martín-Blanco et al. 1999; Baonza et al. 2000). (B) In the adult, the notum (yellow), the hinges (grey) and the proper wing (purple) derive from the wing imaginal discs.

The wing primordium present three-major axis, **antero-posterior (AP), dorso-ventral (DV)** and **proximo-distal (PD)**, where signalling centres along the DV and AP axis organize growth and patterning of both the wing blade and the body wall (Figure 7 A).

There are two main ways by which cells determine their fate, compartment- and non-compartment based mechanisms. The **compartment-based mechanism** (as in AP or DV boundaries) is set up through the establishment of compartment lineage restrictions, defined by the selector genes (Garcia-Bellido & Santamaria 1972). A selector gene acts as a lineage restriction barrier, because it is expressed in a specific population of cells that cannot mix with other from different compartments (Garcia-Bellido et al. 1973).

The progressive subdivision of the disc in different populations of cells causes the expression of different signals in the boundaries, which act as morphogens to pattern the tissue and confer identity and affinity properties on each compartment (Meinhardt 1983). Compartments are considered autonomous units of growth control, because the growth of one compartment is independent to the adjacent one. Interaction between cells in adjacent compartments establishes the organizers or signalling centres at the interface of the boundaries by the secretion of the **morphogens Dpp** and **Wg** to control growth and pattering along the different axes of growth (Figure 8; Lawrence 2001). Hedgehog (Hh), which is transcriptionally activated by Engrailed (En), binds to the receptor Patch (Ptc) and releases Smoothened (Smo), which results in the liberation of Ci transcriptional activation form (Alcedo et al. 1996; van den Heuvel & Ingham 1996; Ohlmeyer & Kalderon 1998) and induces the expression of anterior genes in a concentration dependent fashion. Among others, it promotes the expression of the morphogen **Dpp** at the **AP boundary** (Figure 8; Zecca et al. 1995). The Dpp gradient could lead to th activation of distinct targets depending on the distance from the source (the AP boundary), as *spalt major* (*salm*), *optomotor blind* (*omb*), and *brinker* (*brk*) (Affolter & Basler 2007; Campbell & Tomlinson 1999; Nellen et al. 1996). In late wind disc development, The Dpp gradient is responsible for the positioning of vein L2 and L5.

On the other hand, Apterous, besides specifying the dorsal identity (Diaz-Benjumea & Cohen 1993) induces the expression of **Wg** at the **DV boundary** through Notch (N) and Serrate (Ser) (Figure 8; Diaz-Benjumea & Cohen 1993; Diaz-Benjumea & Cohen 1995). In addition to Wg, Notch induces *vestigial* (*vg)* in the DV boundary. Wg acts as a morphogen as it spreads from its source and forms a gradient along the DV axis, acting at long range up-regulating specific genes at different concentrations (Strigini & Cohen 2000).

Additional mechanisms are implicated in the maintenance of gradients formed by morphogens, such as protein repressors, vesicles for secretion, extracellular matrix modifications and cytonemes, among others (Hsiung et al. 2005; Torroja et al. 2005; Strigini & Cohen 1999).

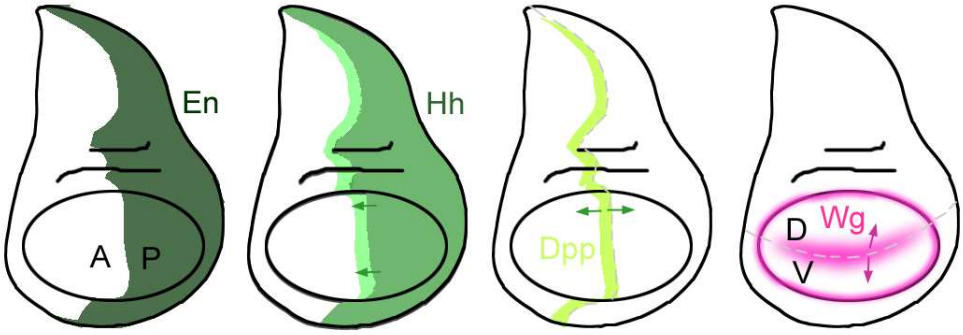

Figure 8. Morphogens act as organizing centres at the AP and DV compartment boundaries. Engrailed (En) is expressed in the posterior (P) compartment, conferring posterior identity and thus establishing the anterior-posterior (AP) boundary. **En** activates **Hh**, a secreted short-range signaling protein, which can cross over the AP boundary and induce the expression of **Dpp** along the AP axis. Its secretion establishes long-range signaling to direct patterning of a wider disc region. **Wg** is another key molecule for wing development produced at the DV boundary.

The **non-compartment based mechanisms** are frequent in development and are defined by the restricted expression and activity of a gene or different combinations of gene products, but with less restrictive segregation (cells can switch from one identity to another) (González-Gaitán et al. 1994; Zirin & Mann 2007). Examples of these domains are the wing pouch, the hinge and the notum (Figure 9 A). Amazingly, cells respond to signals differently depending on the domain they are placed. That is the case of ectopic expression of Wg, which leads to overproliferation without repatterning in the hinge, whereas in the wing blade promotes repatterning and only secondarily proliferation (Neumann & Cohen 1996). Similarly, increased Dpp signalling in proximal cells (where Dpp levels are normally low) causes apoptosis, whereas allowing normal development in distal regions (Adachi-Yamada et al. 1999; Adachi-Yamada & O'Connor 2002; Burke & Basler 1996; Martín-Castellanos & Edgar 2002).

Morphologically, the wing imaginal disc consists of a continuous epithelial monolayer that forms a two-sided epithelial sac, which surrounds the disc lumen. One side of the disc is a columnar pseudostratified epithelium, namely the **columnar epithelium** (CE), and the other side is an outer layer, the **peripodial membrane** (PM), a squamous epithelium of wide and flatten cells (Figure 9 A, B, C). The PM does not contribute to the formation of any adult structure, but facilitates the process of wing disc eversion and thorax fusion during metamorphosis (Pastor-Pareja et al. 2004; Tripura et al. 2011). Most discs also contain some adepithelial cells (mesodermal myoblasts), as well as tracheal cells and a few neurons that reside between the epithelium and the basal lamina (Figure 9 B). The CE will give rise after metamorphosis to the adult wing, the notum, the pleura and the hinge, a structure that joints and articulates the wing to the notum (compare adult in Figure 7 B with imaginal disc in Figure 9 A). The opening of the sac-like structure is connected to the surface of the larva via a narrow stalk, which plays an important role in disc eversion (Pastor-Pareja et al. 2004). During wing disc eversion, the dorsal (D) and ventral (V) surfaces fold and become apposed (Figure 9 D).

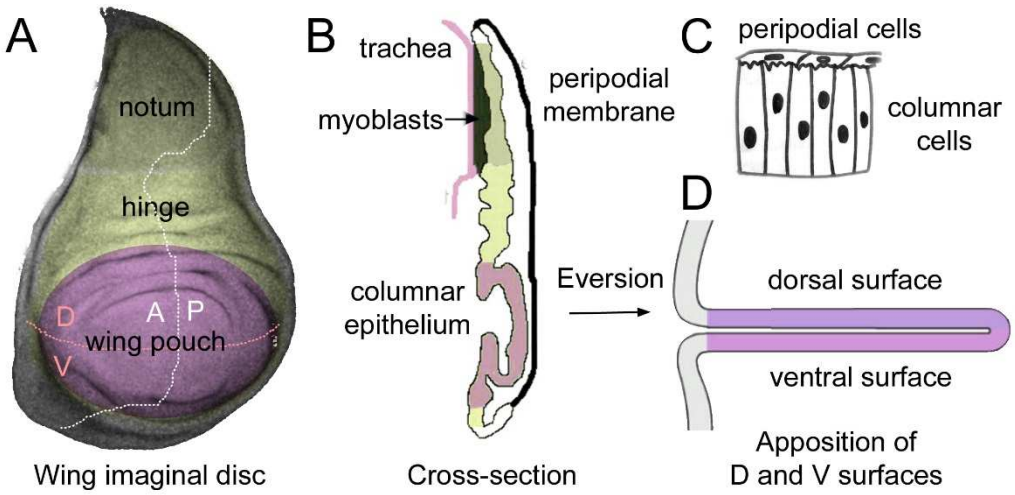

Figure 9. Morphology of wing imaginal disc and wing eversion during metamorphosis. (A) Wing imaginal disc territories: wing pouch (purple), hinge (yellow) and notum (sepia). DV and AP boundaries are labeled with a red and white dotted line, respectively. (B) Schematic cross-section of a wing imaginal disc. The disc is composed by the columnar epithelium and surrounded by a peripodial membrane. Myoblasts and trachea are located close to the notum. (C) Columnar cells belonged to a pseudostratified epithelium, and flat peripodial cells belonged to a squamous one. (D) During wing disc eversion in metamorphosis the dorsal (D) and ventral (V) surfaces fold and become apposed.

Wings are the main evolutionary innovation that originated within hexapods, and its development is constrained to the T2 and T3 segments. The adult wings of pterygotes are formed by a bilayered cuticularized epithelium, with veins set in a taxon-specific pattern in between. Heterometabolous insect's wings appear during an early nymphal instar, without veins and mobility. During metamorphosis, they grow and the hinge allows motion. Nevertheless, in holometabolous species as *Drosophila*, wings are absent during larval stages, and develop as evaginations of the dorsolateral thorax at the pupal molt (Svácha 1992).

How do imaginal discs' regenerate?

Early imaginal disc regeneration studies

The work by Ernst Hadorn, Gerold Schubiger and Peter Bryant in the 60's, established the basis for our current understanding of regeneration in *Drosophila* imaginal discs. They demonstrated that these epithelial tissues have an outstanding capacity to replace lost parts after fragmentation. Discs respond to tissue damage differently depending on the type of fragment; Cells can proliferate and **regenerate** the missing tissue or alternatively, they can **duplicate**. Peter Bryant demonstrated that fragmentation of wing and leg imaginal discs resulted in the regeneration of the larger fragment and the duplication of the smaller one (Bryant 1971). In addition, fragments can **transdeterminate** to a different disc, for example from wing-to-leg. Some of the genes involved in transdetermination are also central for regeneration, and thus, a parallel has been suggested between the molecular mechanisms regulating transdetermination and regeneration (reviewed in Worley et al. 2012; Bergantiños et al. 2010). Although the uncovering of these wonderful capabilities was discovered in parallel, in this work we will focus on the regenerative skills of imaginal discs.

These responses to damage were discovered after Hadorn and colleagues used an *in vivo* culture system that consisted on the **fragmentation** of imaginal discs into pieces and then subsequently **implanted and cultured** for several days in the abdomen of adult females, where those disc' fragments proliferate but do not differentiate (Figure 11 A; Hadorn et al., 1949; Hadorn 1962; Ursprung 1959 and Schubiger 1971).

With this method, disc cultures were maintained for more than 300 transfer generations over a period of even until 12 years (Hadorn 1978). To demonstrate the capacity of regeneration, disc fragments were **re-implanted into mature larvae**, where they differentiated during metamorphosis, thus the adult structures could be recovered (Figure 11 A; Hadorn 1965; Bryant 1975; Bryant 1971). The intercalary growth was demonstrated after confrontation of blastemas from distal parts (Haynie & Bryant 1976). Besides, isolated blastemas were able to recover lost structures (Karpen & Schubiger 1981). In the cut edges, the blastema contains cells that divide faster than in other regions. These fast-proliferating cells are mainly responsible for disc regeneration, although cell death is often observed extending several cell diameters away from the cut (Abbott et al. 1981; Kiehle & Schubiger 1985; Bosch et al. 2008). Of note, disc regeneration depends on the type of injury, the cellular context and the topology of the cut in the fragmented discs.

Regeneration was studied **wounding the wing discs *in situ***, by pinching through the intact larval cuticle to make a cut or remove a fragment while leaving the wounded disc in place to heal and regenerate (Figure 11 C; Bryant 1971; Pastor-Pareja et al. 2008; Díaz-García & Baonza 2013; Handke et al. 2014). Currently, these techniques have been substituted for ***ex vivo* culture** of imaginal discs (Figure 11 D; Handke et al. 2014; Restrepo et al. 2016).

One of the models proposed for imaginal disc regeneration is the **polar coordinate model** (Bryant et al. 1981; French et al. 1976). This model was based on experiments done on amphibian limbs, cockroach legs, and *Drosophila* imaginal discs. It proposes that **positional values** of cellular identity could be determined around the circumference of the disc and that intercalary regeneration would fill in missing positional values. Accordingly, imaginal cells have two coordinates, inherited from the beginning of development, that define their position. To define these values, it is necessary to divide the discs into sectors (triangles) and concentric rings (Figure 10). The circular component corresponds to the position around the outer border of the field, and the radial component is equivalent to the position alongside the PD axis, with the most distal values positioned in the centre. Taken together, they specify all positional values. The intercalary regenerative growth replaces the positional values between the two cut surfaces by the shortest possible route. However, this model was questioned after finding that growth started before healing was completed (Karpen & Schubiger 1981; Dale & Bownes 1981) and because duplicated fragments are much smaller than regenerated ones, while the model predicts that these tissues should intercalate equally (Adler 1981).

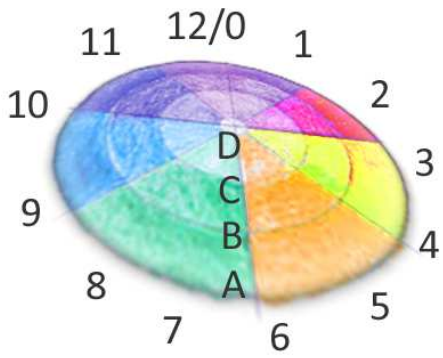

Figure 10. Scheme for polar coordinate model. A series of numbered positional values are arranged in a circle, in which cells have two coordinates that are continuous; One radial, from 1 to 12, and another one along the PD axis, from A to D, where D is the most distal. After fragmentation, apposition of the wound edges is assumed to end in regeneration of positional values that rest along the shortest path between the two cut edges. Consequently, the larger fragment regenerates, whereas the smaller one duplicates.

Hans **Meinhardt** proposed and alternative model, which incorporated compartment boundaries as organizing centres for normal and regenerative growth. It also included the intercalary growth to replace the missing tissue (Meinhardt 1983). Nonetheless, how positional values are distinguished and how regenerated forms are patterned properly is still a mystery.

A breakthrough was the observation of Hayne and Bryant that **irradiated** larvae resulted in about 50% cell death and yet a normal fly developed (Figure 11 B; Haynie & Bryant 1977). They concluded that proliferation compensates the missing cells. Currently, compensatory proliferation refers to tissue recovery after irradiation, massive cell death and induction of apoptosis (Mollereau et al. 2013). Compensatory proliferation may account for reaching the global organ size of the injured epithelium, but genetic and epigenetic signals will be decisive to control regeneration.

However, disc fragmentation and implantation into the abdomen of the flies is extremely laborious and irradiation is difficult to focus to specific zones of the individuals. Because the tremendous advance of the genetic engineering in *Drosophila* technology, flies can be designed with constructs that will allow genetically remove specific zones at specific times (Figure 11 E; Bergantiños et al. 2010; Smith-Bolton et al. 2009). Those genetic systems for

studying regeneration are based on the induction of apoptosis using the Gal4/UAS system (Brand & Perrimon 1993). Expression of the yeast transcription factor Gal4 under the control of different gene promoters was used to express pro-apoptotic genes, such as *eiger* (Smith-Bolton et al. 2009)*, reaper* (Smith-Bolton et al. 2009; Bergantiños et al. 2010)*,* or *hid* (Herrera et al. 2013).

The activity of Gal4 was inhibited by a temperature-sensitive allele Gal80 repressor (Zeidler et al. 2004). Genetic ablation is achieved by a temperature shift from 17°C to 29°C for different periods of time during larval development, and then larvae are shifted back to 17°C to allow tissue recovery (Figure 11 E).

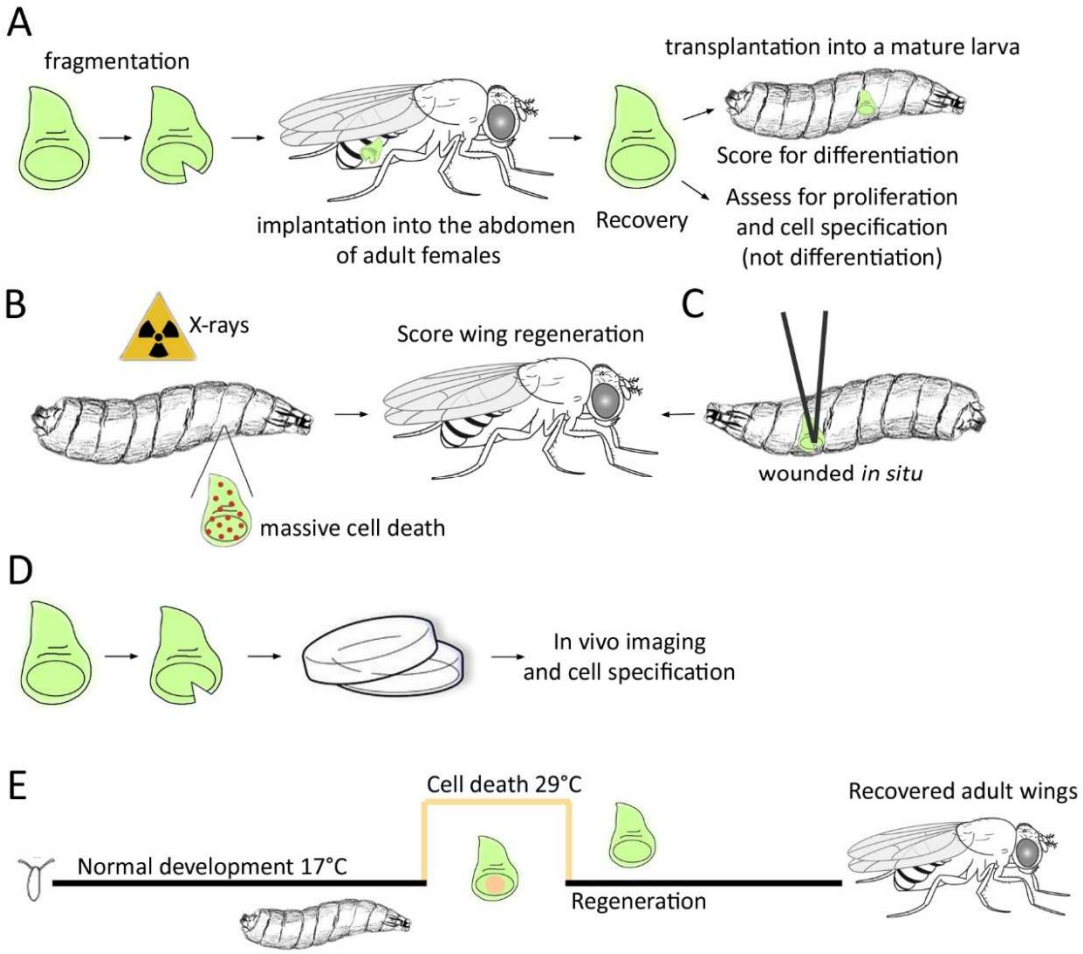

Figure 11. Evolution of the techniques applied for studying imaginal disc regeneration. (A) In the early 40's Hadorn and colleagues fragmented discs and cultured them into the abdomen of adult females, where they regenerated. Then the recovered tissue could be re-implanted into mature larvae for scoring differentiation or could be studied for assessing proliferation and cell specification (Hadorn 1962; Hadorn 1965; Haynie & Bryant 1976; Schubiger 1971). (B) X-rays were used to induce massive cell death in the whole larvae. Imaginal discs regenerated giving rise to normal adult structures (Haynie & Bryant 1977). (C) *In situ* wounds have been done in imaginal discs inside the larvae and then scored for adult appendix regeneration (Pastor-Pareja et al. 2008; Díaz-García & Baonza 2013). (D) Currently, *ex vivo* culture is used in substitution of the tedious implantation into the abdomens of flies (Handke et al. 2014; Restrepo et al. 2016). (E) Genetic ablation was developed for avoiding invasive techniques. Thanks to the Gal4/UAS system the whole larvae are transferred to 29°C to induce cell death and then they are shifted back to 17°C to allow tissue recovery (Smith-Bolton et al. 2009; Bergantiños et al. 2010). More details about D and E are depicted in the section Materials and Methods.

Recent advances

Wound closure

Drosophila embryos and imaginal discs reveal healing efficiently without scaring and resemble epithelial fusion events that occur in normal development, such as the embryonic dorsal closure and thoracic closure (Martin & Parkhurst 2004; Bosch et al. 2005; Mattila et al. 2005).

After **fragmentation or cutting**, transient heterotypic contacts between the cut edges of the columnar and the peripodial epithelium develop during the first day of *in vivo* culture. Contact between both layers is facilitated by filopodia, that extend their tips to close the wound, and closure is mediated by an actin-rich cable (Reinhardt et al. 1977; Reinhardt & Bryant 1981; Bosch et al. 2005). Consequently, the wound is closed in a zippering motion. Within 48 hours of culture, the initial stage of heterotypic healing ends and homotypic contacts are established by cells at both wound edges (Figure 12; Reinhardt et al. 1977; Reinhardt & Bryant 1981; Bosch et al. 2005). Individual cell migration is not involved in healing. Intercellular **calcium** waves seem to respond to mechanical injury (Restrepo & Basler 2016). Similarly, after **genetic ablation**, wound closure involves and actin-rich cable that extends into the wound by cells at the wound edges. The first connections are built at the apical edges of the healing cells, before the healing extends basally. Then wound closure continues in a zippering way extending headed for the edges of the disc (Figure 12; Bergantiños et al. 2010).

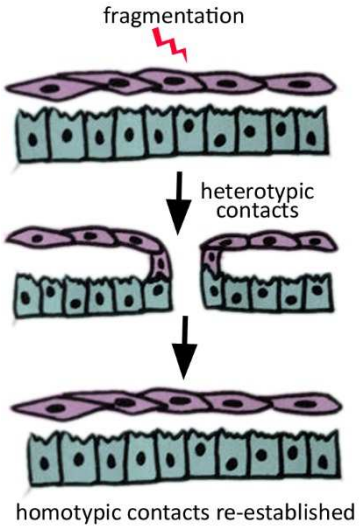

Figure 12. Homotypic contacts are re-established after fragmentation. First, transient heterotypic contacts are formed between columnar and peripodial epithelia, and afterwards homotypic contacts are re-built.

Jun N-terminal kinase (JNK) is crucial for wound healing events (Bosch et al. 2005; Mattila et al. 2005). In *Drosophila*, JNK signalling is activated during dorsal closure of the embryo (reviewed in Noselli & Agnès 1999), imaginal disc eversion (Pastor-Pareja et al. 2004), and in the course of the healing of epidermal wounds (Galko & Krasnow 2004; Rämet et al. 2002). After damage in imaginal discs, JNK is activated in the region near the edges of the wound, and in dying and living cells after genetic ablation. Blocking JNK activity in the dying cells do not impair wound closure or regeneration, demonstrating that the requirement for JNK signalling is in the living cells (Bergantiños et al. 2010). JNK activates the expression of the Matrix metalloprotease 1 (Mmp1), which degrades matrix proteins during wound healing (McClure et al. 2008), as well as the *unpaired* (*upd*) genes, which encode the **JAK/STAT**-activating cytokines (Katsuyama et al. 2015; Pastor-Pareja et al. 2008; Verghese & Su 2016; La Fortezza et al. 2016).

Besides that, JNK is likewise essential for cell proliferation in the blastemas (Bosch et al. 2005; Rämet et al. 2002; Mattila et al. 2005; Lee et al. 2005; Blanco et al. 2010), cytoskeletal rearrangements to close the gap between wounded tissues, cell death around the cut edges

and regulation of chromatin modifiers (Bergantiños et al. 2010; Herrera et al. 2013; Smith-Bolton et al. 2009).

It has also been reported the key role of **Plexin A** (PlexA) and its ligands **semaphorins** to heal wounded discs, revealing that the function of plexins may be evolutionary older than their known function in axonal pathfinding (Yoo et al. 2016).

Blastema formation and regenerative growth

After **fragmentation**, dividing cells accumulate near the wound creating a blastema. During wound healing, cells which were previously widely separated in the disc became neighbours and they reach their original position by intercalation of newly formed tissue (Bryant & Fraser 1988). The localized proliferation occurs as early as 24 hours after fragmentation, similar to a blastema that is observed during the regeneration of appendages in vertebrates (Dale & Bownes 1980; Adler & MacQueen 1984; Kiehle & Schubiger 1985; O'Brochta & Bryant 1987; Bryant & Fraser 1988; Bosch et al. 2008; Abbott et al. 1981), and proliferation peaks two to three days after injury (Bryant & Fraser 1988; Bosch et al. 2008; Mattila et al. 2005). Of note, first signs of cell proliferation begin before the completion of wound closure, thus tissue damage directly stimulates proliferation (Karpen & Schubiger 1981; Kiehle & Schubiger 1985; Bryant & Fraser 1988; Bosch et al. 2008; Mattila et al. 2005).

Cells in the blastema divide more and generate larger clones than cells outside the blastema or cells in unhurt discs (Worley et al. 2013). Moreover, proliferation rate is higher during regenerative growth than during normal development (Gerhold et al. 2011; Wells et al. 2006). Remarkably, cells outside the blastema proliferate less, with most of the cells at a distance from the wound arrested in G_1 or G_2 (O'Brochta & Bryant 1987; Sustar et al. 2011). The high regenerative capabilities of blastemas were not only demonstrated by localized proliferation, but also after isolation and culture blastemas, which regenerate and differentiate most of the misplaced structures in an arranged way (Karpen & Schubiger 1981). Clones of cells near the wound showed an elongated shape, suggesting orientation of cell division toward the wound edge, as well as separation of clonally related cells, signifying that cells are relocated by intercalating neighbours (Sustar et al. 2011).

Proliferation after **genetic ablation** is similarly localized to a blastema near the wound (Smith-Bolton et al. 2009; Bergantiños et al. 2010). Interestingly, proliferation at a distance from the wound is reduced, in a manner similar to the cell-cycle arrest observed after disc fragmentation (Smith-Bolton et al. 2009; Sustar et al. 2011). In contrast to the preferred orientation of mitotic cell divisions during normal growth, proliferating cells at the wound edges after genetic ablation orient toward the wound, similar to cell division near cut edges (Sustar et al. 2011; Repiso et al. 2013). This switch of orientation requires the cell polarity genes *fat (ft)* and *crumbs (crb)*, as well as the growth-promoting transcription factor Yorki (Yki) (Repiso et al. 2013).

Regenerative growth is handled by the same signalling pathways that regulate growth during normal development, but is activated by **damage-responsive signals**. Physical damage results

in the upregulation of the WNT protein **Wg** (Smith-Bolton et al. 2009; Gibson & Schubiger 1999; McClure et al. 2008; Katsuyama et al. 2015). Wg, in turn, activates **Myc** and **Cyclin E** levels. In fact, overexpression of Myc enhance regeneration (Smith-Bolton et al. 2009). In contrast with normal development, the expression of *wg* upon damage is driven by a damage-responsive enhancer (Schubiger et al. 2010; Harris et al. 2016). After fragmentation, the expression of **Dpp** does not upregulates in the wound edges, but the normal pattern is mostly recovered (Mattila et al. 2004). However, after genetic ablation in the wing pouch, Dpp spreads beyond the AP boundary in regenerative growth preceding the re-establishment of the wild-type pattern of Dpp signalling (Smith-Bolton et al. 2009).

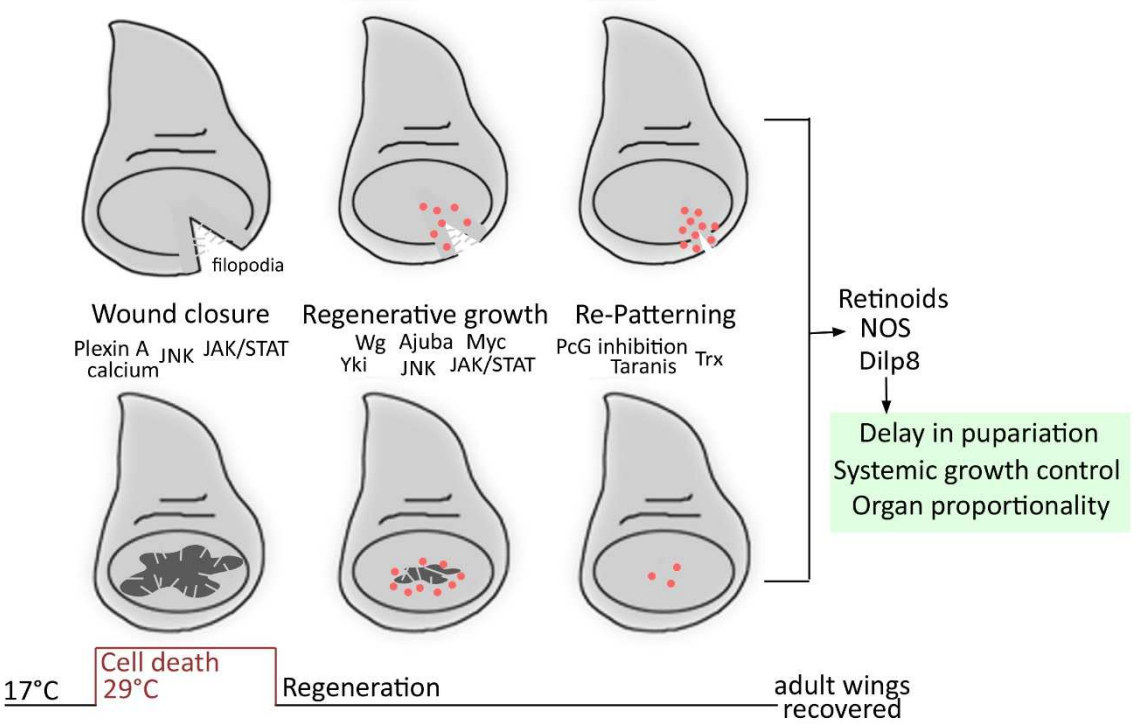

Figure 13. Overview of *Drosophila* imaginal disc regeneration. After fragmentation or genetic ablation, imaginal disc regeneration can be subdivided in three steps, which are not linear and overlap with each other. The first stage is the **wound healing**, where filopodia are emitted to close the wound. JNK, JAK/STAT, calcium waves and Plexin A play a key role in the process. **Regenerative growth** involves developmental pathways activated in a damage-specific manner. JNK, Ajuba, Yki, JAK/STAT, Wg and Myc are essential for proper proliferation. **Pattern respecification** is achieved thanks to Taranis, which protect from cell fate changes, and to the epigenetic machinery PcG and TrxG. Overall, damage in imaginal discs activates molecules as Retinoids, NOS and Dilp8, which delay in pupariation to give more time to the disc for regeneration, systemic growth control and organ proportionality. The bottom bars show temperature shifts to activate cell death and then let the tissue regenerate.

JNK is also indispensable for cell proliferation in the blastemas (Figure 13; Bosch et al. 2005; Rämet et al. 2002; Mattila et al. 2005; Lee et al. 2005; Blanco et al. 2010), and promotes regenerative growth, at least in part, through activating the **Ajuba** LIM domain protein, which targets components of the Hippo signalling pathway that negatively regulate the transcription factor **Yorkie** (Yki) (Sun & Irvine 2011; Sun & Irvine 2013). The activation of Yki is required for full wing disc regeneration, and is JNK-dependent. There is an increase of nuclear Yki in cells within and nearby in the ablated region as well as augmented expression of Yki target genes. In

fact, reductions in Yki levels compromise regeneration (Grusche et al. 2011; Sun & Irvine 2011; Meserve & Duronio 2015; Repiso et al. 2013).

Transcriptome analysis of disc fragmentation and culture in adult abdomens revealed that transcriptional regulators downstream of JNK, Notch, Dpp, and Wg signalling were upregulated at later stages of regeneration (Blanco et al. 2010; Klebes et al. 2005; McClure et al. 2008). The chromatin remodelling factor *absent, small or homeotic discs 2* (*ash2*) stabilizes the histone H3 methyltransferase trithorax-related protein (Carbonell et al. 2013).

Patterning

During regenerative growth, vein cells become respecified as intervein cells to recover the lost area. Thus, eliminated tissue is substituted by **orienting proliferation** toward the wounded area and respecification of cell fates (Repiso et al. 2013). In the same way, hinge cells are capable of generating cells that contribute to the pouch (Smith-Bolton et al. 2009; Herrera et al. 2013; Verghese & Su 2016). Dpp and Hh gradients are not involved in vein and intervein positioning after damage (Repiso et al. 2013).

The mechanism ensuring accurate re-patterning and growth is only starting to be investigated, as demonstrated by the current discovery of a factor protecting regenerating tissues from cell fate changes. This is encoded by ***taranis*** *(tara)*, which controls posterior cell fate during regeneration, and appears unnecessary for normal development (Schuster & Smith-Bolton 2015). **JNK** activity has been proposed to facilitate cell fate changes over the reduction of the **Polycomb group** (PcG) dependent silencing (Figure 13; Lee et al. 2005). Furthermore, additional chromatin factors were retrieved from transcriptome analyses, such as lama, Polycomb (PcG) and Trithorax group (TrxG), and chromatin remodelers as the Brahma complex (Blanco et al. 2010; Klebes et al. 2005).

In normal development, disc cells do not change compartmental identities, although there are unusual exceptions (Gettings et al. 2010). Nevertheless, after **fragmentation**, a regenerating disc composed only of anterior-fated cells can generate a posterior compartment (Abbott et al. 1981; Adler & Bryant 1977; Gibson & Schubiger 1999; Haynie & Bryant 1976; Schubiger 1971). However, the frequency of clones that traverse the compartmental border is low (Gibson & Schubiger 1999; Szabad et al. 1979). During regeneration, boundaries are rapidly reconstructed. In both leg and wing discs, clones of marked cells induced at the time of fragmentation can, albeit in low frequency, cross the A- boundary only when induced before the injury (Abbott et al. 1981; Szabad et al. 1979).

Compartment boundaries are re-established soon after **genetic ablation** (Smith-Bolton et al. 2009; Bergantiños et al. 2010). It has been recently described that these boundaries are transiently disturbed after massive cell death, and the cells close to those boundaries can change their fate and contribute to disc regeneration of compartments outside of their origin. It is the result of the upregulation of JNK and, consequently, a reduction in PcG levels. PcG and TrxG members also play a role in the process, by modulating the potential to transgress the AP boundary (Herrera & Morata 2014).

Signals derived from dead cells

It has been proposed that dying cells are a source of signals that control proliferation. In addition to the investigations in *Drosophila*, links between apoptosis and regeneration have been determined in other model organisms, including *Hydra, Xenopus*, planarians, newts, and mice (reviewed in Bergmann & Steller 2010; King & Newmark 2012).

In flies, in response to apoptotic stimuli, the pro-apoptotic genes *reaper* (***rpr***), *head involution defective* (***hid***), and ***grim*** promote apoptosis through the inhibition of the Caspase Inhibitor **DIAP1** (*Drosophila* inhibitor of apoptosis protein 1) (Goyal et al. 2000; Ryoo et al. 2002). Consequently, the Initiator Caspase **DRONC** (*Drosophila* Nedd2-like caspase, Caspase-9-like) is activated, and in turn activates by proteolysis the two major Effector Caspases, **DrICE** (*Drosophila* Interleukin-1 Converting Enzyme, Caspase-3-like) and **Dcp-1** (Death Caspase-1, Caspase-7-like) (Figure 14; Mills et al. 2005). Caspases are a highly-specialized category of cell-death proteases. Their function consists on the cleavage of several molecules to promote cell death (Xu et al. 2009). Although Caspase activity has been mainly linked to the initiation of the apoptotic pathway, there are rising evidences for non-apoptotic functions of Caspases (Miura 2012), as the activation of the proliferation program upon induction of cell death (Kondo et al. 2006). Additionally, other molecules which control cell death in *Drosophila* have been identified in the last few years (reviewed in Xu et al. 2009).

After disc fragmentation, the production of signals by dying cells is unclear, because the wound edges show only few apoptotic cells (Reinhardt et al. 1977; Bosch et al. 2008). When some tissue is removed by genetic ablation, the regenerative growth continues for several days after removal of the cellular debris (Smith-Bolton et al. 2009; Bergantiños et al. 2010).

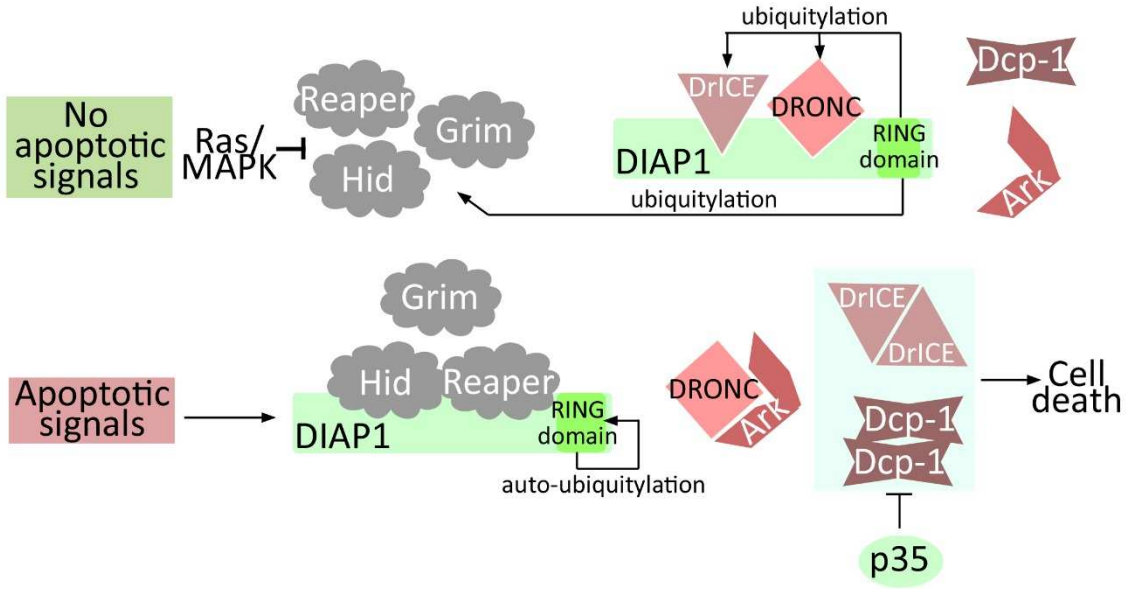

Figure 14. Cell death in *Drosophila*. In the absence of apoptotic signals, the protein DIAP1 is bound to the caspases DRONC and DrICE. This union promotes the ubiquitylation of both caspases by the RING domain of DiAP1. Ubiquitylation inactivates the caspases without proteosomal degradation. DIAP1 can also ubiquitylate Reaper. After apoptotic stimuli, the RHG proteins (Reaper, Hid and Grim) shift the caspases from DIAP1 and stimulate auto-ubiquitylation and proteasomal degradation of DIAP1. Consequently, Dronc binds to Ark for apoptosome formation leading to activation of Dcp-1 and DrICE for cell death induction (Xu et al. 2009). P35 inhibits Dcp-1 and DrICE.

Thus, although an initial contribution of dying cells cannot be discarded, it is unlikely that the dying cells provide the sole source of regenerative signalling.

Injury-induced apoptotic signals are required to maintain tissue homeostasis. For example, when cells of the *Drosophila* midgut are damaged, intestinal enterocytes secrete the cytokine Upd, which stimulates proliferation of intestinal stem cells through activation of the JAK/STAT pathway (Jiang et al. 2009). Moreover, as mentioned before, wing discs can produce appropriately sized adult wings after irradiation-induced cell death of over 50% of the cells, thus apoptosis must provide several signals that can regulate wound healing and regeneration (Haynie & Bryant 1977). This would ensure quick replacement of dead cells. However, the diffusion of these signals may be temporary and may happen in the period of cell death.

To make easy the study of signals released by dying cells, many laboratories used the strategy of the baculovirus p35 protein. It consisted on the activation of pro-apoptotic genes together with the p35, which prevents the completion of cell death by blocking effector caspases. Therefore, apoptotic cells can be maintained in an **"undead" state**. In this situation, these authors found that non-autonomous proliferation increases in compartments containing undead cells, leading to the formation of tumour-like overgrowths (Huh et al. 2004; Perez-Garijo et al. 2004; Ryoo et al. 2004). They observed that undead cells release mitogenic signals such as Dpp and Wg to promote proliferation (Perez-Garijo et al. 2004; Fan & Bergmann 2008; Morata et al. 2011). After a certain time, it was shown that proliferation triggered by undead cells could still occur in compartments that were mutant for *wg*, *dpp* or both (Perez-Garijo et al. 2009). The authors thought that there was a side effect of the necessary activation of the JNK pathway (Shlevkov & Morata 2012; Morata et al. 2011). Currently, how apoptosis contribute to regeneration is still unclear.

Systemic aspects of regeneration

When fragmented discs were implanted into female adult hosts, even discs from early pupae were capable of regenerating after fragmentation (Lee & Gerhart 1973). However, after genetic ablation, the ability for **imaginal discs to regenerate decreases as they mature;** early L3 larvae regenerate efficiently, whereas mature L3 larvae cannot (Smith-Bolton et al. 2009). This loss of regenerative capacity correlates with an inability to upregulate the expression of genes necessaries for regeneration, such as *wg*. It is because the damage-responsive enhancer in the *wg* locus is epigenetically silenced, with a localized increase in H3K27 trimethylation in mature discs (Harris et al. 2016).

What is more, damage in imaginal disc influences on the physiology of the whole larva (Hussey et al. 1927; Poodry & Woods 1990; Simpson et al. 1980). Early studies demonstrated that in the whole larvae there was a **delay in pupariation** in response to X-rays (Hussey et al. 1927) or after damage in imaginal discs (Simpson et al. 1980). This developmental delay is also observed when imaginal discs are damaged using genetic methods (Smith-Bolton et al. 2009; Halme et al. 2010).

Previous studies have revealed a role for **retinoids** in mediating, at least in part, the delay in pupariation in injured imaginal discs. Developmental checkpoints extend larval growth after imaginal disc damage by inhibiting the transcription of the gene encoding prothoracicotropic hormone (PTTH), a neuropeptide that promotes the release of ecdysone. Inhibition of retinoids reduces the delay in pupariation, indicating that those molecules have a role in transmitting a signal from the damaged disc to the PTTH-producing neurons (Halme et al. 2010).

A key finding has been the discovery that **Dilp8**, a member of the insulin/relaxin superfamily, is secreted by imaginal discs to the haemolymph in response to growth perturbations to delay pupariation (Colombani et al. 2012; Garelli et al. 2012). Dilp8 expression is increased directly by JNK (Katsuyama et al. 2015; Colombani et al. 2012) and Yki (Boone et al. 2016), and indirectly by the chromatin modifier Trithorax (Trx) (Skinner et al. 2015). Once released, Dilp8 binds to the **Lgr3** receptor in a subset of neurons, which in turn, synapse with other ones that inhibit the synthesis of ecdysone in the prothoracic grand (PG), the hormone which mediates the developmental delay (Vallejo et al. 2015; Colombani et al. 2015; Garelli et al. 2015; Jaszczak et al. 2016). In addition, Lgr3 is expressed in the PG too, where activates the **Nitric Oxide Synthetase** (NOS), which is necessary to reduce growth of the unharmed discs while damaged tissues are repaired (Figure 13; Jaszczak et al. 2016; Jaszczak et al. 2015).

Finally, a key role for the immune system after tissue damage has been proposed. JNK activates the expression of JAK/STAT-activating cytokines, which are secreted from the injured discs to the haemolymph, amplifying the signal and inducing additional cytokine expression in the **haemocytes** and the **fat body**, resulting in haemocyte proliferation (Pastor-Pareja et al. 2008).

Towards a hypothesis on the onset of regeneration

Although in the last few years substantial improvements on the field have been made, several open questions remain without answer. All the previous works pointed that epithelia can detect damage to restore the missing tissue and that JNK has a key role in regeneration. But the mechanism to sense and initiate regenerative responses is still not known.

Many signals could count for the initiation of regeneration; Growth factors, mechanical forces or changes in cell polarity are all candidates for upstream activation of the regenerative program (Nelson et al. 2005; Igaki et al. 2006). Otherwise, calcium flashes have been found upon damage (Razzell et al. 2013), and propagated via gap junctions in imaginal discs (Narciso et al. 2015; Restrepo & Basler 2016). It has also been proposed that the release of intracellular ATP or calcium by damage or signals secreted by inflammatory cells recruited to the wound may participate in JNK activation (Kushida et al. 2001). In this work, we have focused on the role of **Reactive Oxygen Species** (henceforth **ROS**) for the initiation of imaginal disc regeneration.

Redox signalling as a candidate for triggering regeneration

Response to damage involve oxidative stress (Sen & Roy 2008; Veal et al. 2007) and subsequently, the activation of stress-activated protein kinases (SAPKs). The production of ROS has generally been considered as deleterious (**oxidative stress**) (Cross et al. 1987), but now is being appreciated as a group of highly reactive ions and molecules involved in the regulation of a wide variety of biological processes, what is known as **redox biology** (Figure 15; Finkel 2011; Bigarella et al. 2014). It appears early in evolution, thus even in prokaryotes, nature selected ROS as a signal transduction mechanism to allow for adaptation to changes in environmental nutrients and oxidative environment (Wood et al. 2003; Kiley & Storz 2004; Schieber & Chandel 2014). Key roles of ROS in host defense, regulation of normal an cancer cell proliferation, tissue regeneration, inflammation and aging have been described (reviewed in Gupta et al. 2012; Schieber & Chandel 2014). Moreover, recent works have identified that an oxygen burst is not only required to disinfect wounds and stimulate healing, but that redox signalling represent an essential component of the healing cascade in mammals (reviewed in Sen & Roy 2008).

ROS act as signalling molecules after wounding in mice (Loo et al. 2012), embryos, fin and heart of zebrafish (Yoo et al. 2012; Yoo et al. 2011; Wittmann et al. 2012; Gauron et al. 2013; Han et al. 2014; Niethammer et al. 2009), *Xenopus* tail (Love et al. 2013; Ferreira et al. 2016), gecko tail (Zhang et al. 2016), planarian head and tail (Pirotte et al. 2015) and *Hydra* (Wenger et al. 2014). In *Drosophila,* redox signalling have been linked to wounded embryos (Moreira et al. 2010) and to the differentiation of hematopoietic progenitors through JNK signalling (Owusu-Ansah & Banerjee 2009).

ROS are by-products of aerobic metabolism, protein folding and end-products of several metabolic reactions. Mitochondrial dysfunction and enhanced metabolism lead to ROS production, as it has been reported in cancer cells (Gupta et al. 2012). ROS are intracellular chemical species that are formed upon partial reduction of oxygen (O_2) (Table 3 and Figure 15). Each of them have inherent chemical properties that confer reactivity to different biological targets. One of the most studied ones is oxygen peroxide (H_2O_2), a non-polar molecule that can diffuse across membranes to relatively short distance. It is formed from cytosolic O_2^- by the enzymatic activity of Super Oxide Dismutase (SOD). H_2O_2 can activate signalling pathways to stimulate cell proliferation, differentiation, migration or apoptosis (reviewed in Veal et al. 2007).

The **sources of ROS** are both extracellular and intracellular. Exogenous ROS can be found as pollutants, tobacco, smoke, drugs, diet or radiation. Endogenous ROS are produced in mitochondria, peroxisomes, endoplasmic reticulum (ER) and NADPH oxidases (NOX) in the membranes (Figure 15; reviewed in Gupta et al. 2012; Schieber & Chandel 2014).

Under normal physiologic conditions, cells control ROS levels by balancing their generation and elimination by **scavenging systems** (Winterbourn 2008). On the one hand, non-enzymatic molecules which are in a reduced form ready-to-be oxidized, and on the other hand, a vast variety of enzymes with specialized catalytic mechanisms, cellular localizations and specific regulation (Table 3 and Figure 15). These enzymes can be secreted and even modulated by post-translational modifications, and play a critical role in signalling events (reviewed in Veal et al. 2007).

Reactive Oxygen Species		Antioxidant systems	
Radical ROS	**Non-radical ROS**	**Enzymatic**	**Non-enzymatic**
Superoxide **$O_2^{\cdot -}$**	Hydrogen Peroxide **H_2O_2**	Superoxide dismutase **SOD**	Glutathione **GSH**
Hydroxyl radical **·OH**	Singlet oxygen **$^1O_2$**	Catalase **CAT**	Glutaredoxin **Grx**
Nitric oxide **NO·**	Ozone (trioxygen) **O_3**	Glutathione Peroxidase **GPx**	Thioredoxin **Trx**
Organic radical **R·**	Organic hydroperoxide	Glutathione Reductase **GR**	Peroxiredoxin **Prx**
Peroxyl radical **ROO·**	**ROOH**	Glutathione S-transferase **GST**	Sulfiredoxin **Srx**
Alkoxyl radical **RO·**	Hypochlorous acid **HOCl**	Thioredoxin peroxidase **TrxPx**	Phytochemicals
Thiyl radical **RS·**	Peroxynitrite **$ONOO^-$**	Thioredoxin reductase **TrxR**	Vitamins A,C, E
Sulphonyl radical **ROS·**			Ceruloplasmin
Thiyl peroxyl radical **RSOO·**			

Table 3. List of main Reactive Oxygen Species and antioxidant systems in living organisms. Roughly, there are two types of ROS: the free oxygen radical and the non-radical. Whereas the free oxygen radical ROS contain one or more unpaired electron in their outer molecular orbital, the non-radical ROS lack unpaired electrons but are chemically reactive and can be converted into radical ROS. Intracellular levels of ROS are maintained by a set of antioxidants that can be both enzymatic and non-enzymatic in nature (reviewed in Gupta et al. 2012).

The **susceptibility of proteins to react with ROS** depends on several factors; The generation site, ROS levels, the proximity to antioxidants, the localization or the membrane composition, because the lipid diffusion capacity and the channels could influence how ROS circulate through the membranes. Also, the availability of these molecules, the chemical stability and the pH in the cytoplasm, which can modify the chemical properties of these species (Reczek & Chandel 2015).

Redox signalling can account for several mechanisms. For example, ROS can promote the **oxidation of Cysteine** residues within proteins. This mechanism has been shown for a number of transcription factors, kinases, protein phosphatases and matrix metalloproteases (Meng et al. 2002; Lee et al. 2002; Kamata et al. 2005; Nadeau et al. 2007; Marinho et al. 2014; Nelson & Melendez 2004). Moreover, while kinases usually are activated by ROS, phosphatases are inactivated (Rhee et al. 2000; Rhee 2006).

Another mechanism is that ROS may modify gene expression by mediating **epigenetic changes** and changes in chromatin structure (reviewed in Kreuz & Fischle 2016). DNA could be sensitive to oxidation and methylation too (Clark et al. 2012). Moreover, many **enhancers** are controlled

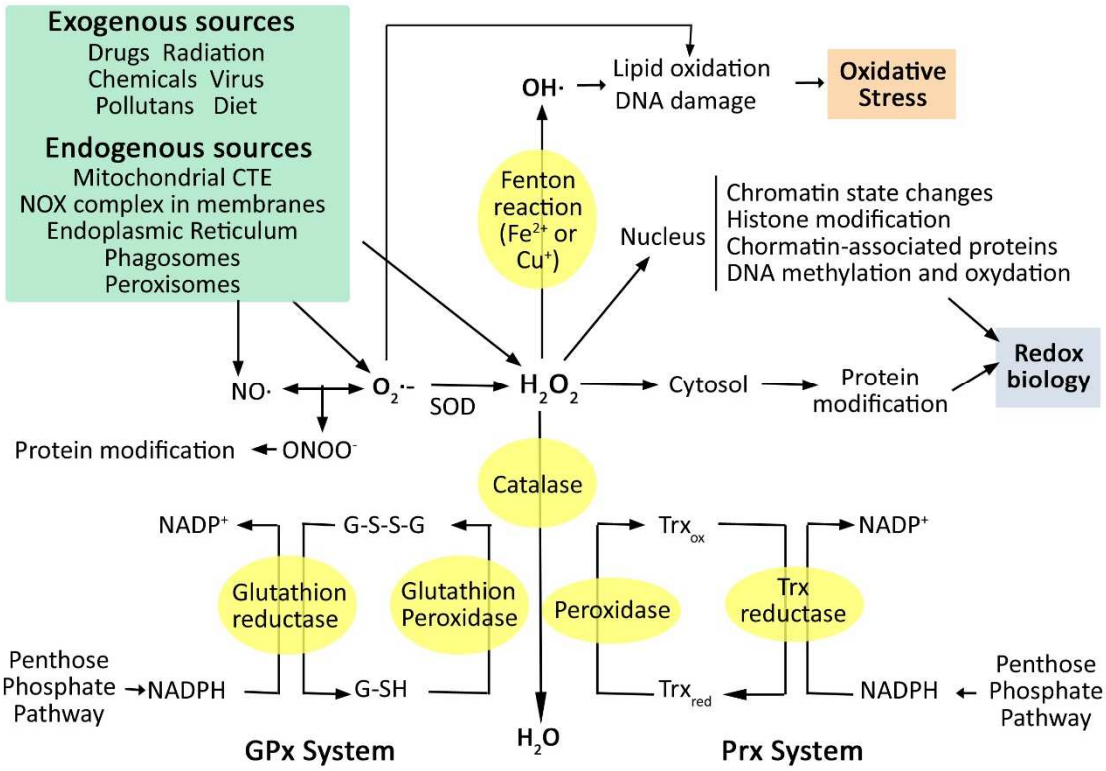

Figure 15. Mechanisms of ROS signalling. ROS can be produced by exogenous and endogenous sources. Many types of ROS can be formed; One of the most deleterious is the hydroxyl radical (**OH·**), which promotes damage and genomic instability (Dizdaroglu & Jaruga 2012). Superoxide (**O_2·-**) is often associated with oxidative stress, but is involved in redox signalling too (Fridovich 1997; Chen et al. 2009). It is converted to **H_2O_2** by the Superoxide Dismutase (**SOD**) (Fridovich 1997). H_2O_2 is one of the most studied signalling molecules. It is produced by mitochondria and NAPDH oxidases in the membrane (NOX) (Lambeth 2004; Brand 2010). It can modify cytosolic proteins or can go to the nucleus and trigger epigenetic changes. H_2O_2 can be converted into water by **Catalase**. To maintain homeostasis, the most relevant antioxidant systems inside the cell are the Peroxidase system (**Prx**), which involves Peroxidase and Thioredoxin reductase enzymes, and Glutathione Peroxidase system (**GPx**). Both achieve its reduced state thanks to the NADPH provided by the Pentose Phosphate Pathway (Veal et al. 2007).

by ROS signalling, as well as epigenetic changes, not only the epigenetic marks but also the chromatin remodellers and associated proteins (reviewed in Kreuz & Fischle 2016).

Mitogen activated protein kinases (MAPKs) in regeneration: P38 and JNK signalling pathways

Mitogen-activated protein kinases (**MAPKs**) are essential molecules that link environmental variations to modify gene expression and intracellular changes. In eukaryotes, ranging from unicellular organisms to mammals, MAPKs and their corresponding phosphatases represent a huge group of evolutionarily conserved enzymes. They are divided into three major groups: the extracellular regulated kinase (ERK) group, the p38 and the JNK group (Hunter 1995; Alonso et al. 2004).

The core MAPK module includes three kinases, firstly a **MAPKKK** (MAPK kinase kinase), and secondly a Ser/Thr kinase that phosphorylates and activates a **MAPKK** (MAPK kinase), which has dual specificity. It phosphorylates a TXY motif in the target requisite MAPK, and thirdly the **MAPK** proper, whose targets are typically transcription factors, but include cytoskeleton associated proteins and other kinases as well. Once triggered, signalling events lead to cellular changes and modification of gene expression, coordinating processes as cellular differentiation, proliferation, apoptosis, stress responses and morphogenesis (Widmann et al. 1999; Raman et al. 2007). This kind of regulation allows for specific and immediate changes in the activity of the module. In *Drosophila*, the three MAPK pathways are well-characterized, with little or no redundancy.

The **Jun-N-terminal Kinase pathway** (**JNK**) has an ancient function as stress mediator, but it has been evolved to develop roles in development, without leaving its original purpose. In flies, it is required for embryonic dorsal closure, follicle cell morphogenesis, pupal thoracic closure and male genitalia disc rotation/closure, all processes with requisite cell shape changes (reviewed in Ríos-Barrera & Riesgo-Escovar 2013). In addition, The JNK pathway has emerged as an early response to cell death and physical damage and appears to play a critical role in proliferation after massive cell death, regeneration and wound healing (Ryoo et al. 2004; Bosch et al. 2005; Bosch et al. 2008; Bergantiños et al. 2010; Smith-Bolton et al. 2009; Mattila et al. 2005; Lee et al. 2005; Fan et al. 2014; Pastor-Pareja et al. 2008). The core of the pathway is depicted in Figure 16. However, little is known about how JNK is triggered in injured imaginal discs, hence we assume that ROS are good candidates.

In mammals, activation of JNK occurs at the edges of wounds, in cells that covering the exposed wound surface during healing. In fact, in mammalian cell lines, ROS are known to act as second messengers to activate diverse redox-sensitive signalling transduction cascades, including the stress-activated protein kinases (SAPKs) p38 and JNK (Droge 2002; McCubrey et al. 2006; Jiang et al. 2011). Indeed, mammalian JNK is activated by hydrogen peroxide via direct oxidation and inactivation of the MAPK phosphatase (Kamata et al. 2005) and by peroxide-induced dissociation of the kinase inhibitor GSTpi (Adler et al. 1999). In *Drosophila*,

Paraquat treatment has been classically used to induce excessive oxidative stress, and activates JNK as well (Chatterjee & Bohmann 2012).

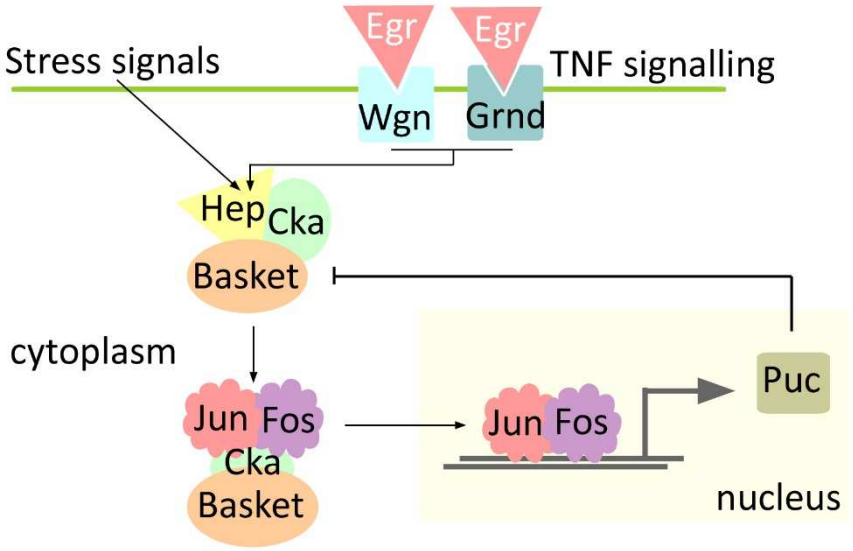

Figure 16. Core of JNK pathway in *Drosophila* after stress stimulus. **Hemipterous** (Hep/JNKK) (Glise et al. 1995) is the mediator between MAPKKKs and **Basket** (Bsk) activation. Hep phosphorylates Bsk (Riesgo-Escovar et al. 1996), the fly JNK homolog, which in turn phosphorylates the **Jun**/Jra transcription factor. This phosphorylation triggers Jun association with **Fos**/Kayak to form the **AP-1** complex (Bogoyevitch & Kobe 2006). **Cka** (Connector of Kinase to AP-1) (Perrimon et al. 1996) is a scaffold molecule thought to form a complex with Hep, Bsk, and AP-1, but how this occurs is not clear. AP-1 complex goes into the nucleus and promotes transcriptional activation of many genes. Among them, ***puckered*** (*puc*) (Martín-Blanco et al. 1998b), which encodes for a dual specificity phosphatase, that turns off the activity of the pathway by dephosphorylating Bsk. Other target genes include cytoskeletal genes, like integrins, matrix metalloproteinases, and stress-related proteins. TNF signaling has been described as upstream molecules of JNK. In *Drosophila*, the **TNF/Eiger** ligand (Igaki et al. 2002; Moreno et al. 2002) has two receptors described, **Wengen** (Wgn) (Kanda et al. 2002) and **Grindelwald** (Grnd) (Andersen et al. 2015). Both can activate the JNK pathway.

We hypothesize that other molecules than ROS could manage JNK activation following damage. An example is the Tumour necrosis factor (TNF), which is an upstream molecule of the JNK pathway. *Drosophila* has a single orthologue of the TNF, called ***eiger*** (*egr*) (Igaki et al. 2002; Moreno et al. 2002). Egr is a membrane protein present in cells as a zymogen. To be activated, it needs to be cleaved and bind to its receptors **Wengen** (Wgn) (Kanda et al. 2002) and/or **Grindelwald** (Grnd) (Andersen et al. 2015) to activate JNK. It has been shown that overexpression of Egr leads to JNK activation and massive cell death in the eye imaginal disc (Igaki et al. 2002; Moreno et al. 2002). JNK activation leads to the expression of stress responsive genes, some pro-apoptotic genes, cytoskeletal and signalling components (Jasper et al. 2001). After the ectopic expression of Egr, a 'non-canonical' JNK pathway was described, and include members from TAB2, CYLD, TRAF1/4 (Tumour necrosis factor receptor associated factor 1/4) to TAK1 (JNKKK/ TGF-β activated kinase 1) (Geuking et al. 2009; Geuking et al. 2005; Xue et al. 2007; Cha et al. 2003). This 'non-canonical' pathway is not required for development. Of note, ectopic expression of TAK1, activates Imd and p38 pathways (Vidal et al. 2001; Geuking et al. 2009).

Thus, we theorized here that the activation of JNK could be ROS-dependent and/or activated by TNF signalling after injury. After that, JNK would be in some way propagated in nearby surviving tissue where beneficial low levels of JNK promote *upd* expression, a family of cytokines linked to the human interleukin-6, which are necessaries for hyperproliferation in *Drosophila* tumours and for wound healing (Álvarez-Fernández et al. 2015; Jiang et al. 2009; Wu et al. 2010; Pastor-Pareja et al. 2008). Upd cytokines are the ligands of **JAK/STAT signalling** (Figure 17).

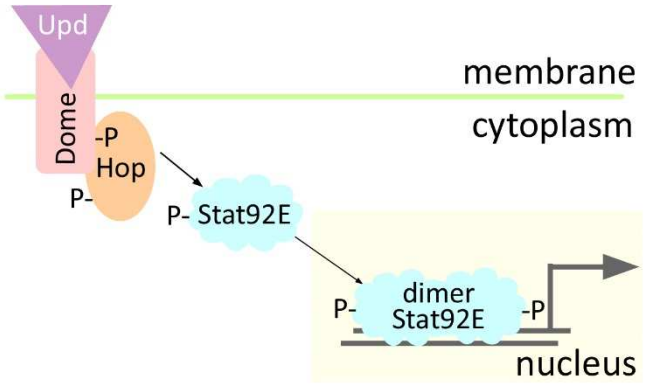

Figure 17. JAK/STAT pathway in *Drosophila*. There are three **Unpaired** ligands, Unpaired (Upd), Upd2 and Upd3 (Gilbert et al. 2005; Harrison et al. 1998; Hombría et al. 2005; Wang et al. 2014). When secreted, they bind to the receptor Domeless (**Dome**) (Brown et al. 2001), resulting in the activation of the receptor-associated JAK, Hopscotch (**Hop**) (Binari & Perrimon 1994). Then, Hop phosphorylates itself and the associated Dome receptor generating docking sites for the SH2 domains of the transcription factor **STAT92E** (Hou et al. 1996; Yan et al. 1996). Once phosphorylated, STAT92E forms dimers and translocate to the nucleus to activate transcription of its target genes.

The conserved **p38 MAPK pathway** is activated in response to different environmental stimuli and stress, and is involved in a diversity of biological processes, including cell proliferation, stress tolerance, immune response, and apoptosis or senescence (Seisenbacher et al. 2011; Craig et al. 2004; Cuadrado & Nebreda 2010). In *Drosophila*, p38 kinase is activated via dual phosphorylation at the Thr-Gly-Tyr motif by a specific MAPKK, **Licorne** (Lic) (Figure 18; Suzanne et al. 1999). Upstream kinases have been proposed to activate the p38 MAPK pathway, including Mekk1, TAK1, Apoptotic signal regulating kinase 1 (ASK1), and Slipper (Slpr) (Inoue et al. 2001; Chen et al. 2010). The *Drosophila* genome encodes three **p38 kinases** named p38a, p38b, and p38c, which do not act redundantly (Figure 18). While p38a regulates stress and the DUOX system in the midgut, p38b is suggested to play a vital role in p38 signalling and p38c may have specific functions in the intestine (Craig et al. 2004; Seisenbacher et al. 2011; Vrailas-Mortimer et al. 2011).

ROS-mediated p38 activation occurs in the course of the inflammatory response in rats (Jia et al. 2007), during the loss of self-renewal and differentiation in glioma-initiating cells (Sato et al. 2014) and to limit the life span of mouse hematopoietic stem cells (Ito et al. 2006). Both p38 and JNK are differentially required during repair. In endothelial cells, TNF-α stimulates repair through the positive action of JNK and negative regulation of p38 (Kanaji et al. 2013), although in corneal repair, p38, and not JNK, is required for epithelial migration (Sharma et al. 2003). In

Drosophila, both MAPK have been associated with stress responses (Karkali & Panayotou 2012).

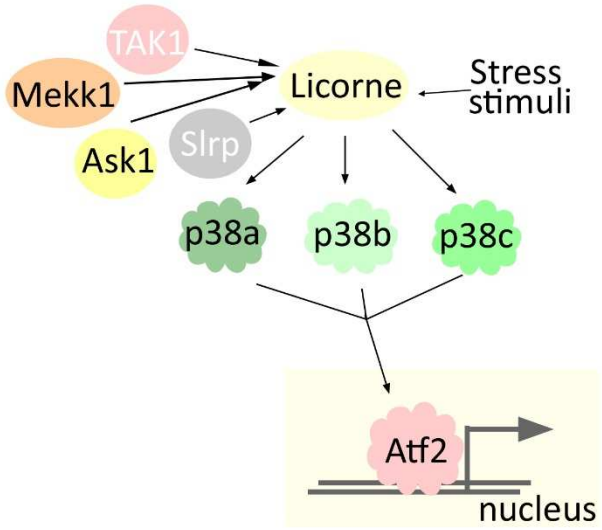

Figure 18. p38 pathway in *Drosophila*. Many stress stimuli are thought to activate **Licorne**, as UV light, heat shock, changes in osmolarity or peptidoglycan (PGN). Indeed, upstream kinases act as activators as well (Ask1, TAK1, SLRP and Mekk1 among others). Licorne, in turn, activates **p38a**, **p38b** and **p38c**, in a context-specific fashion. Those kinases phosphorylate transcription factors as **Atf2** (Activating transcription factor 2), which go to the nucleus and promote the transcriptional response.

Apoptosis signal regulating kinase 1 (Ask1), the candidate to act as a ROS sensor

The **Apoptotic signal-regulating kinase 1** (**ASK1**) is a Serine/Threonine kinase that belongs to the MAPKKK family (Ichijo et al. 1997; Wang et al. 1996). In response to various stresses, it phosphorylates MAPK kinases in JNK and p38 pathways, inducing cellular stress responses (Figure 19). It has long been suggested that ASK1 is highly sensitive to oxidative stress and contributes substantially to apoptosis. Constitutively active ASK1 induces cell death, mainly through mitochondria-dependent caspase activation (Hatai et al. 2000; Kanamoto et al. 2000; Saitoh et al. 1998). In *Drosophila*, *reaper* activates Ask1 and JNK and induce cell death (Kuranaga et al. 2002). However, recent studies have revealed that ASK1 has pleiotropic roles through other mechanisms in addition to apoptosis, such as proliferation, determination of cell fate, differentiation, survival and immune responses (Takeda et al. 2000; Sayama et al. 2001; Rubiolo et al. 2006; Sakauchi et al. 2017).

Mammals have three members of ASK1 family, ASK1, ASK2 and ASK3 (Tobiume et al. 1997; Takeda et al. 2006; Kaji et al. 2010). NSY-1 and *Drosophila* Ask1 are the single orthologues of mammalian ASK1 in *C. elegans* and *Drosophila* and are considered prototypic molecules of ASK family (Sagasti et al. 2001; Kuranaga et al. 2002).

The activity of this protein is tightly **regulated by redox signalling**. In a reduced environment Thioredoxin (Trx) is bound to ASK1, thereby blocking its activity. But upon oxidative stress the redox sensitive Cysteines of Trx are oxidized, which allow the dissociation of Trx from ASK1. As a consequence ASK1 oligomerizes and the kinase domain becomes phosphorylated (Saitoh et al. 1998; Liu et al. 2000). After that, TNF receptor associated factor 2 (TRAF2) and TRAF6 are recruited to the ASK1 complex and activate JNK and p38 pathways in mammals (Figure 19; Fujino et al. 2007; Nishitoh et al. 1998).

Moreover, **Ask1-interacting proteins** can modulate its activity, promoting conformational changes which will lead to various cellular responses. Many Ask1 positive and negative regulators were described (reviewed in Takeda et al. 2008; Sakauchi et al. 2017). For example **AKT**, which is a kinase activated by PI3K pathway in response to insulin receptor activation, phosphorylates Ask1 and decrease its activity (Kim et al. 2001). It is relevant because ROS produced by endogenous sources can also enhance cell proliferation through **PI3K pathway**, which components have been highly conserved through evolution, playing an crucial role in regulation of growth as well as modulation of central neuroendocrine pathways in response to nutrient availability (reviewed in Nässel & Broeck 2016).

***Drosophila* Ask1** protein locus has two possible transcripts isoforms encoding two different length peptides, **Ask1-RB** and **Ask1-RC**. Both have a protein kinase-like domain which presents a highly-conserved core of threonines (henceforth Thr-rich domain) and is responsible for the functional activation of the protein. After Trx release, the Ask1 oligomer undergoes conformational change leading to trans-autophosphorylation of the threonine residues corresponding to Thr838 in human ASK1 (Thr845, Thr806, Thr747 and Thr825 of mouse, human ASK2, *Drosophila* Ask1 and *C.elegans* NSY-1, respectively) (reviewed in Takeda et al. 2008). In *Drosophila,* Ask1 was found upstream of JNK and p38 in many contexts (Takeda et al. 2008), thus seems to be a good candidate to sense ROS and trigger the regenerative response in imaginal discs.

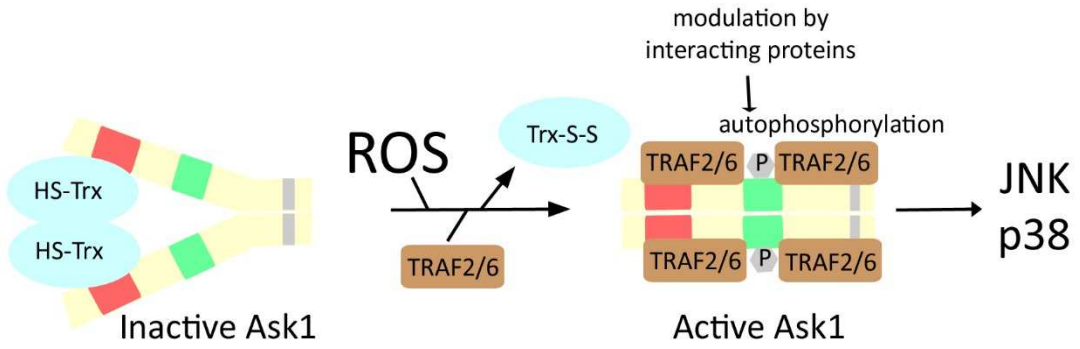

Figure 19. Ask1 activation is ROS-dependent. Ask1 is activated in a ROS-dependent fashion. In normal conditions, Thioredoxin (Trx) is bound to Ask1 in the cytoplasm, thereby blocking its activity. But upon ROS signaling, Trx is released and Ask1 is autophosphorylated in the Thr-rich domain. After that, Ask1 can recruit TRAF factors and activate JNK and p38 pathways. Besides that, Ask1 can be modulated positively or negatively by many interacting proteins (Sakauchi et al. 2017; Takeda et al. 2008).

OBJECTIVES

Many evolutionary conserved molecules are being thought to be implicated in imaginal disc regeneration, but how this process is initiated is still unknown. We wondered if ROS are candidate upstream molecules that initiate the regenerative program and if there is a sensor coupling oxidative changes and the stress-activated machinery. For that, we have proposed three main goals:

1. Describe the **first signals** which trigger regeneration in imaginal discs after injury or cell death. To this aim, we have accomplished the following objectives:

    - Test if Reactive Oxygen Species have an active role in wound healing and regenerative growth.
    - Set up the combination of two binary expression systems (LexA/LexO and Gal4/UAS) to determine what kind of cells are involved in regenerative response.
    - Characterize the function of p38 and JNK as response to ROS.

2. Determine if during the initiation of regeneration, the ROS-dependent MAPK signalling trigger the JAK/STAT pathway.

3. Define the **genetic mechanisms** by which regeneration is controlled.

    - Analyse the role of Apoptosis signal regulating kinase 1 (Ask1) as a ROS sensor and as a coupling mechanism between oxidation an MAPK signalling.
    - Decipher if PI3K pathway controls Ask1 besides growth.

MATERIALS AND METHODS

Drosophila strains

Fly strains utilized in this work were maintained in temperature-controlled chambers at 17 and 25 degrees. They were fed with the standard fly food (Table 4).

Ingredient	Quantity per litre
Distilled water	1 L
Yeast	64 g
Dextrose	67,2 g
Agar	8,8 g
Flour	40 g
Nipagin (methyl p-hydroxibenzoate)	1,6 g
Propionic Acid	5 ml

Table 4. Composition of Standard fly food. In the left column ingredients are detailed and in the right the quantity of each one for 1L.

The *Drosophila* strains used in this work and their origin are depicted in table 5:

Stock	Origin
ptc-Gal4	Hinz et al. 1994
tub-Gal80^{TS}	McGuire et al. 2003
UAS-rpr	Wing et al. 1998
ci-Gal4	Martin & Morata 2006
nub-Gal4	Baena-Lopez & García-Bellido 2006
sal-Gal4	Barrio & de Celis 2004
sal$^{E/Pv}$-Gal4	Barrio & de Celis 2004
en-Gal4	Bloomington Stock Center
ap-Gal4	Bloomington Stock Center
p38b^{d27}	Cully et al. 2010
lic^{d13}	Cully et al. 2010
dATF2^{PB}	Seong et al. 2011a
p38a^{1}	Seisenbacher et al. 2011a
LexO-rCD2::GFP	Yagi et al. 2010
UAS-bsk^{DN}	Weber et al. 2000
TRE-DsRed.T4	Chatterjee & Bohmann 2012
puc-LacZ	Martín-Blanco et al. 1998
UAS-upd	Harrison et al. 1998
upd-Gal4	Dr. Douglas Harrison
10XSTAT92E-GFP	Bach et al. 2007
UAS-GFP	Bloomington Stock Center
UAS-myrtomato	Bloomington Stock Center
UAS-Sod.A	Bloomington Stock Center
UAS-Cat.A	Bloomington Stock Center
UAS-dome^{DN}	Bloomington Stock Center

UAS-Socs36E	Callus & Mathey-Prevot 2002
hop^{2}	Bloomington Stock Center
upd^{YM55}	Eberl et al. 1992
hop^{27}	Bloomington Stock Center
stat92e^{06346}	Bloomington Stock Center
stat92e^{397}	Hou et al. 1996
hep^{r75}	Glise et al. 1995
Canton S	Bloomington Stock Center
w^{118}	Bloomington Stock Center
sal$^{E/Pv}$*-LHG*	Santabárbara-Ruiz et al. 2015
LexO-rpr	Santabárbara-Ruiz et al. 2015
UAS-RNAi-atf2	Vienna Drosophila RNAi Center (VDRC)
UAS-RNAi-licorne	Vienna Drosophila RNAi Center (VDRC)
UAS-RNAi-p38b	Vienna Drosophila RNAi Center (VDRC)
UAS-RNAi-p38a	Vienna Drosophila RNAi Center (VDRC)
ask1^{MB06489}	Metaxakis et al. 2005
ask1^{M102915}	Venken et al. 2011
UAS-RNAi Ask1	Bloomington Stock Center - 35331
egr^{3}	Igaki et al. 2002
grnd^{minos}	Andersen et al. 2015
wgn^{KO}	Andersen et al. 2015
UAS-grnd^{extra}	Andersen et al. 2015
UAS-RNAi eiger	Vienna Drosophila RNAi Center (VDRC)
UAS-RNAi wgn	Vienna Drosophila RNAi Center (VDRC)
UAS-RNAi grnd	Vienna Drosophila RNAi Center (VDRC)
UAS-dp110^{DN}	Bloomington Stock Center - D954A
UAS-dp110^{CAAX}	Bloomington Stock Center - 25908
akt^{1}	Staveley et al. 1998
UAS-ecto-eiger	Moreno et al. 2002
UAS-RNAi DUOX	Bloomington Stock Center - 59037
Hml-Gal4 (A)	Bloomington Stock Center - 30139
Hml-Gal4 (B)	Bloomington Stock Center - 30141
hml^{MB01940}	Bloomington Stock Center - 23381
UAS-RNAi aqp	Bloomington Stock Center
UAS-RNAi inx1	Vienna Drosophila RNAi Center (VDRC)
UAS-RNAi inx2	Vienna Drosophila RNAi Center (VDRC)
pnt^{d88}	Gift from J. Casanovas
ras^{c40b}	Gift from G. Jiménez
rl^{1}	Gift from E. Hafen
top^{1}	Gift from E. Hafen

Table 5. List of *Drosophila* strains utilized in this work. The genotype is indicated in the left column and origin in the right one.

Bacterial strains

To manipulate plasmidic DNA we used *E. coli* DH5α competent cells (Invitrogen).

Plasmids utilized and generated

sal$^{E/Pv}$-LHG → The *sal$^{E/Pv}$-LHG* construct was created cutting the wing specific enhancer of *spalt*, *sal$^{E/Pv}$* (Barrio & de Celis 2004) from *pC4LacZ-Spalt$^{E/Pv}$* EcoRI/BamHI and cloning this fragment into the plasmid *attB-LHG* containing a *Gal80*-suppressible form of *LexA* transcriptional activator (*LHG*) (Yagi et al. 2010). *LHG* contains both the binding domain of *LexA* and the activator domain of *Gal4*, which is recognized by the inhibitor *Gal80^{TS}*.

LexO-rpr → The *LexO-rpr* strain was obtained subcloning the pro-apoptotic gene *reaper* (*rpr*) from *pOT2-rpr* (IP02529) EcoRI/XhoI in the *pLOTattB* plasmid (Lai & Lee 2006) carrying the *lexA* operator *LexO*.

***upd*-pOTB7** → *upd* full sequence cloned into pOTB7 plasmid (AT1366 of DGRC).

***upd3*-pOT2** →*upd3* full sequenced cloned into pOT2 plasmid (FI03911 of DGRC).

Antibodies and dyes

Primary antibodies used are indicated in Table 6:

Primary antibodies			
Antigen	**Host**	**Concentration**	**Origin**
P-p38	rabbit	1:50	Cell Signalling
P-Histone-H3	rabbit	1:1000	Millipore
P-Histone-H3	mouse	1:1000	Millipore
ß-Galactosidase	rabbit	1:1000	ICN Biochemicals
Upd	rabbit	1:800	Gift from Dr Harrison
Cleaved Caspase-3	rabbit	1:100	Millipore
Anti-Digoxigenin-POD	sheep	1:2000	Roche
Ask1 P-Ser83	rabbit	1:100	Santa Cruz Biotechnology sc-101633
Ask1 P-Thr845	rabbit	1:100	Santa Cruz Biotechnology sc-109911
Mmp1	rabbit	1:100	Cocktail of 3A6B4, 5H7B11, 3B8D12 (DSHB)
P-Akt (S473)	rabbit	1:100	Cell Signalling
Ci	rat	1:10	DSHB 2A1
En	mouse	1:20	DSHB 4D9

Table 6. List of Primary antibodies used. Characteristics of each antigen as host, concentration and origin are detailed.

Fluorescently labelled secondary antibodies were from Life Technologies and Jackson Immunochemicals. The working concentration was 1:200.

To label nuclei TO-PRO-3 and YO-PRO-1 (Life Technologies) were utilized.

For general ROS detection in vivo, we employed the CellROX Green Reagent (Life Technologies), which is an indicator of oxidative stress in living cells and the cell-permeant 2',7' dichlorodihydrofluorescein diacetate (H2DCFDA, Life Technologies) which upon oxidation is converted to the highly fluorescent 2',7'-dichlorofluorescein (DCF). For Superoxide detection, the MitoSOX™ Red mitochondrial superoxide indicator was used.

For calcium imaging, we utilized the Fluo-4 Calcium Imaging Kit (Thermofisher).

Methods to study regeneration

In vivo: Genetic ablation with *Gal4/UAS* system

To induce cell death in a particular domain of the wing disc, expression of the pro-apoptotic gene *rpr* (Yoo et al. 2002) was driven using the *Gal4/UAS* binary system (Brand & Perrimon 1993) in combination with a thermo-sensitive *Gal80* repressor (*Gal80^{TS}*), which blocks *Gal4* activity (Salmeron et al. 1990). At 17°C, *Gal80* is ubiquitously expressed and functional. In contrast, at 25-29°C, *Gal80^{TS}* is inactive (Zeidler et al. 2004), thus relieving the inhibition of *Gal4* and activating *rpr* expression (Figure 20 A). This method was previously described by Smith-Bolton et al. 2009, Bergantiños et al. 2010 and Repiso et al. 2013.

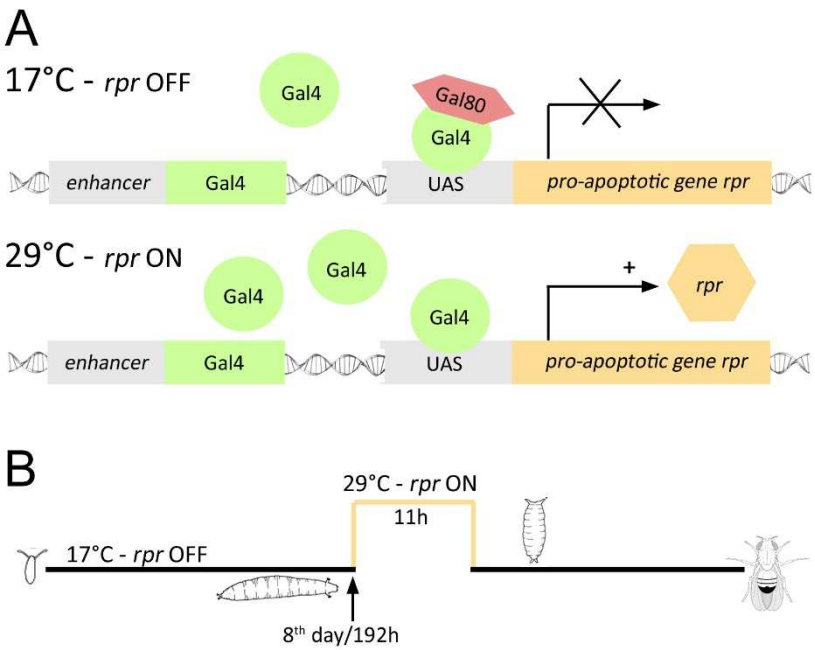

Figure 20. *In vivo* Genetic ablation with Gal/UAS system. (A) At 17°C, Gal80^{TS} is active and blocks Gal4 activity. However, at 25°C Gal80^{TS} is inactive and Gal4 can bind to UAS sequences and promote *rpr* expression to induce cell death. (B) Scheme that shows the time course of cell death and regeneration. Cell death starts the 8th day when larvae are transferred to 29°C for 11 hours. Then they are shifted back to 17°C to allow tissue recovery.

We used two different drivers to induce cell death; the first, *ptc-Gal4*, which is expressed in a narrow stripe in the centre of the disc (Figure 21). This strain was used to induce cell death in imaginal discs (*ptc>rpr*), because the dead domain can be easily discerned from the neighbouring living domain. The second, *sal$^{E/Pv}$-Gal4* strain, which consists of *spalt* wing enhancer with expression confined to the wing (Barrio & de Celis 2004), has been used in this work to score adult wing parameters as well as imaginal disc analysis (*sal$^{E/Pv}$>rpr)*. We also used the *sal$^{E/Pv}$-LHG* and *LexO-rpr* strains for genetic ablation using the same design as for Gal4/UAS. Freshly laid eggs were kept at 17°C to prevent *rpr* expression. The 8th day/192 h after egg

laying (equivalent to 96 hours at 25°C) were subsequently moved to 29°C for 11 hours and then back to 17°C to allow tissue regeneration (Figure 20 B). Controls without *rpr* expression were always treated in parallel. In dual transactivation experiments, we used the *sal$^{E/Pv}$-LHG LexO-rpr* to ablate the *sal$^{E/Pv}$* domain, whereas the *Gal4* was used to express different transgenes under the control of *nub-Gal4*, *ci-Gal4* or *ap-Gal4*.

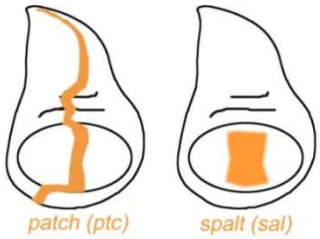

Figure 21. Wing disc domains used for cell death induction. Left image shows the *patch* domain, whereas right picture indicates the *spalt* zone.

Ex vivo: Imaginal disc culture after physical injury

Wing discs were dissected from third instar larvae in Schneider's insect medium (Sigma-Aldrich) and a small fragment was removed very carefully with tungsten needles. Discs were cultured in Schneider's insect medium supplemented with 2% heat activated foetal calf serum, 2.5% fly extract and 5 µg/ml insulin, for different periods of time (from 1 to 10 hours) at 25°C (Figure 22). *Ex vivo* images were taken using a Leica SPE confocal microscope and processed with Fiji software.

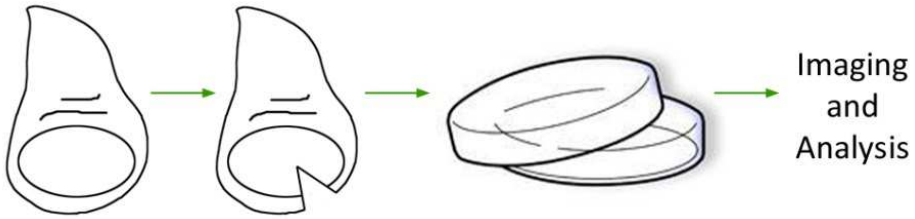

Figure 22. Design for physical injury and imaginal disc *ex vivo* culture. Discs are injured al cultured for different periods and then imaged and analysed.

Analysis of adult phenotypes and statistics

For testing the capacity to regenerate we used adult wings emerged from *sal$^{E/Pv}$>rpr* individuals, in which patterning defects can be easily scored (Figure 23). Flies were fixed in glycerol:ethanol (1:2) for 24 h and wings were dissected on water and then washed with ethanol. Then they were mounted on 6:5 lactic acid:ethanol and analysed and imaged under a microscope. We consider a non-regenerated wing when veins or interveins are absent, because they have lost the capacity to restore the normal pattern. Therefore, the % of regenerated wings was calculated after the number of wings with the complete set of veins and interveins. For each sample, we scored the percentage of individuals that belong to the "regenerated wings" class and calculated the standard error of sample proportion based on binomial distribution (regenerate complete wing or not) $SE=\sqrt{p}\ (1-p)/n$, where p is the proportion of successes in the population. Ratios between wing areas were used as an

indication of the size achieved after cell death for each genetic background, and consisted of a comparison between wing size with and without *rpr* induction.

Figure 23. *Spalt*$^{E/Pv}$ domain in wing imaginal discs and adult wings.

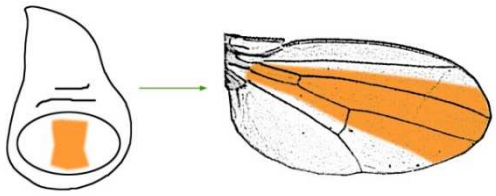

DNA analysis and manipulation

Transformation of competent cells

DH5α Competent cells (Invitrogen) were taken out of -80°C and thaw on ice approximately 30 minutes. Then DNA (usually 100 ng) was put into 50 µL of competent cells and gently mixed by flicking the bottom of the tube with the fingers a few times. After that the tube was transferred into a 42°C water bath and heat shocked 20 seconds, and then put back on ice for 2 minutes. Pre-warmed 950 µl LB media (without antibiotic) was added to the bacteria, which have grown in a 37°C shaking incubator for 1 hour. Finally, the transformation was spread into agar plates containing the appropriate antibiotic (in our case chloramphenicol and ampicillin).

Extraction of plasmidic DNA

Bacterial cells were cultured in LB medium containing the appropriate selective antibiotic for 12-16 hours at 37°C with vigorous shaking. To extract and purify the plasmidic DNA, we used the NZYTech's miniprep procedure, based on the alkaline lysis of bacterial cells followed by adsorption of DNA into silica in the presence of high salt.

Standard Polymerase Chain Reaction (PCR)

Standard PCRs were used for DNA amplification. All reaction components were assembled on ice and quickly transferring to a thermocycler preheated to the denaturation temperature (95°C) (Table 7 and Figure 24).

Template DNA	2µl (50-300ng)
10mM dNTPs	0.5µl
25mM $MgCl_2$	1.5µl
20mM Primer FW	1µl
20mM Primer RV	1µl
5X Taq Reaction Buffer	4µl
Taq polymerase	0.2µl
H_20	9.8µl
Total volume	20µl

Table 7. List of components of a classical PCR reaction. Left column shows all components necessaries for standard PCRs, and right column indicates the quantity of each one for a final volume of 20µl.

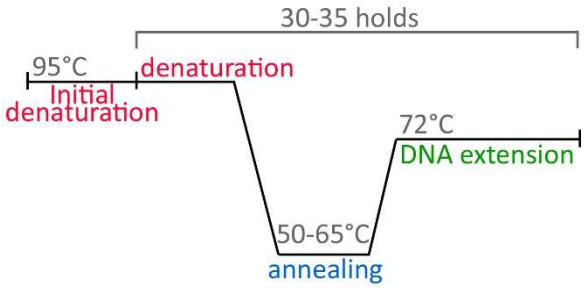

Figure 24. Thermocycling conditions for a routine PCR. The first step consisted on an initial denaturation, followed by 30 to 35 holds of denaturation, annealing and DNA extension. The lengh and temperature or each step depends on the polymerase, the primers and the fragment final size.

RNA analysis

Riboprobe synthesis for *In Situ* Hybridization

Riboprobes for *upd* and *upd3* were synthesized using cDNA clones from DGRC AT1366 (*upd*-pOTB7) and FI03911 (*upd3*-pOT2). They were isolated and purified with NZYMiniprep kit (NZYTech). For *upd* riboprobe, 10µg of plasmidic DNA were linearizing with MluI (sense) and BamHI (antisense) restriction enzymes. For *upd3,* XhoI (sense) and EcoRV (antisense) were utilized.

The resulted digestions were purified with Quiaquik PCR kit (Qiagen). For *in vitro* transcription, we used DNA polymerases SP6 (sense) and T7 (antisense), and dNTPs labelled with Digoxigenin (Dig RNA labelling mix Roche). The conditions were established according to the company.

Then samples were incubated with DNase (Zymo Research) to eliminate DNA. RNA was purified with the RNA Clean and Concentrator kit (Zymo Research). After that, the Digoxigenin-labelled riboprobes were hydrolysed with Carbonate Buffer 2X at 65°C for 40 minutes, and purified again.

Fluorescence *In Situ* Hybridization (FISH)

Wing imaginal discs were dissected and injured in Schneider's insect medium (Sigma-Aldrich). They were first fixed 20' in 4%FA/PBS 1X and second 20' in 4% FA/PBTween. Next they were washed 3 times in PBTween. Samples were progressively dehydrated in Ethanol and then they were frozen at -20°C. After that they were washed in Ethanol and fixed again 5' in 5% FA/PBS 1X and 20' in 5% FA. Immediately, discs were washed three times in PBTween.

The Pre-Hybridization step consisted on two incubations in Proteinase K to eliminate the remained proteins, two washes in Glycine, two more in PBTween and 20 minutes of fixation in 5% FA in PBTween, followed by the last three washes in PBTween.

Hybridization was carried out at 55°C. Discs were incubated 10' in PBTween/Solution A and then 1h in Solution A. After that discs hybridised overnight in a solution containing the riboprobe diluted 1:250 in Solution A.

The day after, samples were progressively washed in Solution B/PBTween at 55ºC. Then they were transferred at room temperature (RT) and washed again 4 times in PBTween. Subsequently, discs were incubated 30' in BSA and then 1h30' in the preadsorbed antibody

anti-Digoxigenin-POD diluted 1:2000 in BSA. Later they were washed four times in PBTween and two times in TNT. The detection reaction was carried out incubating samples 1h in Tyramide diluted in commercial buffer 1:50, in the dark.

Samples were finally washed several times in PBTween and mounted with SlowFade (Life Technologies) supplemented with 1µM TO-PRO-3 to label nuclei. All the Solutions used are summarized in table 8.

PBS 1X	125mM NaCl, 16mM Na_2HPO_4 and 8.4mM NaH_2PO_4, pH 7.3 diluted in miliQ water
FA 10%	1,37ml FA 36.5% and 8.63 ml PBTween
Proteinase K	5mg/ml Proteinase K solved in PBTween
Glycine	2mg/ml Glycine dissolved in PBTween
PBTween	PBS 1X and Tween20 0.1%.
Solution A	100µg/ml denatured herring sperm DNA and 50µg/ml heparin diluted in solution B
Solution B	50% Formamide, 5x SSC and 0.1% Tween20 diluted in miliQ water
TNT	0.05M MgCl2, 0.15M NaCl and 0.1M TrisHCl pH 7.5 diluted in miliQ water
BSA	2% BSA (without NaN_3) diluted in PBTween

Table 8. Solutions for Fluorescence *in situ* hybridization (FISH). Left column shows the name of the solution mentioned in the protocol and right column the composition of each one.

Protein analysis

Immunostaining of imaginal discs

Discs were dissected in Schneider's Insect medium and fixed for 30-60 minutes at RT in 4% PF. Then they were washed twice in PBS 1X, twice in PBT and incubated with Blocking Solution (BS) for 1 hour. After that the sample was transferred to a 4°C chamber and incubated with the primary antibody diluted in BS overnight.

The next day, discs were washed several times at RT and then incubated with the secondary antibody diluted in BS for 3 hours. Afterwards samples were washed three times in PBT and mounted in Slowfade (Life Technologies) supplemented with 1µM TO-PRO-3/YO-PRO-1 (Life Technologies) to label nuclei. Components necessaries for immunostaining are depicted in table 9.

4% PF	4% Formaldehyde diluted in PBS 1X
PBS 1X	125mM NaCl, 16mM Na_2HPO_4 and 8.4mM NaH_2PO_4, pH 7.3 diluted in miliQ water
PBT	0.3% TritonX-100 diluted in PBS 1X
Blocking solution	2% Bovine Serum Albumin and 0.05% NaN_3 diluted in PBT

Table 9. Solutions for immunostaining. Left column shows the name of the solution and right column indicates the composition of each one.

Apoptotic cell detection with TUNEL assay

After fixation and immunostaining of imaginal discs, apoptotic cells were detected using labelled dUTP ChromaTide® BODIPY® FL-14- or Alexa Fluor® 647-aha-dUTP (Life Technologies) and the Terminal deoxynucleotidyl transferase (TdT, Roche). The sample was incubated in the Reaction Mix (Table 10) for 1h 30' at 37°C. Then, EDTA was added to stop the reaction and discs were washed and mounted as explained in the immunostaining protocol.

Reaction Mix	5µl of $CoCl_2$, 10µl of 5X Buffer TdT, 1µl (24.5u) of TdT, 1.5µl of 10% TritonX-100, 0.5µl of ChromaTide BODIPY FL-14-dUTP/ Alexa Fluor® 647-aha-dUTP and 32µl of GIBCO water
EDTA	15 mM EDTA pH 8

Table 10. Composition of solutions for TUNEL assay. Note that the reaction mix is prepared just before use.

EdU incorporation

For 5-ethynyl-2'-deoxyuridine (EdU) incorporation into the sample, the Click-iT® EdU Imaging Kit (Life Technologies) was utilized. Imaginal discs were dissected after cell death induction and incubated in Schneider's insect medium supplemented with 1 mg/ml EdU (Life Technologies) for 5 minutes. Then they were fixed 20' in 4% PF, washed with BSA for 30' and permeabilized with PBT for 20'.

Subsequently discs were incubated with the Click-iT® EdU reaction cocktail for 30' to detect EdU and washed again with BSA. Following this step, discs were fixed and immunostained as explained before. Reagents for EdU detection are summarized in table 11.

4% PF	4% Formaldehyde diluted in PBS 1X
PBT	0.3% TritonX-100 diluted in PBS 1X
BSA	3% Bovine Serum Albumin diluted in PBT
Click-iT® EdU reaction cocktail	430 µl 1X Click-iT® reaction buffer, 20µl $CuSO_4$, 1.2µl Alexa Fluor® azide and 50 µl Reaction buffer additive

Table 11. Reagents for EdU detection with the Click-iT® EdU Imaging Kit. Note that the EdU reaction cocktail is prepared just before use.

Detection and modification of Reactive Oxidative Species in imaginal discs

ROS detection *ex vivo*

Experiments for ROS detection were done in living conditions. To detect the presence of general ROS we used two dyes. First, the CellROX Green Reagent (Life Technologies), which is an indicator of oxidative stress in living cells and second, the cell-permeant 2',7'-dichlorodihydrofluorescein diacetate (H2DCFDA, Life Technologies) which upon oxidation is converted to the highly fluorescent 2',7'-dichlorofluorescein (DCF). For Superoxide detection, the MitoSOX™ Red mitochondrial superoxide indicator was used.

Third instar discs were dissected in Schneider´s insect medium immediately after cell death or injury and incubated for 15 minutes in medium containing 5µM CellROX Green Reagent, 5µM H2DCFDA or 5 µM MitoSOX reagent, followed by three washes. Samples were protected from light throughout. Then they were mounted using culture medium supplemented with 1 µM TO-PRO-3 (Life Technologies) nucleic acid stain. As TO-PRO-3 only enters into dead cells, we used it to distinguish dead cells from living cells in the *ex vivo* experiments.

ROS scavenging *in vivo* and *ex vivo*

To prevent ROS production, we used two protocols. The first was mainly used for *rpr*-ablation discs. It consisted on antioxidant supplementation into standard fly food. As antioxidants, we used vitamin C (250 µg/ml), Trolox (an analog of vitamin E; 20 µg/ml) and N-acetyl cysteine (NAC) (100 µg/ml), all from Sigma-Aldrich.

To score adult wings, larvae were transferred from vials containing standard food to vials containing food with the desired antioxidant concentration. Antioxidant treatment was administered at 168 h of development at 17°C (equivalent to 84 h AEL at 25°C). After 24 hours, experimental larvae were moved to 29°C for 11 hours to promote *rpr* apoptosis (Figure 25 A). One control consisted on larvae maintained at 17°C and another control consisted on larvae transferred to a vial with standard food and moved to 29°C for the same period as in the experimental group. After *rpr* induction temperature was returned to 17°C to allow tissue recovery.

The second protocol was used for *ex vivo* cultured discs. Injured wing imaginal discs were incubated for 30 minutes in Schneider's insect medium supplemented with antioxidants (NAC 100 µg/ml, vitamin C 250 µg/ml or Trolox 20 µg/ml). Then, they were transferred to Schneider's containing 5µM CellROX Green (Figure 25 B) following the ROS detection protocol. After antioxidant incubation discs were also used for immunostaining as explained before.

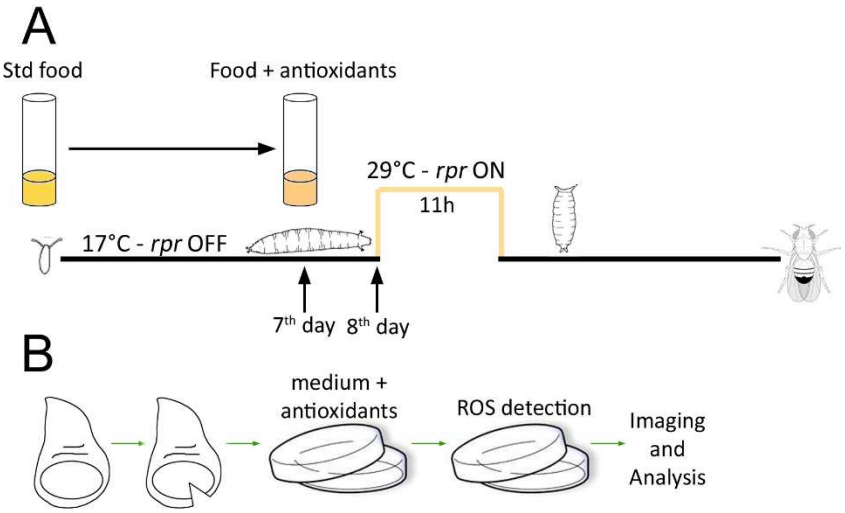

Figure 25. ROS scavenging in imaginal discs. (A) Design for ROS scavenging before genetic ablation. Larvae are transferred to a vial supplemented with antioxidants 24 hours before cell death induction. (B) Design for ROS scavenging in *ex vivo* culture. Discs are incubated for 30 minutes in medium supplemented with antioxidants and then with CellROX Green to monitor ROS production.

Oxidative stress induction

Third instar larvae were transferred to vials with 5mL of special medium containing 1,3% UltraPure™ LMP agarose (Invitrogen) 5% sucrose (Fluka) and the desired concentration of H_2O_2 0,1% and 1% (Merck) or Tunicamycin 1ng/µl (Sigma-Aldrich). To avoid loss of oxidative capacity, H_2O_2 was added at a temperature under 45°C. Larvae were fed for 2 h in this medium prior dissection and fixation of the discs. Controls without H_2O_2 were done in parallel.

Measurement of life span

Freshly emerged flies of both sexes were collected over a 24-h period and placed into plastic vials (20 flies/vial), males and females separately. Minimal food was composed by water, 1,3% UltraPure™ LMP agarose (Invitrogen) and 5% Sucrose (Fluka). H_2O_2-supplemented food contained also 0,1% H_2O_2 (Merck) and Tunicamycin-supplemented food contained 1µg/ml of Tunicamycin (Sigma-Aldrich). Survivorship was recorded daily and food was renewed twice a week. Five replicates were performed for each condition. For life span determination, we used the isogenic line w^{118} as a control and $ask1^{MB06489}$ and as experimental group. A scheme of this experiment is depicted in Figure 26.

For statistical analysis, the mean life span of each strain was calculated as the time (in days) at which survival reached 50% of the starting population. Survival data were analysed by stratified log rank tests, using Microsoft Excel.

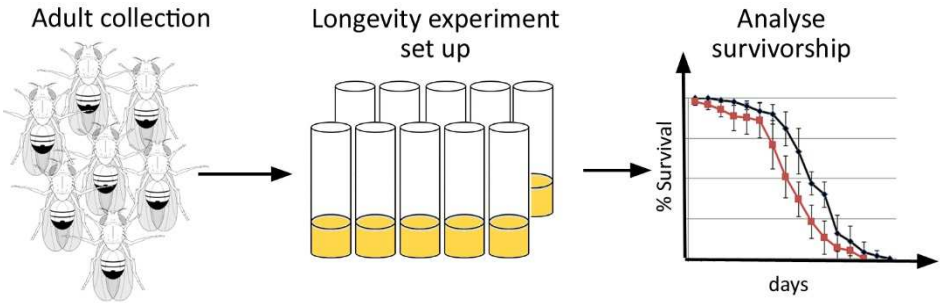

Figure 26. Analysis of the life span in *Drosophila* adults. Adults are collected and then survivorship is daily recorded.

Chemical inhibition of MAPK pathways

To prevent p38 activation the imidazole drug SB202190 (Sigma-Aldrich) was added into standard fly food. We used three different concentrations (0.12 µM, 1 µM and 5 µM), and DMSO as the control.

To inhibit chemically JNK we used the JNK Inhibitor IX (5 µM, Selleckchem) which is a thienylnaphthamide compound that is a selective and potent inhibitor of the ATP binding site of JNK. The timing and protocol followed to inhibit both pathways were the same as that to scavenge ROS (Figure 25).

Calcium imaging

To identify calcium signaling, we utilized the Fluo-4 Calcium imaging Kit (#F10489 Thermofisher), which displays high sensitivity and a large fluorescent increase upon calcium binding. Third instar discs were dissected in Schneider´s medium immediately after cell death or injury and incubated for 30 minutes in 1mL of Fresh Fluo-4 Solution (10µL Powerload 100X,1µL Fluo-4 1000X, 10µL Probencid 100X Stock Solution and 1mL Fresh Schneider's insect medium), followed by two washes.

Samples were protected from light throughout. Then they were mounted using culture medium supplemented with 1 µM TO-PRO3 (Life Technologies) nucleic acid stain. As nuclear markers only enter dead cells, we used it to distinguish dead from living cells.

Imaging

Confocal images were obtained with Leica SP2 and SPE confocal microscopes. Bright flied images were taken with Leica DMLB microscope. All pictures were processed with Fiji and Adobe® Photoshop software.

Bioinformatics

UCSC genome browser was used for gene analysis as well as for in silico PCRs.

RESULTS

CHAPTER I

ROS are produced after tissue damage

As the first signals to initiate regeneration must be extremely rapid and efficient, we first examined the production and propagation of ROS over time after tissue damage. To do that, we used CellROX Green, a cell-permeant fluorogenic probe that is non-fluorescent in the reduced state and exhibits bright fluorescence upon oxidation.

Immediately after cut (0-5') we found elevated levels of CellROX Green near the wound edges, thus the oxidative burst is rapidly occurring after damage. Few CellROX Green positive cells were labelled with TO-PRO-3 (dying cells), indicating that most ROS-producing cells were alive (Figure 27 A). After that**,** *ex vivo* imaging showed that fluorescence propagates to the neighbouring cells during the first 30' after damage (Figure 27 A).

We next monitored ROS production after controlled induction of cell death in the *patched* domain (*ptc>rpr* discs, Figure 27 B, C). Those discs show a stripe of apoptotic cells that eventually extrudes basally and is replaced apically by living cells (Figure 27 C; Bergantiños et al. 2010). CellROX Green was strongly incorporated into the apoptotic cells (TO-PRO-3 positive) (Figure 27 D) but also in adjacent living cells, albeit at much lower levels than in dead cells (Figure 27 D, E).

Equivalent results were obtained using 2',7'-dichlorodihydrofluorescein diacetate (H2DCFDA), a molecule which upon oxidation is converted to the highly fluorescent DCF. Both cut or *rpr*-ablated discs, showed important level of fluorescence on the wound edges, in the apoptotic cells and in the living cells near the apoptotic (Figure 27 F).

These results demonstrated that both physical injury and genetically induced apoptosis are insults that result in the production of ROS.

ROS are required for tissue repair

After finding an oxidative burst following death or damage we hypothesized that it could propagate from dying to living cells in sub-toxic doses and initiate repair. To explore this issue, we scavenged ROS production and examined adult wings after cell death.

We first checked whether antioxidants (Vitamin C, Trolox or N-acetyl cysteine [NAC]) were capable of blocking ROS production. To do that, we incubated cut discs in Schneider's medium containing antioxidants and detected strong reduction of CellROX Green fluorescence (Figure 28 A).

Next, we studied the effects of ROS scavenging on regeneration. For that we induced cell death with the $sal^{E/Pv}$-Gal4 driver which allows analysis in adult wings while not affecting the rest of the organism (henceforth $sal^{E/Pv}$*>rpr* discs). To deplete intracellular ROS, $sal^{E/Pv}$*>rpr* larvae were fed with food supplemented with antioxidants (Figure 28 B).

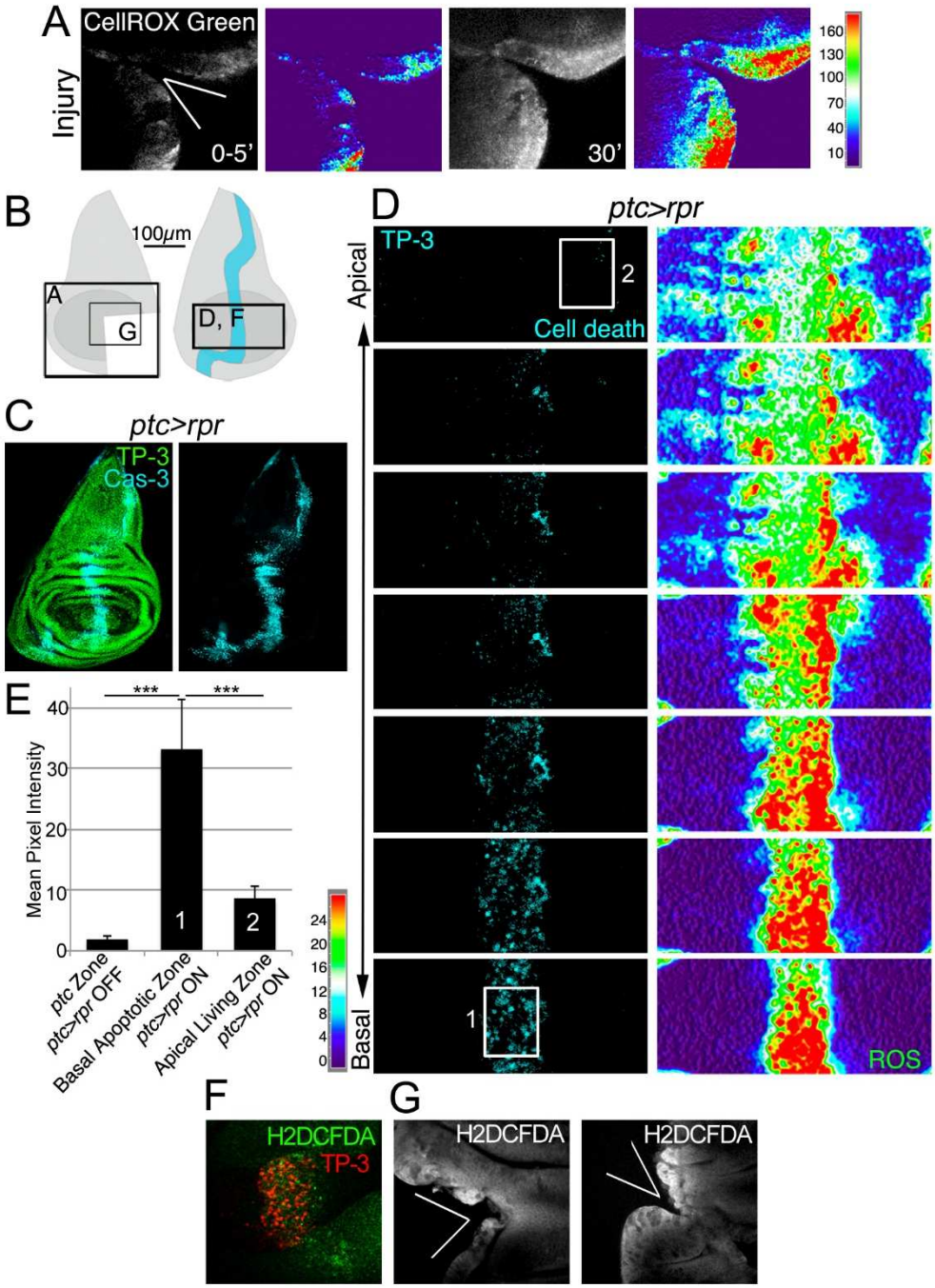

Figure 27. ROS are produced after physical injury and after cell death. (A) Cut disc cultured *ex vivo* (white wedge indicates cut edges) and thermal LUT of CellROX Green. Left image just after cut (0–5') and right image 30' later. Thermal scale indicates pixel intensity. (B) Sketch of wing imaginal discs with the area (black square) shown in A, D, F and G. (C) Fixed disc stained for nuclei to show disc contour (TP-3: TO-PRO-3) and Caspase-3 after *ptc>rpr* activation for 11h at 29°C. (D) *ptc>rpr* disc cultured *ex vivo*; basal images at the bottom, apical at the top. Left, cell death (TO-PRO-3). Right, thermal LUT taken from the ROS channel (CellROX Green) of the same preparation. (E) Mean pixel intensity (grey value) of the indicated zones in control discs without cell death (*ptc>rpr* OFF) and discs with cell death (*ptc>rpr* ON). The pixel intensity in the *ptc* domain in the absence of cell death (*ptc>rpr* OFF) was 1.76 ± 0.55 (SD; from 48 regions of interest [ROI] in n = 5 discs). The mean pixel intensity for the apoptotic region (basal; *ptc>rpr* ON) was 33.14±8.18 (SD), measured in 27 ROI on confocal images taken from n = 6 discs. Living cells adjacent to the apoptotic zone showed a mean grey value of 8.51±2.12 (SD; 15 ROI from 6 discs taken from cells near the *ptc* domain). White rectangles in D: Example ROI for Basal Apoptotic Zone (1) and Apical Living Zone (2). The ROI's for the *ptc* zone, in discs in which *ptc>rpr* is OFF, were placed as (1). ***P<0.001. Thermal scale indicates sample values from raw images. (F) ROS detected with H2DCFDA after *ptc>rpr*. ROS are found in dead cells and in adjacent living cells. TP-3: TO-PRO-3. (G) ROS detected with H2DCFDA after physical injury (white wedge).

ROS scavengers in *sal$^{E/Pv}$>rpr* controls kept at 17ºC to prevent cell death did not show any alteration of wing morphology (Figure 28 E). Conversely, a *sal$^{E/Pv}$>rpr* control group without scavengers moved to 29ºC for 11 h showed complete wing regeneration (Figure 28 C, D). However, the *sal$^{E/Pv}$>rpr* experimental group with ROS scavengers and induced cell death showed incomplete regeneration in about 50% of the cases (Figure 28 C, D).

Then we checked whether proliferation is impaired after ROS depletion. We counted the number of mitoses after cell death induction in discs from NAC-fed larvae and found a significant decrease compared to discs from larvae fed in the absence of antioxidants (Figure

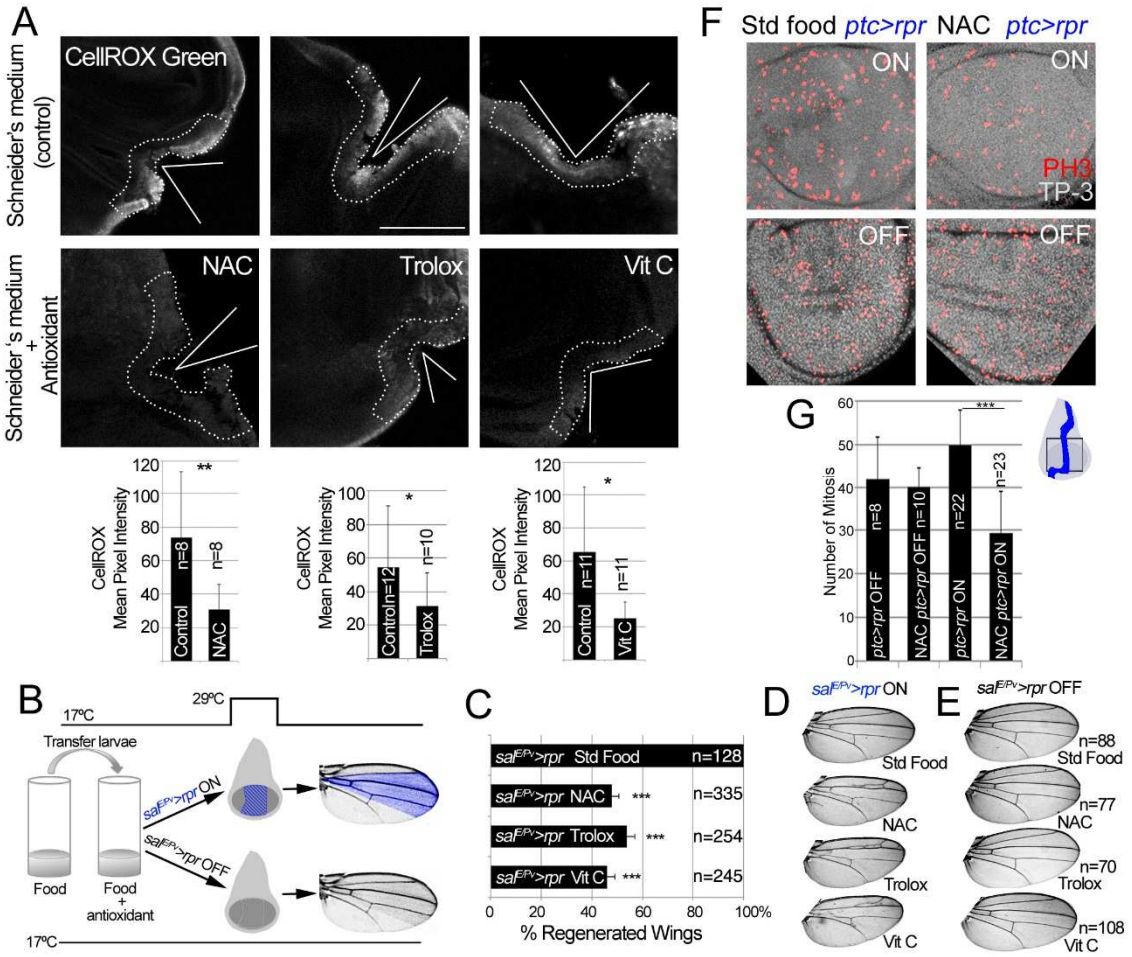

Figure 28. ROS are required for tissue repair. (A) *Ex vivo* analysis of cut imaginal discs cultured in Schneider's medium, incubated with NAC, Trolox or Vitamin C. Top row shows control discs (no antioxidant). Lower row shows discs incubated with the indicated antioxidant. Dotted lines indicate zones used as ROI for pixel intensity measurements (below). White wedges indicate the position of the cut. *P<0.05 **P<0.01. (B) Design for chemical antioxidant intake and cell death induction. At 17°C and 24 h before cell death, larvae were transferred to a vial with food supplemented with antioxidant. Cell death (*sal$^{E/Pv}$>rpr* ON) was induced by shifting temperature to 29°C for 11 h (blue zone in the disc). Then Larvae were moved to 17ºC where they regenerated and emerged into adults, in which wings were scored. Blue color in the wing: area emerged from *sal$^{E/Pv}$*. Controls *sal$^{E/Pv}$>rpr* OFF were kept at 17°C to avoid cell death. (C) Percentage of regenerated wings after cell death (*sal$^{E/Pv}$>rpr* ON) in Standard Food or in the presence of antioxidants (NAC, Trolox or Vitamin C). ***P<0.001. (D) Examples of *sal$^{E/Pv}$>rpr* ON wings with the indicated food supplement. In controls wings were completely recovered (Std Food). For each antioxidant, an example of incomplete regeneration after cell death induction is shown. (E) Examples of control wings kept at 17°C (*sal$^{E/Pv}$>rpr* OFF). (F) Mitosis in *ptc>rpr* discs from larvae fed with and without NAC and with or without *rpr*-ablation (ON versus OFF). Red dots labeled phospho-histone 3 (PH3) positive cells. Nuclei were labeled with TP-3: TO-PRO-3. (G) Mitosis number in *ptc>rpr* OFF: 41.86 ± 9.84 (S.D.); NAC *ptc>rpr* OFF: 39.9 ± 4.68 (S.D.); *ptc>rpr* ON: 49.73 ± 8.18 (S.D.); NAC *ptc>rpr* ON: 29.52 ± 9.41 (S.D.). ***P<0.001.

28 F, G). The number of mitoses in controls fed with or without antioxidants and kept at 17°C to block cell death did not vary (Figure 28 F, G).

In addition, we manipulated ROS enzymatically. Superoxide dismutase (**Sod**) catalyzes the dismutation of superoxide anion into oxygen and hydrogen peroxide. In the presence of hydrogen peroxide, Catalase (**Cat**) catalyzes its breakdown into water and oxygen. Thus, overexpression of Sod or Cat will remove their respective ROS substrates, whereas simultaneous activation of both will enhance the depletion of O_2^- and H_2O_2. *UAS-Sod*, *UAS-Cat* or *UAS-Sod:UAS-Cat* were ectopically expressed under the *nub-Gal4* driver, which operates throughout the wing pouch (Figure 29 A). To induce cell death we used a *sal$^{E/Pv}$-LHG* transgene, which includes a Gal80 suppressible form of LexA (Yagi et al. 2010), to conditionally express *lexO-rpr* in the *sal$^{E/Pv}$* domain. This combination permits control of the temporary expression of two binary systems (*sal$^{E/Pv}$-LHG lexO-rpr* and *nub-Gal4 UAS*-transgene) by *tubGal80^{TS}* (Figure 29 A). After *sal$^{E/Pv}$-LHG lexO-rpr* genetic ablation and *nub-Gal4 UAS*-transgene expression we allowed the larvae to develop to adulthood and found a drop in the number of regenerated wings (Figure 29 B, C). Controls kept at 17°C to prevent cell death did not show any alteration of wing morphology (Figure 29 D).

The NADPH oxidase **DUOX** acts as a source of H_2O_2. Only 75% of adult wings with DUOX inhibition in the anterior compartment and simultaneous cell death in *sal$^{E/Pv}$* domain could regenerate, which is consistent with previous results (Figure 29 E-H). Together, these results indicate that chemical and enzymatic ROS scavengers interfere with regeneration.

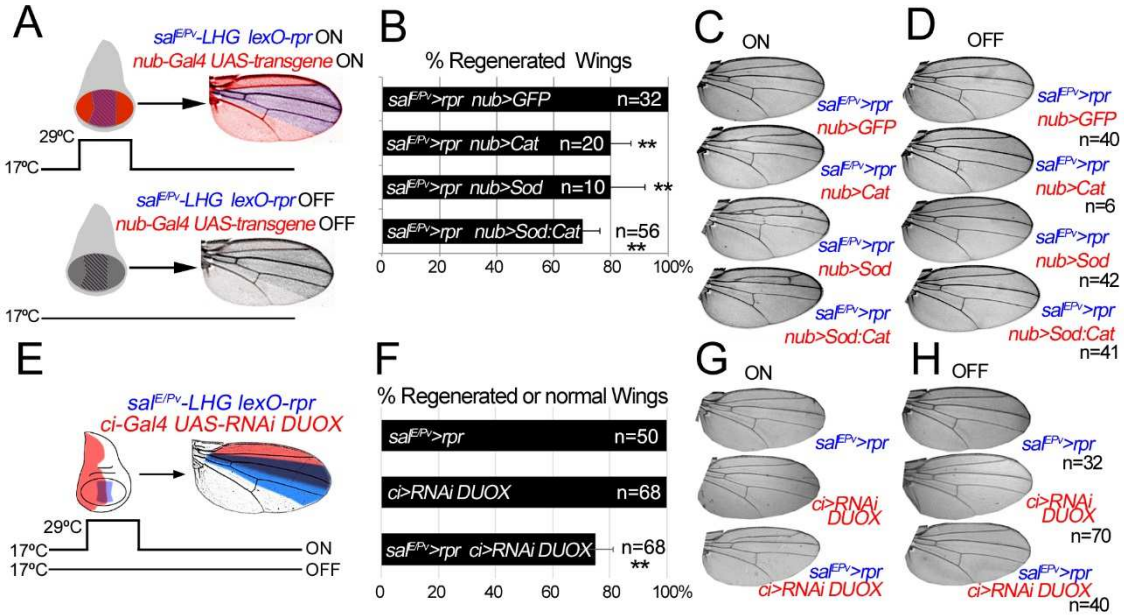

Figure 29. ROS inhibition impairs regeneration. (A, E) Design for ectopic expression of enzymatic antioxidant transgenes and simultaneous cell death induction when shifted to 29°C for 11 h. The Gal4/UAS (red) activate Cat, Sod or Cat+Sod transgenes. Blue area: *sal$^{E/Pv}$-LHG lexO-rpr*. Adult wings were scored for complete regeneration of the missing zone. Red coloration indicates zone influenced by the enzymatic antioxidant; purple: zone influenced by enzymatic antioxidant and cell death. Transgenes are under the control of *tubGal80^{TS}*. (B, F) Percentage of regenerated wings in Cat, Sod, Cat:Sod and RNAi DUOX ectopically expressed transgenes. (C, G) Wings from individuals after cell death and transgene activation (ON). For Cat, Sod, Sod:Cat or RNAi DUOX and example of incomplete regeneration is shown. (D, H) Examples of control wings kept at 17°C (*sal^{EPv}>rpr* OFF). ** P>0,01. Error bars show Standard Deviation.

ROS control JNK activity

The JNK signalling pathway has emerged as an early response to cell death and physical damage and appears to play a critical role in compensatory proliferation, regeneration and wound healing (Ryoo et al. 2004; Bosch et al. 2005; Bosch et al. 2008; Bergantiños et al. 2010; Smith-Bolton et al. 2009; Mattila et al. 2005; Lee et al. 2005; Fan et al. 2014; Pastor-Pareja et al. 2008).

Thus, we wondered whether ROS could act on JNK during wing disc repair. To achieve that, we first monitored the activity of this pathway in wing discs after damage. We used two different reporters: *puc-lacZ*, which marks *puc*-expressing cells (Martin-Blanco et al. 1998) and the *TRE-DsRed.T4* reporter, which monitors the JNK substrate *AP1* transcription factor (hereafter *TRE-red* reporter) (Figure 30; Chatterjee & Bohmann 2012).

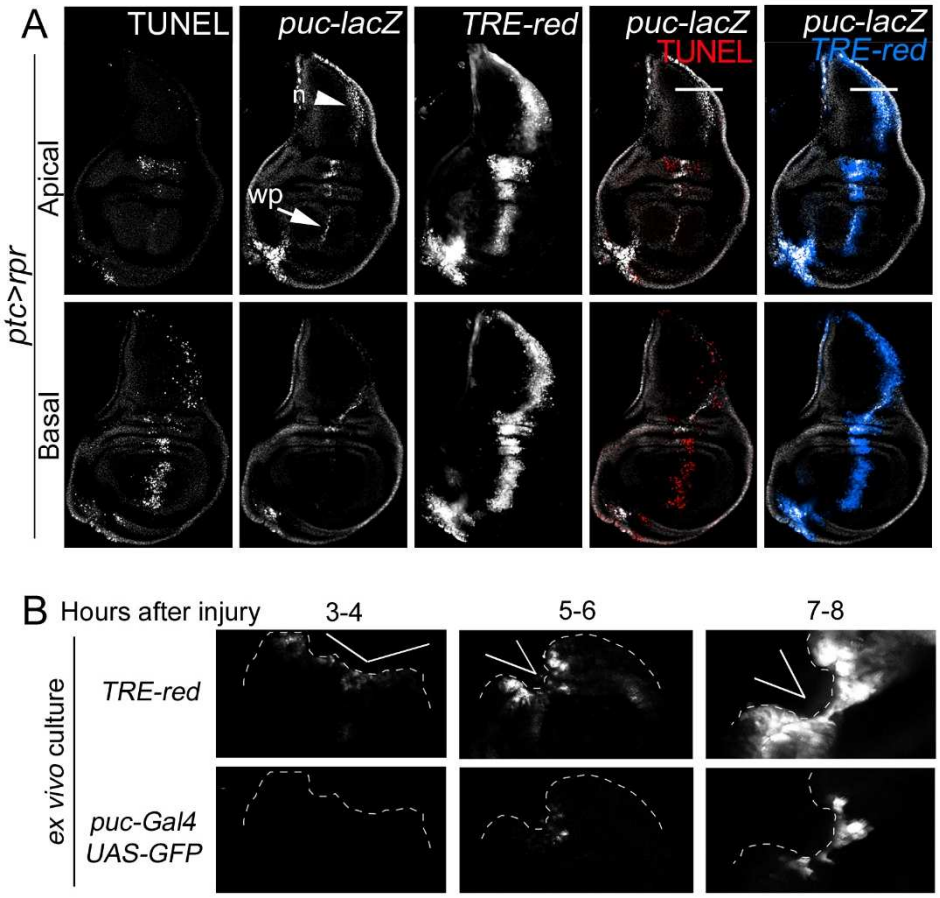

Figure 30. JNK is activated upon cell death and physical injury. (A) Test of JNK reporters. All images in A correspond to the same disc after *ptc>rpr* induction. Top row: apical sections. Bottom row: basal sections. Notum: n (arrowhead). Wing pouch: wp (arrow). Cell death: TUNEL. (B) *TRE-red* and *puc>GFP* expression after physical injury. *TRE-red* expression is activated earlier and more extensive than *puc>GFP*. White wedges indicate the position of the cut. Dotted line indicates the edges of the disc.

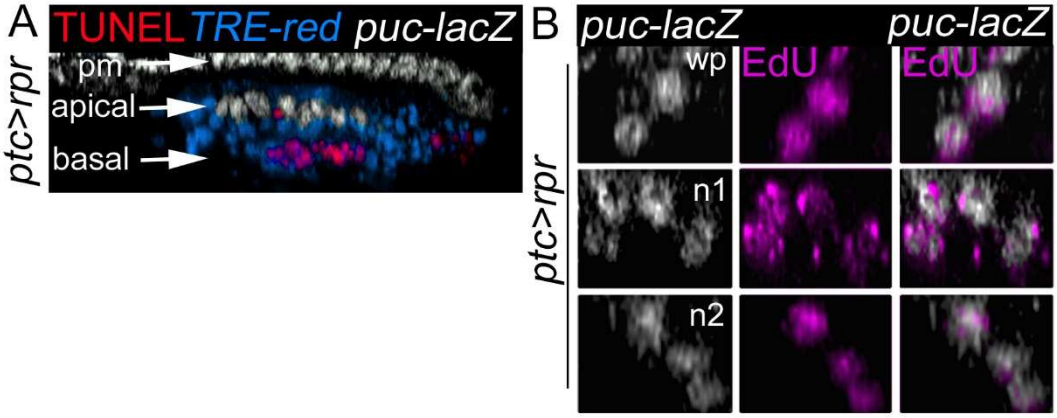

Figure 31. Puckered positive cells incorporate EdU. (A) Zoom of a digital cross section of the zone marked with a white line in Figure 30 A. Endogenous *puc-lacZ* was found in the outer layer of peripodial membrane cells (pm). *Puc-lacZ* cells in the disc columnar epithelium are apical (white), most apoptotic cells are basal (red), and *TRE-red* positive cells are apical and basal (blue). (B) Three digital cross sections in an apical *ptc>rpr* section; *puc-lacZ* zone of the wing pouch (wp) and notum (n1, n2).

In *ptc>rpr* discs, we found elevated levels of *TRE-red* reporter in the basal apoptotic zone and, to a lesser extent, in the apical living cells (Figure 30 A, 31 A). In contrast, *puc-lacZ* positive cells were found in the apical zone, as described previously (Bergantiños et al. 2010), and rarely in the apoptotic zone (Figure 30 A, 31 A). After physical injury, *TRE-red* reporter appeared 3 hours after cut, and spreads throughout the wound edges. However, *puc>GFP* positive cells were found later (5 hours) and with restricted expression close the wound site (Figure 30 B). Some *puc* positive cells incorporated EdU, supporting that JNK is also induced in living cells (Figure 31 B).

As in previous studies, we blocked JNK activity and regeneration was impaired. First, we fed $sal^{E/Pv}$>*rpr* larvae with a JNK inhibitor and we observed that only 23% of adult wings were recovered (Figure 32 B). Indeed, only 16% of adult wings with JNK inhibition in the anterior compartment and simultaneous cell death in $sal^{E/Pv}$ domain could regenerate ($sal^{E/Pv}$>*rpr ci*>bsk^{DN} discs, Figure 32 C, D). These results confirmed previous findings about the essential role of JNK pathway after cell death (Bergantiños et al. 2010; Smith-Bolton et al. 2009).

To determine the relationship between ROS and JNK in *rpr*-ablated discs we modified ROS with the antioxidant NAC. This molecule is the acetylated variant of the amino acid L-cysteine, an excellent source of sulfhydryl (SH) groups, and is converted in the body into metabolites capable of stimulating glutathione (GSH) synthesis, promoting detoxification, and acting directly as free radical scavengers (Kelly 1998).

To test NAC effects on JNK, we used the *TRE-red* reporter because is more rapidly and extensively expressed than *puc-lacZ* (Figure 30 A, 31 A) and because its activity is blocked in JNK mutants (Chatterjee & Bohmann 2012) or after chemical JNK inhibitors (Figure 32 A).

We found that the mean pixel intensity of the *TRE-red* reporter in *ptc>rpr* discs from animals grown in NAC-supplemented food was lower than in the same zone of individuals fed with Standard food (Figure 33 A, B). Moreover, discs cultured *ex vivo* in which NAC was added into the medium resulted in a drop of *TRE-red* activity after physical injury (Figure 33 C, D). These observations indicate that activation of JNK is ROS dependent.

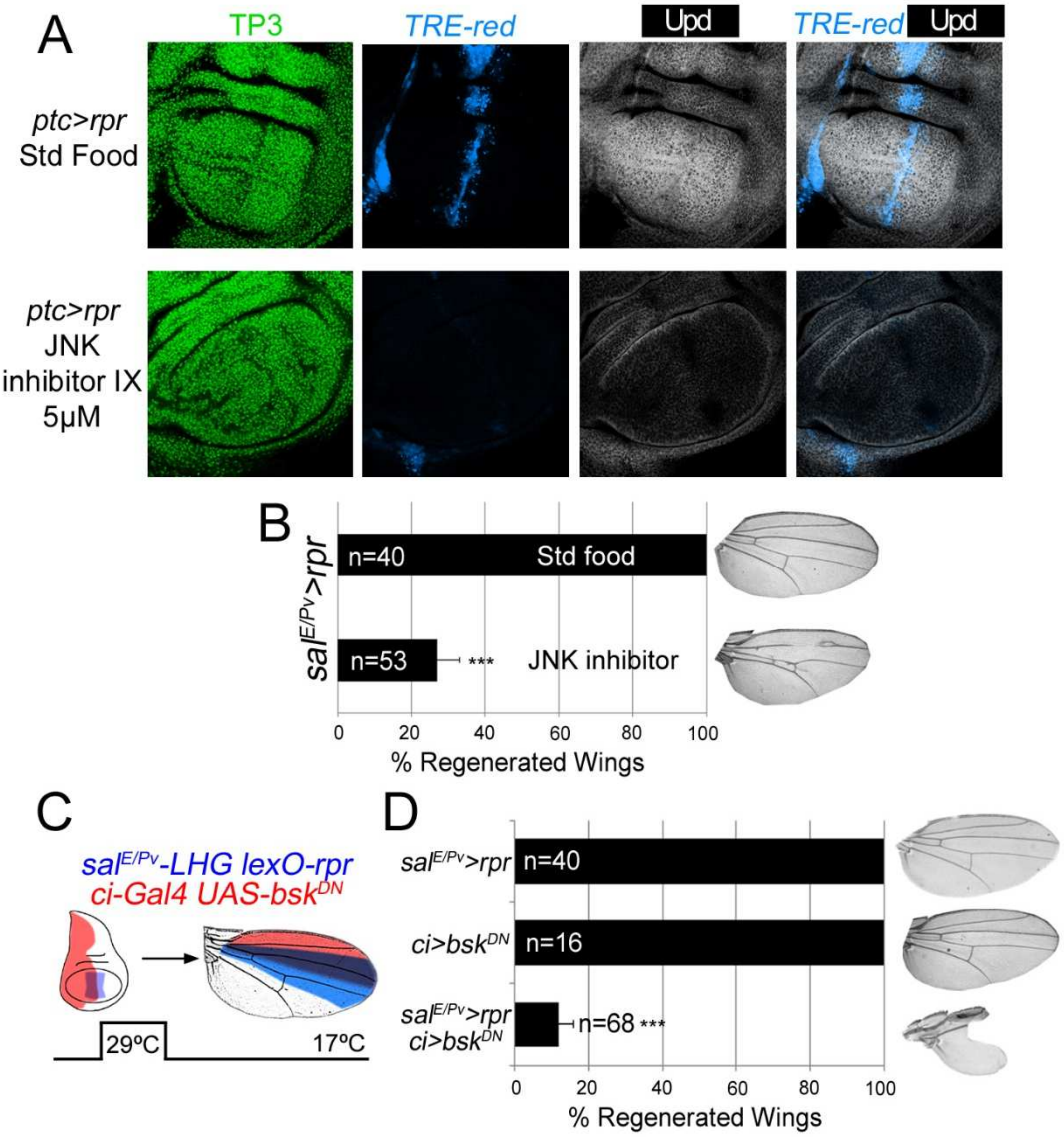

Figure 32. JNK inhibition impairs regeneration and JAK/STAT signalling. (A) The JNK Inhibitor IX eliminates *TRE-red* activity and *upd* expression after cell death. Top row: *rpr*–ablated disc from larvae fed with Standard food stained for nuclei (TP3: TO-PRO-3), AP1 (*TRE-red* reporter) and anti-Upd. Bottom row: *rpr*–ablated disc from larvae supplemented with JNK Inhibitor IX. (B) JNK Inhibitor IX inhibits regeneration. Quantification of regenerated sal^{EPv}*>rpr* wings after feeding with Standard or JNK Inhibitor IX supplemented food. (C) Design for ectopic expression of bsk dominant negative transgene and simultaneous cell death induction when shifted to 29°C for 11 h. The Gal4/UAS (red) activates the bsk^{DN}. Blue area: $sal^{E/Pv}$*-LHG lexO-rpr*. Adult wings were scored for complete regeneration of the missing zone. Transgenes are under the control of *tubGal80*^{TS}. (D) Percentage of regenerated or normal wings after shifting to 29°C for 11 h. Right: Wings from individuals after cell death and transgene activation. *** P>0.001. Error bars show Standard Deviation.

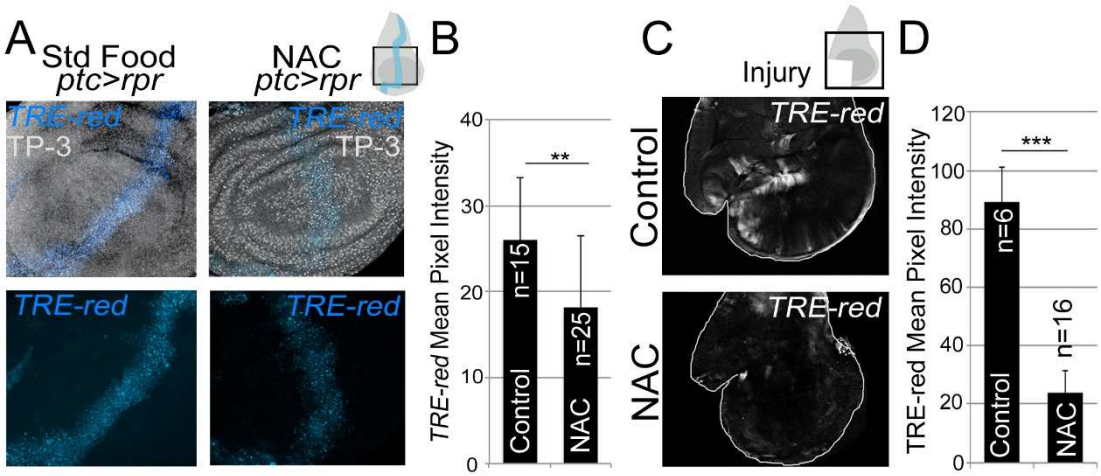

Figure 33. Antioxidants decrease JNK activity. (A) *TRE-red* reporter in *ptc>rpr* discs of larvae fed with Standard food or NAC-supplemented food (NAC). TP-3: TO-PRO-3. (B) Mean pixel intensities of *TRE-red* reporter in *ptc>rpr* discs with Standard or NAC food. The pixel intensity for Standard food was 26.06 ± 7.22 (S.D.; n=15) and for NAC 18.12 ± 8.32 (S.D.; n= 25). (C) *TRE-red* reporter expression in physically injured discs, cultured for 7 h *ex vivo* in Schneider's culture medium with or without NAC. Outline: disc contour. (D) Mean pixel intensities of *TRE-red* reporter in *ex vivo* cultured discs with or without NAC. The pixel intensity for Standard culture was 88.98 ± 22.25 (S.D.; n=6) and for NAC 23.98 ± 10.26 (S.D.; n= 16). **P<0.01, ***P<0.001.

ROS stimulates p38 phosphorylation

Another potential response to ROS increase is the activation of the p38 signalling cascade (McCubrey et al. 2006; Craig et al. 2004; Seisenbacher et al. 2011). Active p38 signalling can be monitored using anti-phosphorylated p38 (P-p38).

After physical injury wing discs showed P-p38 staining around the wound. P-p38 localization was variable and depended on the severity of the injury. Intact discs did not show P-p38 (Figure 34 A). However, discs cultured for 3 to 8 hours with or without injury showed P-p38 staining throughout the disc. This general staining is likely due to the stress generated by culturing, and contrasts with the fast local P-p38 response around the damaged zone (Figure 34 A). We next wondered whether the boost of ROS that propagates to the surviving tissue triggers p38 activation. We observed that the early P-p38 staining was blocked in discs cut and cultured *ex vivo* in medium containing NAC (Figure 34 B, C).

We also analysed p38 activation after inducing cell death and found P-p38 only in living cells but never in the basal apoptotic zone (Figure 34 E). In the absence of cell death, no P-p38 was detected (data not shown). Blocking of ROS production with NAC resulted in a significant drop in P-p38-labeled cells (Figure 34 E, F). In addition, we used the double transcriptional trans-activator system consisting of the *sal$^{E/Pv}$-LHG lexO-rpr* to induce apoptosis and simultaneously interfere with ROS production by inducing *UAS-Sod:UAS-Cat* in the anterior (*ci-Gal4*) compartment (Figure 34 D). A strong reduction of P-p38 was found in the anterior (*ci-Gal4 UAS-Sod:UAS-Cat*) compartment in comparison to the posterior one (Figure 34 D).

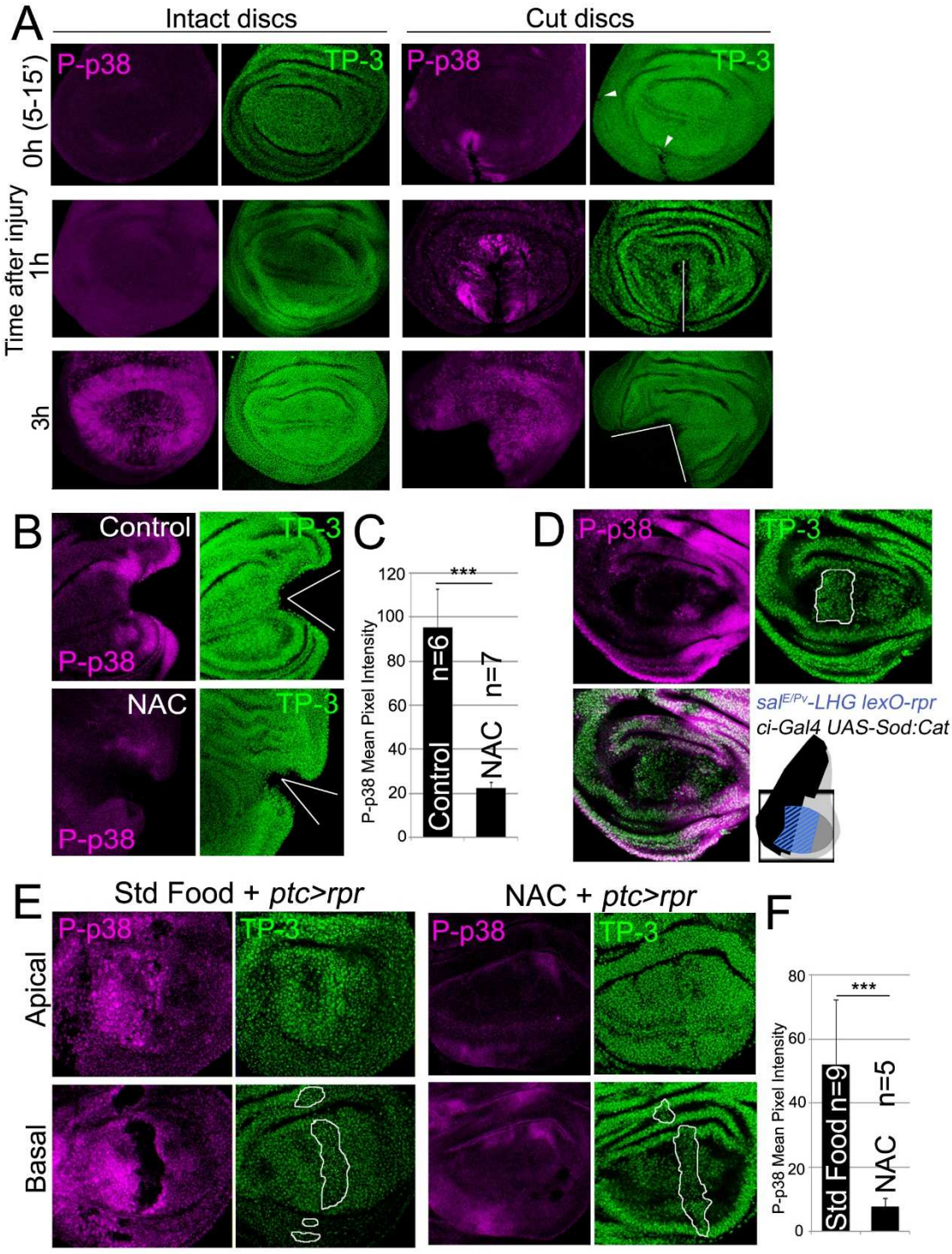

Figure 34. ROS stimulate p38 phosphorylation. (A) P-p38 staining of intact (uncut, controls) and cut discs cultured for the indicated times after injury. White lines: wound edges; white arrowhead: small incision. (B) Discs cut and cultured with or without NAC and stained for P-p38. (C) Mean pixel intensities of P-p38 fluorescence from cut discs cultured with standard medium (95.29 ± 17.52; S.D.) or NAC-supplemented (22.45±2.56; S.D.). (D) Genetic ROS scavenging using *ci>Sod:Cat*, activated in the anterior compartment (*ci*, black in the sketch). *Sal^{EPv}>rpr* cell death (blue in the sketch) in the same disc results in inhibition of P-p38 only in anterior compartment. TP-3: TO-PRO-3. Outlined white in D and E: apoptotic zone. (E) Apical and basal images of P-p38 after *ptc>rpr* induction with or without NAC supplementation. (F) Mean pixel intensities of P-p38 fluorescent labeling from *ptc>rpr* discs fed with standard (52.17±19.96; S.D.) or NAC-supplemented food (7,85 ± 2,42; S.D.). ***P<0.001.

To test whether an independent source of ROS could activate P-p38 in discs, we fed larvae for 2h with food supplemented with 1% H_2O_2 and checked for P-p38. Intact discs dissected from these larvae resulted in elevated levels of P-p38 as well as high CellROX Green fluorescence (Figure 35 A, B).

Together, these observations show that ROS scavengers inhibit P-p38 and therefore indicate that oxidative stress is required for p38 activation.

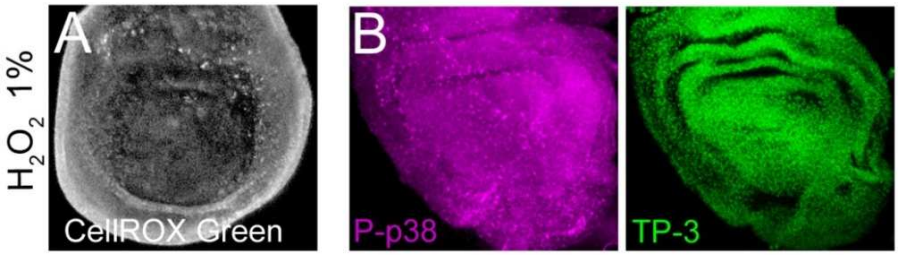

Figure 35. Oxidative stress promotes p38 phosphorylation. Discs from larvae were fed with 1% H_2O_2 for 2 h before processed for imaging. (A) Live imaging showing high ROS in the entire disc. (B) Fixed disc stained with P-p38. TP-3: TO-PRO-3 nuclear staining.

p38 signalling is required for tissue repair

Next, we wondered how p38 inhibition could affect regeneration. Thus, we scored wing regeneration after *sal$^{E/Pv}$>rpr* induction of cell death in different mutant backgrounds of the p38 pathway. As most of the alleles are lethal or semilethal in homozygosis (Cully et al. 2010), we tested them in heterozygosis.

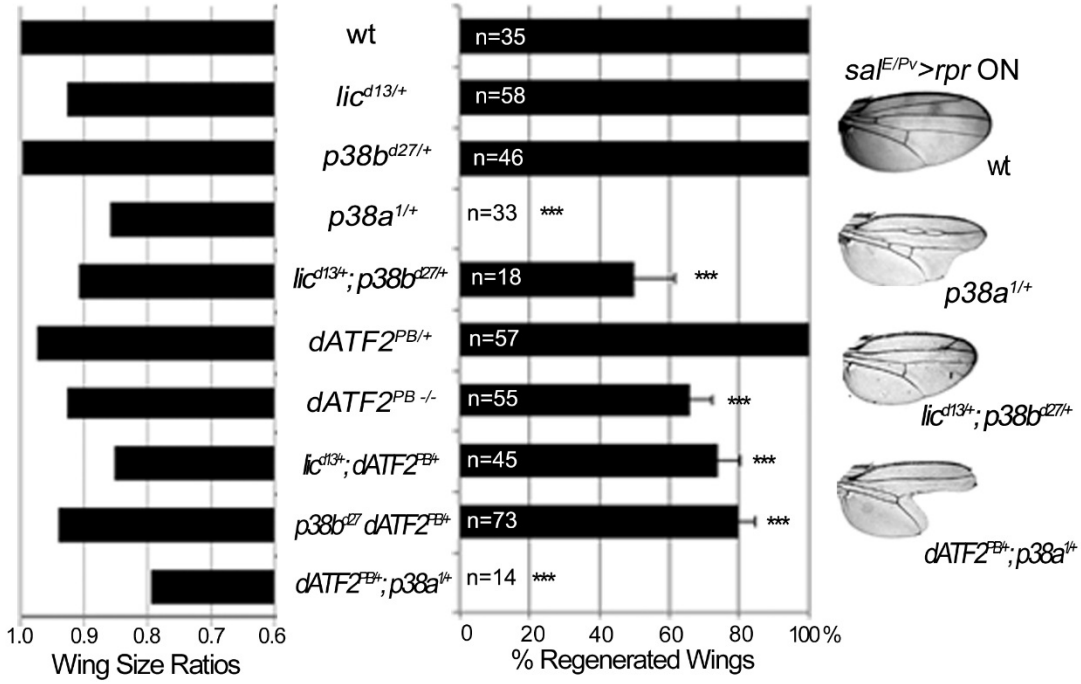

Figure 36. p38 is necessary for tissue repair. Adult wing parameters in p38 signaling mutant backgrounds after genetic ablation. Left: ratios of the wing areas between experimental groups (*rpr* induction *sal$^{E/Pv}$>rpr* ON) and control (no *rpr* induction *sal$^{E/Pv}$>rpr* OFF). Right: percentage of fully regenerated wings. Far right: examples of wings with full regeneration (wt: control) and incomplete regeneration (indicated genotypes) after *sal$^{E/Pv}$>rpr* induction.

We found that heterozygous *p38b*^{d27} animals regenerated entire wings (Figure 36). However, a severe effect was observed with *p38a*^{1} as the resulting wings lacked some sectors and presented notches in the margin. *Drosophila* p38 signalling is activated by MKK3/licorne (*lic*)-mediated phosphorylation (Suzanne et al. 1999). Heterozygous *lic*^{d13} showed all wing sectors albeit wings were smaller than controls. However, double heterozygotes for *lic*^{d13} and *p38b*^{d27} were unable to regenerate some wing sectors. We also tested *Atf2*^{PB}, a hypomorphic allele of the ATF2 transcription factor downstream of p38 (Seong et al. 2011) either in homozygosis or in double heterozygous combinations (*lic*^{d13} *Atf2*^{PB} or *p38b*^{d27} *Atf2*^{PB}). We found in all cases defects in size and pattern after *sal*$^{E/Pv}$*>rpr* induction. Regeneration was severely impaired in double heterozygotes for *p38a*^{1} (MAPK) and *Atf2*^{PB} (Figure 36).

We also blocked the pathway with UAS-RNAi constructs for *lic*, *p38b*, *p38a* and *Atf2* and analysed the adult wings. These transgenes were activated in the anterior compartment (*ci-Gal4 UAS-RNAi*) and cell death was induced in the *sal*$^{E/Pv}$ domain (*sal*$^{E/Pv}$*-LHG lexO-rpr)*. We found a reduction of individuals capable to fully regenerate wings for those RNAi's (Figure 37).

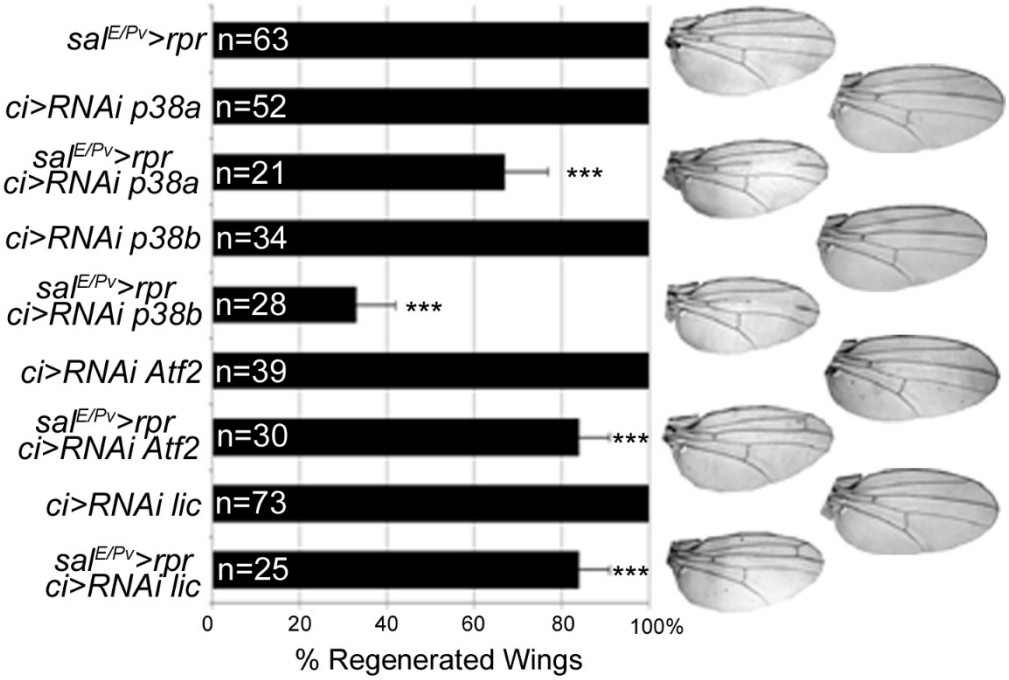

Figure 37. p38 inhibition impairs tissue repair. Ectopic expression of p38 RNAis under the control of *ci-Gal4* and simultaneous cell death induction with *sal*$^{E/Pv}$*-LHG LexO-rpr* when shifted to 29°C for 11 h. Adult wing size was measured after ectopic expression of the indicated RNAi transgenes.

To gain further insight into the requirement for p38, we chemically blocked the pathway using the imidazole drug SB202190, a specific cell permeable p38 MAP kinase inhibitor that has been reported to do not interfere JNK or ERK kinases and is known to prevent phosphorylation of Atf2 in *Drosophila* S2 cells (Frantz et al. 1998). We first tested the specificity of the SB202190 on P-p38 in *rpr*-ablated discs and found significant differences between individuals fed with the drug and controls. In contrast, the differences on *TRE-red* reporter were not significant (Figure 38 A). This indicates that SB202190 strongly blocked P-p38 and weakly the *TRE-red*.

Sal$^{E/Pv}$*>rpr* larvae grown at 17°C to prevent cell death and fed with food containing SB202190 (0.12, 1.0 or 5.0 µM) emerged into normal adults (*sal*$^{E/Pv}$*>rpr* OFF in Figure 38 B). However, *sal*$^{E/Pv}$*>rpr*-induced larvae fed with SB202190 developed wings lacking some sectors. The highest percentage of aberrant wings was found using 5 µM SB202190 (*sal*$^{E/Pv}$*>rpr* ON in Figure 38 B), indicating that this inhibitor act in a doses-dependent manner. This observation confirms that activation of p38 is required for wing repair.

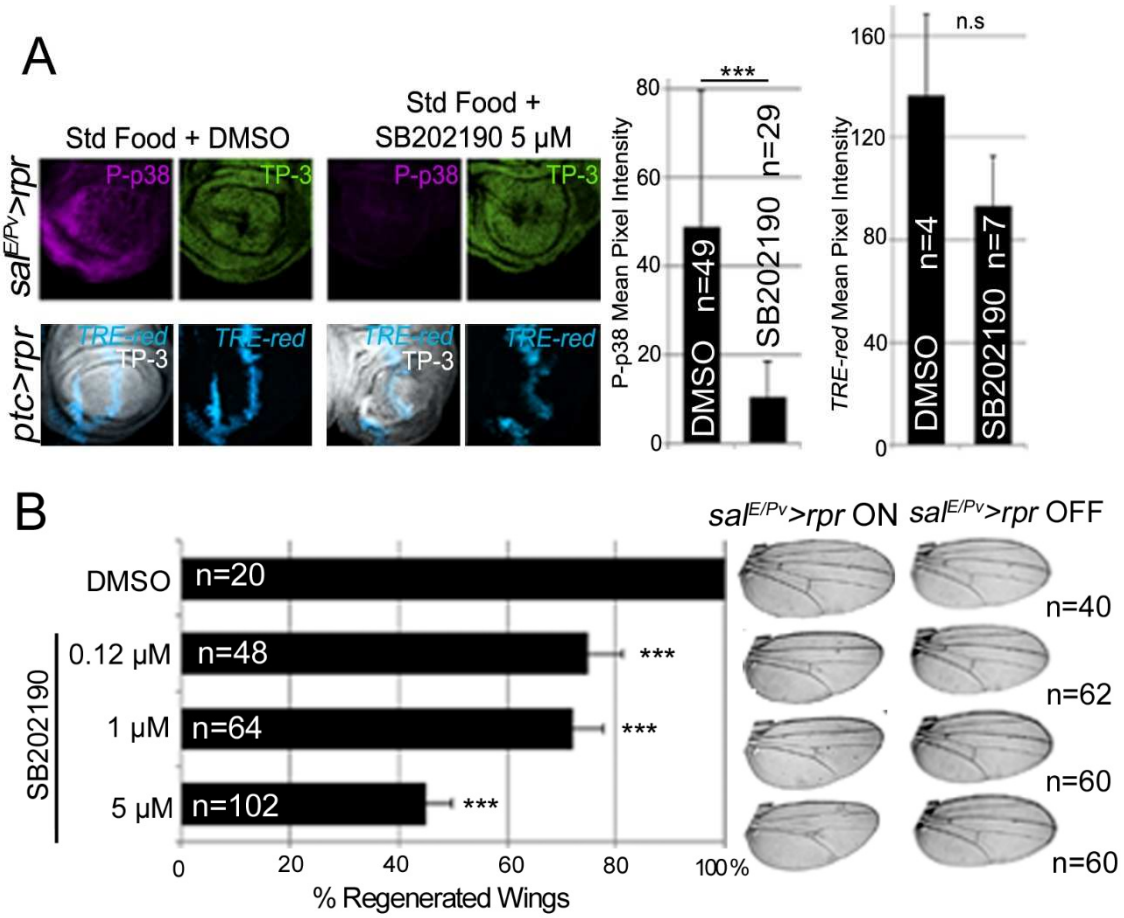

Figure 38. p38 inhibition impairs regeneration but does not affect JNK. (A) Test for the reliability of the SB202190. Discs were dissected from *rpr*-ablated larvae that were fed with 5 µM SB202190, fixed and imaged. SB202190 intake reduces P-p38 activation after cell death as measured from the Mean Pixel Intensity in comparison to DMSO fed larvae. *TRE-red* in individuals fed with 5 µM SB202190 is active. Right: Mean Pixel Intensities for both experiments. For p38: control 48.77 ± 30.82 (S.D.); SB202190 10.52 ± 8.09 (S.D.). For TRE-red: control 136.46 ± 44.5 (S.D.); SB202190 93.5 ± 23.19 (S.D.). ***P<0.001 for the P-p38 and P=0.15 n.s. for *TRE-red*. (B) Percentage of fully regenerated wings after SB202190 intake in *sal*$^{E/Pv}$*>rpr* flies. *sal*$^{E/Pv}$*>rpr* ON: wing fully regenerated (top) and examples of incomplete regeneration for each SB202190 concentration. *sal*$^{E/Pv}$*>rpr* OFF: Examples of control wings in which no rpr-ablation was induced (kept at 17°C) for the indicated concentrations of the p38 inhibitor SB202190. ***P<0.001.

p38 and JNK act independently

To assess the relationship between JNK and p38, we tested p38 activation in wounded null hemizygous JNKK *hemipterous* (*hep*^{r75}) discs. P-p38 was localized near the wound after physical injury (Figure 39 A). This contrasts with the decrease in P-p38 when the MAPK kinase *lic*, which is the p38 activating kinase, was interfered with RNAi in injured discs (Figure 39 B).

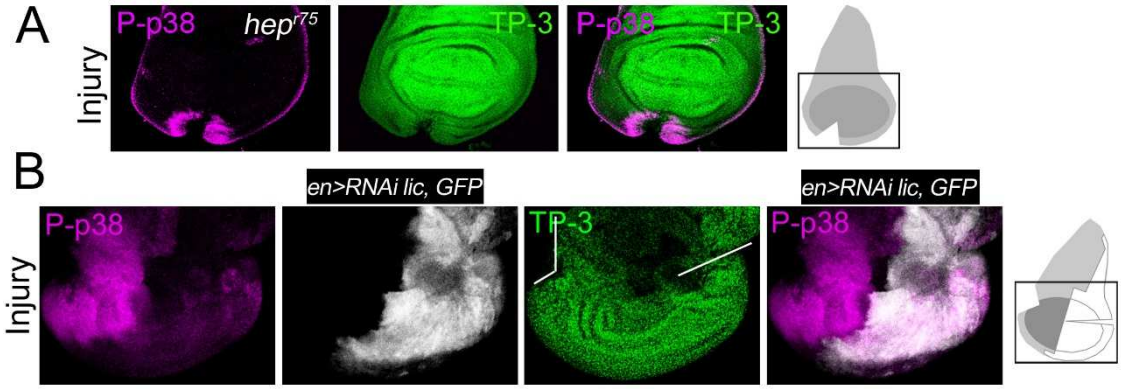

Figure 39. p38 and JNK are activated independently. (A) *Hep*^{r75} hemizygous disc cut and stained with P-p38. Sketch of wing disc with square indicate location of images. (B) RNA interference of MKK *lic* inhibits p38 phosphorylation after injury. The *UAS-RNAi lic* was activated in the posterior compartment together with *UAS-GFP* (white). Two injuries were inflected, one in the anterior and one in the posterior compartment. The cuts were performed in Schneider's medium, and fixation for immunostaining 20' after injury. P-p38 activation was localized in the anterior compartment and almost absent around the posterior cut.

Moreover, P-p38 staining was localized in *hep*^{r75} discs after *ptc>rpr* induction, as in the wt (Figure 40 A, compare with Figure 34 E) indicating that JNK and p38 act independently. We also fed animals with the JNK Inhibitor IX, which abolishes *TRE-red* reporter expression and inhibits regeneration (Figure 32 A, B), and found that P-p38 after *rpr*-ablation was not affected (Figure 40 B).

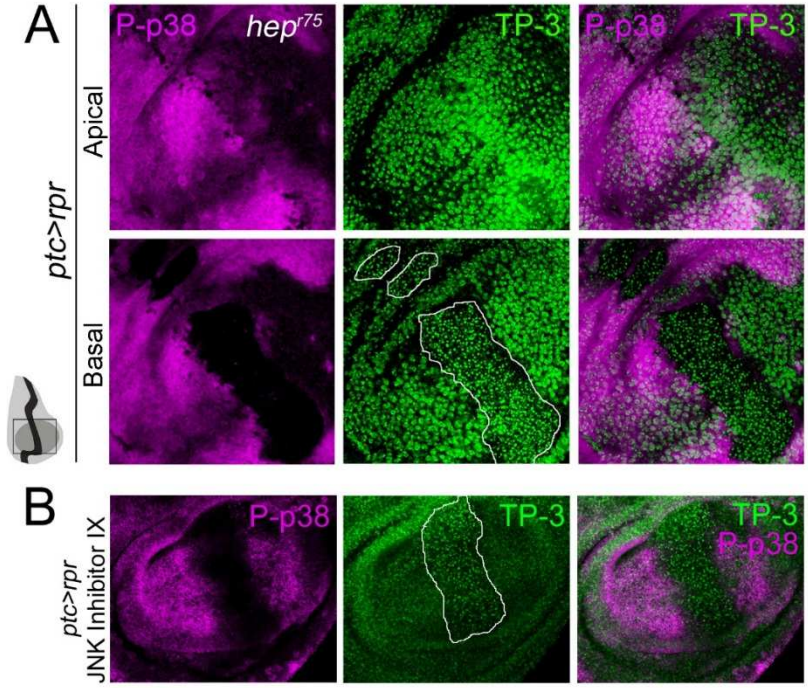

Figure 40. p38 is phosphorylated in the absence of JNK. (A) Apical and basal images of *hep*^{r75} hemizygous disc after *ptc>rpr* induction and stained for P-p38. Dead domain is outlined white. TP-3: TO-PRO-3. (B) Blocking JNK with JNK Inhibitor IX does not affect P-p38 after *rpr*-ablation. The dead domains are outlined in white. The sketch of the wing disc with square indicate the location of images.

To confirm that JNK and p38 act independently, we blocked the *p38* pathway and checked for *TRE-red* reporter activity. As the *p38a*^{1} allele in heterozygosis strongly affects regeneration (Figure 36), we used this null allele in homozygosis and tested *TRE-red* activity after physical injury. Our results showed that *TRE-red* is induced at the wound edges of *p38a*$^{1-/-}$ mutant discs (Figure 41). Together, these results demonstrate that p38 and JNK stress responses act independently in damaged imaginal discs.

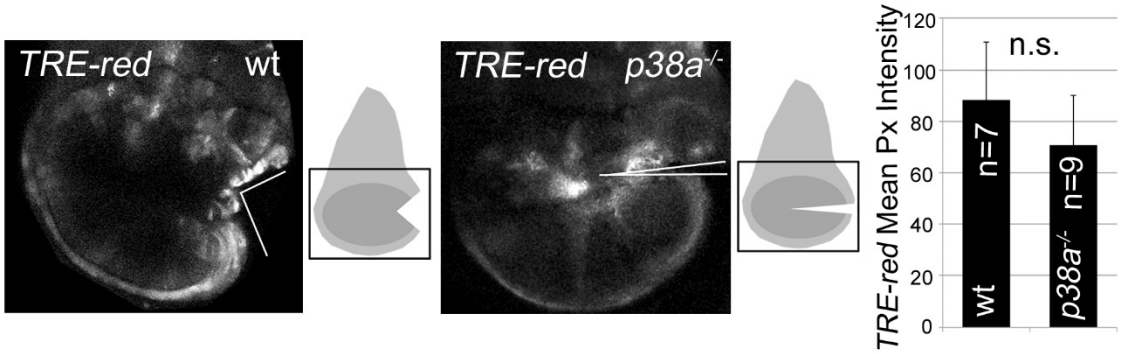

Figure 41. JNK is activated after injury in p38 mutant background. Wild type and *p38a*$^{1-/-}$ discs, cultured for 7h showing *TRE-red* activation close to the cut edges. Right: Mean pixel intensity for *TRE-red* measured in discs with physical injury in wild type (88.24 ± 22.58; S.D.) and *p38a*$^{1-/-}$ (70.80 ± 19.14; S.D.). P =0.33 n.s.

Upd expression is triggered by ROS

It has been found that JNK is active in the living tissue located near damaged zones (Figure 30 A, B), and its inhibition results in defects in repair (Figure 32; Bosch et al. 2005; Lee et al. 2005; Mattila et al. 2005; Galko & Krasnow 2004; Bergantiños et al. 2010). Moreover, JNK activation promotes *upd* expression in different contexts (Pastor-Pareja et al. 2008; Bunker et al. 2015). We wondered whether those low non-deleterious JNK levels are capable of triggering tissue repair through *upd* expression.

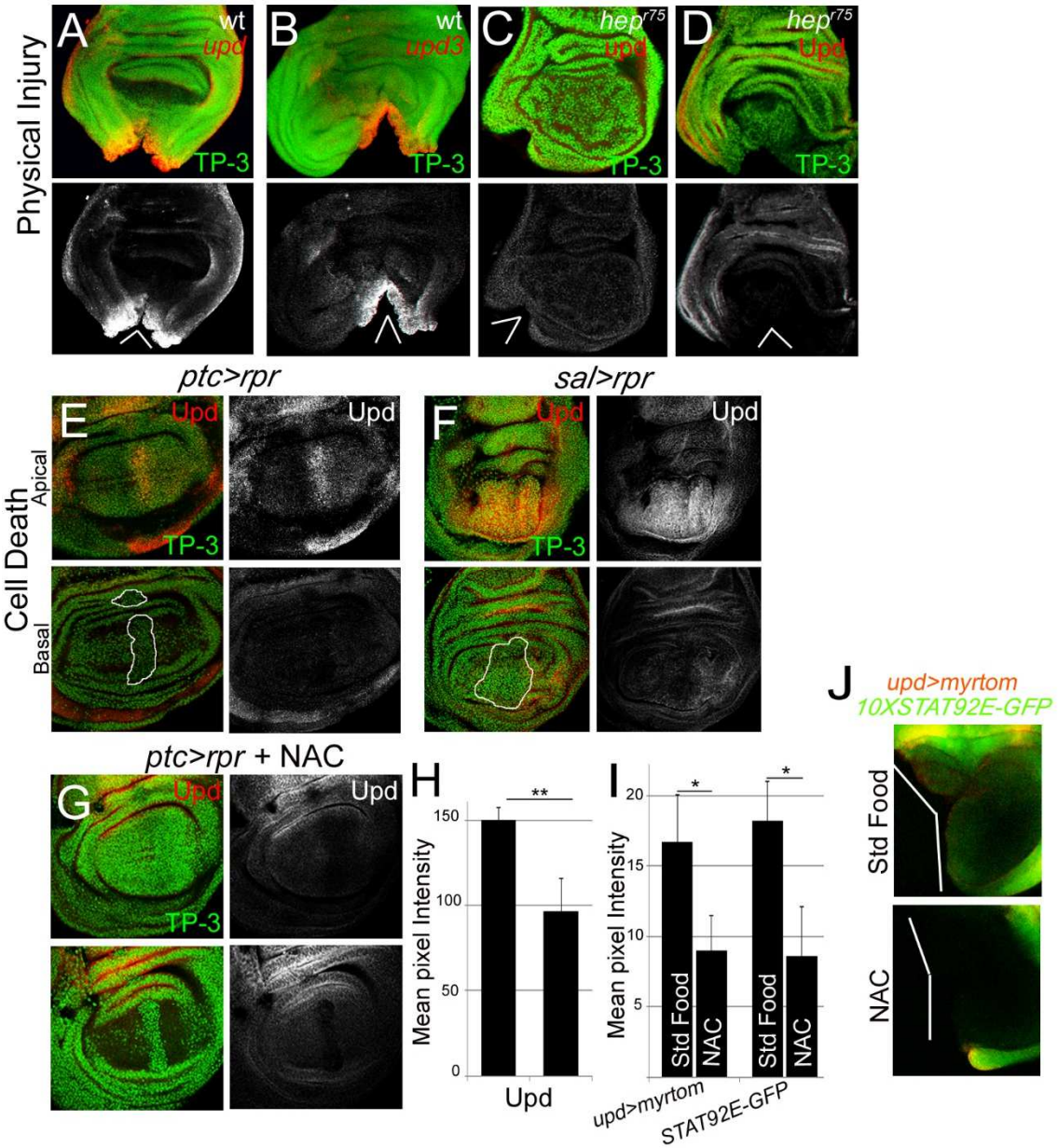

Figure 42. Unpaired signaling is controlled by ROS and JNK. (A, B) FISH of *upd* (A) and *upd3* (B) in wild type (wt) discs and JNKK *hep*^{r75} hemizygotes (C) after injury. (D) *hep*^{r75} hemizygote stained with anti-Upd after injury. (E, F) Upd (anti-Upd) is mainly expressed in living cells and not in dead cells after *ptc>rpr* or *sal>rpr.* (G) Upd expression declines after NAC intake. TP-3: TP-PRO-3 nuclei staining. (H) Mean pixel intensities of Upd stained *ptc>rpr* discs with or without NAC feeding (150.29 ± 7.11 and 96.69 ± 18.97, S.D.). (I, J) Mean pixel intensities of *upd* reporter (*upd>myrtom* Std food: 16.68 ± 3.22 and NAC: 9.01 ± 3.41, S.D.) and STAT92E reporter (*10xSTAT92E-GFP* Std food: 18.24 ± 2.73 and NAC: 8.63 ± 4.07, S.D.) after standard or NAC-supplemented food. White wedges indicate zone of injury. **P<0.01 *P<0.05.

Upd cytokines are ligands that binds to the receptor *domeless* (*dome*) to activate the kinase activity of the receptor associated protein kinase *hopscotch* (*hop*), which in turn phosphorylates dimers of the transcription factor STAT92E (Amoyel et al. 2014). Fluorescence *in situ* hybridization revealed *upd* and *upd3* expression near the wound after both physical injury and cell death (Figure 42 A, B and E, F). This injury-induced *upd* expression was blocked in JNKK hep^{r75} hemizygous mutant background (Figure 42 C, D) and by JNK Inhibitor IX (Figure 32 A), which is consistent with previous observations (Álvarez-Fernández et al. 2015; Pastor-Pareja et al. 2008).

We next analysed if JAK/STAT signalling requires ROS in this context. Two different reporters (*10XSTAT92E-GFP* and *upd-Gal4 UAS-myrtomato*) were used in physically injured discs and showed reduced expression after NAC feeding (Figure 42 I, F). In addition, *ptc>rpr* induced discs from NAC fed larvae showed a reduction of *upd* expression (Figure 42 E-H). Thus, this expression is ROS dependent after both physical injury and cell death.

To study the requirement of JAK/STAT for regeneration, we used the $sal^{E/Pv}$*-LHG lexO-rpr* to induce apoptosis and simultaneously interfered with the receptor *dome* using the dominant

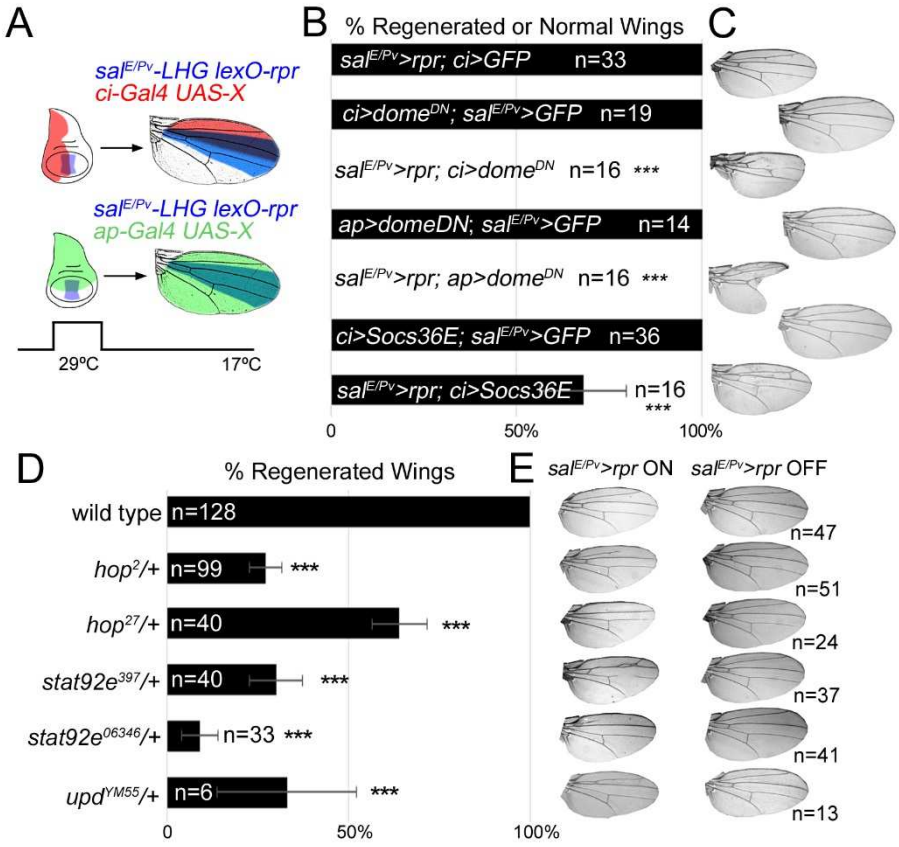

Figure 43. Inhibition of the JAK/STAT signalling impairs wing regeneration. (A) Genetic design for double transactivator system to induce death (blue) and activate transgenes in anterior (red) or dorsal compartment (green). (B) Percentage of regenerated wings for controls (*rpr*, $dome^{DN}$ or Socs36E expression only) and experimental (*rpr* and $dome^{DN}$/Socs36E dual expression). Note that $dome^{DN}$ wings were not able to regenerate, whereas $dome^{DN}$ wings in the absence of cell death are normal. (C) Examples of wings of controls and experimentals. (D) Percentages of regenerated wings for the indicated genetic background after $sal^{E/Pv}$>*rpr* ablation. (E) $sal^{E/Pv}$>*rpr* ON column: top (wt) is an example of fully regenerated wing. The rest of wings are examples of non-regenerated or incomplete regeneration in the heterozygous condition indicated $sal^{E/Pv}$>rpr OFF column: wings of those genetic backgrounds without cell death (kept at 17°C). All wings raised in those conditions contain the normal set of veins and interveins.

negative form *UAS-dome^{DN}* driven by *ci-Gal4* or *ap-Gal4,* as well as with the negative regulator of the pathway Sosc36E. These wings lacked most of the tissue where cell death was induced and *dome* was blocked (Figure 43 A, B, C). Socs36E overexpression in regenerating discs leads to 68% of regeneration (Figure 43 A, B, C), indicating that JAK/STAT signalling is needed for tissue recovery. Moreover, heterozygous alleles for the JAK/STAT pathway resulted in partial disruption of adult wing recovery after cell death (Figure 43 D, E).

We speculated that if ROS operate upstream *upd*, the impairment of regeneration resulting from NAC feeding should be rescued by activating Upd. To this aim, we used the double transactivation system to induce cell death in NAC-fed individuals and concomitantly activate *upd* expression (Figure 44 A). Analysis of the resulting wings showed that *upd* ectopic expression rescued the NAC inhibition phenotype (Figure 44 B, C). These observations demonstrate that ROS function upstream of JAK/STAT during repair.

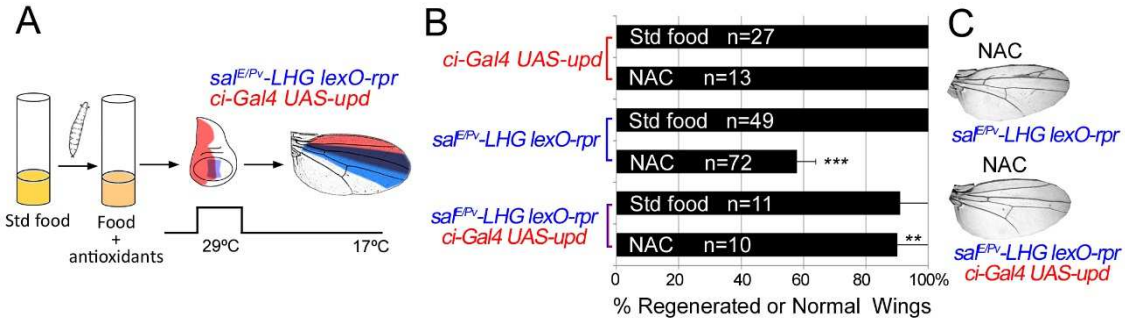

Figure 44. Inhibition of regeneration by NAC is rescued by ectopic expression of *upd*. (A) Experimental design for testing the rescue of NAC effects by ectopic activation of *upd*. (B) Quantification of the percentage of wings that regenerate after NAC feeding for the indicated genotypes. (C) Examples of wings from NAC-feeding with *rpr*-ablation defects (upper) and with rescue after *rpr*-ablation and *upd* activation (lower). **P<0.01 ***P<0.001.

p38 controls *upd* expression

We wondered whether p38 is also required for *upd* expression in damaged discs. Expression of *upd* or *upd3* was severely reduced in *p38a*$^{1-/-}$ wound edges (Figure 45 A-F). This suggests that in addition to JNK, p38 is essential for *upd* expression upon stress.

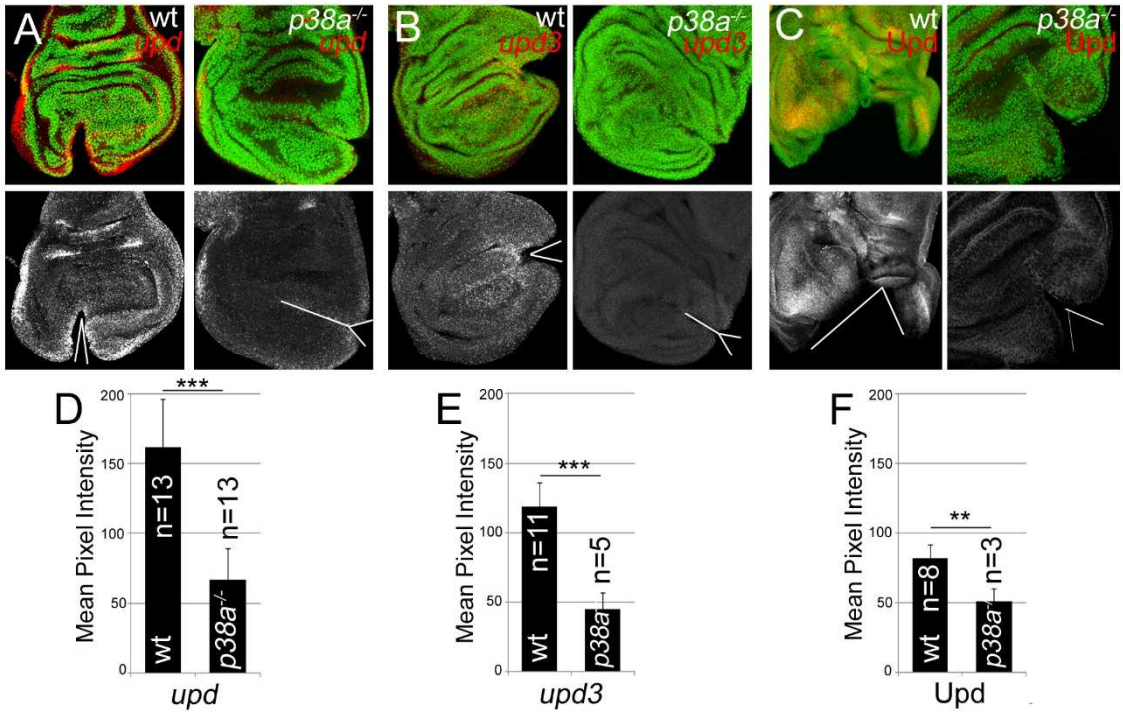

Figure 45. p38 controls *upd* expression after injury. (A) In situ hybridization of *upd* in wild type (wt) and *p38a*$^{1-/-}$ cut discs. (B) In situ hybridization of *upd3* in wild type (wt) and *p38a*$^{1-/-}$ cut discs. (C) Immunostaining with anti-Upd in wild type (wt) and *p38a*$^{1-/-}$ cut discs. White lines indicate the position of the cut. (D, E, F) Quantification of in situ hybridizations of *upd* mRNA (D), *upd3* mRNA (E) and antibody localization for Upd (F). Regions of interest were determined around the wound edges. ***P<0.001 **P<0.01. Error bars indicate standard deviation.

Finally, we argued that if p38 is required for repair through *upd,* its ectopic expression should rescue the impaired regeneration after inhibition of p38. We, again, used the double transactivation system to induce cell death in SB202190-fed individuals, to block p38 phosphorylation and alongside activate *upd* expression (Figure 46 A). Indeed, we found that the number of wings that regenerated after p38 inhibition significantly increased (Figure 46 B, C).

Altogether these results position Upd cytokines downstream from the ROS/p38/JNK module.

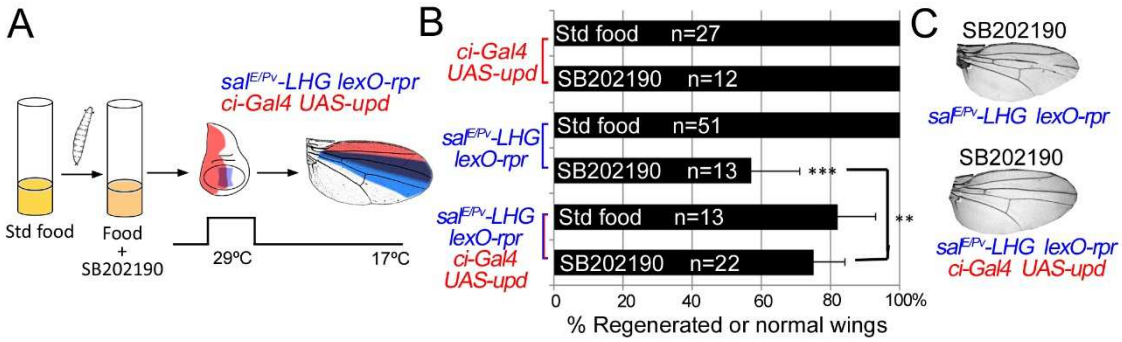

Figure 46. SB202190 phenotype is rescued by ectopic expression of *upd*. (A) Experimental design for testing the rescue of SB202190 effects by ectopic activation of *upd*. (B) Quantification of the percentage of wings that regenerate after SB202190 feeding for the indicated genotypes. (C) Examples of wings from SB202190-feeding with *rpr*-ablation defects (upper) and with rescue after *rpr*-ablation and *upd* activation (lower). **P<0.01 ***P<0.001.

CHAPTER II

Ask1 is necessary for imaginal disc regeneration

Drosophila Ask1 is the single orthologue of mammalian ASK1 (Kuranaga et al. 2002). In response to oxidative stress, ASK1 phosphorylates MAP kinases in JNK and p38 pathways. It contributes substantially to apoptosis, but is also implicated in determination of cell fate, differentiation, survival and immune responses (reviewed in Sakauchi et al. 2017). Thus, in this second chapter, we investigated whether Ask1 could sense ROS upstream of SAPK p38 and JNK during imaginal disc repair.

We first asked if Ask1 could be involved in imaginal disc regeneration. To achieve that, we scored wing regeneration of *ask1* heterozygous mutants after cell death in *spalt*$^{E/Pv}$ domain (*sal*$^{E/Pv}$*>rpr*). We found that both heterozygous *ask1*^{MB06489} (Metaxakis et al. 2005) and *ask1*^{M102915} alleles (Venken et al. 2011) presented wings smaller in size, lacking some sectors and with vein defects. In *ask1*^{MB06489} heterozygous allele, only 15% of wings could regenerate properly, whereas in *ask1*^{M102915} heterozygous regenerated 23% of the total wings. *Sal*$^{E/Pv}$*>rpr* controls showed completely regenerated wings (Figure 47 A).

We also used an UAS-RNAi construct to block *ask1*. The transgene was activated in the anterior compartment (*ci-Gal4 UAS-RNAi*) and cell death was induced in the *sal*$^{E/Pv}$ domain (*sal*$^{E/Pv}$*-LHG lexO-rpr*) (Figure 47 B). Neither wing could regenerate after inhibition of *ask1* in the anterior

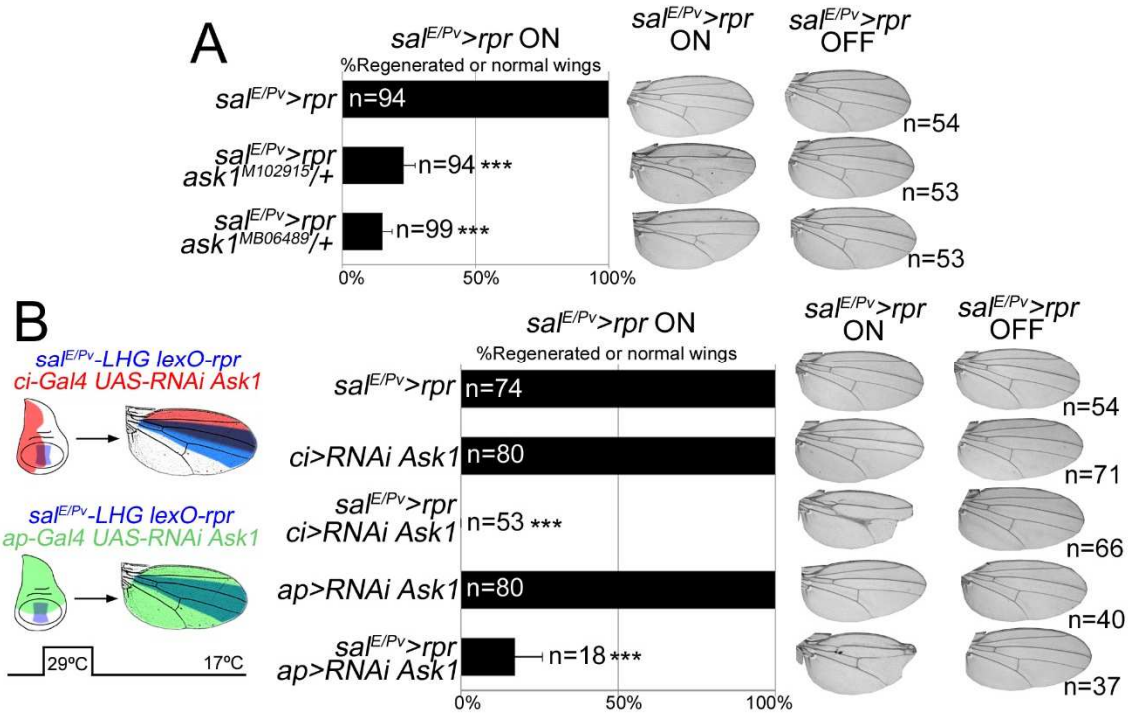

Figure 47. Ask1 is necessary for imaginal disc regeneration. (A) Percentage of fully regenerated wings in *ask1* mutant backgrounds after genetic ablation. Close to the indicated genotypes are examples of wings with full regeneration (control *sal*$^{E/Pv}$*>rpr*) and incomplete regeneration after *rpr*-ablation (*sal*$^{E/Pv}$*>rpr* ON). (B) Genetic design for double transactivator system to induce death (blue) and to activate transgenes in anterior (red) or dorsal compartment (green). Percentage of regenerated wings for controls (*rpr* or *RNAi Ask1* expression only) and experimental (*rpr* and *RNAi Ask1* dual expression) and examples of wings with complete regeneration (controls *sal*$^{E/Pv}$*>rpr, ci>RNAi Ask1 and ap>RNAi Ask1*) and incomplete regeneration (indicated genotypes). Right: Examples of wings without *rpr*-ablation (kept at 17°C, *sal*$^{E/Pv}$*>rpr* OFF) for each genotype. Error Bars indicate Standard Deviation. ***P<0.001.

compartment (*ci>RNAi Ask1 sal$^{E/Pv}$>rpr,* Figure 47 B). All wings were smaller than controls and most wings lacked some sectors in addition to show notches in the margins. Blocking *Ask1* in *ci* without cell death does not affect wing size or pattern (*ci>RNAi Ask1*) (Figure 47 B). Using the dorsal driver *apGal4* to inhibit *ask1*, we observed similar phenotypes. Only 17% of wings were fully regenerated (*ap>RNAi Ask1 sal$^{E/Pv}$>rpr*). For all the experiments controls of the same genotype without cell death induction resulted in normal wings (*sal$^{E/Pv}$>rpr* OFF wings in Figure 47 A, B).

Ask1 is activated after cell death or injury

Drosophila Ask1 protein locus has two possible transcript isoforms encoding two different length peptides, Ask1-RB and Ask1-RC. Both have a protein kinase-like domain which presents a highly-conserved core of threonines (henceforth Thr-rich domain) and is the responsible for the functional activation of the protein (green domain in Figure 48). After Trx release, the Ask1 oligomer undergoes conformational change leading to trans-autophosphorylation of the threonine residues corresponding to Thr838 in human ASK1 (Thr845, Thr806, Thr747 and Thr825 of mouse, human ASK2, *Drosophila* Ask1 and *C.elegans* NSY-1, respectively) (Figure 48 B; reviewed in Takeda et al. 2008).

However, Only the longer RC isoform possesses a domain called DUF4071, conserved throughout evolution (Figures 48 A in red, 49). We found a consensus sequence in the DUF4071 domain, which contains a Serine in position 83 surrounded by other characteristic residues (YHLGVRESF, Figures 48 A, 49). Remarkably, the AKT kinase downstream the PI3K pathway phosphorylates the Ser83 of human ASK1 to attenuate the activity of ASK1 *in vitro* (Kim et al. 2001).

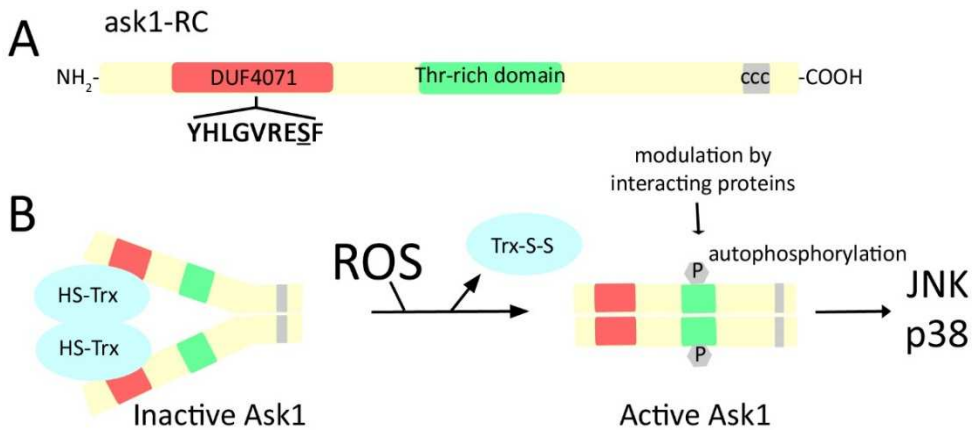

Figure 48. Ask1 activation is ROS-dependent. (A) Structural features of *ask1*-RC isoform. It possesses a phosphokinase domain in its midportion with a highly-conserved core of threonines (Thr-rich domain in green). In the N-terminal domain *ask1*-RC presents a DUF4071 domain, in which there is a consensus sequence surrounding the Serine 83 residue (in red). In the C-terminal domain RC isoform presents a coiled coil domain (ccc), which allow interactions between Ask1 monomers to form oligomers. (B) Activation of Ask1 is ROS-dependent. Inactive Ask1 is constituted by association of Ask1 monomers through the ccc domain and the reduced form of thioredoxin (Trx-SH) in the N-terminal domain. Upon oxidation, Trx is oxidized (Trx-S-S) and released, which allows the Ask1 auto phosphorylation in the Thr-rich domain leading to an active Ask1. In this state, Ask1 activates JNK and p38 pathways (Sakauchi et al. 2017; Takeda et al. 2008).

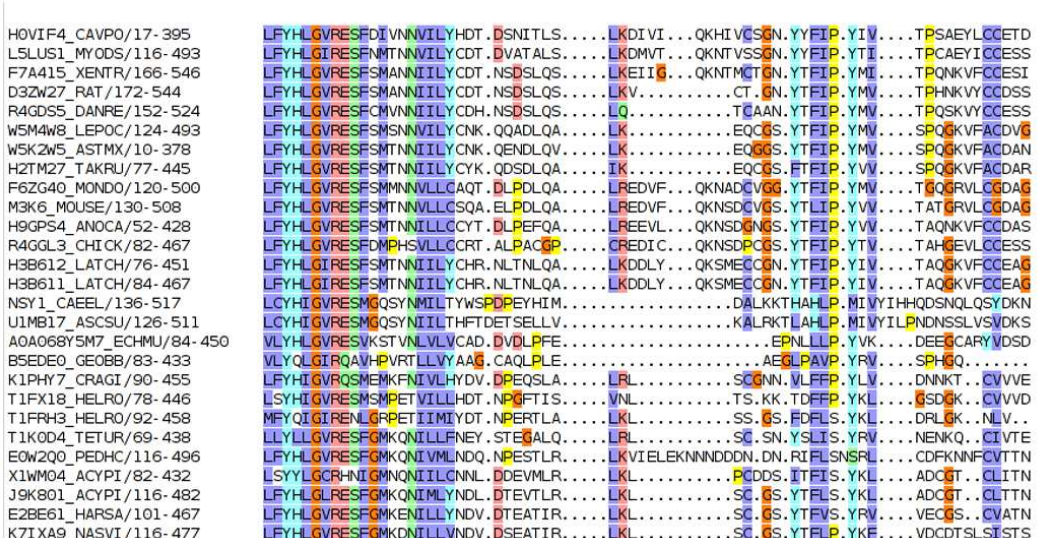

Figure 49. Sequence alignment for DUF4071 domain. First block of the core alignment of DUF4071 that was produced from 27 protein sequences from a range of species from diverse taxons with HMM model. The serine S83 (highlighted in green) is within a highly-conserved region. It can describe a pattern with the following context of most frequent amino acids: YHLGVRESF.

We decided to study the activation of the Thr-rich domain of Ask1 after *sal$^{E/Pv}$>rpr* cell death. We monitored the activity of this domain with an antibody against the mouse Ask1 phosphorylated Thr845 which also recognizes the Thr-rich domain in *Drosophila* (Choi & Chung 2011). In the absence of cell death, no phosphorylation of Thr-rich domain was found (Figure 50 A), as well as in injured discs (Figure 50 B). Curiously, we found activation of the Thr-rich domain in mitotic cells (Figures 50 A, 51).

Apoptotic cells of *sal$^{E/Pv}$>rpr* discs showed a high localization of the activated Thr-rich domain. (Figure 50 D), which concurs with high activity of Ask1 in dying cells. This agrees with the proposal that high Ask1 activity will activate high levels of JNK that trigger apoptosis (Tobiume et al. 2001).

We next studied the phosphorylation of the DUF4071 domain of Ask1, which is highly conserved with a Serine residue in position 83 (Figures 48 A, 49). We monitored the activity of the DUF4071 domain with a mammalian antibody against the Ser83 phosphorylated Ask1. Wild type discs show low levels of P-Ser83 at the basal side of the columnar epithelium (Figure 54). After the activation of apoptosis in *sal$^{e/Pv}$>rpr* discs, we found an increase in the P-Ser83 in living cells surrounding the apoptotic domain. P-Ser83 was absent in apoptotic cells (Figure 50 E). The localization in cells bordering the dying domain is more evident in younger third instar discs than in mature, perhaps because the folding masks the staining (8/8 young discs and 11/27 mature discs analysed). After physical injury, P-Ser83 was found localized in the wound edges (Figure 50 C). In the absence of apoptosis, endogenous P-Ser83 staining dropped in *Ask1* RNAi discs (Figure 52 A). In the presence of apoptosis, the P-Ser83 staining abutting the cell death domain was absent in the anterior compartment of *ci>RNAi Ask1 sal$^{E/Pv}$>rpr* discs (Figure 52 B). Moreover, the Thr-rich domain activation decrease in these discs too, both in dying cells as well as in mitotic cells close to the dying zone (compare Figure 52 C with 50 D).

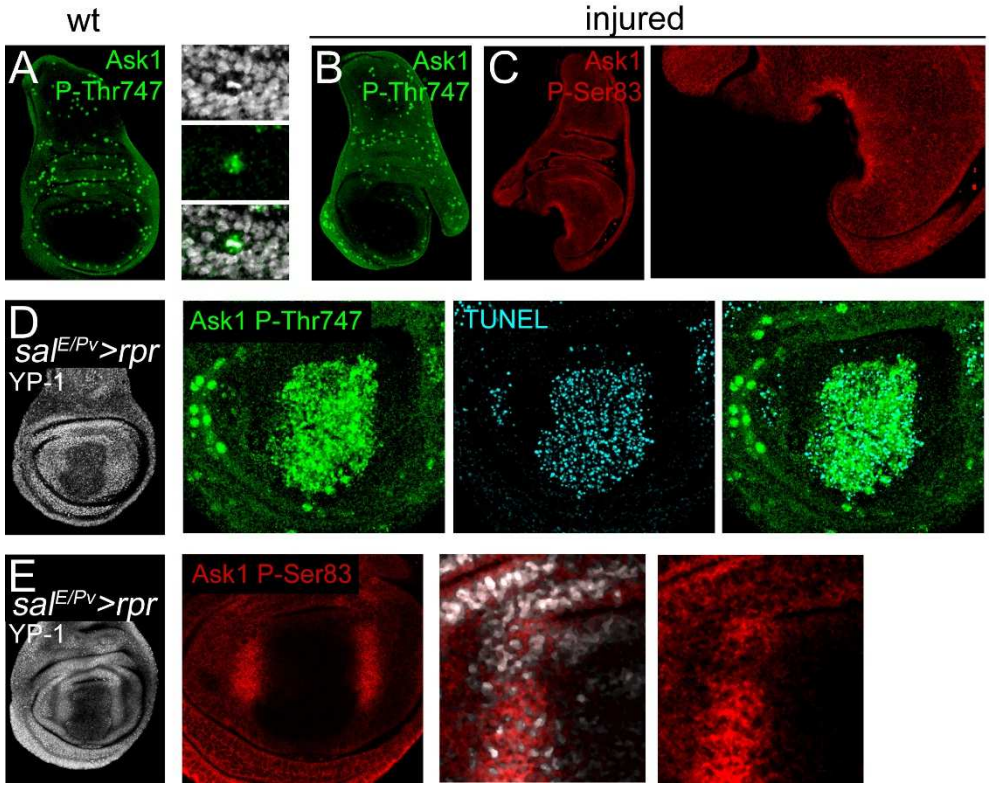

Figure 50. Ask1 is activated in imaginal disc regeneration. (A) Wild-type (n= 14), (B) physically injured discs (n= 7) and (D) *sal$^{E/Pv}$>rpr* (n= 21) stained with Ask1 P-Thr747. Note that Ask1 P-Thr747 is mainly expressed in dying cells. Cell death was labelled with TUNEL assay (in blue). Mitotic cells were labelled too. (C) physically injured discs (n= 6) and (E) *sal$^{E/Pv}$>rpr* (n= 35) stained with Ask1 P-Ser83, only detected in the wound edges and living cells after cell death. YP-1: YO-PRO-1 nuclei staining.

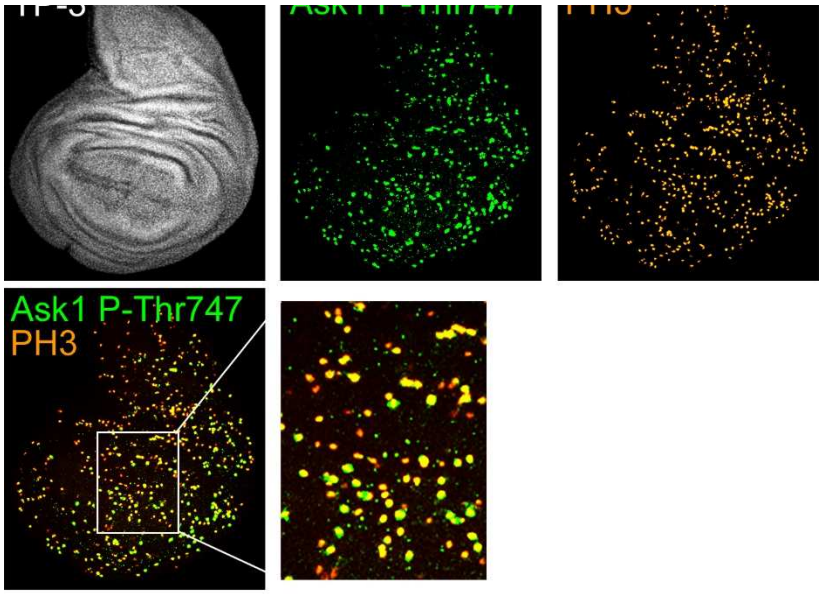

Figure 51. PH3 positive cells present Ask1 P-Thr747 labelling. Wt disc stained for Ask1 P-Thr747 and phospho-Histone 3 (PH3). Merged images show PH3- and Ask1 P-Thr747 positive cells in yellow. White square indicates the magnification of the centre of the wing pouch. TP-3: TO-PRO-3 nuclei.

These observations suggest that after cell death two states of activity can be associated to the disc. One in the apoptotic cells, where the Thr-rich activation domain is highly activated and another in the regenerating cells, where the P-Ser83 of the DUF4071 domain attenuates Ask1 activity.

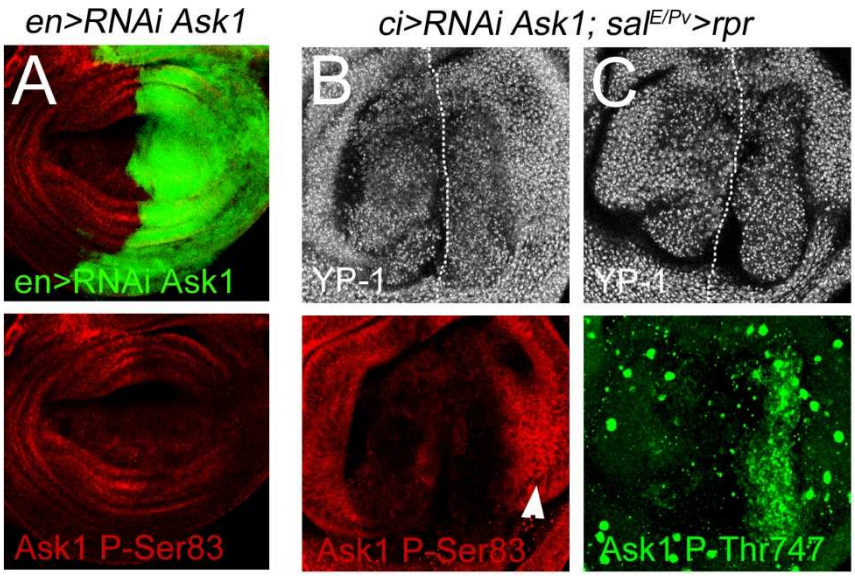

Figure 52. Ask1 RNAi prevents its activation. (A) Inhibition of Ask1 in posterior compartment with an UAS-RNAi construct (*en> RNAi Ask1, GFP*) decreases basal levels of P-Ser83. (B, C) After cell death and simultaneous inhibition of Ask1 with an UAS-RNAi in the anterior compartment (*sal$^{E/Pv}$>rpr, ci> RNAi Ask1)* both P-Ser83 (B) and P-Thr747 (C) are inhibited in this domain. White-dotted line indicates the AP boundary.

Phosphorylation of the Serine 83 in Ask1 depends on PI3K pathway

The AKT kinase, downstream of PI3K and the Insulin/IGF signalling pathway, is responsible for the phosphorylation of ASK1 Ser83 in mammals in order to attenuate its activity (Kim et al. 2001). To determine if a similar event occurs in the fly Ask1 activity, we used a dominant negative form of PI3K/dp110 to drop the activity of the pathway (Figure 53 A, B) and test for Ask1 activity (*ci>dp110^{DN} sal$^{E/Pv}$>rpr*). After PI3K inhibition, Ask1 P-Thr747 was not affected (Figure 53 C), whereas P-Ser83 dropped (Figure 53 D, E). Note that in these experiments the inhibition of the pathway is directed into one compartment, whereas the other acts as control. Moreover, ectopic activation of PI3K (*ap> dp110^{CAAX}*), increased Ask1 P-Ser83 (Figure 54).

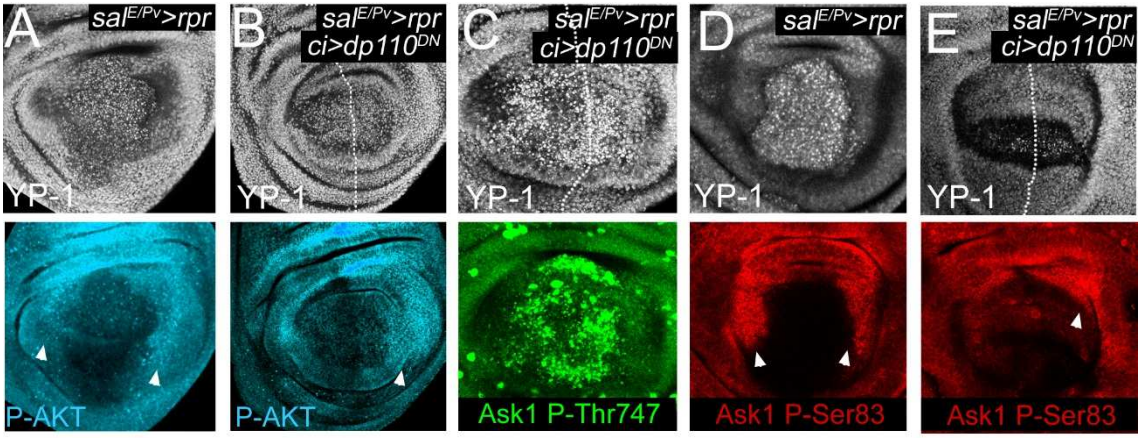

Figure 53. Inhibition of Insulin/IGF signalling impedes Ask1 Ser83 phosphorylation. (A) P-AKT staining after *sal$^{E/Pv}$>rpr* cell death. AKT is activated in living cells surrounding the dead cells. (B) P-AKT staining after *sal$^{E/Pv}$>rpr* cell death and simultaneous inhibition of PI3K in the ci compartment (*sal$^{E/Pv}$>rpr ci>dp110^{DN}*). P-AKT drops off in the anterior compartment. (C) The activation of the Ask1 Thr-rich domain does not vary after PI3K inhibition. (D) Control for Ask1 P-Ser83 staining after *sal$^{E/Pv}$>rpr* cell death. (E) Ask1 P-Ser83 decrease in the anterior compartment of *sal$^{E/Pv}$>rpr ci>dp110^{DN}* discs, indicating that Insulin/IGF signalling controls Ser83 phosphorylation. YP-1: YO-PRO-1 nuclear staining. White arrows indicate activation of proteins in these territories.

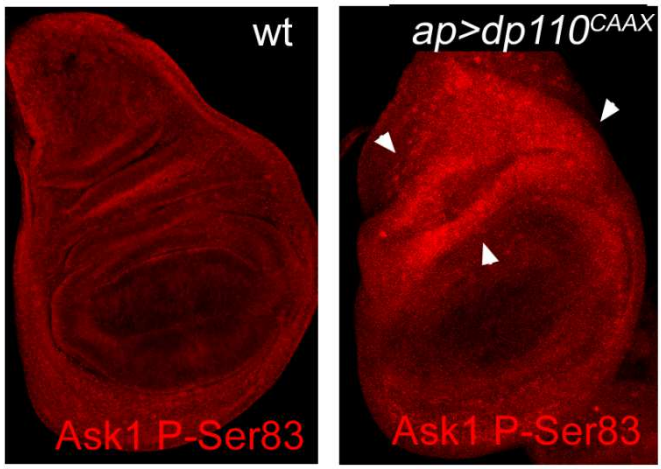

Figure 54. Insulin/IGF signalling promotes Ask1 Serine 83 phosphorylation. Left image: wt disc stained with Ask1 P-Ser83. Right image: Overexpression of PI3K in the dorsal compartment of a disc with the *dp110^{CAAX}* construct (*ap>dp110^{CAAX}*) increases Ask1 P-Ser83. White squares show magnification of those areas below. White arrows indicate Ask1 P-ser83 activation in these territories.

We also scored the effects on wing regeneration after blocking the PI3K pathway. In *akt*^{1} heterozygous mutant background, only 44% of the total wings could regenerate properly. The dominant negative form of PI3K/dp110 (*ci>dp110*^{DN} *sal*$^{E/Pv}$*>rpr*) also impaired regeneration. Double heterozygous combinations of *akt*^{1} and *ask1*^{MB06489} or *ask1*^{M102915} severely block regeneration too (Figure 55).

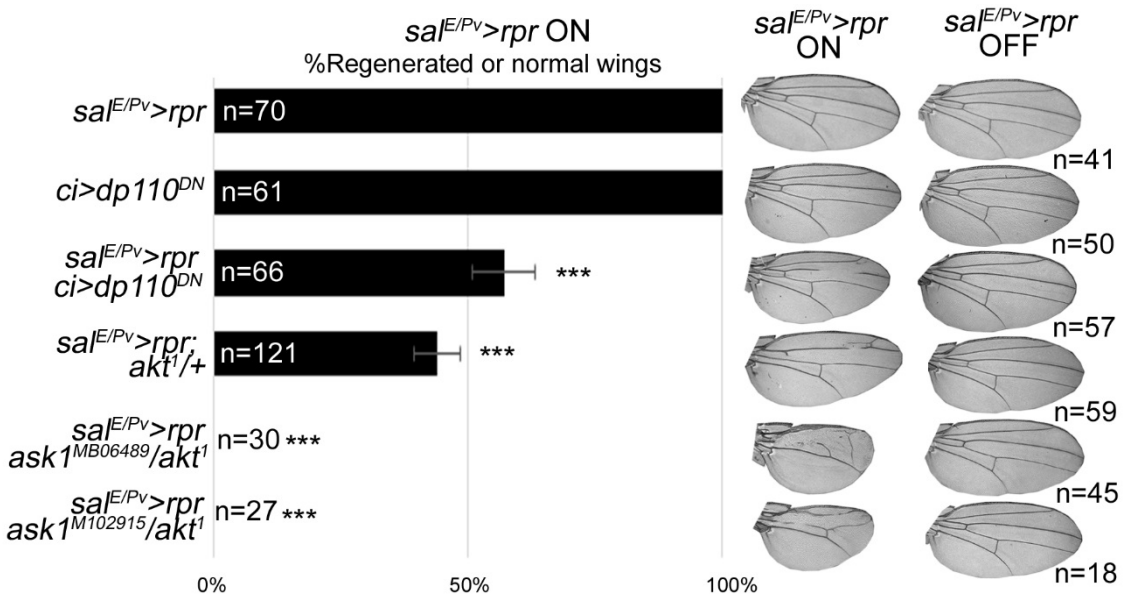

Figure 55. Insulin/IGF signalling is necessary for proper imaginal disc regeneration. Percentage of fully regenerated wings after genetic ablation and PI3K pathway inhibition alone or in combination with *ask1* mutant backgrounds (indicated genotypes). Right: Examples of wings with full regeneration (control *sal*$^{E/Pv}$*>rpr* ON) and incomplete regeneration after *sal*$^{E/Pv}$*>rpr*. In control wings *sal*$^{E/Pv}$*>rpr* OFF, no *rpr*-ablation was induced (kept at 17ºC). Error Bars indicate Standard Deviation. ***P<0.001.

Activation of Ask1 depends on oxidative stress

To test whether Ask1 activation is ROS-dependent, we depleted ROS production and examined Ask1 activation (Figure 56 A). We fed *sal$^{e/Pv}$>rpr* larvae with food supplemented with NAC (N-acetyl cysteine), a potent non-enzymatic scavenger that decreases ROS production. After cell death induction, we found a significant decrease of P-Thr747 (Figure 56 B, C). Similarly, the localization of Ask1 P-Ser83 in living cells was also reduced in NAC-fed larvae (Figure 56 D, E).

In addition, we fed larvae with H_2O_2-supplemented food for 2 hours and observed a significant increase in P-Thr747 and P-Ser83 (Figure 57). This increase was not detected in *ask1^{MB06489}* mutant discs (Figure 57). In addition we performed the same experiments with the ER stressor tunicamycin (Nishitoh et al. 2002), and found similar results. Summarizing, Ask1 activity in Drosophila imaginal discs is sensitive to oxidative stress.

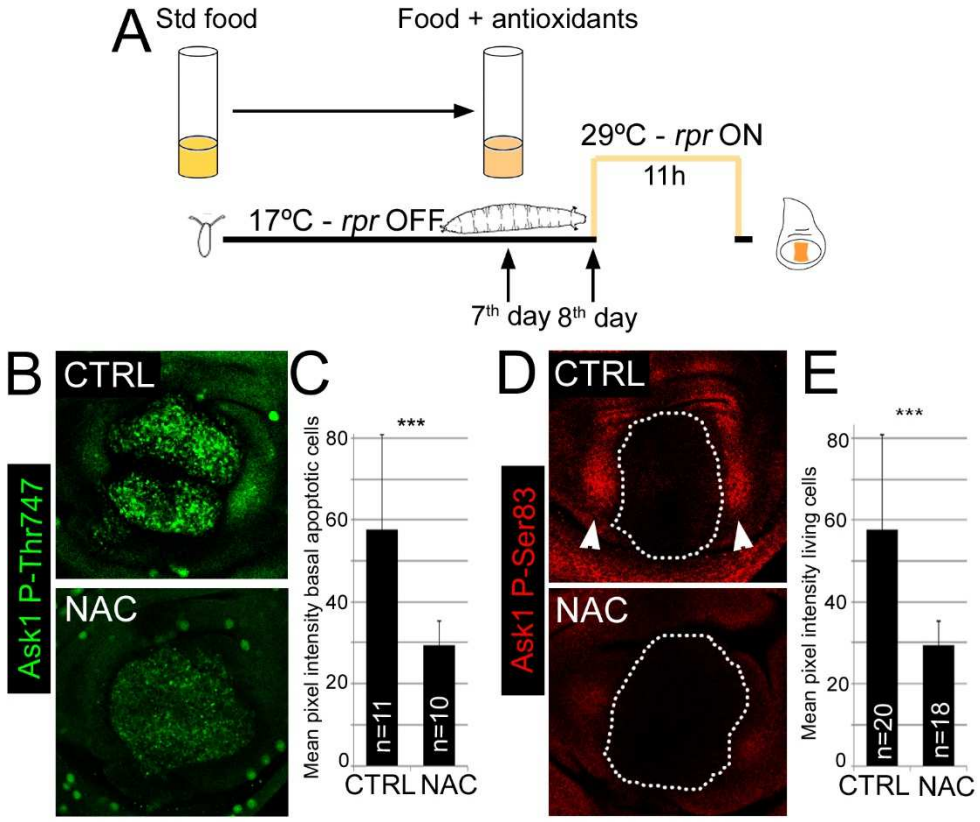

Figure 56. Activation of Ask1 depends on oxidative stress. (A) Protocol for antioxidant treatment before cell death induction. Larvae were transferred to NAC-supplemented food 24 hours before cell death induction. After *sal$^{E/Pv}$>rpr* cell death, discs were analysed. (B) Images of Ask1 P-Thr747 after *sal$^{E/Pv}$>rpr* induction in Standard or NAC-supplemented food. (C) Mean pixel intensities of Ask1 P-Thr747 fluorescent labelling from *sal$^{E/Pv}$>rpr* discs fed with Standard (dead cells 94.01±17.04; S.D., living cells 53.15±8.53; S.D.) or NAC-supplemented food (dead cells 31.07±9.38; S.D., living cells 23.75±5.99; S.D.). (D) Images of Ask1 P-Ser83 after *sal$^{E/Pv}$>rpr* induction in Standard or NAC-supplemented food. White dotted line indicates the dying domain. White arrowheads show Ask1 P-Ser83 in the living cells. (E) Mean pixel intensities of Ask1 P-Ser83 fluorescent labelling from *sal$^{E/Pv}$>rpr* discs fed with Standard (living cells 57.56±23.27; S.D.) or NAC-supplemented food (living cells 29.54±5.92; S.D.).

These observations point to Ask1 as a pro-survival molecule that integrates the PI3K and ROS signals to maintains cellular homeostasis under stress conditions. To further dig into this we asked if under oxidative stress conditions Ask1 is required for life span. To this aim, we monitored the life span of *ask1*^{MB06489} mutant flies in H_2O_2-supplemented food and tunicamycin-supplemented food. As non-experimental group, *w*^{118} flies were scored. Five replicates were carried out independently. In minimal food, not significant changes were appreciated between strains (Figure 58). However, in H_2O_2- or in tunicamycin-food, life span of *ask1*^{MB06489} flies was strongly compromised (Figure 58).

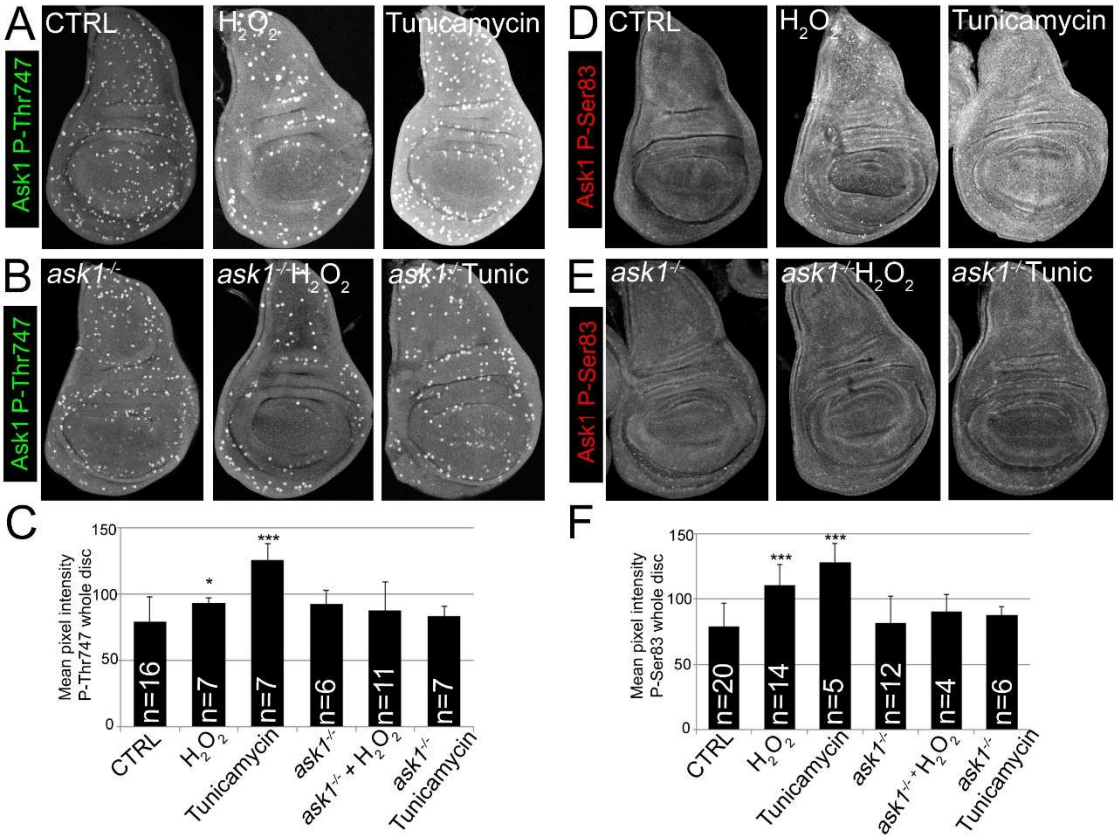

Figure 57. Oxidative stress activates Ask1. (A, B) Wing imaginal discs from wt (A) or *ask1*^{MB06489} (B) flies labelled with Ask1 P-Thr747 belonged to larvae fed with Standard food, H_2O_2- and Tunicamycin-supplemented food. (C) Ask1 P-Thr747 Mean pixel intensity of discs from larvae fed with Standard food (wt 79.36±18.65; S.D. and *ask1*^{MB06489} 92.92±9.75; S.D.), H_2O_2- (wt 93.37±3.87; S.D. and *ask1*^{MB06489} 83.66±7.11; S.D.) and Tunicamycin-supplemented food (wt 125.49±12.51; S.D. and *ask1*^{MB06489} 87.99±21.38; S.D.). (D, E) Wing imaginal discs from wt (D) or *ask1*^{MB06489} (E) flies labelled with Ask1 P- Ser83 belonged to larvae fed with Standard food, H_2O_2- and Tunicamycin-supplemented food. (F) Ask1 P-Ser83 Mean pixel intensity of discs from larvae fed with Standard food (wt 79.14±17.69; S.D. and *ask1*^{MB06489} 81.83±20.25; S.D.), H_2O_2- (wt 110.89±15.43; S.D. and *ask1*^{MB06489} 87.51±6.40; S.D.) and Tunicamycin-supplemented food (wt 128.35±14.42; S.D. and *ask1*^{MB06489} 90.27±13.26; S.D.). *P<0.05., ***P<0.001. Error bars indicate Standard Deviation.

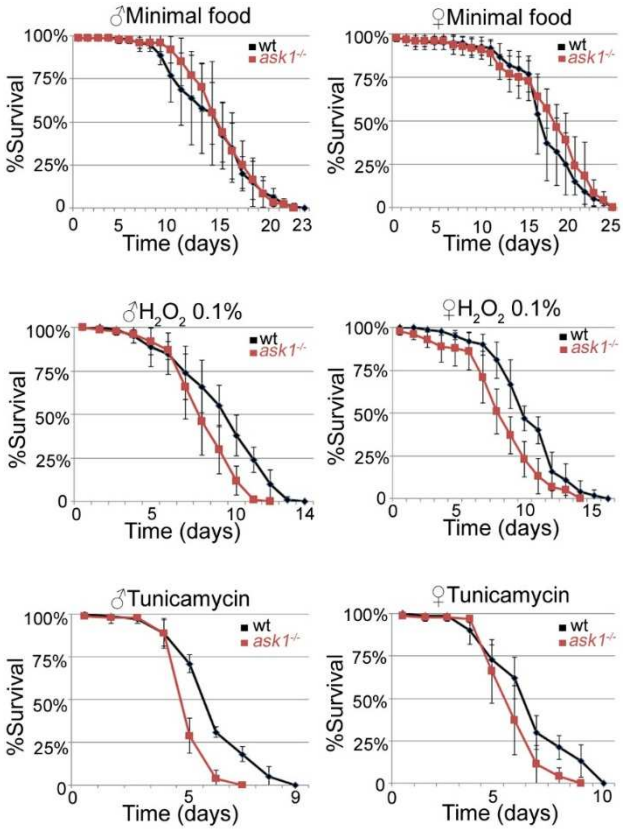

Figure 58. Ask1 acts as a pro-survival molecule. Longevity determination of *ask1*^{MB06489} homozygous mutant flies versus *w*^{118} flies in minimal food, 0.1% H_2O_2 and 1µg/ml Tunicamycin-supplemented food. In minimal food, no significant changes were appreciated between both strains, meanwhile *ask1*^{MB06489} flies are significantly more sensitive to H_2O_2 and Tunicamycin oxidative treatment compared to control flies Error bars showed Standard Deviation.

Ask1 promotes JNK and p38 activation

Next, we examined whether Ask1 operates upstream the SAPKs. We blocked Ask1 in the anterior compartment and used the posterior as internal control for the same disc. When cell death is driven with the *sal*$^{E/Pv}$*>rpr* system, which operates in the central zone of anterior and posterior compartments, activated p38 (P-p38) is found in surviving cells of both compartments (Figures 34 E, 59 A). However, *ci>RNAi Ask1 sal*$^{E/Pv}$*>rpr* discs showed P-p38 only in the posterior compartment (Figure 59 B).

We also analysed whether Ask1 was required for SAPK after physical damage. Few minutes after physical injury, P-p38 appeared in the wound edges (Figure 34 B and 59 C). However, in injured *en>GFP, RNAi Ask1* discs, we found that p38 is activated strongly in the anterior compartment (wt) comparing with the posterior (Figure 59 C, D).

The effects of Ask1 on JNK activity were monitored using Mmp1 expression as read out of the pathway (Uhlirova & Bohmann 2006). After cell death in *sal$^{E/Pv}$>rpr* discs, Mmp1 appeared both in dying and in living domain of both compartments (Figure 59 E). Nevertheless, in *ci>RNAi Ask1 sal$^{E/Pv}$>rpr* discs, a severe decrease of Mmp1 staining in the anterior compartment was found (Figure 59 F). Likely, cut *en>GFP, RNAi Ask1* discs resulted in a decrease of Mmp1 in the posterior compartment (Figure 59 G, H). In summary, these results demonstrated that Ask1 is upstream the p38 and JNK activation in regeneration.

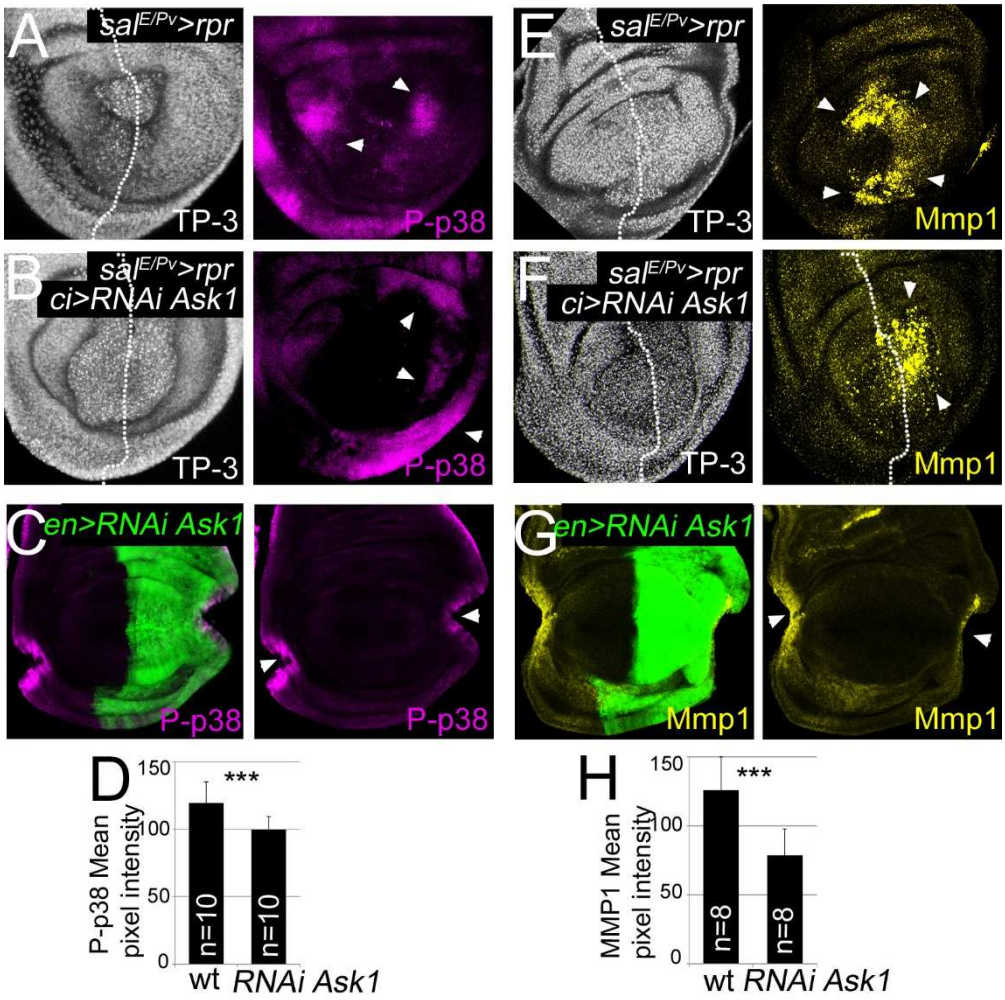

Figure 59. Ask1 promotes JNK and p38 signalling after damage. (A) P-p38 staining after *sal$^{E/Pv}$>rpr* induction. P38 is activated in living cells around the dying domain (n= 14). (B) P-p38 staining after *sal$^{E/Pv}$>rpr* induction and simultaneously inhibition of Ask1 in the anterior compartment (*ci>RNAi Ask1*). Note that p38 is only activated in the posterior compartment (n=7). (C, D) RNA interference of Ask1 inhibits p38 after injury. The *UAS-RNAi Ask1* was activated in the posterior compartment together with *UAS-GFP* (green). Two injuries were inflected with tungsten needles in Schneider's medium, one in the anterior and one in the posterior compartment. (C) For P-p38 staining discs were immediately fixed after injury. (D) Quantification of P-p38 activation in the wound site. P-38 significantly decreased after Ask1 inhibition in the posterior compartment. (E) Mmp1 staining after *sal$^{E/Pv}$>rpr* induction. Mmp1 is activated in dying and living cells (n=16). (F) Mmp1 staining in *sal$^{E/Pv}$>rpr ci>RNAi Ask1* discs (n= 14). Mmp1 is only activated in the posterior compartment. TP-3: TO-PRO-3 nuclei staining. White dotted line divides the discs into anterior (Ask1 inhibition) and posterior (wt) compartments. (G) RNA interference of Ask1 inhibits JNK after injury. For Mmp1 staining discs were first cut and cultured for 5 hours. (H) Quantification of Mmp1 in the wound site. White arrows indicate the wound site. Error Bars indicate Standard Deviation. ***P<0.001.

TNF/Eiger is involved in JNK activation in regeneration

Tumour necrosis factor (TNF) is a cytokine that acts upstream of JNK pathway. In mammals, TNF could activate ASK1, while there are ROS (Tobiume et al. 2001; Liu et al. 2000; Fujino et al. 2007; Nishitoh et al. 1998; Saitoh et al. 1998). Moreover, when cells are incubated with TNF, they generate intracellular ROS, which is consistent with Ask1 activation (Lin et al. 2004; Goossens et al. 1995).

Drosophila has a single orthologue of TNF, called *eiger* (e*gr*) (Igaki et al. 2002; Moreno et al. 2002). Egr is a membrane protein present in cells as a zymogen. To be activated, it needs to be cleaved and then, it can bind to its receptors Wengen (Wgn) (Kanda et al. 2002) and Grindelwald (Grnd) (Andersen et al. 2015). Both receptors have been proposed to operate upstream the JNK pathway.

As a previous link was established between TNF and ASK1, we first scored wing regeneration after *sal$^{E/Pv}$>rpr* induction in different mutant backgrounds of TNF/Egr signalling. We found that homozygous *grnd^{minos}* animals as well as *ci or ap>RNAi grnd sal$^{E/Pv}$>rpr* regenerated entire wings. However, strong defects were detected in *egr^{3}*, in egr RNAi or in *grnd^{extra}*, a transgene which binds to *egr* but does not transduce the signal (Andersen et al. 2015) (Figures 60, 61). The resulting wings lacked some sectors and presented notches in wing margins. We also found anomalous regeneration after *wgn* inhibition using *wgn* RNAi (*ci* or *ap>RNAi wgn sal$^{e/Pv}$>rpr*) (Figures 60, 61).

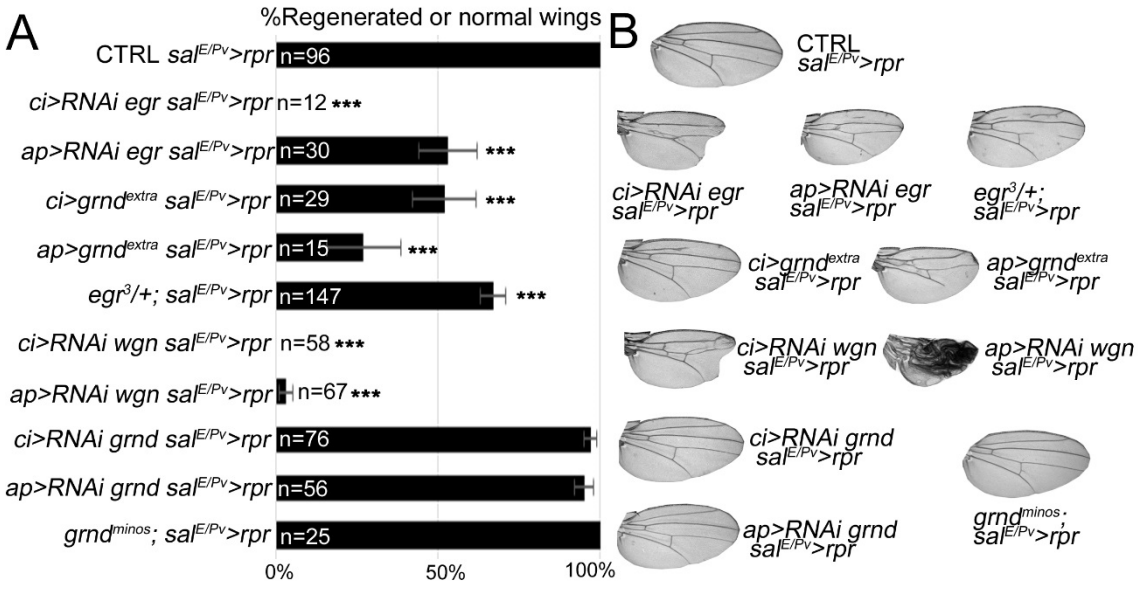

Figure 60. TNF/Eiger signalling is necessary for proper regeneration. (A) Percentage of fully regenerated wings in Eiger signalling mutant backgrounds after genetic ablation. (B) Examples of wings with full regeneration (control *sal$^{E/Pv}$>rpr*) and incomplete regeneration (indicated genotypes) after *sal$^{E/Pv}$>rpr*. Error Bars indicate Standard Deviation. ***P<0.001.

.

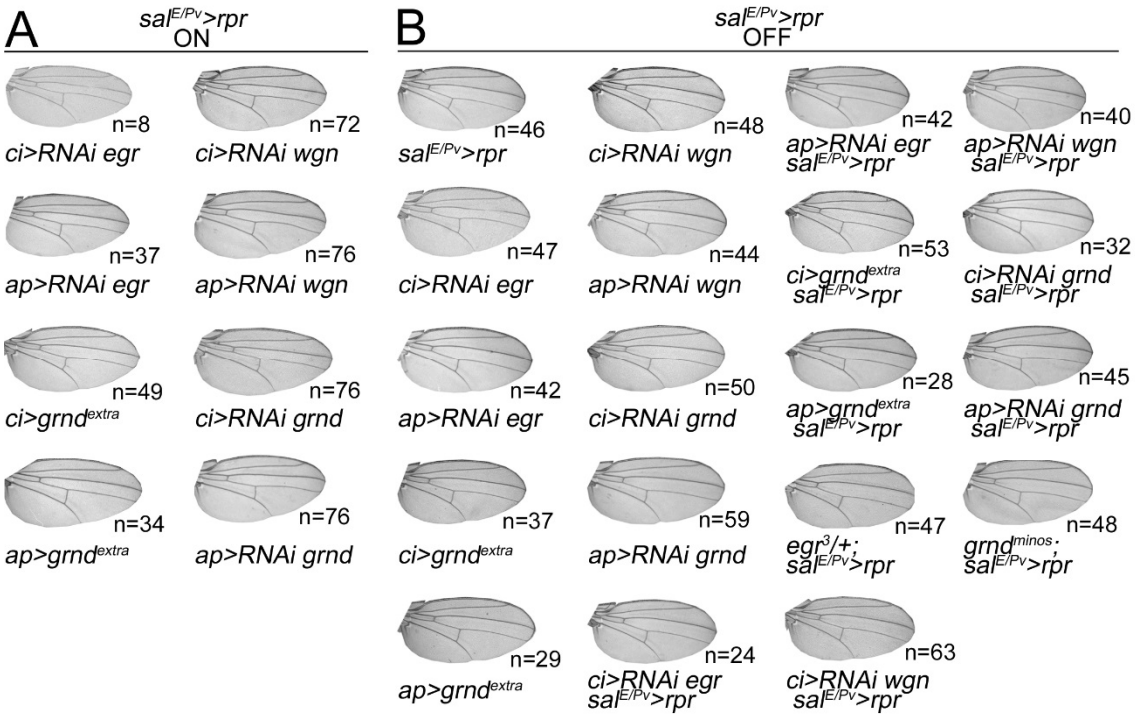

Figure 61. Control wings for TNF/Egr signalling is necessary for proper regeneration. (A) Examples of control wings for Figure 60 A, B in which the RNAi construct was activated for 11h (29°C ON). (B) Examples of control wings of Figure 60 A, B in which no *rpr*-ablation was induced (kept at 17°C, *sal$^{E/Pv}$>rpr* OFF) for the indicated genotypes. The 'n' number indicates the number of wings analyzed per each indicated phenotype.

To be sure that Egr could act through Wgn, we expressed ectopically the soluble form of Egr in *spalt$^{E/Pv}$* domain (*sal$^{E/Pv}$>ecto-eiger*). In those conditions Egr promotes cell death, and 100% of adult wings were smaller and presented vein defects (Figure 62). However, *wgn* inhibition with an UAS-RNAi construct (*sal$^{E/Pv}$>ecto-eiger, RNAi wgn*) rescues partially the phenotype associated with Egr-dependent cell death (Figure 62). Those experiments confirmed that Egr could act through Wgn, and that both are implicated in wing imaginal disc regeneration.

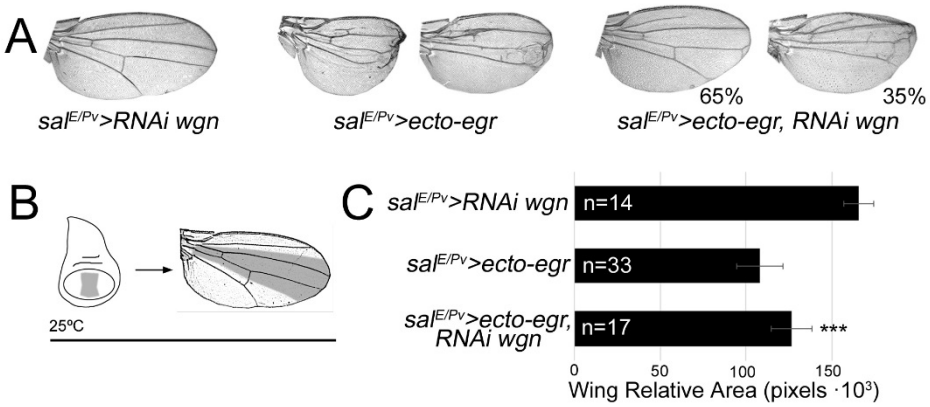

Figure 62. Loss of Wgn partially rescues Egr-induced apoptosis. (A) Wgn Inhibition in *spalt$^{E/Pv}$* domain does not affect wing size or vein pattern. Ectopic expression of *ecto-egr* in *spalt$^{E/Pv}$* domain promotes autonomous and non-autonomous cell death, thus wings are reduced in size and presented vein defects. Wgn inhibition partially rescues Egr-induced cell death (65% wings partially recovered). (B) Sketch showing *spalt$^{E/Pv}$* domain in imaginal disc and adult wing, were transgenes are expressed at 25 degrees. (C) Wing size of indicated genotypes. Error Bars indicate Standard Deviation. ***P<0.001

To confirm that Egr and Wgn are necessaries for JNK signalling, we analysed JNK after its inhibition. We used the *sal$^{E/Pv}$-LHG lexO-rpr* to induce apoptosis and simultaneously interfered with *UAS-RNAi egr* and/or *UAS-RNAi wgn* driven by *ci-Gal4*. Then we utilized Mmp1 staining as a read-out of JNK activation.

We also observed that Mmp1, which in flies is downstream of JNK, dropped after *egr* or *wgn* inhibition (Figure 63 A-C). Moreover, in physically injured *en>RNAi wgn* discs, the *TRE-red* reporter significantly decrease after *wgn* inhibition (Figure 63 D-E), as well as Mmp1 in injured *egr^{3}* and *wgn^{KO}* mutant discs (Figure 63 F-I).

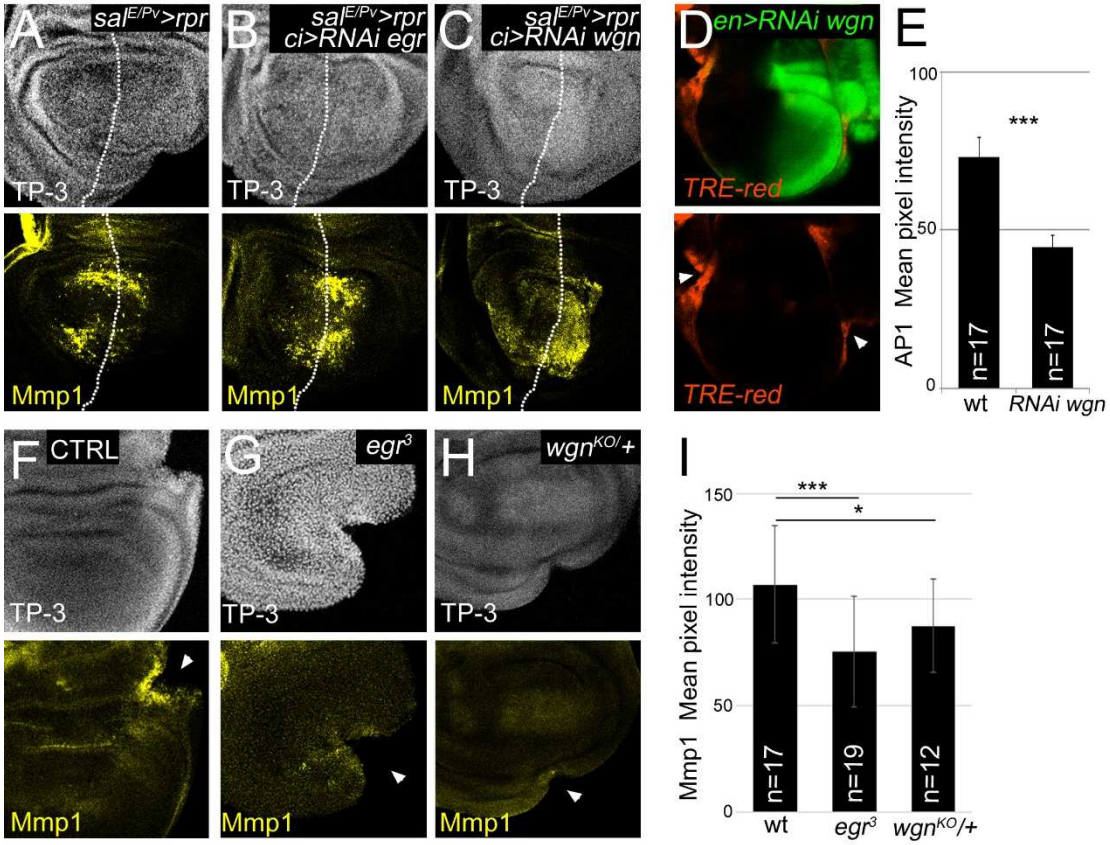

Figure 63. TNF/Eiger activates JNK in imaginal disc regeneration. (A) Mmp1 staining after *sal$^{E/Pv}$>rpr* induction. In *sal$^{E/Pv}$>rpr* discs Mmp1 is activated in *sal$^{E/Pv}$* zone. (B, C) After *sal$^{E/Pv}$>rpr* induction and simultaneous inhibition of *egr* or *wgn* in the anterior compartment (*ci>RNAi egr/wgn*) Mmp1 drops off. White dotted line divides the discs into anterior (*egr* or *wgn* inhibition) and posterior (wt) compartments. (D, E) RNA interference of *wgn* decrease JNK signalling after injury. The *UAS-RNAi wgn* was activated in the posterior compartment together with *UAS-GFP* (green). Two injuries were inflected with tungsten needles in Schneider's medium, one in the anterior and one in the posterior compartment. Note that *TRE-red* reporter expression decrease after *wgn* inhibition. (F-I) wt, *egr^{3}* and *wgn^{KO}/+* cut and cultured discs stained for Mmp1. Note that in *egr^{3}* and *wgn^{KO}* background Mmp1 expression dropped off. White arrows indicate the wound site. TP-3: TO-PRO-3 nuclei staining. ***P<0.001. *P<0.05.

Ask1 and p38 activation are independent of TNF/Eiger

Once we found a second input for JNK activation after damage, we assessed if Ask1 activation depended on TNF/Egr too. After *sal$^{E/Pv}$>rpr* cell death and simultaneous inhibition of *wgn* with an UAS-RNAi construct in *ci* compartment (*ci>RNAi wgn sal$^{e/Pv}$>rpr* disc), Ask1 P-Ser83, P-Thr747 and P-p38 appeared as in *sal$^{E/Pv}$>rpr* control discs (compare Figure 64 with Figures 50 and 59). Moreover, in physically injured *en>RNAi wgn* discs, P-p38 did not change after Wgn inhibition (Figure 64 D, E).

Altogether, we confirmed that there are two inputs for JNK in regeneration, Eiger through Wengen, and ROS-Ask1 module, which act independently.

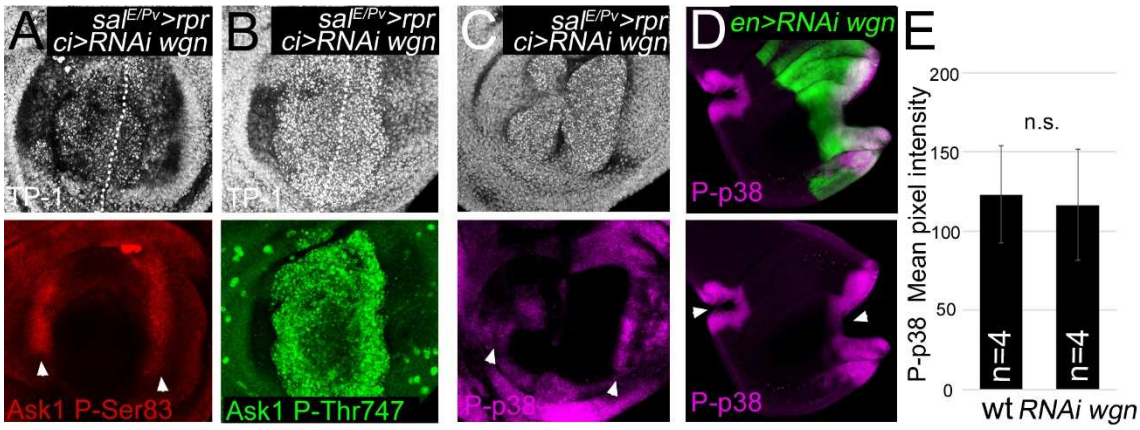

Figure 64. Ask1 and p38 activation are independent of TNF/Eiger. (A, B, C) Ask1 P-Ser83, P-Thr747 and P-p38 staining after *sal$^{E/Pv}$>rpr* induction and simultaneous inhibition of *wgn* in the anterior compartment (*sal$^{E/Pv}$>rpr ci>RNAi wgn*). Note that the pattern does not change comparing to *sal$^{E/Pv}$>rpr* controls in Figures 49, 51, 53 and 56. White arrows show P-Ser83 and P-p38 in living cells and white dotted line establish the A-P boundary. (D, E) P-p38 does not vary in injured *en>RNAi wgn* discs.

DISCUSSION

The results of this work contribute to the understanding of how regeneration is initiated. We demonstrated the activation of a stress-responsive module upon cell death or physical damage. This module consists of an early boost of ROS that triggers non-deleterious levels of JNK and p38 MAPKs necessaries for the expression of Upd and JAK/STAT signalling, which drives regeneration. Moreover, Ask1 integrates the burst of ROS with JNK and p38 activation to initiate regeneration. Insulin signalling attenuates Ask1 activity, very likely to prevent deleterious effects of an excess of Ask1 and JNK, and promotes survival. The TNF/Egr ligand activates JNK through Wgn independently of Ask1. Therefore, JNK is activated, at least, by two different inputs, oxidative stress and TNF (Figure 65).

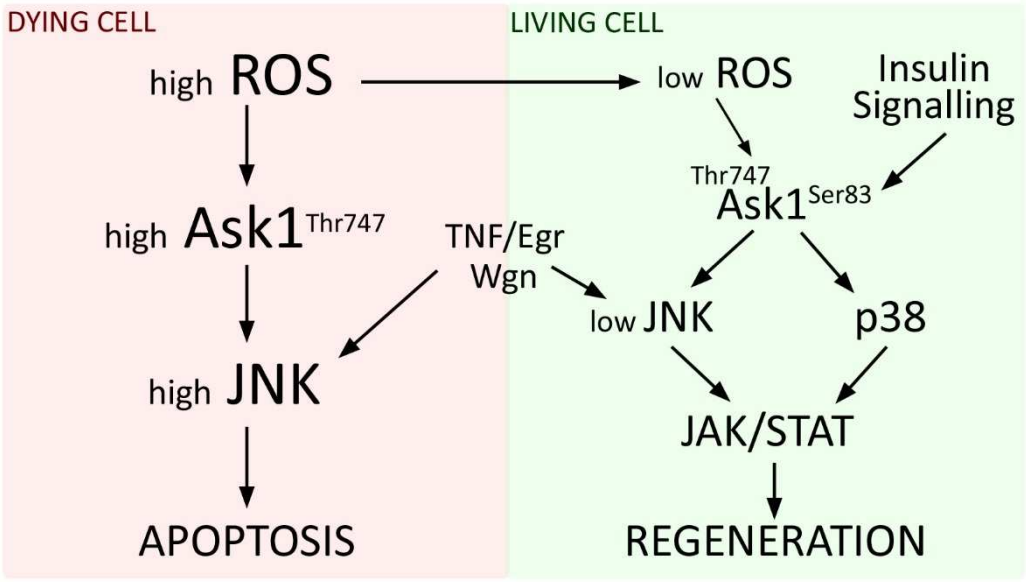

Figure 65. Model for imaginal disc regeneration. Dying cells present prominent levels of ROS that activate deleterious Ask1 and JNK, which in turn promote the pro-apoptotic program. However, in living cells, non-deleterious ROS activate JNK and p38 MAPKs necessaries for the expression of Upd and JAK/STAT signalling. Moreover, Ask1 integrates ROS signalling with JNK and p38 activation. Insulin signalling attenuates Ask1 activity and promotes survival. The TNF/Egr ligand activates JNK through Wgn independently of Ask1, therefore JNK is activated, at least, by two different inputs. All those molecules form a stress-responsive module in living cells to initiate regenerative program and replace the missing tissue.

Towards the initiation of imaginal disc regeneration: ROS

After damage, **ROS** signalling is conserved within the animal kingdom as a mechanism to trigger regeneration (Loo et al. 2012; Yoo et al. 2011; Yoo et al. 2012; Wittmann et al. 2012; Gauron et al. 2013; Han et al. 2014; Niethammer et al. 2009; Love et al. 2013; Ferreira et al. 2016; Zhang et al. 2016; Pirotte et al. 2015; Wenger et al. 2014; Moreira et al. 2010; Fogarty et al. 2016; Santabárbara-Ruiz et al. 2015). Our results demonstrated that ROS are produced in the wound site and propagated throughout the living cells, both after cell death and physical injury.

We concluded that the burst of ROS is necessary to initiate regeneration, chiefly because larvae fed with antioxidants cannot regenerate properly. Cells surrounding the dying domain should proliferate to recover lost tissue (Bergantiños et al. 2010), and we found that antioxidant treatment affects regenerative growth. Acordingly, low doses of H_2O_2 and superoxide accelerate cell proliferation in a wide variety of cancer cell types (reviewed in Liou & Storz 2010). Moreover, ROS can upregulate the mRNA levels of Cyclins that contribute to the G1 to S phase transition in breast cancer cells, including cyclin B2, cyclin D3, cyclin E1 and cyclin E2 (Felty et al. 2005). Conversely, antioxidants inhibit tumour cell proliferation (Behrend et al. 2003). In plants, ROS have a role in cell cycle activation of differentiated leaf cells, having a positive effect on the plant cell cycle machinery (Fehér et al. 2008). Our observations point to that an initial, very likely transitory, burst of ROS is key to activate the first signals that trigger regeneration and tissue repair.

The same results were obtained after enzymatic manipulation of ROS. Superoxide dismutase (**SOD**) catalyses the dismutation of superoxide anion into oxygen and hydrogen peroxide. In the presence of hydrogen peroxide, Catalase (**Cat**) catalyses its breakdown into water and oxygen. The NADPH oxidase **DUOX** is activated by calcium waves in embryonic epidermal wounds and acts as a source of H_2O_2, recruiting macrophages to the wound within minutes (Razzell et al. 2013). Misexpression of those enzymes impairs regeneration. We thought that the low percentage of non-regenerated wings after enzymatic inhibition compared to the antioxidant treatment is because we only activated the transgenes for 11 hours, the same time as we induced cell death in $sal^{e/Pv}$ domain. As DUOX inhibition leads to only 75% of wings recovered, we hypothesized that wound-induced calcium flashes are also occurring in injured imaginal discs to activate DUOX and trigger H_2O_2, which could act autonomously and non-autonomously to initiate an inflammatory response involving haemocytes.

In fact, we would like to include in this discussion some unpublished results that support our findings and our understanding of initial regeneration steps. For example, preliminary experiments in our laboratory pointed out that **calcium** flashes occur in injured or damaged

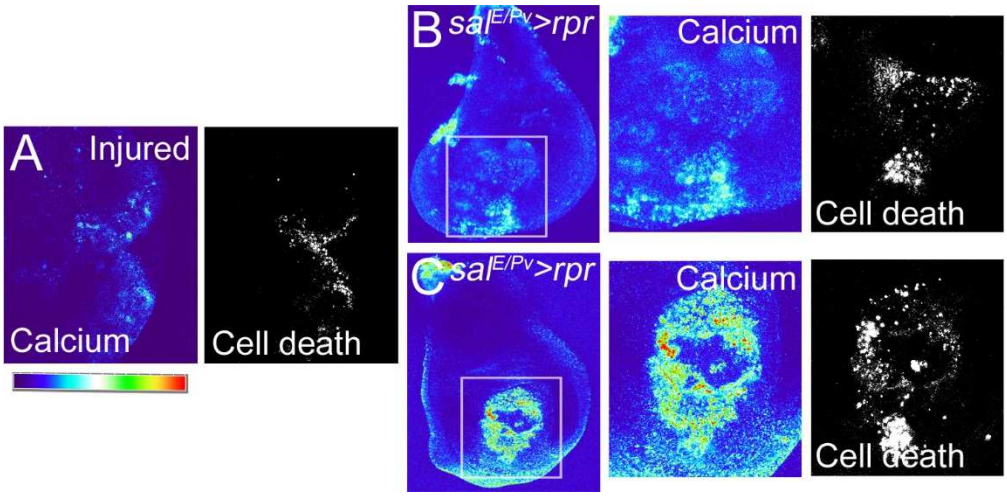

Figure 66. A burst of calcium is found after physical injury or cell death. (A) Injured imaginal discs show high Calcium levels in necrotic cells in the wound site and lower levels in the surrounding tissue. (B, C) Two examples of Calcium imaging after $sal^{e/Pv}$>*rpr* cell death. Thermal LUT indicates pixel intensity (red high, blue low). Fluo-4 was used to label Calcium and TO-PRO-3 to label cell death *in vivo*.

imaginal tissues (Figure 66). We used the Fluo-4 calcium indicator *ex vivo*, which emits fluorescence upon Ca^{2+} binding. We found elevated levels of calcium in dying cells, as well as low levels in the surrounding living tissue (Figure 66). These results have been already published by others (Restrepo & Basler 2016).

Thus, as suggested by others, Ca^{2+} activates DUOX, in turn DUOX produces H_2O_2, and H_2O_2 attracts macrophages (Love et al. 2013; Niethammer et al. 2009; Razzell et al. 2013). Therefore, we decided to deplete **haemocytes** from the whole larvae and analyse wings after *sal$^{e/Pv}$>rpr* cell death. In the absence of cell death, removal of haemocytes (*hml>rpr* larvae) does not show any phenotype in the wing. However, upon cell death, only about 60% of the wings regenerated properly (Figure 67). Moreover, in heterozygous *hemolectin* (*hml^{MB01940}*), a gene crucial for haemostasis and coagulation after wounding (Chang et al. 2012; Goto et al. 2003), regeneration is not fully achieved (Figure 67, unpublished observations). These findings indicate that, in addition to the epithelial response found in this thesis, haemocytes also contribute to repair, although their function and mechanism is still unknown. Similar observations have been published by others (Fogarty et al. 2016).

Another key point that needs to be addressed is how ROS are produced and how they spread between cells. We used two dyes to detect general ROS in living tissues, the CellROX Green Reagent, which is an indicator of oxidative stress in living cells and the cell-permeant H2DCFDA which upon oxidation is converted to the highly fluorescent DCF. Both reagents are non-fluorescent or very weakly fluorescent when reduced and upon oxidation exhibit strong

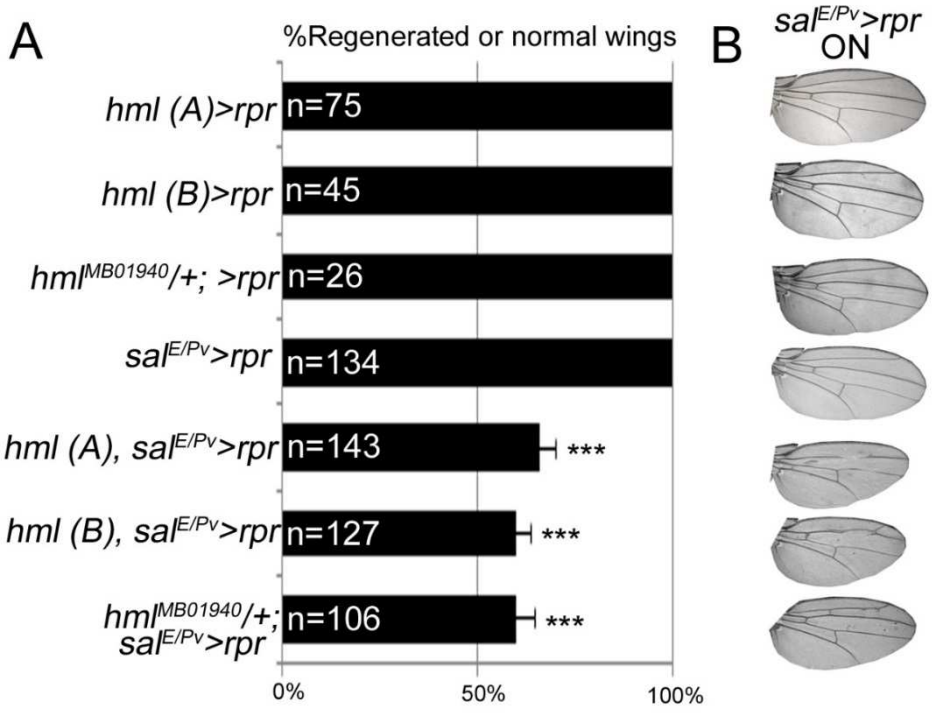

Figure 67. Haemocytes are required in imaginal disc regeneration. (A) Percentage of fully regenerated wings after haemocyte and wing imaginal disc ablation. Note that adult wings are normal in the absence of haemocytes. However, the wings cannot regenerate properly if haemocytes are ablated too. (B) Examples of wings with full regeneration and incomplete regeneration (indicated genotypes) after *sal$^{E/Pv}$>rpr*. Error Bars indicate Standard Deviation. ***P<0.001.

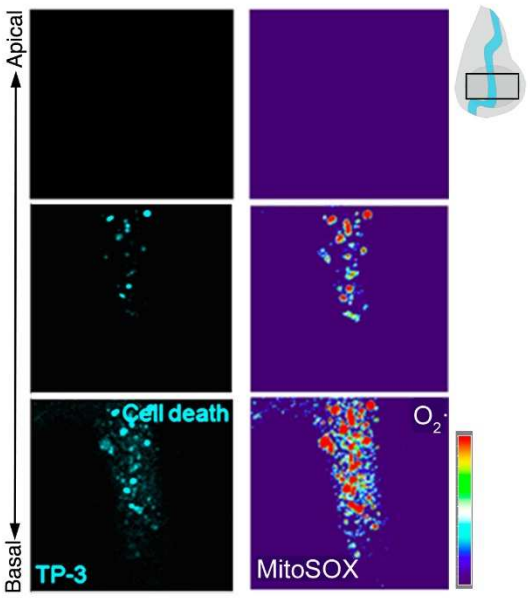

Figure 68. Superoxide is only present in dying cells. After *ptc>rpr* cell death, MitoSOX indicator, which detects the mitochondrial superoxide, was only found in dying cells (TP-3 positive). Thermal LUT shows pixel intensity (red high, blue low). Images correspond to different sections of the same disc, from the basal side (bottom images) to the apical side (upper images).

fluorogenic signal. They detect a wide range of ROS and therefore we cannot discriminate between membrane oxidases or mitochondrial origin. However, since Rpr acts on mitochondria (Freel et al. 2008; Abdelwahid et al. 2007), mitochondrial alterations could cause the burst of ROS in apoptotic cells. Of note, we observed that high ROS levels are associated with elevated levels of JNK in apoptotic cells. Preliminar experiments in the laboratory suggested that the superoxide anion is concentrated only in dying cells (Figure 68). To achieve that, we used the **MitoSOX** indicator, which is a fluorogenic dye for highly selective detection of superoxide, which is generated as a byproduct of oxidative phosphorylation, primarily in mitochondria. Lethal bursts in superoxide production have been implicated in cardiovascular and neurodegenerative diseases (reviewed in Schieber & Chandel 2014), which is consisted with MitoSOX labelling only in dying cells.

As **H_2O_2** has been suggested as signalling molecule (Veal et al. 2007), we propose the use of specific dyes and inhibitors of this molecule to decipher its properties in regeneration.

Mitochondrial superoxide can be converted into H_2O_2 in the cytoplasm by the action of SOD, thus one possibility is that the source of general ROS after damage would be the mitochondria. Another possibility, is that damage induced calcium waves propagated via **gap junctions** (Narciso et al. 2015; Restrepo & Basler 2016) could activate DUOX and subsequently generate H_2O_2 (Razzell et al. 2013). This ROS could propagate across **aquaporin** channels. Aquaporins have been proposed, in addition to water, as ''open doors'' by which ROS could break through cell membranes (Bienert & Chaumont 2014; Miller et al. 2010; Ferreira et al. 2016). In a first approach, current work of our lab is pointing to that both innexins and aquaporins are required for regeneration (Figure 69). Experiments to detect ROS diffusion into cells will reveal potential new targets to modulate regeneration.

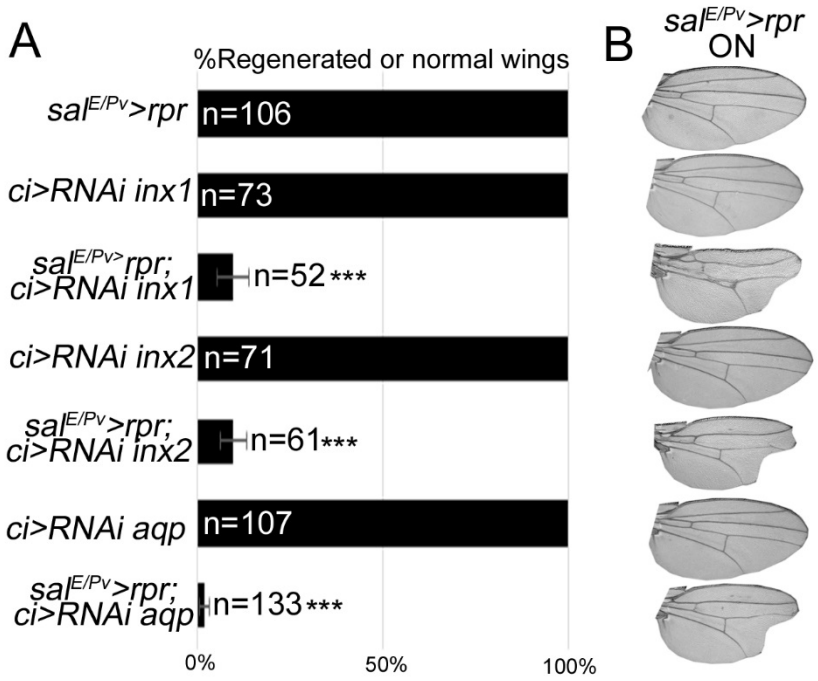

Figure 69. Innexins and Aquaporins are necessaries for imaginal disc regeneration. (A) Percentage of regenerated wings for controls (*rpr* or *RNAi inx* or *aqp* expression only) and experimental (*rpr* and *RNAi inx* or *aqp* dual expression). (B) Examples of wings with full regeneration and incomplete regeneration (indicated genotypes) after *sal$^{E/Pv}$>rpr*. Error Bars indicate Standard Deviation. ***P<0.001.

Nitric Oxide Synthase (NOS) activity in the prothoracic gland seems to be involved in the decrease of the growth rate in undamaged tissues when regeneration occurs in the damaged one through regulation of endocrine signals (Jaszczak et al. 2015; Jaszczak et al. 2016). Thus, systemic response also involves ROS signalling.

Recent findings showed that ROS produced during dorsal closure, which is a model for wound healing, operate as a tuning mechanism for cytoskeleton reorganization (Muliyil & Narasimha 2014). Therefore, it could be that changes in **mechanical stress** generated during wounding and epithelial disruption (mechanical stretching) results in ROS production. Interestingly, mechanical forces have been proposed as growth regulators (Shraiman 2005).

Changes in mechanical tension could affect the voltage gradients across the plasma membrane. These transmembrane potentials arise from the combined activity of numerous ion channels, pumps and gap junction complexes. It has been proposed that the mitotic rate can be regulated by **bioelectric signals**, because the function of membrane voltage and specific potassium, sodium and chloride ion channels influence cell proliferation (Blackiston et al. 2009; Levin 2009). In *Xenopus* tadpole tail regeneration, NADPH oxidases in the membrane produce both H_2O_2 and modify the membrane electrogenic properties, allowing wound healing and regenerative growth (Ferreira et al. 2016). The interplay between ultra-fast biochemical and biophysical signals will shed some light on the initial steps of tissue response to damage.

Redox signalling can account for quite a lot of mechanisms. Among them, ROS can promote the **oxidation of cysteine** residues within proteins (Rhee 2006), as in the case of Ask1. ROS, and in particular H_2O_2, can oxidize the protonated cysteine (Cys-SH) to the thiolate anion (Cys-S·), which in turn can be oxidized into its sulfenic form (Cys-SOH) causing allosteric changes

that modify protein function (Finkel 2012). The protein can be returned to its original state by enzymatic and non-enzymatic scavengers, creating a reversible signal transduction mechanism (Winterbourn & Hampton 2008). This mechanism has been described for a many transcription factors, kinases, protein phosphatases and matrix metalloproteases (Meng et al. 2002; Lee et al. 2002; Kamata et al. 2005; Nadeau et al. 2007; Marinho et al. 2014; Nelson & Melendez 2004). While kinases can be activated by ROS, phosphatases are inactivated (Rhee et al. 2000; Rhee 2006). Although our findings revealed a decisive role of ROS in Ask1 activation, we cannot discard that can also inhibit phosphatases as Puckered, which is a JNK inhibitor, or PTEN, which attenuates Insulin signalling.

Furthermore, ROS could be implicated in **epigenetic changes** and modifications in chromatin structure leading to changes in gene expression (Halicka et al. 2009; Frost et al. 2014). ROS not only modulate histone folding, stability and post-translational modifications, altering histone marks leading to aberrant transcription or chromatin packaging but also chromatin-associated proteins (reviewed in Kreuz & Fischle 2016). In addition, DNA could be sensitive to oxidation and methylation (Clark et al. 2012). In mammals, many **enhancers** are controlled by ROS (reviewed in Kreuz & Fischle 2016), and in *Drosophila*, the localized epigenetic silencing of WNT damage-responsive enhancer restrict regenerative capacity in maturing organisms (Harris et al. 2016). Actually, some trithorax group genes control JNK and Dilp8 expression to delay pupariation (Skinner et al. 2015). JNK, in turn, downregulates polycomb group genes to facilitate cell fate changes (Lee et al. 2005). Indeed, the chromatin regulator Taranis, protects regenerating tissue from deleterious side effects of wound healing and regeneration by controlling JNK (Schuster & Smith-Bolton 2015).

The ability to regenerate as well as to prevent damage are two determinants of **aging**. In many organisms, regenerative skills may decrease with age, and the implication of ROS signalling in this process has been extensively studied (Schieber & Chandel 2014). How ROS could influence the epigenetic status in younger and older organisms is an exciting question that scientists will answer soon.

MAPKs as key molecules driving regenerative growth

JNK pathway has been extensively described to be needed in wound healing and regenerative growth (Bosch et al. 2005; Bosch et al. 2008; Mattila et al. 2005; Lee et al. 2005; Smith-Bolton et al. 2009; Bergantiños et al. 2010; Blanco et al. 2010). Although JNK has often been linked to apoptosis because the pro-apoptotic genes *reaper* and *hid* can activate this pathway (Adachi-Yamada et al. 1999; Shlevkov & Morata 2012; Ryoo et al. 2004). it is currently accepted that JNK signalling can switch from the pro-apoptotic role to a proliferative function in the presence of oncogenic Ras or upon JNK activation (Uhlirova & Bohmann 2006; Uhlirova et al. 2005; Zhu et al. 2010).

After *ptc>rpr* cell death, we monitored JNK activity with the *puc-lacZ* and the *TRE-red* reporter, which monitors the JNK substrate AP1 transcription factor. Whereas *TRE-red* reporter

expression was found extensively in the apoptotic zone and, to a lesser extent, in the apical living cells, Puc positive cells were found apically. Indeed, some of them incorporated *EdU*, which is consistent with previous studies about the role of JNK in proliferation and regeneration.

We verified that JNK is crucial for imaginal disc regeneration. Larvae treated with JNK inhibitor IX-supplemented food could not regenerate properly. In fact, when we observed those wing imaginal discs after *ptc>rpr* or $sal^{E/Pv}$*>rpr* cell death, we could not detect healing. The combination of Gal4 and LexA binary systems allowed us to inhibit JNK signalling in a whole compartment and simultaneously induce cell death in $sal^{E/Pv}$ domain (*ci>*bsk^{DN} $sal^{E/Pv}$*>rpr*). With this combination, we demonstrated that JNK is mainly required in living cells to trigger regenerative growth.

In addition, after tissue damage, as for tumorous growth, Dilp8 is secreted from imaginal discs in response to JNK, Yki and JAK/STAT, in order to delay metamorphosis and obtain extra time to reach the final size (Colombani et al. 2012; Garelli et al. 2012; Katsuyama et al. 2015; Boone et al. 2016). Nevertheless, the precise mechanisms controlling systemic response after growth perturbations are largely unknown.

In front of this plethora of functions of the JNK, we propose here that JNK is required essentially in the imaginal disc cells to push healing and regeneration. From our observations, we conclude that two different inputs control JNK activity after damage, ROS and the TNF/Egr signalling. Imaginal discs exposed to antioxidants result not only in less incidence of regeneration but also of JNK activity. Interestingly, the decrease of JNK after ROS inhibition was always partial or mild, which suggests that JNK may be activated by other inputs.

Besides ROS, we described that the **TNF/Egr** through **Wgn** are necessaries for JNK activation after tissue damage. Inhibition of both molecules after cell death or physical injury prevent the expression of the *TRE-red* reporter and the protein Mmp1, a known target of the pathway (Uhlirova & Bohmann 2006; McClure et al. 2008). We hypothesized that TNF/Egr could contribute not only in TRAF2/6 activation to activate Ask1 as it has been studied in ASK1-deficient mice (Nishitoh et al. 1998b; Kei Tobiume et al. 2001; Liu et al. 2000b; Fujino et al. 2007b; Noguchi et al. 2005) but also to trigger JNK and Dilp8 expression to activate the PI3K pathway autonomously, thus attenuate Ask1 and promotes survival.

Both Wgn (Kanda et al. 2002) and Grnd (Andersen et al. 2015) have been described as receptors for TNF/Egr ligand. In this work we found that only Wgn was implicated in imaginal disc regeneration, whereas Grnd has been proposed to act as an effector of Egr-dependent cell death, and a JNK promoter both in the eye (Andersen et al. 2015) and in the Insulin Producing cells of the brain (IPCs) (Agrawal et al. 2016). This suggests that TNF/Egr could act in a context specific manner and promote different responses.

The activation of JNK by ROS seems to be a conserved mechanism. Not only in *Drosophila*, where ROS associated with tumour-like overgrowths lead to JNK activation (Fogarty et al. 2016; Clemente-Ruiz et al. 2016), but also in lower organisms as in the yeast *S. pombe*, where the AP1-like transcription factor Pap1, as well as the Atf1, drive the transcriptional response of cells to low levels of H_2O_2 (Quinn et al. 2002). Actually, in mammalian cell lines, the inhibition

of the scavenger PrxII (Peroxidaxin II), enhances H_2O_2 production and therefore JNK and p38 activation as well (Kang et al. 2004). Nevertheless, there are exceptions. For example, in breast cancer cells, the theaflavin, a bioactive flavonoid of black tea, suppress breast cancer metastasis by activating the p53-ROS-p38MAPK and inhibiting JNK (Adhikary et al. 2010).

We cannot discard the implication of other molecules upstream of JNK. For example, the Rho family of **small GTPses** (Rac, Cdc42 and Rho1), that participate in dorsal and thorax closure (Jacinto et al. 2002; Agnès et al. 1999; Baek et al. 2010). Indeed, The **PVR/PVF** signalling, the *Drosophila* homolog of the PDGF/VEGF, is a potent mitogen which has been associated with JNK induction during thorax closure and in neoplastic tumours (Ishimaru et al. 2004; Ohsawa et al. 2011). Moreover, members of **apicobasal polarity** complexes (*lgl-dlg-scrib*) suppress JNK, therefore, its modulation after damage could involve changes in JNK activity (Igaki et al. 2006; Uhlirova et al. 2005).

Transcriptomic analysis of regenerating discs revealed that a major class of genes, whose expression increases during early regeneration, possesses AP1 binding sites in their regulatory regions, sequences targeted by the AP1 complex Fos and Jun (Blanco et al. 2010). Many of these genes are transcription factors that somehow might be involved in tissue remodelling. Moreover, JNK activity is responsible for increasing **Yki** translocation into the nucleus through Ajuba proteins (Sun & Kenneth D. Irvine 2011; Sun & Irvine 2013). Besides proliferation, Yki induces the expression of the DIAP1 inhibitor of apoptosis, being other feasible way to promote JNK-dependent proliferation.

ROS are stressors involved in **p38** activation (Son et al. 2013; Plotnikov et al. 2011). We demonstrated that antioxidants decrease p38 activation not only after cell death but also after physical injury. Moreover, we described that not only JNK but also p38 is required for imaginal disc regeneration. In different p38 mutant backgrounds, as well as after p38 inhibition with UAS-RNAi constructs, we appreciated that regeneration was impaired. Particularly the $p38a^{1}$ allele, seems to affect *upd* expression and regeneration. This is consistent with the finding that *Drosophila* p38a is more susceptible to environmental stressors, such as oxidative stress (Craig et al. 2004). However, other p38 members also contribute to tissue regeneration. Indeed, heterozygous alleles of the p38 activating kinase *lic,* which normally do not show patterning defects after *rpr*-mediated ablation, can result in incomplete regeneration when a dose of *p38b* is missing.

Many other proteins have been described as upstream activators of p38, as ASK1, DLK1 (dual-leucine zipper-bearing kinase 1), TAK1, TAO (thousand-and-one amino acid) 1 and 2, TPL2 (tumour progression loci 2), MLK3 (mixed lineage kinase 3), MEKK3 (MEK kinase 3), MEKK4, and ZAK1 (leucine zipper and sterile-a motif kinase 1) (Cuadrado & Nebreda 2010). Of note, some of these MAPKs that trigger p38 MAPK activation can also activate the JNK pathway. We found that Ask1 is implicated in p38 activation, but little is known about the function of these upstream molecules of the pathway. Besides *p38a* and *p38b*, we cannot discard a function of *p38c* after damage, which is involved in intestinal immune homeostasis (Chakrabarti et al. 2014). We focused on the Atf-2 transcription factor, but many other downstream molecules of p38 kinases have been described (Zarubin & Han 2005). The *Drosophila* Activating transcription

factor 3 (Atf3), preserves metabolic and immune system homeostasis, and its loss, results in chronic inflammation and starvation responses (Rynes et al. 2012).

In mammals, the p38 MAPKs are activated by various pro-inflammatory and stressful stimuli, such as tumour necrosis factor-α (TNF-α) and interleukin-1b (IL-1b), and therefore have been broadly studied in the field of inflammation (Yong et al. 2009). In *Drosophila,* we uncovered that both cytokines and TNF/Egr play a role after damage. We found that TNF/Egr is not involved in p38 activation, because although TNF/Egr inhibition, P-p38 is in the wound sites. However, we cannot discard a positive feedback loop after *upd* expression to amplify the p38 pro-survival signal.

In contrast to JNK, p38 activation was only found in living cells surrounding the wounded area. Hence, although there could be both stimulatory and inhibitory interactions within and across MAPK signalling, upstream signals may differ from dying to living cells to initiate regeneration. We have found that both hep^{r75} and $p38a^{1}$ mutant backgrounds inhibit *upd* expression. But hep^{r75} mutants, which block JNK signalling, do not affect p38 phosphorylation and vice versa, $p38a^{1}$ mutants, which block at least the p38a branch of the p38 kinase, do not interfere with the *TRE-red* reporter expression. This suggests that ROS activate p38 and JNK independently and that both MAPKs stimulate the transcriptional expression of the cytokines *unpaired* to drive tissue repair.

The p38 cascade exhibits a considerable crosstalk and shared components with JNKs (Kyriakis & Avruch 2001). Similarly, these cascades are activated primarily by stress stimuli, but p38 respond to a wide variety of other molecules and cellular events (Zarubin & Han 2005). The variances in activation of these two pathways after damage should be mediated by specific scaffold proteins, compartmentalization, and available substrates. Consequently, although JNK and p38 are evolutionary conserved pathways that participate in stress response, seems that the interactions and crosstalk between both depend on the cellular context, thus future efforts should provide more information to consider those molecules as therapeutic targets in regenerative medicine.

The role of JAK/STAT signalling has been well-characterized in hinge (Ayala-Camargo et al. 2013; Johnstone et al. 2013) and in wing pouch development (Recasens-Alvarez et al. 2017).

Our results showed that JAK/STAT signalling must be activated by the cytokines Unpaired to promote regeneration after damage. In this work, we utilized an antibody against Upd and the reporter line 10XSTAT-GFP (Bach et al. 2007) after cell death or injury, and found localization surrounding the wounded area, in addition to the endogenous expression in the hinge region.

in mammals, the activation of JAK/STAT signalling pathway is triggered by a wide range of interleukins, interferons and growth factors, whereas in *Drosophila* is mediated by only three Upd ligands (Gilbert et al. 2005; Harrison et al. 1998; Hombría et al. 2005; Wang et al. 2014). After injury, FISH of *upd* and *upd3* revealed that transcription of both genes is confined near the wound. In $p38a^{-/-}$ and hep^{r75} discs, *upd* and *upd3* expression associated to the wound significantly decreases, revealing that the transcription of those molecules is dependent on MAPK activation. In fact, ectopic expression of *upd* rescued the phenotype caused by p38 and ROS inhibition. The other *unpaired* gene, *upd2*, has been related with systemic response after fasting (Rajan & Perrimon 2012), and its function in regeneration is still not known.

We also found that ectopic expression of a dominant negative form of the receptor Domeless as well as the Socs36E inhibitor impairs regeneration. Socs36E is both a target (it contains multiple high affinity STAT92E binding sites) and an inhibitor of the pathway and therefore promotes a negative feedback loop to attenuate JAK/STAT signalling upon pathway activation (Callus & Mathey-Prevot 2002; Karsten et al. 2002; Stec et al. 2013). In fact, the 10xSTAT-GFP activity reporter in based on the STAT92E binding sites present in the first intron of *socs36E* gene (Bach et al. 2007). Socs36E inhibits JAK/STAT signalling at the level of the Dome receptor, regulating its stability and lysosomal degradation as well as preventing its phosphorylation by Hop (Stec et al. 2013).

Socs36E has also been shown to inhibit the EGFR pathway in imaginal tissues as well as to limit EGFR-induced overgrowth in *Drosophila* epithelial transformation models (Almudi et al. 2009; Callus & Mathey-Prevot 2002; Herranz et al. 2012). The role of EGRF after damage has not been described yet, although preliminary experiments in the lab showed that is also implicated in the genetic network controlling the recovery of imaginal tissues (Figure 70).

JAK/STAT signalling promotes cell proliferation in different cellular contexts (Zeidler et al. 2000). In neoplastic tumours, the JAK/STAT pathway is activated in a JNK-dependent manner, inducing proliferation and metastasis (Pastor-Pareja et al. 2008; Wu et al. 2010; Igaki et al. 2009). Interestingly, epithelial tumours are often originated from tumour hotspots located in the hinge region, which concurs with elevated STAT92E activity (Tamori et al. 2016). This region appears to be particularly resistant to irradiation and drug-induced apoptosis (Verghese & Su 2016). STAT92E can protect cells from irradiation-induced apoptosis directly upregulating dIAP1 through two conserved STAT92E binding sites on the *diap1* locus (Betz et al. 2008). After wounding wing discs or gut, *upd* genes expression, are elevated in a JNK dependent manner, and are required to increase proliferation (Wu et al. 2010; Jiang et al. 2009). Moreover, activation of the JAK/STAT pathway upregulates CycD and CycB levels (Mukherjee et al. 2005;

Tsai & Sun 2004), as well as the competitive status of proliferating cells in imaginal discs. It has been reported that cells with hyperactivated STAT92E become winners and display super competitor features (Rodrigues et al. 2012).

Constitutive activation of several STATs has been observed in numerous human diseases, as in blood cancers (Calò et al. 2003). In humans, STAT promotes G1/S transition and activates c-Myc, which is a transcriptional regulator of cell cycle progression and cell growth (Bowman et al. 2000; Calò et al. 2003).

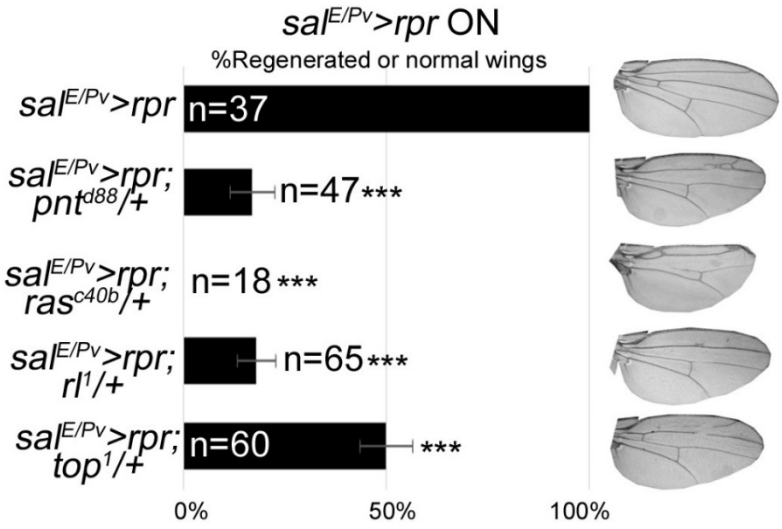

Figure 70. Inhibition of EGFR signalling impairs regeneration. Percentage of regenerated wings in heterozygous mutant background of EGFR signalling. Right: Examples of wings with full regeneration and incomplete regeneration (indicated genotypes) after *sal$^{E/Pv}$>rpr* cell death. Error Bars indicate Standard Deviation. ***P<0.001.

Ask1 as a ROS sensor to promote tissue repair

To uncover the molecular mechanisms of ROS-mediated activation of JNK and p38 MAPK pathways we focused on **Ask1**, which is activated when ROS oxidizes Trx and dissociates from Ask1 (Katagiri et al. 2010). We observed that Ask1 inhibition impairs regeneration. Ask1 is an evolutionary conserved signalling intermediate between cytotoxic stress and cellular responses (Saitoh et al. 1998b; Nishitoh et al. 2002; Takeda et al. 2004; Matsuzawa et al. 2005). The mechanism by which Trx is oxidized and released was discovered more than twenty years ago (Saitoh et al. 1998; Liu et al. 2000), and is an extremely accurate system to initiate stress responses. In mice, after Trx release, the Thr845 is auto-phosphorylated, which is essential for ASK1 activation. However, it has been proposed that this residue can also be trans-phosphorylated by an unidentified kinase in response to ROS (Tobiume et al. 2002). In *Drosophila,* we also found that after cell death and the subsequent burst of ROS, there is an activation of the Thr-rich domain in dead cells, whereas lower or unappreciated levels in surrounding living cells. No other kinases have been identified upstream of Ask1.

ASK1 function was initially related to cell death. Constitutively active ASK1 induces cell death, mainly through mitochondria-dependent caspase activation (Hatai et al. 2000; Kanamoto et al. 2000; Saitoh et al. 1998a). In *Drosophila*, *reaper* activates Ask1 and JNK and induce cell death (Kuranaga et al. 2002), which is consistent with our results.

However, it has been demonstrated a role of ASK1 in proliferation, survival and differentiation (Takeda et al. 2000; Sayama et al. 2001; Rubiolo et al. 2006). We found that PH3-positive cells present Ask1 P-Thr747. In interphase, the hypophosphorylated Cdc25C (cell division cycle 25C) phosphatase suppresses mammalian ASK1, by dephosphorylating P-Thr-838 *in vitro*. But during mitotic arrest, hyperphosphorylated Cdc25C has significantly reduced affinity to ASK1, suggesting that enhanced ASK1 activity in mitosis was due to reduced binding of hyperphosphorylated Cdc25C to ASK1 (Cho et al. 2015).

Several of our findings point to that Ask1 acts as key molecule in regenerating tissue. First, *ask1* mutant flies develop normal and are healthy in standard laboratory conditions. However, under stress insults, their life span is compromised, which is consistent with experiments done in ASK1-deficient mice (Yokoi et al. 2006; Izumiya et al. 2003; Yamaguchi et al. 2003; Watanabe et al. 2005; Izumi et al. 2003; Yamaguchi et al. 2004; Izumi et al. 2005; Harada et al. 2006). Second, inhibition or reduction of Ask1 impairs regeneration. Third, blocking the PI3K/Akt, which is key for the inhibitory phosphorylation of Ser83, results in regeneration defects.

Many Ask1 positive and negative regulators were reported (reviewed in Takeda et al. 2008; Sakauchi et al. 2017). In this study, we proposed a new role of **Akt** in flies by promoting stress tolerance and survival through Ask1. We uncovered that Insulin signalling controls the phosphorylation of the Ask1 Ser83. The role of Insulin signalling in growth and metabolism has been extensively described (reviewed in Nässel & Broeck 2016; Nässel et al. 2015). The inhibition of this pathway leads to defects in regeneration, presumably by preventing attenuation of Ask1 activity. Additionally, the combination of *akt* and *ask1* mutant alleles blocks entirely the regenerative response. These results are in agreement with the notion that

PI3K/AKT are required for cell survival as their loss of function results in apoptosis (Staveley et al. 1998) (Scanga et al. 2000).

AKT activity is regulated by PI3K via synthesis of 3-phosphoinositides (3-PPIs), and by the lipid phosphatase **PTEN**, via degradation of PPIs. In breast cancer cells ROS-mediated tumour progression was found to be dependent on activation of PI3K pathway and reduction of PTEN activity (De Luca et al. 2010). It is noteworthy that PTEN, a tumour suppressor and negative regulator of the PI3K pathway, can be oxidized and inactivated by ROS (Leslie et al. 2003; Kwon et al. 2004; Lee et al. 2002). Moreover, H_2O_2 has also been shown to promote metastasis by upregulating P-AKT and inactivating PTEN in prostate cancer cells (Chetram et al. 2011). Therefore, we propose that soon, the role of tumour suppressor genes as PTEN in imaginal disc regeneration must be explored.

General overview of the regenerative response to damage

This work contributes to the understanding of the robustness of *Drosophila* imaginal discs to overcome growth perturbations. In nature, *Drosophila* populations adapted to live in relatively extreme conditions. The regenerative capacity of the imaginal discs can be considered as a mechanism of adaptation for survival in life-threatening environmental conditions. This wonderful ability of adaptation, allows the imaginal tissues to be modulated by external inputs, such as nutrient availability and temperature to reach its final size before metamorphosis (reviewed in Boulan et al. 2015).

Although it has been proposed that the same pathways act in normal and in regenerative growth, as Wg (Gibson & Schubiger 1999; McClure et al. 2008; Katsuyama et al. 2015) by increasing Myc (Smith-Bolton et al. 2009), JAK/STAT (Katsuyama et al. 2015; Pastor-Pareja et al. 2008b; La Fortezza et al. 2016; Verghese & Su 2016) and Hippo/Yki (Repiso et al. 2013; Grusche et al. 2011; Sun & Irvine 2011; Meserve & Duronio 2015), the **damage-induced signals** differ from the development in the mechanism that they are recruited. For example, the WNT protein wingless (Wg) is likely activated by a damage responsive enhancer (Harris et al. 2016). Unpaired is activated by JNK and p38, which in turn depend on ROS. How ROS activate those pathways throughout Ask1 has been analyzed in this work, demonstrating the presence of another stress signal necessary for tissue repair and regeneration.

Taking together, we propose the following model (Figure 71). After cell death or injury, damage-induced signals as **ROS** or calcium trigger the response in imaginal tissues. **Calcium** could activate the Dual oxidase **DUOX**, with in turn will produce H_2O_2. Besides that, other calcium-dependent proteins could be involved in cytoskeletal rearrangements, secretion or in the transcriptional response. Calcium and ROS propagation between adjacent cells could be accomplished by **gap junctions** and/or **aquaporin** channels. ROS oxidize thioredoxin that releases Ask1. The Ask1 protein will have a dual function. First, in cells committed to die will contribute to apoptosis. Second, in surviving cells where the insulin pathway is active, its deleterious function will be attenuated and the tolerable levels of Ask1 will be sufficient to activate JNK and p38. In addition, **JNK** can be also modulated by **TNF/Egr**. Downstream of MAPKs, **Yki** (Sun & Irvine 2011; Sun & Irvine 2013), **JAK/STAT** (Pastor-Pareja et al. 2008;

Katsuyama et al. 2015; Santabárbara-Ruiz et al. 2015) and the **epigenetic machinery** (Lee et al. 2005c; Smith-Bolton et al. 2009) will induce the transcriptional response for wound healing, regenerative growth and re-patterning of the missing tissue. Moreover, **Dilp8** and **retinoids** will be secreted from the disc epithelium to turn on the **systemic response** (Garelli et al. 2012; Colombani et al. 2012; Halme et al. 2010) . These systemic molecules will circulate through the hemolimph and bind to their receptors in the neurans that trigger the ecdysone response from the Prothoracic gland (**PG**). **Haemocytes** could provide signals to improve the regenerative response. We cannot discard the implication of cues coming from the **fat body**, the organ which senses nutrient availability and has a well-characterised crosstalk with neurons to control **systemic growth**.

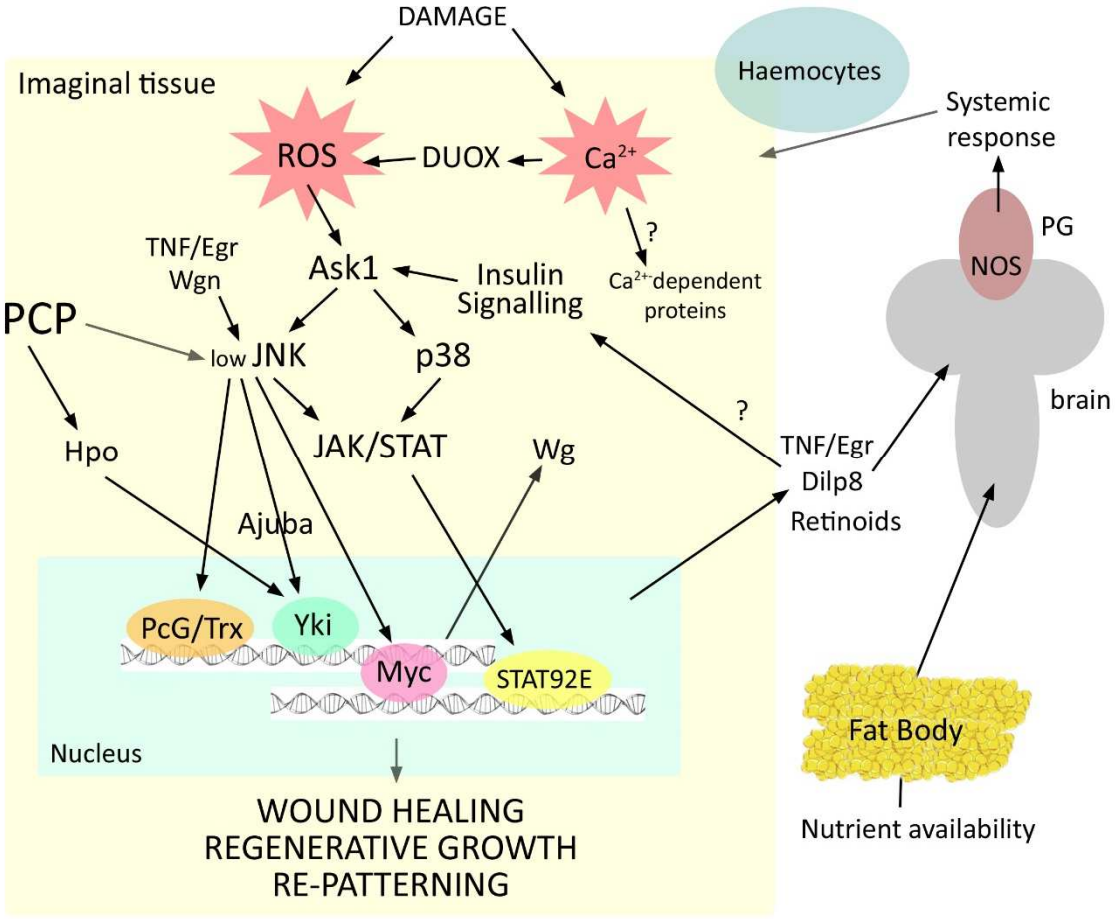

Figure 71. Hypothetical model for imaginal disc regeneration. Scheme of molecules involved in imaginal disc regeneration and their probable connections between them, as well as the possible crosstalk concerning different organs to initiate the systemic response.

Biological relevance of *Drosophila* regeneration

All multicellular organisms can respond to injury, but there is an enormous variety in how this process occurs. The study of wound repair in different creatures could provide information on the different strategies to replace cells in nature. The parallelism in the mechanisms underlying some types of regeneration in vertebrates and invertebrates, has contributed to the proposal that an ancient patterning system is being repeatedly used to recover lost tissues and organs.

The old perception regarding the deleterious effects of ROS has been substituted by so-called '**redox biology**', which primarily supports that oxidative protein modifications can be specific and reversible and, consequently, may play a crucial role in cellular physiology. It has been shown that ROS are cellular stimuli capable of activating MAPK pathways in a number of different cell types (Son et al. 2013). After damage, these MAPKs drive the regenerative response, thus the study of the site, concentration and kinetics of ROS production as well as scavenger molecules controlling redox state are most likely to be potential targets determining the regenerative ability of tissues and organs.

The use of *Drosophila* imaginal discs as a model for tissue repair has allowed scientists the identification and functional characterization of the molecules involved in wound repair, particularly in re-epithelialization. These discoveries have been made thanks to the genetic tools developed in these organisms, as well as to the recent advances in live-imaging techniques. Not only after damage, but also the morphological events, such as dorsal closure and tracheal fusion, have a remarkable resemblance to healing in mammalian skin wounds (Gurtner et al. 2008).

Similarities between fly and vertebrate wound healing have been proposed. First, the formation of an actin cable upon wounding. Cells orient and migrate towards the wound by extending their filopodia. Then they re-specificate in the blastema to recover lost tissue. Moreover, it seems that JNK signalling and the consequent activation of the transcription factor AP1 in the wound site, are crucial for successful wound repair in *Drosophila* (Bosch et al. 2005d; Smith-Bolton et al. 2009; Bergantiños et al. 2010). Likewise, AP1 proteins have a similar role in the mammalian wound repair (Li et al. 2003), although some of their functions are probably hidden by redundancy between the many members of the mammalian AP1 family (Schäfer & Werner 2007). We found that JAK/STAT activation is crucial after damage. In mammals, the transcription factor STAT3 is involved in re-epithelialization after wounding (Sano et al. 1999).

Many **differences** have been reported. In mammals, the gap caused by injury is filled by a clot, in which many types of cells as well as stem cells are recruited to the wound site. However, in *Drosophila* imaginal discs, these processes do not occur. It seems that in mammals, the rapid interposition of fibrotic tissue, prevents subsequent regeneration. As the fruit fly is one of the most genetic tractable models, screenings can be easily performed. Perhaps if we fully understand how the epithelium of the imaginal disc is able to recover, we will be ready to design some genetic strategies to trigger epithelial recovery in mammals.

FUTURE PERSPECTIVES

From my point of view, the study of regeneration in *Drosophila* has a special social interest. First, taking in account that the fruit fly is an extraordinarily genetic tractable organism and that shares more than half of its genome with humans, it can be used as a source of information to improve the field of regenerative biology. Moreover, *Drosophila*, also offers the opportunity to test the coordination between regeneration and tissue homeostasis, besides the hormonal control of growth.

For more than a century, traditional regenerative research has focused on the understanding of the mechanisms of regeneration in lower species. One should consider if now is the time to apply this knowledge to enhance wound repair in humans. The current therapies are mainly focused on **skin substitutes**, **stem cell** biology and innovative **biomaterials** for manipulation and delivery of patient-compatible tissues which could recapitulate the regenerative response. The creation of **bioartificial functional limbs** will be possible in a few years, thanks to the HEAL (Hartford Engineering a Limb) project, which aims to regenerate human limbs by 2030.

Truthfully, the direct biomedical applications of *Drosophila* knowledge of wound healing and regeneration are narrow, but research in fruit flies has contributed to the detection of novel genes and epigenetic mechanisms that could help in the development of new therapies, due to the evolutionary conserved molecules underlying regeneration. For example, I firmly believe the sequence of events ROS ->Ask1->Trx, JNK->cytokines->repair and its dependence on the insulin pathway can be of interest in pharmaceutical applications.

One strategy to improve regeneration includes the use of **soluble factors and molecular cocktails**. In this regard, *Drosophila* could facilitate the identification of drugs capable of accelerating and stimulate wound healing and repair. The high-throughput methodology and the easy handling of flies, allow the performance of large-scale compound screenings *in vivo*, such as those performed in fly models of human diseases (Chang et al. 2008). One question I am particularly interested, is how nutrition could enhance regeneration. Many molecules have been proposed to modify the cellular redox state, as curcumin, flavonoids, vitamins, soy, green tea or carotenoids (Nimse & Pal 2015). But their role in cancer and wound healing is still not described. Hence, large-scale diet screens could reveal innovative roles of these molecules in this process. Numerous genes involved in wound healing are also present in human highly malignant tumours, as prostate, liver, colon and breast cancers (reviewed in Arnold et al. 2015). Therefore, these studies highlight the importance of functional genomic research in fruit flies to provide additional information about the role of tumour inducers and tumour suppressors in wound healing events.

Thanks to the revolutionary CRISPR methodology, **gene therapy** has emerged as one of the most challenged techniques to improve any disease. The identification of essential genes implicated in chronic wounds and metastatic events could be easily applied to *Drosophila*, by performing *in vivo* genetic screens. The main advantages are the reproducibility, the speed, because they could be done faster than in other organisms, and the obtaining of a large number of progeny. Moreover, not only genes but enhancer regions could be identified simply in this type of screenings.

CONCLUSIONS

As a summary of this work, we described how imaginal disc regeneration starts, and how these early signals are transduced to recover lost tissue after cell death or injury.

1. Specific conclusions:

    - One of the earliest responses to damage consisted on the production of Reactive Oxygen Species, in higher levels in dying cells and in lower levels in surrounding living cells. This burst of ROS is necessary for JNK and p38 MAPK signalling, which are independent pathways that transduce the damage induced-signal to recover lost tissue. Besides ROS, the TNF/Eiger throughout Wengen acts as a second input controlling JNK pathway.

    - The Apoptotic signal-regulating kinase 1 (Ask1) is the intermediate between the boost of ROS and MAPK activation. This protein integrates oxidation and Insulin signalling in the living tissue to promote regeneration.

    - JNK and p38 signalling initiate tissue recovery regulating JAK/STAT pathway at the level of the cytokines *unpaired*. The activation of JAK/STAT is crucial for regenerative growth.

2. Global conclusion:

    - Although antioxidants usually present health benefits, we demonstrated that they impair the onset of regeneration in imaginal discs.

BIBLIOGRAPHY

A

Abbott, L.C., Karpen, G.H. & Schubiger, G., 1981a. Compartmental restrictions and blastema formation during pattern regulation in Drosophila imaginal leg discs. *Developmental biology*, 87(1), pp.64–75.

Abdelwahid, E. et al., 2007. Mitochondrial disruption in Drosophila apoptosis. *Developmental cell*, 12(5), pp.793–806.

Achituv, Y. & Sher, E., 1991. Sexual Reproduction and Fission in the Sea Star Asterina Burtoni from the Mediterranean Coast of Israel.

Adachi-Yamada, T. et al., 1999. Distortion of proximodistal information causes JNK-dependent apoptosis in Drosophila wing. *Nature*, 400(6740), pp.166–9.

Adachi-Yamada, T. & O'Connor, M.B., 2002. Morphogenetic apoptosis: a mechanism for correcting discontinuities in morphogen gradients. *Developmental biology*, 251(1), pp.74–90.

Adams, M.D. et al., 2000. The genome sequence of Drosophila melanogaster. *Science (New York, N.Y.)*, 287(5461), pp.2185–95.

Adhikary, A. et al., 2010. Theaflavins retard human breast cancer cell migration by inhibiting NF-kappaB via p53-ROS cross-talk. *FEBS letters*, 584(1), pp.7–14.

Adler, P.N., 1981. Growth during pattern regulation in imaginal discs. *Developmental biology*, 87(2), pp.356–73.

Adler, P.N. & Bryant, P.J., 1977. Participation of lethally irradiated imaginal disc tissue in pattern regulation in Drosophila. *Developmental biology*, 60(1), pp.298–304.

Adler, P.N. & MacQueen, M., 1984. Cell proliferation and DNA replication in the imaginal wing disc of Drosophila melanogaster. *Developmental biology*, 103(1), pp.28–37.

Adler, V. et al., 1999. Regulation of JNK signaling by GSTp. *The EMBO journal*, 18(5), pp.1321–34.

Affolter, M. & Basler, K., 2007. The Decapentaplegic morphogen gradient: from pattern formation to growth regulation. *Nature Reviews Genetics*, 8(9), pp.663–674.

Agata, K., Saito, Y. & Nakajima, E., 2007. Unifying principles of regeneration I: Epimorphosis versus morphallaxis. *Development, growth & differentiation*, 49(2), pp.73–8.

Agnès, F., Suzanne, M. & Noselli, S., 1999. The Drosophila JNK pathway controls the morphogenesis of imaginal discs during metamorphosis. *Development (Cambridge, England)*, 126(23), pp.5453–62.

Agrawal, N. et al., 2016. The Drosophila TNF Eiger Is an Adipokine that Acts on Insulin-Producing Cells to Mediate Nutrient Response. *Cell Metabolism*, 23(4), pp.675–684.

Alcedo, J. et al., 1996. The Drosophila smoothened gene encodes a seven-pass membrane protein, a putative receptor for the hedgehog signal. *Cell*, 86(2), pp.221–32.

Aldaz, S., Escudero, L.M. & Freeman, M., 2010. Live imaging of Drosophila imaginal disc development. *Proceedings of the National Academy of Sciences of the United States of America*, 107(32), pp.14217–22.

Almudi, I. et al., 2009. SOCS36E specifically interferes with Sevenless signaling during Drosophila eye development. *Developmental biology*, 326(1), pp.212–23.

Alonso, A. et al., 2004. Protein tyrosine phosphatases in the human genome. *Cell*, 117(6), pp.699–711.

Álvarez-Fernández, C. et al., 2015b. Identification and functional analysis of healing regulators in Drosophila. *PLoS genetics*, 11(2), p.e1004965.

Alves, S.L.S., Pereira, A.A.D. & Ventura, A.C.R.R., 2002. Sexual and asexual reproduction of Coscinasterias tenuispina (Echinodermata: Asteroidea) from Rio de Janeiro, Brazil.

Amoyel, M., Anderson, A.M. & Bach, E.A., 2014. JAK/STAT pathway dysregulation in tumors: a Drosophila perspective. *Seminars in cell & developmental biology*, 28, pp.96–103.

Andersen, D.S. et al., 2015. The Drosophila TNF receptor Grindelwald couples loss of cell polarity and neoplastic growth. *Nature*, 522(7557), pp.482–486.

Arnold, K.M. et al., 2015. Wound healing and cancer stem cells: inflammation as a driver of treatment resistance in breast cancer. *Cancer growth and metastasis*, 8, pp.1–13.

Ayala-Camargo, A. et al., 2013. JAK/STAT signaling is required for hinge growth and patterning in the Drosophila wing disc. *Developmental biology*, 382(2), pp.413–26.

Azpiazu, N. & Morata, G., 2000. Function and regulation of homothorax in the wing imaginal disc of Drosophila. *Development (Cambridge, England)*, 127(12), pp.2685–93.

B

Bach, E.A. et al., 2007. GFP reporters detect the activation of the Drosophila JAK/STAT pathway in vivo. *Gene Expr Patterns*, 7(3), pp.323–331.

Baek, S.H. et al., 2010. Rho-family small GTPases are required for cell polarization and directional sensing in Drosophila wound healing. *Biochemical and biophysical research communications*, 394(3), pp.488–92.

Baena-López, L.A., Baonza, A. & García-Bellido, A., 2005. The Orientation of Cell Divisions Determines the Shape of Drosophila Organs. *Current Biology*, 15(18), pp.1640–1644.

Baena-Lopez, L.A. & García-Bellido, A., 2006. Control of growth and positional information by the graded vestigial expression pattern in the wing of Drosophila melanogaster. *Proceedings of the National Academy of Sciences of the United States of America*, 103(37), pp.13734–9.

Baguñà, J., Saló, E. & Auladell, C., 1989. Regeneration and pattern formation in planarians \nIII. Evidence that neoblasts are totipotent stem cells and the source of blastema cells. *Development*, 107(December 2015), pp.77–86.

Baonza, A., Roch, F. & Martin-Blanco, E., 2000. DER signaling restricts the boundaries of the wing field during Drosophila development. *Proceedings of the National Academy of Sciences of the United States of America*, 97(13), pp.7331–5.

Barrio, R. & de Celis, J.F., 2004. Regulation of spalt expression in the Drosophila wing blade in response to the Decapentaplegic signaling pathway. *Proceedings of the National Academy of Sciences of the United States of America*, 101(16), pp.6021–6.

Bate, M. & Arias, A.M., 1991. The embryonic origin of imaginal discs in Drosophila. *Development (Cambridge, England)*, 112(3), pp.755–61.

Bayat, A., McGrouther, D.A. & Ferguson, M.W.J., 2003. Skin scarring. *BMJ (Clinical research ed.)*, 326(7380), pp.88–92.

Becher, M.U., Nickenig, G. & Werner, N., 2010. Regeneration of the vascular compartment. *Herz*, 35(5), pp.342–51.

Behrend, L., Henderson, G. & Zwacka, R.M., 2003. Reactive oxygen species in oncogenic transformation. *Biochemical Society transactions*, 31(Pt 6), pp.1441–4.

Belacortu, Y. & Paricio, N., 2011. Drosophila as a model of wound healing and tissue regeneration in vertebrates. *Developmental Dynamics*, 240(11), pp.2379–2404.

Beltrami, A.P. et al., 2001. Evidence that human cardiac myocytes divide after myocardial infarction. *The New England journal of medicine*, 344(23), pp.1750–7.

Bely, A.E. & Nyberg, K.G., 2010. Evolution of animal regeneration: re-emergence of a field. *Trends in ecology & evolution*, 25(3), pp.161–70.

Bergantiños, C. et al., 2010. Imaginal discs: Renaissance of a model for regenerative biology. *Bioessays*, 32(3), pp.207–217.

Bergantiños, C., Corominas, M. & Serras, F., 2010. Cell death-induced regeneration in wing imaginal discs requires JNK signalling. *Development (Cambridge, England)*, 137(7), pp.1169–79.

Bergmann, A. & Steller, H., 2010. Apoptosis, Stem Cells, and Tissue Regeneration. *Science Signaling*, 3(145), p.re8-re8.

Betz, A. et al., 2008. STAT92E is a positive regulator of Drosophila inhibitor of apoptosis 1 (DIAP/1) and protects against radiation-induced apoptosis. *Proceedings of the National Academy of Sciences of the United States of America*, 105(37), pp.13805–10.

Bienert, G.P. & Chaumont, F., 2014. Aquaporin-facilitated transmembrane diffusion of hydrogen peroxide. *Biochimica et Biophysica Acta (BBA) - General Subjects*, 1840(5), pp.1596–1604.

Bigarella, C.L., Liang, R. & Ghaffari, S., 2014. Stem cells and the impact of ROS signaling. *Development*, 141(22), pp.4206–4218.

Binari, R. & Perrimon, N., 1994. Stripe-specific regulation of pair-rule genes by hopscotch, a putative Jak family tyrosine kinase in Drosophila. *Genes & development*, 8(3), pp.300–12.

Blackiston, D.J., McLaughlin, K.A. & Levin, M., 2009. Bioelectric controls of cell proliferation: Ion channels, membrane voltage and the cell cycle. *Cell Cycle*, 8(21), pp.3527–3536.

Blanco, E. et al., 2010. Gene expression following induction of regeneration in Drosophila wing imaginal discs. Expression profile of regenerating wing discs. *BMC Developmental Biology*, 10(1), p.94.

Bogoyevitch, M.A. & Kobe, B., 2006. Uses for JNK: the many and varied substrates of the c-Jun N-terminal kinases. *Microbiology and molecular biology reviews : MMBR*, 70(4), pp.1061–95.

Boone, E. et al., 2016. The Hippo signalling pathway coordinates organ growth and limits developmental variability by controlling dilp8 expression. *Nature communications*, 7, p.13505.

Borgens, R.B., 1982. Mice regrow the tips of their foretoes. *Science (New York, N.Y.)*, 217(4561), pp.747–50.

Bosch, M. et al., 2005. JNK signaling pathway required for wound healing in regenerating Drosophila wing imaginal discs. *Dev Biol*, 280(1), pp.73–86.

Bosch, M., Baguna, J. & Serras, F., 2008. Origin and proliferation of blastema cells during regeneration of Drosophila wing imaginal discs. *Int J Dev Biol*, 52(8), pp.1043–1050.

Boulan, L., Milán, M. & Léopold, P., 2015. The Systemic Control of Growth. *Cold Spring Harbor Perspectives in Biology*, 7(12), p.a019117.

Bowman, T. et al., 2000. STATs in oncogenesis. *Oncogene*, 19(21), pp.2474–2488.

Brand, A.H. & Perrimon, N., 1993. Targeted gene expression as a means of altering cell fates and generating dominant phenotypes. *Development (Cambridge, England)*, 118(2), pp.401–15.

Brand, M.D., 2010. The sites and topology of mitochondrial superoxide production. *Experimental Gerontology*, 45(7–8), pp.466–472.

Brockes, J.P. & Kumar, A., 2008. Comparative aspects of animal regeneration. *Annual review of cell and developmental biology*, 24(1), pp.525–49.

Brockes, J.P., Kumar, A. & Velloso, C.P., 2001. Regeneration as an evolutionary variable. *Journal of anatomy*, 199(Pt 1-2), pp.3–11.

Brockes, J.P., Kumar, A. & Velloso, C.P., Regeneration as an evolutionary variable. *Journal of anatomy*, 199(Pt 1-2), pp.3–11.

Brown, S., Hu, N. & Hombría, J.C., 2001. Identification of the first invertebrate interleukin JAK/STAT receptor, the Drosophila gene domeless. *Current biology : CB*, 11(21), pp.1700–5.

Bryant, P.J., 1975. Pattern formation in the imaginal wing disc of Drosophila melanogaster: fate map, regeneration and duplication. *The Journal of experimental zoology*, 193(1), pp.49–77.

Bryant, P.J., 1971. Regeneration and duplication following operations in situ on the imaginal discs of Drosophila melanogaster. *Developmental biology*, 26(4), pp.637–51.

Bryant, P.J., 1975. Regeneration and duplication in imaginal discs. *Ciba Foundation symposium*, 0(29), pp.71–93.

Bryant, P.J. & Fraser, S.E., 1988. Wound healing, cell communication, and DNA synthesis during imaginal disc regeneration in Drosophila. *Developmental biology*, 127(1), pp.197–208.

Bryant, P.J. & Simpson, P., 1984. Intrinsic and extrinsic control of growth in developing organs. *The Quarterly review of biology*, 59(4), pp.387–415.

Bryant, S. V, French, V. & Bryant, P.J., 1981. Distal regeneration and symmetry. *Science (New York, N.Y.)*, 212(4498), pp.993–1002.

Bullard, K.M., Longaker, M.T. & Lorenz, H.P., 2003. Fetal wound healing: current biology. *World journal of surgery*, 27(1), pp.54–61.

Bunker, B.D. et al., 2015. The transcriptional response to tumorigenic polarity loss in Drosophila. *eLife*, 4.

Burke, R. & Basler, K., 1996. Dpp receptors are autonomously required for cell proliferation in the entire developing Drosophila wing. *Development (Cambridge, England)*, 122(7), pp.2261–9.

C

Calleja, M. et al., 2000. Generation of medial and lateral dorsal body domains by the pannier gene of Drosophila. *Development (Cambridge, England)*, 127(18), pp.3971–80.

Callus, B.A. & Mathey-Prevot, B., 2002. SOCS36E, a novel Drosophila SOCS protein, suppresses JAK/STAT and EGF-R signalling in the imaginal wing disc. *Oncogene*, 21(31), pp.4812–21.

Calò, V. et al., 2003. STAT proteins: From normal control of cellular events to tumorigenesis. *Journal of Cellular Physiology*, 197(2), pp.157–168.

Campbell, G. & Tomlinson, A., 1999. Transducing the Dpp morphogen gradient in the wing of Drosophila: regulation of Dpp targets by brinker. *Cell*, 96(4), pp.553–62.

Cannizzo, F.T. et al., 2010. Thymus atrophy and regeneration following dexamethasone administration to beef cattle. *The Veterinary record*, 167(9), pp.338–43.

Carbonell, A. et al., 2013. Ash2 acts as an ecdysone receptor coactivator by stabilizing the histone methyltransferase Trr. *Molecular Biology of the Cell*, 24(3), pp.361–372.

Carlson, B.M., 2007. *Principles of regenerative biology*, Elsevier/Academic.

Casares, F. & Mann, R.S., 2000. A dual role for homothorax in inhibiting wing blade development and specifying proximal wing identities in Drosophila. *Development (Cambridge, England)*, 127(7), pp.1499–508.

Cha, G.-H. et al., 2003. Discrete functions of TRAF1 and TRAF2 in Drosophila melanogaster mediated by c-Jun N-terminal kinase and NF-kappaB-dependent signaling pathways. *Molecular and cellular biology*, 23(22), pp.7982–91.

Chakrabarti, S., Poidevin, M. & Lemaitre, B., 2014. The Drosophila MAPK p38c Regulates Oxidative Stress and Lipid Homeostasis in the Intestine D. A. Garsin, ed. *PLoS Genetics*, 10(9), p.e1004659.

Chang, H.-J. et al., 2012. Loss of Hemolectin reduces the survival of Drosophila larvae after wounding. *Developmental & Comparative Immunology*, 36(2), pp.274–278.

Chang, S. et al., 2008. Identification of small molecules rescuing fragile X syndrome phenotypes in Drosophila. *Nature chemical biology*, 4(4), pp.256–63.

Chatterjee, N. & Bohmann, D., 2012. A versatile ΦC31 based reporter system for measuring AP-1 and Nrf2 signaling in Drosophila and in tissue culture. B. Jennings, ed. *PloS one*, 7(4), p.e34063.

Chen, J. et al., 2010. Participation of the p38 pathway in Drosophila host defense against pathogenic bacteria and fungi. *Proceedings of the National Academy of Sciences of the United States of America*, 107(48), pp.20774–9.

Chen, Y., Azad, M.B. & Gibson, S.B., 2009. Superoxide is the major reactive oxygen species regulating autophagy. *Cell Death and Differentiation*, 16(7), pp.1040–1052.

Chesney, J. & Bucala, R., 2000. Peripheral blood fibrocytes: mesenchymal precursor cells and the pathogenesis of fibrosis. *Current rheumatology reports*, 2(6), pp.501–5.

Chetram, M.A., Don-Salu-Hewage, A.S. & Hinton, C. V., 2011. ROS enhances CXCR4-mediated functions through inactivation of PTEN in prostate cancer cells. *Biochemical and Biophysical Research Communications*, 410(2), pp.195–200.

Cho, Y.-C. et al., 2015. Cell cycle-dependent Cdc25C phosphatase determines cell survival by regulating apoptosis signal-regulating kinase 1. *Cell Death and Differentiation*, 22(10), pp.1605–1617.

Choi, H.K. & Chung, K.C., 2011. Dyrk1A Positively Stimulates ASK1-JNK Signaling Pathway during Apoptotic Cell Death. *Experimental Neurobiology*, 20(1), p.35.

Christiano, A.M., 2004. Epithelial stem cells: stepping out of their niche. *Cell*, 118(5), pp.530–2.

Cifuentes, F.J. & García-Bellido, A., 1997. Proximo-distal specification in the wing disc of Drosophila by the nubbin gene. *Proceedings of the National Academy of Sciences of the United States of America*, 94(21), pp.11405–10.

Clark, D.W. et al., 2012. Promoter G-quadruplex sequences are targets for base oxidation and strand cleavage during hypoxia-induced transcription. *Free Radical Biology and Medicine*, 53(1), pp.51–59.

Clemente-Ruiz, M. et al., 2016. Gene Dosage Imbalance Contributes to Chromosomal Instability-Induced Tumorigenesis. *Developmental Cell*, 36(3), pp.290–302.

Cohen, B. et al., 1992. apterous, a gene required for imaginal disc development in Drosophila encodes a member of the LIM family of developmental regulatory proteins. *Genes & development*, 6(5), pp.715–29.

Cohen, B., Simcox, A.A. & Cohen, S.M., 1993. Allocation of the thoracic imaginal primordia in the Drosophila embryo. *Development (Cambridge, England)*, 117(2), pp.597–608.

Colombani, J. et al., 2015. Drosophila Lgr3 Couples Organ Growth with Maturation and Ensures Developmental Stability. *Current biology : CB*, 25(20), pp.2723–9.

Colombani, J., Andersen, D.S. & Leopold, P., 2012. Secreted Peptide Dilp8 Coordinates Drosophila Tissue Growth with Developmental Timing. *Science*, 336(6081), pp.582–585.

Craig, C.R. et al., 2004. A Drosophila p38 orthologue is required for environmental stress responses. *EMBO reports*, 5(11), pp.1058–63.

Cross, C.E. et al., 1987. Oxygen radicals and human disease. *Annals of internal medicine*, 107(4), pp.526–45.

Cuadrado, A. & Nebreda, A.R., 2010. Mechanisms and functions of p38 MAPK signalling. *The Biochemical journal*, 429(3), pp.403–17.

Cully, M. et al., 2010. A role for p38 stress-activated protein kinase in regulation of cell growth via TORC1. *Molecular and cellular biology*, 30(2), pp.481–95.

D

Dale, L. & Bownes, M., 1980. Is regeneration inDrosophila the result of epimorphic regulation? *Wilhelm Roux's archives of developmental biology*, 189(2), pp.91–96.

Dale, L. & Bownes, M., 1981. Wound healing and regeneration in the imaginal wing disc of Drosophila. *Wilhelm Roux's archives of developmental biology*, 190(4), pp.185–190.

Dalle Carbonare, L., Innamorati, G. & Valenti, M.T., 2012. Transcription factor Runx2 and its application to bone tissue engineering. *Stem cell reviews*, 8(3), pp.891–7.

Delavary, B.M. et al., 2011. Macrophages in skin injury and repair. *Immunobiology*, 216(7), pp.753–762.

Dent, J.N., 1962. Limb regeneration in larvae and metamorphosing individuals of the South African clawed toad. *Journal of morphology*, 110(1), pp.61–77.

Desai, B.M. et al., 2007. Preexisting pancreatic acinar cells contribute to acinar cell, but not islet beta cell, regeneration. *The Journal of clinical investigation*, 117(4), pp.971–7.

Diaz-Benjumea, F.J. & Cohen, S.M., 1993. Interaction between dorsal and ventral cells in the imaginal disc directs wing development in Drosophila. *Cell*, 75(4), pp.741–52.

Diaz-Benjumea, F.J. & Cohen, S.M., 1995. Serrate signals through Notch to establish a Wingless-dependent organizer at the dorsal/ventral compartment boundary of the Drosophila wing. *Development (Cambridge, England)*, 121(12), pp.4215–25.

Díaz-García, S. & Baonza, A., 2013. Pattern reorganization occurs independently of cell division during Drosophila wing disc regeneration in situ. *Proceedings of the National Academy of Sciences of the United States of America*, 110(32), pp.13032–7.

Diez del Corral, R. et al., 1999. The Iroquois homeodomain proteins are required to specify body wall identity in Drosophila. *Genes & development*, 13(13), pp.1754–61.

Dimitriou, R. et al., 2011. Bone regeneration: current concepts and future directions. *BMC medicine*, 9(1), p.66.

Dizdaroglu, M. & Jaruga, P., 2012. Mechanisms of free radical-induced damage to DNA. *Free radical research*, 46(4), pp.382–419.

Dong-Yun, S. et al., 2003. Redox stress regulates cell proliferation and apoptosis of human hepatoma through Akt protein phosphorylation. *FEBS letters*, 542(1–3), pp.60–4.

Droge, W., 2002. Free Radicals in the Physiological Control of Cell Function. *Physiol Rev*, 82(1), pp.47–95.

E

Eberl, D.F. et al., 1992. Genetic and developmental analysis of polytene section 17 of the X chromosome of Drosophila melanogaster. *Genetics*, 130(3).

Echeverri, K., Clarke, J.D. & Tanaka, E.M., 2001. In vivo imaging indicates muscle fiber dedifferentiation is a major contributor to the regenerating tail blastema. *Developmental biology*, 236(1), pp.151–64.

Edgar, B.A., 2006. How flies get their size: genetics meets physiology. *Nature reviews. Genetics*, 7(12), pp.907–16.

Einhorn, T.A., 1998. The cell and molecular biology of fracture healing. *Clinical orthopaedics and related research*, (355 Suppl), pp.S7-21.

Engeland, W.C. et al., 1996. Phenotypic changes and proliferation of adrenocortical cells during adrenal regeneration in rats. *Endocrine research*, 22(4), pp.395–400.

Evans, M.J. et al., 1976. Renewal of the terminal bronchiolar epithelium in the rat following exposure to NO2 or O3. *Laboratory investigation; a journal of technical methods and pathology*, 35(3), pp.246–57.

F

Fan, Y. et al., 2014. Genetic models of apoptosis-induced proliferation decipher activation of JNK and identify a requirement of EGFR signaling for tissue regenerative responses in Drosophila. N. Perrimon, ed. *PLoS genetics*, 10(1), p.e1004131.

Fan, Y. & Bergmann, A., 2008. Distinct Mechanisms of Apoptosis-Induced Compensatory Proliferation in Proliferating and Differentiating Tissues in the Drosophila Eye. *Developmental Cell*, 14(3), pp.399–410.

Farber, E., 1956. Similarities in the sequence of early histological changes induced in the liver of the rat by ethionine, 2-acetylamino-fluorene, and 3'-methyl-4-dimethylaminoazobenzene. *Cancer research*, 16(2), pp.142–8.

Fehér, A. et al., 2008. The involvement of reactive oxygen species (ROS) in the cell cycle activation (G(0)-to-G(1) transition) of plant cells. *Plant signaling & behavior*, 3(10), pp.823–6.

Felty, Q., Singh, K.P. & Roy, D., 2005. Estrogen-induced G1/S transition of G0-arrested estrogen-dependent breast cancer cells is regulated by mitochondrial oxidant signaling. *Oncogene*, 24(31), pp.4883–4893.

Ferguson, C. et al., 1999. Does adult fracture repair recapitulate embryonic skeletal formation? *Mechanisms of development*, 87(1–2), pp.57–66.

Ferguson, M.W. et al., 1996. Scar formation: the spectral nature of fetal and adult wound repair. *Plastic and reconstructive surgery*, 97(4), pp.854–60.

Ferreira, F. et al., 2016. Early bioelectric activities mediate redox-modulated regeneration. *Development*, 143(24), pp.4582–4594.

Finkel, T., 2012. From sulfenylation to sulfhydration: what a thiolate needs to tolerate. *Science signaling*, 5(215), p.pe10.

Finkel, T., 2011. Signal transduction by reactive oxygen species. *The Journal of cell biology*, 194(1), pp.7–15.

Fogarty, C.E. et al., 2016. Extracellular Reactive Oxygen Species Drive Apoptosis-Induced Proliferation via Drosophila Macrophages. *Current biology : CB*, 26(5), pp.575–84.

La Fortezza, M. et al., 2016. JAK/STAT signalling mediates cell survival in response to tissue stress. *Development (Cambridge, England)*, 143(16), pp.2907–19.

Frantz, B. et al., 1998. The activation state of p38 mitogen-activated protein kinase determines the efficiency of ATP competition for pyridinylimidazole inhibitor binding. *Biochemistry*, 37(39), pp.13846–53.

Freel, C.D. et al., 2008. Mitochondrial localization of Reaper to promote inhibitors of apoptosis protein degradation conferred by GH3 domain-lipid interactions. *The Journal of biological chemistry*, 283(1), pp.367–79.

Freeman, G., 1963. LENS REGENERATION FROM THE CORNEA IN XENOPUS LAEVIS. *The Journal of experimental zoology*, 154, pp.39–65.

French, V., Bryant, P.J. & Bryant, S. V, 1976. Pattern regulation in epimorphic fields. *Science (New York, N.Y.)*, 193(4257), pp.969–81.

Fridovich, I., 1997. Superoxide anion radical (O2-.), superoxide dismutases, and related matters. *The Journal of biological chemistry*, 272(30), pp.18515–7.

Fristrom, DK. Fristrom, J., 1993. The metamorphic development of the adult epidermis. *Cold Spring Harbor Laboratory Press*, pp.843–897.

Fristrom, D. et al., 1994. Blistered: a gene required for vein/intervein formation in wings of Drosophila. *Development (Cambridge, England)*, 120(9), pp.2661–71.

Frost, B. et al., 2014. Tau promotes neurodegeneration through global chromatin relaxation. *Nature Neuroscience*, 17(3), pp.357–366.

Fuchs, E., Tumbar, T. & Guasch, G., 2004. Socializing with the neighbors: stem cells and their niche. *Cell*, 116(6), pp.769–78.

Fujino, G. et al., 2007. Thioredoxin and TRAF family proteins regulate reactive oxygen species-dependent activation of ASK1 through reciprocal modulation of the N-terminal homophilic interaction of ASK1. *Molecular and cellular biology*, 27(23), pp.8152–63.

G

Galko, M.J. & Krasnow, M.A., 2004. Cellular and Genetic Analysis of Wound Healing in Drosophila Larvae Alfonso Martinez Arias, ed. *PLoS Biology*, 2(8), p.e239.

Galliot, B. et al., 2006. Hydra, a niche for cell and developmental plasticity. *Seminars in cell & developmental biology*, 17(4), pp.492–502.

Galliot, B. & Ghila, L., 2010. Cell plasticity in homeostasis and regeneration. *Molecular Reproduction and Development*, 77(10), pp.837–855.

Garcia-Bellido, A. & Merriam, J.R., 1971. Parameters of the wing imaginal disc development of Drosophila melanogaster. *Developmental biology*, 24(1), pp.61–87.

Garcia-Bellido, A., Ripoll, P. & Morata, G., 1973. Developmental compartmentalisation of the wing disk of Drosophila. *Nature: New biology*, 245(147), pp.251–3.

Garcia-Bellido, A. & Santamaria, P., 1972. Developmental analysis of the wing disc in the mutant engrailed of Drosophila melanogaster. *Genetics*, 72(1), pp.87–104.

Garelli, A. et al., 2015. Dilp8 requires the neuronal relaxin receptor Lgr3 to couple growth to developmental timing. *Nature communications*, 6, p.8732.

Garelli, A. et al., 2012. Imaginal discs secrete insulin-like peptide 8 to mediate plasticity of growth and maturation. *Science (New York, N.Y.)*, 336(6081), pp.579–82.

Garza-Garcia, A.A., Driscoll, P.C. & Brockes, J.P., 2010. Evidence for the Local Evolution of Mechanisms Underlying Limb Regeneration in Salamanders. *Integrative and Comparative Biology*, 50(4), pp.528–535.

Gauron, C. et al., 2013. Sustained production of ROS triggers compensatory proliferation and is required for regeneration to proceed. *Scientific Reports*, 3, p.2084.

Gemberling, M. et al., 2013. The zebrafish as a model for complex tissue regeneration. *Trends in Genetics*, 29(11), pp.611–620.

Gerhold, A.R. et al., 2011. Identification and characterization of genes required for compensatory growth in Drosophila. *Genetics*, 189(4), pp.1309–26.

Gettings, M. et al., 2010. JNK signalling controls remodelling of the segment boundary through cell reprogramming during Drosophila morphogenesis. K. Basler, ed. *PLoS biology*, 8(6), p.e1000390.

Geuking, P. et al., 2009. A non-redundant role for Drosophila Mkk4 and hemipterous/Mkk7 in TAK1-mediated activation of JNK. A. Bergmann, ed. *PloS one*, 4(11), p.e7709.

Geuking, P., Narasimamurthy, R. & Basler, K., 2005. A genetic screen targeting the tumor necrosis factor/Eiger signaling pathway: identification of Drosophila TAB2 as a functionally conserved component. *Genetics*, 171(4), pp.1683–94..

Ghosh-Roy, A. & Chisholm, A.D., 2010. Caenorhabditis elegans: a new model organism for studies of axon regeneration. *Developmental dynamics : an official publication of the American Association of Anatomists*, 239(5), pp.1460–4.

Gibson, M.C. & Schubiger, G., 1999. Hedgehog is required for activation of engrailed during regeneration of fragmented Drosophila imaginal discs. *Development (Cambridge, England)*, 126(8), pp.1591–9.

Gierer, A. et al., 1972. Regeneration of hydra from reaggregated cells. *Nature: New biology*, 239(91), pp.98–101.

Gilbert, M.M. et al., 2005. A novel functional activator of the Drosophila JAK/STAT pathway, unpaired2, is revealed by an in vivo reporter of pathway activation. *Mechanisms of development*, 122(7–8), pp.939–48.

Glise, B., Bourbon, H. & Noselli, S., 1995. hemipterous encodes a novel Drosophila MAP kinase kinase, required for epithelial cell sheet movement. *Cell*, 83(3), pp.451–61.

González-Gaitán, M., Capdevila, M.P. & García-Bellido, A., 1994. Cell proliferation patterns in the wing imaginal disc of Drosophila. *Mechanisms of development*, 46(3), pp.183–200.

Goossens, V. et al., 1995. Direct evidence for tumor necrosis factor-induced mitochondrial reactive oxygen intermediates and their involvement in cytotoxicity. *Proceedings of the National Academy of Sciences of the United States of America*, 92(18), pp.8115–9.

Goto, A., Kadowaki, T. & Kitagawa, Y., 2003. Drosophila hemolectin gene is expressed in embryonic and larval hemocytes and its knock down causes bleeding defects. *Developmental biology*, 264(2), pp.582–91.

Gould, E., 2007. How widespread is adult neurogenesis in mammals? *Nature Reviews Neuroscience*, 8(6), pp.481–488.

Goyal, L. et al., 2000. Induction of apoptosis by Drosophila reaper, hid and grim through inhibition of IAP function. *The EMBO Journal*, 19(4), pp.589–597.

Grusche, F.A. et al., 2011. The Salvador/Warts/Hippo pathway controls regenerative tissue growth in Drosophila melanogaster. *Developmental Biology*, 350(2), pp.255–266.

Gupta, S.C. et al., 2012. Upsides and downsides of reactive oxygen species for cancer: the roles of reactive oxygen species in tumorigenesis, prevention, and therapy. *Antioxidants & redox signaling*, 16(11), pp.1295–322.

Gurtner, G.C. et al., 2008. Wound repair and regeneration. *Nature*, 453(7193), pp.314–321.

H

Hadorn E., Bertani G., G.J., 1949. Regulative capacity and field organization of male genital discs in Drosophila melanogaster. *Roux's Arch. Entwickl*, 144, pp.31–70.

Hadorn E., B.D., 1962. On the differentiation of transplanted wing imaginal disc fragments of Drosophila melanogaster. *Rev. Suisse Zool.*, 69:302–10.

Hadorn E., 1965. Problems of determination and transdetermination. *Brookhaven Symp Biol*.

Hadorn E., 1978. Transdetermination. *The Genetics and Biology of Drosophila*, 2c, pp.556–617.

Halicka, H.D. et al., 2009. Cytometric detection of chromatin relaxation, an early reporter of DNA damage response. *Cell Cycle*, 8(14), pp.2233–2237.

Halme, A., Cheng, M. & Hariharan, I.K., 2010. Retinoids regulate a developmental checkpoint for tissue regeneration in Drosophila. *Current biology : CB*, 20(5), pp.458–63.

Han, M. et al., 2005. Limb regeneration in higher vertebrates: developing a roadmap. *Anatomical record. Part B, New anatomist*, 287(1), pp.14–24.

Han, P. et al., 2014. Hydrogen peroxide primes heart regeneration with a derepression mechanism. *Cell research*, 24(9), pp.1091–107.

Handke, B. et al., 2014. Towards Long Term Cultivation of Drosophila Wing Imaginal Discs In Vitro M. Kango-Singh, ed. *PLoS ONE*, 9(9), p.e107333.

Harada, C. et al., 2006. Role of Apoptosis Signal-Regulating Kinase 1 in Stress-Induced Neural Cell Apoptosis in Vivo. *The American Journal of Pathology*, 168(1), pp.261–269.

Harding, K.G., Morris, H.L. & Patel, G.K., 2002. Science, medicine and the future: healing chronic wounds. *BMJ (Clinical research ed.)*, 324(7330), pp.160–3.

Harris, R.E. et al., 2016. Localized epigenetic silencing of a damage-activated WNT enhancer limits regeneration in mature *Drosophila* imaginal discs. *eLife*, 5.

Harrison, D.A. et al., 1998. Drosophila unpaired encodes a secreted protein that activates the JAK signaling pathway. *Genes & development*, 12(20), pp.3252–63.

Hatai, T. et al., 2000. Execution of Apoptosis Signal-regulating Kinase 1 (ASK1)-induced Apoptosis by the Mitochondria-dependent Caspase Activation. *Journal of Biological Chemistry*, 275(34), pp.26576–26581.

Haynie, J.L. & Bryant, P.J., 1976. Intercalary regeneration in imaginal wing disk of Drosophila melanogaster. *Nature*, 259(5545), pp.659–62.

Haynie, J.L. & Bryant, P.J., 1977. The effects of X-rays on the proliferation dynamics of cells in the imaginal wing disc ofDrosophila melanogaster. *Wilhelm Roux's archives of developmental biology*, 183(2), pp.85–100.

Heber-Katz, E. & Gourevitch, D., 2009. The relationship between inflammation and regeneration in the MRL mouse: potential relevance for putative human regenerative(scarless wound healing) capacities? *Annals of the New York Academy of Sciences*, 1172(1), pp.110–4.

Henry, J.J. & Tsonis, P.A., 2010. Molecular and cellular aspects of amphibian lens regeneration. *Progress in retinal and eye research*, 29(6), pp.543–55.

Herranz, H. et al., 2012. Oncogenic cooperation between SOCS family proteins and EGFR identified using a Drosophila epithelial transformation model. *Genes & development*, 26(14), pp.1602–11.

Herrera, S.C., Martin, R. & Morata, G., 2013. Tissue homeostasis in the wing disc of Drosophila melanogaster: immediate response to massive damage during development. *PLoS genetics*, 9(4), p.e1003446.

Herrera, S.C. & Morata, G., 2014. Transgressions of compartment boundaries and cell reprogramming during regeneration in Drosophila. *eLife*, 3, p.e01831.

van den Heuvel, M. & Ingham, P.W., 1996. smoothened encodes a receptor-like serpentine protein required for hedgehog signalling. *Nature*, 382(6591), pp.547–51.

Hinz, U., Giebel, B. & Campos-Ortega, J.A., 1994. The basic-helix-loop-helix domain of Drosophila lethal of scute protein is sufficient for proneural function and activates neurogenic genes. *Cell*, 76(1), pp.77–87.

Hombría, J.C.-G. et al., 2005. Characterisation of Upd2, a Drosophila JAK/STAT pathway ligand. *Developmental biology*, 288(2), pp.420–33.

Horne, K.A. & Jahoda, C.A., 1992. Restoration of hair growth by surgical implantation of follicular dermal sheath. *Development (Cambridge, England)*, 116(3), pp.563–71.

Hoshi, N. et al., 2007. Side population cells in the mouse thyroid exhibit stem/progenitor cell-like characteristics. *Endocrinology*, 148(9), pp.4251–8.

Hou, X.S., Melnick, M.B. & Perrimon, N., 1996. Marelle acts downstream of the Drosophila HOP/JAK kinase and encodes a protein similar to the mammalian STATs. *Cell*, 84(3), pp.411–9.

Hsiung, F. et al., 2005. Dependence of Drosophila wing imaginal disc cytonemes on Decapentaplegic. *Nature*, 437(7058), pp.560–3.

Huh, J.R., Guo, M. & Hay, B.A., 2004. Compensatory proliferation induced by cell death in the Drosophila wing disc requires activity of the apical cell death caspase Dronc in a nonapoptotic role. *Current biology : CB*, 14(14), pp.1262–6.

Hunter, T., 1995. Protein kinases and phosphatases: the yin and yang of protein phosphorylation and signaling. *Cell*, 80(2), pp.225–36.

Hussey, R.G., Thompson, W.R. & Calhoun, E.T., 1927. THE INFLUENCE OF X-RAYS ON THE DEVELOPMENT OF DROSOPHILA LARVAE. *Science (New York, N.Y.)*, 66(1698), pp.65–6.

I

Ichijo, H. et al., 1997. Induction of apoptosis by ASK1, a mammalian MAPKKK that activates SAPK/JNK and p38 signaling pathways. *Science (New York, N.Y.)*, 275(5296), pp.90–4.

Igaki, T. et al., 2002. Eiger, a TNF superfamily ligand that triggers the Drosophila JNK pathway. *The EMBO Journal*, 21(12), pp.3009–3018.

Igaki, T. et al., 2009. Intrinsic tumor suppression and epithelial maintenance by endocytic activation of Eiger/TNF signaling in Drosophila. *Developmental cell*, 16(3), pp.458–65.

Igaki, T., Pagliarini, R.A. & Xu, T., 2006. Loss of Cell Polarity Drives Tumor Growth and Invasion through JNK Activation in Drosophila. *Current Biology*, 16(11), pp.1139–1146.

Inoue, H. et al., 2001. A Drosophila MAPKKK, D-MEKK1, mediates stress responses through activation of p38 MAPK. *The EMBO journal*, 20(19), pp.5421–30.

Ishikawa, F. et al., 2006. Purified human hematopoietic stem cells contribute to the generation of cardiomyocytes through cell fusion. *FASEB journal : official publication of the Federation of American Societies for Experimental Biology*, 20(7), pp.950–2.

Ishimaru, S. et al., 2004. PVR plays a critical role via JNK activation in thorax closure during Drosophila metamorphosis. *The EMBO journal*, 23(20), pp.3984–94.

Iten, L.E. & Bryant, S. V, 1975. The interaction between the blastema and stump in the establishment of the anterior--posterior and proximal--distal organization of the limb regenerate. *Developmental biology*, 44(1), pp.119–47.

Ito, K. et al., 2006. Reactive oxygen species act through p38 MAPK to limit the lifespan of hematopoietic stem cells. *Nature Medicine*, 12(4), pp.446–451.

Izumi, Y. et al., 2003. Activation of apoptosis signal-regulating kinase 1 in injured artery and its critical role in neointimal hyperplasia. *Circulation*, 108(22), pp.2812–8.

Izumi, Y. et al., 2005. Important role of apoptosis signal-regulating kinase 1 in ischemia-induced angiogenesis. *Arteriosclerosis, thrombosis, and vascular biology*, 25(9), pp.1877–83.

Izumiya, Y. et al., 2003. Apoptosis signal-regulating kinase 1 plays a pivotal role in angiotensin II-induced cardiac hypertrophy and remodeling. *Circulation research*, 93(9), pp.874–83.

J

Jacinto, A. et al., 2002. Dynamic analysis of actin cable function during Drosophila dorsal closure. *Current biology : CB*, 12(14), pp.1245–50.

Jasper, H. et al., 2001. The genomic response of the Drosophila embryo to JNK signaling. *Developmental cell*, 1(4), pp.579–86.

Jaszczak, J.S. et al., 2016. Growth Coordination During Drosophila melanogaster Imaginal Disc Regeneration Is Mediated by Signaling Through the Relaxin Receptor Lgr3 in the Prothoracic Gland. *Genetics*, 204(2), pp.703–709.

Jaszczak, J.S. et al., 2015. Nitric Oxide Synthase Regulates Growth Coordination During Drosophila melanogaster Imaginal Disc Regeneration. *Genetics*, 200(4), pp.1219–1228.

Jensen, J.N. et al., 2005. Recapitulation of elements of embryonic development in adult mouse pancreatic regeneration. *Gastroenterology*, 128(3), pp.728–41.

Jia, Y.-T. et al., 2007. Activation of p38 MAPK by reactive oxygen species is essential in a rat model of stress-induced gastric mucosal injury. *Journal of immunology (Baltimore, Md. : 1950)*, 179(11), pp.7808–19.

Jiang, F., Zhang, Y. & Dusting, G.J., 2011. NADPH oxidase-mediated redox signaling: roles in cellular stress response, stress tolerance, and tissue repair. *Pharmacological reviews*, 63(1), pp.218–42.

Jiang, H. et al., 2009. Cytokine/Jak/Stat signaling mediates regeneration and homeostasis in the Drosophila midgut. *Cell*, 137(7), pp.1343–55.

Johnson, S.L. & Weston, J.A., 1995. Temperature-sensitive mutations that cause stage-specific defects in Zebrafish fin regeneration. *Genetics*, 141(4), pp.1583–95.

Johnstone, K. et al., 2013. Localised JAK/STAT pathway activation is required for Drosophila wing hinge development. *PloS one*, 8(5), p.e65076.

Jopling, C. et al., 2010. Zebrafish heart regeneration occurs by cardiomyocyte dedifferentiation and proliferation. *Nature*, 464(7288), pp.606–9.

K

Kaji, T. et al., 2010. ASK3, a novel member of the apoptosis signal-regulating kinase family, is essential for stress-induced cell death in HeLa cells. *Biochemical and Biophysical Research Communications*, 395(2), pp.213–218..

Kamata, H. et al., 2005. Reactive oxygen species promote TNFalpha-induced death and sustained JNK activation by inhibiting MAP kinase phosphatases. *Cell*, 120(5), pp.649–61.

Kanaji, N. et al., 2013. Differential roles of JNK, ERK1/2, and p38 mitogen-activated protein kinases on endothelial cell tissue repair functions in response to tumor necrosis factor-α. *Journal of vascular research*, 50(2), pp.145–56.

Kanamoto, T. et al., 2000. Role of apoptosis signal-regulating kinase in regulation of the c-Jun N-terminal kinase pathway and apoptosis in sympathetic neurons. *Molecular and cellular biology*, 20(1), pp.196–204.

Kanda, H. et al., 2002. Wengen, a Member of the Drosophila Tumor Necrosis Factor Receptor Superfamily, Is Required for Eiger Signaling. *Journal of Biological Chemistry*, 277(32), pp.28372–28375.

Kang, S.W. et al., 2004. Cytosolic Peroxiredoxin Attenuates The Activation Of Jnk And P38 But Potentiates That Of Erk In Hela Cells Stimulated With Tumor Necrosis Factor-α. *Journal of Biological Chemistry*, 279(4), pp.2535–2543.

Karkali, K. & Panayotou, G., 2012. The Drosophila DUSP Puckered is phosphorylated by JNK and p38 in response to arsenite-induced oxidative stress. *Biochemical and Biophysical Research Communications*, 418(2), pp.301–306.

Karpen, G.H. & Schubiger, G., 1981. Extensive regulatory capabilities of a Drosophila imaginal disk blastema. *Nature*, 294(5843), pp.744–7.

Karsten, P., Häder, S. & Zeidler, M.P., 2002. Cloning and expression of Drosophila SOCS36E and its potential regulation by the JAK/STAT pathway. *Mechanisms of development*, 117(1–2), pp.343–6.

Katagiri, K., Matsuzawa, A. & Ichijo, H., 2010. Regulation of Apoptosis Signal-Regulating Kinase 1 in Redox Signaling. In *Methods in enzymology*. pp. 277–288.

Katsuyama, T. et al., 2015. During Drosophila disc regeneration, JAK/STAT coordinates cell proliferation with Dilp8-mediated developmental delay. *Proceedings of the National Academy of Sciences of the United States of America*, 112(18), pp.E2327-36.

Kelly, G.S., 1998. Clinical applications of N-acetylcysteine. *Alternative Medicine Review*, 3(2), pp.114–127.

Kiehle, C.P. & Schubiger, G., 1985. Cell proliferation changes during pattern regulation in imaginal leg discs of Drosophila melanogaster. *Developmental biology*, 109(2), pp.336–46.

Kikuchi, K. et al., 2010. Primary contribution to zebrafish heart regeneration by gata4(+) cardiomyocytes. *Nature*, 464(7288), pp.601–5.

Kiley, P.J. & Storz, G., 2004. Exploiting thiol modifications. *PLoS biology*, 2(11), p.e400.

Kim, A.H. et al., 2001. Akt Phosphorylates and Negatively Regulates Apoptosis Signal-Regulating Kinase 1. *Molecular and Cellular Biology*, 21(3), pp.893–901.

Kimura, Y. et al., 2003. Expression of complement 3 and complement 5 in newt limb and lens regeneration. *Journal of immunology (Baltimore, Md. : 1950)*, 170(5), pp.2331–9.

King, R.S. & Newmark, P.A., 2012. The cell biology of regeneration. *The Journal of Cell Biology*, 196(5), pp.553–562.

Klebes, A. et al., 2005. Regulation of cellular plasticity in Drosophila imaginal disc cells by the Polycomb group, trithorax group and lama genes. *Development (Cambridge, England)*, 132(16), pp.3753–65.

Knopf, F. et al., 2011. Bone regenerates via dedifferentiation of osteoblasts in the zebrafish fin. *Developmental cell*, 20(5), pp.713–24.

Kondo, S. et al., 2006. DRONC Coordinates Cell Death and Compensatory Proliferation. *Molecular and Cellular Biology*, 26(19), pp.7258–7268.

Kornberg, T., 1981. Engrailed: a gene controlling compartment and segment formation in Drosophila. *Proceedings of the National Academy of Sciences of the United States of America*, 78(2), pp.1095–9.

Kornberg, T. et al., 1985. The engrailed locus of Drosophila: in situ localization of transcripts reveals compartment-specific expression. *Cell*, 40(1), pp.45–53.

Kragl, M. et al., 2009. Cells keep a memory of their tissue origin during axolotl limb regeneration. *Nature*, 460(7251), pp.60–5.

Kreuz, S. & Fischle, W., 2016. Oxidative stress signaling to chromatin in health and disease. *Epigenomics*, 8(6), pp.843–62.

Kumar, A. et al., 2004. The regenerative plasticity of isolated urodele myofibers and its dependence on MSX1. Brigid Hogan, ed. *PLoS biology*, 2(8), p.E218.

Kumar, R.D. & Babu, N.M., 2014. DER PHARMACOLOGIA SINICA WOUND HEALING AND IT'S IMPORTANCE-A REVIEW. , 1(1), pp.24–30.

Kuranaga, E. et al., 2002. Reaper-mediated inhibition of DIAP1-induced DTRAF1 degradation results in activation of JNK in Drosophila. *Nature Cell Biology*, 4(9), pp.705–710.

Kurosaka, H. et al., 2008. Comparison of molecular and cellular events during lower jaw regeneration of newt (Cynops pyrrhogaster) and West African clawed frog (Xenopus tropicalis). *Developmental dynamics : an official publication of the American Association of Anatomists*, 237(2), pp.354–65.

Kushida, N. et al., 2001. Essential role for extracellular Ca(2+) in JNK activation by mechanical stretch in bladder smooth muscle cells. *American journal of physiology. Cell physiology*, 281(4), pp.C1165-72.

Kwon, J. et al., 2004. Reversible oxidation and inactivation of the tumor suppressor PTEN in cells stimulated with peptide growth factors. *Proceedings of the National Academy of Sciences of the United States of America*, 101(47), pp.16419–24.

Kyriakis, J.M. & Avruch, J., 2001. Mammalian mitogen-activated protein kinase signal transduction pathways activated by stress and inflammation. *Physiological reviews*, 81(2), pp.807–69.

L

L. Belecky-Adams, T. et al., 2008. The Chick as a Model for Retina Development and Regeneration. In *Animal Models in Eye Research*. Elsevier, pp. 102–119.

Lai, S.-L. & Lee, T., 2006. Genetic mosaic with dual binary transcriptional systems in Drosophila. *Nature neuroscience*, 9(5), pp.703–9.

Lambeth, J.D., 2004. NOX enzymes and the biology of reactive oxygen. *Nature Reviews Immunology*, 4(3), pp.181–189.

Lan, L. et al., 2007. Stem cells derived from goiters in adults form spheres in response to intense growth stimulation and require thyrotropin for differentiation into thyrocytes. *The Journal of clinical endocrinology and metabolism*, 92(9), pp.3681–8.

Laube, F. et al., 2006. Re-programming of newt cardiomyocytes is induced by tissue regeneration. *Journal of cell science*, 119(Pt 22), pp.4719–29.

Lawrence, P.A., 2001. Morphogens: how big is the big picture? *Nature cell biology*, 3(7), pp.E151-4.

Lawrence, P.A. & Morata, G., 1976. Compartments in the wing of Drosophila: a study of the engrailed gene. *Developmental biology*, 50(2), pp.321–37.

Leaper, D.J. & Harding, K.G. (Keith G.., 1998. *Wounds : biology and management*, Oxford University Press.

Lee, L.W. & Gerhart, J.C., 1973. Dependence of transdetermination frequency on the developmental stage of cultured imaginal discs of Drosophila melanogaster. *Developmental biology*, 35(1), pp.62–82.

Lee, N. et al., 2005. Suppression of Polycomb group proteins by JNK signalling induces transdetermination in Drosophila imaginal discs. *Nature*, 438(7065), pp.234–237.

Lee, S.-R. et al., 2002. Reversible Inactivation of the Tumor Suppressor PTEN by H2O2. *Journal of Biological Chemistry*, 277(23), pp.20336–20342.

Leslie, N.R. et al., 2003. Redox regulation of PI 3-kinase signalling via inactivation of PTEN. *The EMBO journal*, 22(20), pp.5501–10.

Levin, M., 2009. Bioelectric mechanisms in regeneration: Unique aspects and future perspectives. *Seminars in Cell & Developmental Biology*, 20(5), pp.543–556.

Lewis I.Held, 2005. Imaginal discs. *Cambridge University Press*. Available at: www.cambridge.org [Accessed March 20, 2017].

Li, G. et al., 2003. c-Jun is essential for organization of the epidermal leading edge. *Developmental cell*, 4(6), pp.865–77.

Lin, Y. et al., 2004. Tumor Necrosis Factor-induced Nonapoptotic Cell Death Requires Receptor-interacting Protein-mediated Cellular Reactive Oxygen Species Accumulation. *Journal of Biological Chemistry*, 279(11), pp.10822–10828.

Liou, G.-Y. & Storz, P., 2010. Reactive oxygen species in cancer. *Free radical research*, 44(5), pp.479–96.

Liu, H. et al., 2000. Activation of apoptosis signal-regulating kinase 1 (ASK1) by tumor necrosis factor receptor-associated factor 2 requires prior dissociation of the ASK1 inhibitor thioredoxin. *Molecular and cellular biology*, 20(6), pp.2198–208.

Lo, D.C., Allen, F. & Brockes, J.P., 1993. Reversal of muscle differentiation during urodele limb regeneration. *Proceedings of the National Academy of Sciences of the United States of America*, 90(15), pp.7230–4.

Loo, A.E.K. et al., 2012. Effects of Hydrogen Peroxide on Wound Healing in Mice in Relation to Oxidative Damage J. Sastre, ed. *PLoS ONE*, 7(11), p.e49215.

Love, N.R. et al., 2013. Amputation-induced reactive oxygen species are required for successful Xenopus tadpole tail regeneration. *Nature Cell Biology*, 15(2), pp.222–228.

De Luca, A. et al., 2010. Methionine sulfoxide reductase A down-regulation in human breast cancer cells results in a more aggressive phenotype. *Proceedings of the National Academy of Sciences of the United States of America*, 107(43), pp.18628–33.

M

Macmahon, H.E., 1937. Hyperplasia and Regeneration of the Myocardium in Infants and in Children. *The American journal of pathology*, 13(5), p.845–854.5.

Maden, M., 2008. Axolotl/Newt. In *Methods in molecular biology (Clifton, N.J.)*. pp. 467–480.

Mandaravally Madhavan, M. & Schneiderman, H.A., 1977. Histological analysis of the dynamics of growth of imaginal discs and histoblast nests during the larval development ofDrosophila melanogaster. *Wilhelm Roux's Archives of Developmental Biology*, 183(4), pp.269–305.

Marinho, H.S. et al., 2014. Hydrogen peroxide sensing, signaling and regulation of transcription factors. *Redox Biology*, 2, pp.535–562.

Martin-Blanco, E. et al., 1998. puckered encodes a phosphatase that mediates a feedback loop regulating JNK activity during dorsal closure in Drosophila. *Genes Dev*, 12(4), pp.557–570.

Martín-Blanco, E. et al., 1999. A temporal switch in DER signaling controls the specification and differentiation of veins and interveins in the Drosophila wing. *Development (Cambridge, England)*, 126(24), pp.5739–47.

Martín-Blanco, E. et al., 1998. puckered encodes a phosphatase that mediates a feedback loop regulating JNK activity during dorsal closure in Drosophila. *Genes & development*, 12(4), pp.557–70.

Martín-Castellanos, C. & Edgar, B.A., 2002. A characterization of the effects of Dpp signaling on cell growth and proliferation in the Drosophila wing. *Development (Cambridge, England)*, 129(4), pp.1003–13.

Martin, F.A. & Morata, G., 2006. Compartments and the control of growth in the Drosophila wing imaginal disc. *Development*, 133(22), pp.4421–4426.

Martin, P. & Parkhurst, S.M., 2004. Parallels between tissue repair and embryo morphogenesis. *Development (Cambridge, England)*, 131(13), pp.3021–34.

Martino, G. et al., 2011. Brain Regeneration in Physiology and Pathology: The Immune Signature Driving Therapeutic Plasticity of Neural Stem Cells. *Physiological Reviews*, 91(4), pp.1281–1304.

Matsuzawa, A. et al., 2005. ROS-dependent activation of the TRAF6-ASK1-p38 pathway is selectively required for TLR4-mediated innate immunity. *Nature Immunology*, 6(6), pp.587–592.

Mattila, J. et al., 2005. Role of Jun N-terminal Kinase (JNK) signaling in the wound healing and regeneration of a Drosophila melanogaster wing imaginal disc. *Int J Dev Biol*, 49(4), pp.391–399.

Mattila, J., Omelyanchuk, L. & Nokkala, S., 2004. Dynamics of decapentaplegic expression during regeneration of the Drosophila melanogaster wing imaginal disc. *The International journal of developmental biology*, 48(4), pp.343–7.

McClure, K.D., Sustar, A. & Schubiger, G., 2008. Three genes control the timing, the site and the size of blastema formation in Drosophila. *Developmental Biology*, 319(1), pp.68–77.

McCubrey, J.A., Lahair, M.M. & Franklin, R.A., 2006. Reactive oxygen species-induced activation of the MAP kinase signaling pathways. *Antioxidants & redox signaling*, 8(9–10), pp.1775–89.

McCusker, C., Bryant, S. V. & Gardiner, D.M., 2015. The axolotl limb blastema: cellular and molecular mechanisms driving blastema formation and limb regeneration in tetrapods. *Regeneration*, 2(2), pp.54–71.

McGuire, S.E. et al., 2003. Spatiotemporal rescue of memory dysfunction in Drosophila. *Science (New York, N.Y.)*, 302(5651), pp.1765–8.

Meinhardt, H., 1983. Cell determination boundaries as organizing regions for secondary embryonic fields. *Developmental biology*, 96(2), pp.375–85.

Meng, T.-C., Fukada, T. & Tonks, N.K., 2002. Reversible oxidation and inactivation of protein tyrosine phosphatases in vivo. *Molecular cell*, 9(2), pp.387–99.

Meserve, J.H. & Duronio, R.J., 2015. Scalloped and Yorkie are required for cell cycle re-entry of quiescent cells after tissue damage. *Development (Cambridge, England)*, 142(16), pp.2740–51.

Metaxakis, A. et al., 2005. Minos as a genetic and genomic tool in Drosophila melanogaster. *Genetics*, 171(2), pp.571–81.

Milán, M., Campuzano, S. & García-Bellido, A., 1996. Cell cycling and patterned cell proliferation in the Drosophila wing during metamorphosis. *Proceedings of the National Academy of Sciences of the United States of America*, 93(21), pp.11687–92.

Milán, M., Campuzano, S. & García-Bellido, A., 1997. Developmental parameters of cell death in the wing disc of Drosophila. *Proceedings of the National Academy of Sciences of the United States of America*, 94(11), pp.5691–6.

Milán, M. & Cohen, S.M., 1999. Regulation of LIM homeodomain activity in vivo: a tetramer of dLDB and apterous confers activity and capacity for regulation by dLMO. *Molecular cell*, 4(2), pp.267–73.

Miller, E.W., Dickinson, B.C. & Chang, C.J., 2010. Aquaporin-3 mediates hydrogen peroxide uptake to regulate downstream intracellular signaling. *Proceedings of the National Academy of Sciences*, 107(36), pp.15681–15686.

Mills, K., Daish, T. & Kumar, S., 2005. The Function of the Drosophila Caspase DRONC in Cell Death and Development. *Cell Cycle*, 4(6), pp.744–746.

Mitani, F. et al., 2003. The undifferentiated cell zone is a stem cell zone in adult rat adrenal cortex. *Biochimica et biophysica acta*, 1619(3), pp.317–24.

Mitashov, V.I., 1996. Mechanisms of retina regeneration in urodeles. *The International journal of developmental biology*, 40(4), pp.833–44..

Miura, M., 2012. Apoptotic and Nonapoptotic Caspase Functions in Animal Development. *Cold Spring Harbor Perspectives in Biology*, 4(10), pp.a008664–a008664.

Mollereau, B. et al., 2013. Compensatory proliferation and apoptosis-induced proliferation: a need for clarification. *Cell death and differentiation*, 20(1), p.181.

Montagne, J. et al., 1996. The Drosophila Serum Response Factor gene is required for the formation of intervein tissue of the wing and is allelic to blistered. *Development (Cambridge, England)*, 122(9), pp.2589–97.

Moore, K.A. & Lemischka, I.R., 2006. Stem cells and their niches. *Science (New York, N.Y.)*, 311(5769), pp.1880–5.

Morata, G. & Lawrence, P.A., 1975. Control of compartment development by the engrailed gene in Drosophila. *Nature*, 255(5510), pp.614–7.

Morata, G., Shlevkov, E. & Pérez-Garijo, A., 2011. Mitogenic signaling from apoptotic cells in Drosophila. *Development, growth & differentiation*, 53(2), pp.168–76.

Moreira, S. et al., 2010. Prioritization of Competing Damage and Developmental Signals by Migrating Macrophages in the Drosophila Embryo. *Current Biology*, 20(5), pp.464–470.

Moreno, E., Yan, M. & Basler, K., 2002. Evolution of TNF signaling mechanisms: JNK-dependent apoptosis triggered by Eiger, the Drosophila homolog of the TNF superfamily. *Current biology : CB*, 12(14), pp.1263–8.

Morgan, T.H., *Regeneration*.

Morgan, T.H. 1898. Experimental Studies of the Regeneration of Planaria maculata.

Mukherjee, T., Hombría, J.C.-G. & Zeidler, M.P., 2005. Opposing roles for Drosophila JAK/STAT signalling during cellular proliferation. *Oncogene*, 24(15), pp.2503–11.

Muliyil, S. & Narasimha, M., 2014. Mitochondrial ROS regulates cytoskeletal and mitochondrial remodeling to tune cell and tissue dynamics in a model for wound healing. *Developmental cell*, 28(3), pp.239–52.

Muller, T.L. et al., 1999. Regeneration in higher vertebrates: limb buds and digit tips. *Seminars in cell & developmental biology*, 10(4), pp.405–13.

Mummery, C.L. & Passier, R., 2011. New perspectives on regeneration of the heart. *Circulation research*, 109(8), pp.828–9.

Muneoka, K. et al., 2008. Mammalian regeneration and regenerative medicine. *Birth Defects Research Part C: Embryo Today: Reviews*, 84(4), pp.265–280.

Muneoka, K., Holler-Dinsmore, G. & Bryant, S. V, 1986. Intrinsic control of regenerative loss in Xenopus laevis limbs. *The Journal of experimental zoology*, 240(1), pp.47–54.

N

Nacu, E. & Tanaka, E.M., 2011. Limb regeneration: a new development? *Annual review of cell and developmental biology*, 27(1), pp.409–40.

Nadeau, P.J. et al., 2007. Disulfide Bond-mediated Multimerization of Ask1 and Its Reduction by Thioredoxin-1 Regulate H2O2-induced c-Jun NH2-terminal Kinase Activation and Apoptosis. *Molecular Biology of the Cell*, 18(10), pp.3903–3913.

Narciso, C. et al., 2015. Patterning of wound-induced intercellular Ca(2+) flashes in a developing epithelium. *Physical biology*, 12(5), p.56005.

Nässel, D.R. & Broeck, J. Vanden, 2016. Insulin/IGF signaling in Drosophila and other insects: factors that regulate production, release and post-release action of the insulin-like peptides. *Cellular and Molecular Life Sciences*, 73(2), pp.271–290.

Nellen, D. et al., 1996. Direct and long-range action of a DPP morphogen gradient. *Cell*, 85(3), pp.357–68.

Nelson, C.M. et al., 2005. Emergent patterns of growth controlled by multicellular form and mechanics. *Proceedings of the National Academy of Sciences of the United States of America*, 102(33), pp.11594–9.

Nelson, K.K. & Melendez, J.A., 2004. Mitochondrial redox control of matrix metalloproteinases. *Free Radical Biology and Medicine*, 37(6), pp.768–784.

Neumann, C.J. & Cohen, S.M., 1996. Distinct mitogenic and cell fate specification functions of wingless in different regions of the wing. *Development (Cambridge, England)*, 122(6), pp.1781–9.

Niethammer, P. et al., 2009. A tissue-scale gradient of hydrogen peroxide mediates rapid wound detection in zebrafish. *Nature*, 459(7249), pp.996–9.

Nimse, S.B. & Pal, D., 2015. Free radicals, natural antioxidants, and their reaction mechanisms. *RSC Adv.*, 5(35), pp.27986–28006.

Nishitoh, H. et al., 2002. ASK1 is essential for endoplasmic reticulum stress-induced neuronal cell death triggered by expanded polyglutamine repeats. *Genes & development*, 16(11), pp.1345–55.

Nishitoh, H. et al., 1998a. ASK1 is essential for JNK/SAPK activation by TRAF2. *Molecular cell*, 2(3), pp.389–95.

Noda, K., 1971. Reconstitution of dissociated cells of Hydra. *Zoology Magazine*, 80:27–31.

Noguchi, T. et al., 2005. Recruitment of Tumor Necrosis Factor Receptor-associated Factor Family Proteins to Apoptosis Signal-regulating Kinase 1 Signalosome Is Essential for Oxidative Stress-induced Cell Death. *Journal of Biological Chemistry*, 280(44), pp.37033–37040.

Noselli, S. & Agnès, F., 1999. Roles of the JNK signaling pathway in Drosophila morphogenesis. *Current Opinion in Genetics & Development*, 9(4), pp.466–472.

Nye, H.L.D. et al., 2003. Regeneration of the urodele limb: A review. *Developmental Dynamics*, 226(2), pp.280–294.

0

O'Brochta, D.A. & Bryant, P.J., 1987. Distribution of S-phase cells during the regeneration of Drosophila imaginal wing discs. *Developmental biology*, 119(1), pp.137–42.

Oberpriller, J.O. & Oberpriller, J.C., 1974. Response of the adult newt ventricle to injury. *The Journal of experimental zoology*, 187(2), pp.249–53.

Ohlmeyer, J.T. & Kalderon, D., 1998. Hedgehog stimulates maturation of Cubitus interruptus into a labile transcriptional activator. *Nature*, 396(6713), pp.749–53.

Ohsawa, S. et al., 2011. Elimination of oncogenic neighbors by JNK-mediated engulfment in Drosophila. *Developmental cell*, 20(3), pp.315–28.

Okamoto, M. et al., 2007. Regeneration of retinotectal projections after optic tectum removal in adult newts. *Molecular vision*, 13, pp.2112–8.

Owusu-Ansah, E. & Banerjee, U., 2009. Reactive oxygen species prime Drosophila haematopoietic progenitors for differentiation. *Nature*, 461(7263), pp.537–41.

P

Padmanabha, D. & Baker, K.D., 2014. Drosophila gains traction as a repurposed tool to investigate metabolism. *Trends in endocrinology and metabolism: TEM*, 25(10), pp.518–27.

Pastor-Pareja, J.C. et al., 2004. Invasive cell behavior during Drosophila imaginal disc eversion is mediated by the JNK signaling cascade. *Developmental cell*, 7(3), pp.387–99.

Pastor-Pareja, J.C., Wu, M. & Xu, T., 2008. An innate immune response of blood cells to tumors and tissue damage in Drosophila. *Disease Models and Mechanisms*, 1(2–3), pp.144–154.

Perez-Garijo, A., Martín, F.A. & Morata, G., 2004. Caspase inhibition during apoptosis causes abnormal signalling and developmental aberrations in Drosophila. *Development*, 131(22), pp.5591–5598.

Perez-Garijo, A., Shlevkov, E. & Morata, G., 2009. The role of Dpp and Wg in compensatory proliferation and in the formation of hyperplastic overgrowths caused by apoptotic cells in the Drosophila wing disc. *Development*, 136(7), pp.1169–1177.

Perrimon, N. et al., 1996. Zygotic lethal mutations with maternal effect phenotypes in Drosophila melanogaster. II. Loci on the second and third chromosomes identified by P-element-induced mutations. *Genetics*, 144(4), pp.1681–92.

Pirotte, N. et al., 2015. Reactive Oxygen Species in Planarian Regeneration: An Upstream Necessity for Correct Patterning and Brain Formation. *Oxidative medicine and cellular longevity*, 2015, p.392476.

Plotnikov, A. et al., 2011. The MAPK cascades: Signaling components, nuclear roles and mechanisms of nuclear translocation. *Biochimica et Biophysica Acta (BBA) - Molecular Cell Research*, 1813(9), pp.1619–1633.

Podolsky, D.K., 1999. Mucosal immunity and inflammation. V. Innate mechanisms of mucosal defense and repair: the best offense is a good defense. *The American journal of physiology*, 277(3 Pt 1), pp.G495-9.

Pomerantz, J. & Blau, H.M., 2004. Nuclear reprogramming: a key to stem cell function in regenerative medicine. *Nature cell biology*, 6(9), pp.810–6.

Poodry, C., Imaginal discs: morphology and development. In The Genetics and Biology of Drosophila''. , 2d, pp.407–441.

Poodry, C.A. & Woods, D.F., 1990. Control of the developmental timer forDrosophila pupariation. *Roux's archives of developmental biology : the official organ of the EDBO*, 199(4), pp.219–227.

Porrello, E.R. et al., 2011. Transient regenerative potential of the neonatal mouse heart. *Science (New York, N.Y.)*, 331(6020), pp.1078–80.

Poss, K.D., 2010. Advances in understanding tissue regenerative capacity and mechanisms in animals. *Nature Reviews Genetics*, 11(10), pp.710–722.

Poss, K.D., Wilson, L.G. & Keating, M.T., 2002. Heart regeneration in zebrafish. *Science (New York, N.Y.)*, 298(5601), pp.2188–90.

Potente, M., Gerhardt, H. & Carmeliet, P., 2011. Basic and therapeutic aspects of angiogenesis. *Cell*, 146(6), pp.873–87.

Price, J.S. et al., 2005. Deer antlers: a zoological curiosity or the key to understanding organ regeneration in mammals? *Journal of Anatomy*, 207(5), pp.603–618.

Q

Quinn, J. et al., 2002. Distinct regulatory proteins control the graded transcriptional response to increasing H(2)O(2) levels in fission yeast Schizosaccharomyces pombe. *Molecular biology of the cell*, 13(3), pp.805–16.

Quiñones, J.L. et al., 2002. Extracellular matrix remodeling and metalloproteinase involvement during intestine regeneration in the sea cucumber Holothuria glaberrima. *Developmental biology*, 250(1), pp.181–97.

R

Rajan, A. & Perrimon, N., 2012. Drosophila cytokine unpaired 2 regulates physiological homeostasis by remotely controlling insulin secretion. *Cell*, 151(1), pp.123–37.

Raman, M., Chen, W. & Cobb, M.H., 2007. Differential regulation and properties of MAPKs. *Oncogene*, 26(22), pp.3100–12.

Rämet, M. et al., 2002. JNK Signaling Pathway Is Required for Efficient Wound Healing in Drosophila. *Developmental Biology*, 241(1), pp.145–156.

Ramírez-Gómez, F. et al., 2008. Immune-related genes associated with intestinal tissue in the sea cucumber Holothuria glaberrima. *Immunogenetics*, 60(7), pp.409–409.

Razzell, W. et al., 2013. Calcium flashes orchestrate the wound inflammatory response through DUOX activation and hydrogen peroxide release. *Current biology : CB*, 23(5), pp.424–9.

Recasens-Alvarez, C., Ferreira, A. & Milán, M., 2017. JAK/STAT controls organ size and fate specification by regulating morphogen production and signalling. *Nature Communications*, 8, p.13815.

Reczek, C.R. & Chandel, N.S., 2015. ROS-dependent signal transduction. *Current opinion in cell biology*, 33, pp.8–13.

Reinhardt, C.A. & Bryant, P.J., 1981. Wound healing in the imaginal discs of Drosophila. II. Transmission electron microscopy of normal and healing wing discs. *The Journal of experimental zoology*, 216(1), pp.45–61.

Reinhardt, C.A., Hodgkin, N.M. & Bryant, P.J., 1977. Wound healing in the imaginal discs of Drosophila. I. Scanning electron microscopy of normal and healing wing discs. *Developmental biology*, 60(1), pp.238–57.

Reiter, L.T. et al., 2001. A systematic analysis of human disease-associated gene sequences in Drosophila melanogaster. *Genome research*, 11(6), pp.1114–25.

Repiso, A., Bergantinos, C. & Serras, F., 2013. Cell fate respecification and cell division orientation drive intercalary regeneration in Drosophila wing discs. *Development (Cambridge, England)*, 140(17), pp.3541–3551.

Repiso, A., Bergantiños, C. & Serras, F., 2013. Cell fate respecification and cell division orientation drive intercalary regeneration in Drosophila wing discs. *Development (Cambridge, England)*, 140(17), pp.3541–51.

Resino, J., Salama-Cohen, P. & García-Bellido, A., 2002. Determining the role of patterned cell proliferation in the shape and size of the Drosophila wing. *Proceedings of the National Academy of Sciences of the United States of America*, 99(11), pp.7502–7.

Restrepo, S. & Basler, K., 2016. Drosophila wing imaginal discs respond to mechanical injury via slow InsP3R-mediated intercellular calcium waves. *Nature communications*, 7, p.12450.

Restrepo, S., Zartman, J.J. & Basler, K., 2016. Cultivation and Live Imaging of Drosophila Imaginal Discs. In *Methods in molecular biology (Clifton, N.J.)*. pp. 203–213.

Reyer, R.W., 1954. Regeneration of the lens in the amphibian eye. *The Quarterly review of biology*, 29(1), pp.1–46.

Rhee, S.G., 2006. Cell signaling. H2O2, a necessary evil for cell signaling. *Science (New York, N.Y.)*, 312(5782), pp.1882–3.

Rhee, S.G. et al., 2000. Hydrogen Peroxide: A Key Messenger That Modulates Protein Phosphorylation Through Cysteine Oxidation. *Science Signaling*, 2000(53), p.pe1-pe1.

Riehle, K.J. et al., 2011. New concepts in liver regeneration. *Journal of gastroenterology and hepatology*, 26 Suppl 1, pp.203–12.

Riesgo-Escovar, J.R. et al., 1996. The Drosophila Jun-N-terminal kinase is required for cell morphogenesis but not for DJun-dependent cell fate specification in the eye. *Genes & development*, 10(21), pp.2759–68.

Ríos-Barrera, L.D. & Riesgo-Escovar, J.R., 2013. Regulating cell morphogenesis: The drosophila jun N-terminal kinase pathway. *genesis*, 51(3), pp.147–162.

Roch, F. et al., 1998. Genetic interactions and cell behaviour in blistered mutants during proliferation and differentiation of the Drosophila wing. *Development (Cambridge, England)*, 125(10), pp.1823–32.

Rodrigues, A.B. et al., 2012. Activated STAT regulates growth and induces competitive interactions independently of Myc, Yorkie, Wingless and ribosome biogenesis. *Development (Cambridge, England)*, 139(21), pp.4051–61.

Rubilar, T., Pastor, C. & Díaz De Vivar, E., 2005. Timing of fission in the starfish Allostichaster capensis (Echinodermata:Asteroidea) in laboratory. *Rev. Biol. Trop. (Int. J. Trop. Biol*, 53, pp.299–303.

Rubiolo, C. et al., 2006. A balance between Raf-1 and Fas expression sets the pace of erythroid differentiation. *Blood*, 108(1), pp.152–9.

Rynes, J. et al., 2012. Activating Transcription Factor 3 Regulates Immune and Metabolic Homeostasis. *Molecular and Cellular Biology*, 32(19), pp.3949–3962.

Ryoo, H.D. et al., 2002. Regulation of Drosophila IAP1 degradation and apoptosis by reaper and ubcD1. *Nature Cell Biology*, 4(6), pp.432–438.

Ryoo, H.D., Gorenc, T. & Steller, H., 2004. Apoptotic cells can induce compensatory cell proliferation through the JNK and the Wingless signaling pathways. *Dev Cell*, 7(4), pp.491–501.

S

Sabbahy, M. El & Vaidya, V.S., 2011. Ischemic kidney injury and mechanisms of tissue repair. *Wiley Interdisciplinary Reviews: Systems Biology and Medicine*, 3(5), pp.606–618.

Sagasti, A. et al., 2001. The CaMKII UNC-43 activates the MAPKKK NSY-1 to execute a lateral signaling decision required for asymmetric olfactory neuron fates. *Cell*, 105(2), pp.221–32.

Saitoh, M. et al., 1998. Mammalian thioredoxin is a direct inhibitor of apoptosis signal-regulating kinase (ASK) 1. *The EMBO Journal*, 17(9), pp.2596–2606.

Sakauchi, C. et al., 2017. Pleiotropic properties of ASK1. *Biochimica et Biophysica Acta (BBA) - General Subjects*, 1861(1), pp.3030–3038.

Salmeron, J.M., Leuther, K.K. & Johnston, S.A., 1990. GAL4 mutations that separate the transcriptional activation and GAL80-interactive functions of the yeast GAL4 protein. *Genetics*, 125(1), pp.21–7.

Sánchez Alvarado, A., 2000. Regeneration in the metazoans: why does it happen? *BioEssays : news and reviews in molecular, cellular and developmental biology*, 22(6), pp.578–90.

Sánchez Alvarado, A. & Tsonis, P.A., 2006. Bridging the regeneration gap: genetic insights from diverse animal models. *Nature reviews. Genetics*, 7(11), pp.873–84.

Sano, S. et al., 1999. Keratinocyte-specific ablation of Stat3 exhibits impaired skin remodeling, but does not affect skin morphogenesis. *The EMBO journal*, 18(17), pp.4657–68.

Santabárbara-Ruiz, P. et al., 2015. ROS-Induced JNK and p38 Signaling Is Required for Unpaired Cytokine Activation during Drosophila Regeneration G. P. Copenhaver, ed. *PLOS Genetics*, 11(10), p.e1005595.

Sato, A. et al., 2014. Pivotal role for ROS activation of p38 MAPK in the control of differentiation and tumor-initiating capacity of glioma-initiating cells. *Stem cell research*, 12(1), pp.119–31.

Sayama, K. et al., 2001. Apoptosis Signal-regulating Kinase 1 (ASK1) Is an Intracellular Inducer of Keratinocyte Differentiation. *Journal of Biological Chemistry*, 276(2), pp.999–1004.

Scanga, S.E. et al., 2000. The conserved PI3'K/PTEN/Akt signaling pathway regulates both cell size and survival in Drosophila. *Oncogene*, 19(35), pp.3971–3977.

Schäfer, M. & Werner, S., 2007. Transcriptional control of wound repair. *Annual review of cell and developmental biology*, 23(1), pp.69–92.

Schieber, M. & Chandel, N.S., 2014. ROS Function in Redox Signaling and Oxidative Stress. *Current Biology*, 24(10), pp.R453–R462.

Schubiger, G., 1971. Regeneration, duplication and transdetermination in fragments of the leg disc of Drosophila melanogaster. *Developmental biology*, 26(2), pp.277–95.

Schubiger, M., Sustar, A. & Schubiger, G., 2010. Regeneration and transdetermination: the role of wingless and its regulation. *Developmental biology*, 347(2), pp.315–24.

Schuster, K.J. & Smith-Bolton, R.K., 2015. Taranis Protects Regenerating Tissue from Fate Changes Induced by the Wound Response in Drosophila. *Developmental cell*, 34(1), pp.119–28.

Seisenbacher, G., Hafen, E. & Stocker, H., 2011. MK2-dependent p38b signalling protects Drosophila hindgut enterocytes against JNK-induced apoptosis under chronic stress. E. Rulifson, ed. *PLoS genetics*, 7(8), p.e1002168.

Sen, C.K. & Roy, S., 2008. Redox signals in wound healing. *Biochimica et biophysica acta*, 1780(11), pp.1348–61.

Seong, K.-H. et al., 2011a. Inheritance of stress-induced, ATF-2-dependent epigenetic change. *Cell*, 145(7), pp.1049–61.

Seong, K.-H. et al., 2011b. Inheritance of stress-induced, ATF-2-dependent epigenetic change. *Cell*, 145(7), pp.1049–61.

Sharma, G.-D., He, J. & Bazan, H.E.P., 2003. p38 and ERK1/2 coordinate cellular migration and proliferation in epithelial wound healing: evidence of cross-talk activation between MAP kinase cascades. *The Journal of biological chemistry*, 278(24), pp.21989–97.

Shi, Y.B. & Ishizuya-Oka, A., 1996. Biphasic intestinal development in amphibians: embryogenesis and remodeling during metamorphosis. *Current topics in developmental biology*, 32, pp.205–35.

Shibata, T.F. et al., 2010. Staging of regeneration process of an arm of the feather star Oxycomanthus japonicus focusing on the oral-aboral boundary. *Developmental Dynamics*, 239(11), pp.2947–2961.

Shlevkov, E. & Morata, G., 2012. A dp53/JNK-dependant feedback amplification loop is essential for the apoptotic response to stress in Drosophila. *Cell Death and Differentiation*, 19(3), pp.451–460.

Shraiman, B.I., 2005. Mechanical feedback as a possible regulator of tissue growth. *Proceedings of the National Academy of Sciences of the United States of America*, 102(9), pp.3318–23.

Simmonds, A.J. et al., 1995. Distinguishable functions for engrailed and invected in anterior-posterior patterning in the Drosophila wing. *Nature*, 376(6539), pp.424–7.

Simpson, P., Berreur, P. & Berreur-Bonnenfant, J., 1980. The initiation of pupariation in Drosophila: dependence on growth of the imaginal discs. *Journal of embryology and experimental morphology*, 57, pp.155–65.

Skinner, A., Khan, S.J. & Smith-Bolton, R.K., 2015. Trithorax regulates systemic signaling during *Drosophila* imaginal disc regeneration. *Development*, 142(20), pp.3500–3511.

Slack, J.M.W. et al., 2004. Cellular and molecular mechanisms of regeneration in Xenopus. *Philosophical transactions of the Royal Society of London. Series B, Biological sciences*, 359(1445), pp.745–51.

Smith-Bolton, R.K. et al., 2009. Regenerative Growth in Drosophila Imaginal Discs Is Regulated by Wingless and Myc. *Developmental Cell*, 16(6), pp.797–809.

Son, Y. et al., 2013. Reactive oxygen species in the activation of MAP kinases. *Methods in enzymology*, 528, pp.27–48.

Staveley, B.E. et al., 1998. Genetic analysis of protein kinase B (AKT) in Drosophila. *Current biology : CB*, 8(10), pp.599–602.

Stec, W., Vidal, O. & Zeidler, M.P., 2013. Drosophila SOCS36E negatively regulates JAK/STAT pathway signaling via two separable mechanisms. *Molecular biology of the cell*, 24(18), pp.3000–9.

Strigini, M. & Cohen, S.M., 1999. Formation of morphogen gradients in the Drosophila wing. *Seminars in cell & developmental biology*, 10(3), pp.335–44.

Strigini, M. & Cohen, S.M., 2000. Wingless gradient formation in the Drosophila wing. *Current biology : CB*, 10(6), pp.293–300.

Strub, S., 1979. Leg regeneration in insects. An experimental analysis in Drosophila and a new interpretation. *Developmental biology*, 69(1), pp.31–45.

Sturtevant, M.A., Roark, M. & Bier, E., 1993. The Drosophila rhomboid gene mediates the localized formation of wing veins and interacts genetically with components of the EGF-R signaling pathway. *Genes & development*, 7(6), pp.961–73.

Sun, G. & Irvine, K.D., 2013. Ajuba family proteins link JNK to Hippo signaling. *Science signaling*, 6(292), p.ra81.

Sun, G. & Irvine, K.D., 2011. Regulation of Hippo signaling by Jun kinase signaling during compensatory cell proliferation and regeneration, and in neoplastic tumors. *Developmental Biology*, 350(1), pp.139–151.

Sustar, A. et al., 2011. Drosophila twin spot clones reveal cell division dynamics in regenerating imaginal discs. *Developmental biology*, 356(2), pp.576–87.

Suzanne, M. et al., 1999. The Drosophila p38 MAPK pathway is required during oogenesis for egg asymmetric development. *Genes & development*, 13(11), pp.1464–74.

Svácha, P., 1992. What are and what are not imaginal discs: reevaluation of some basic concepts (Insecta, Holometabola). *Developmental biology*, 154(1), pp.101–17.

Szabad, J., Simpson, P. & Nöthiger, R., 1979. Regeneration and compartments in Drosophila. *Journal of embryology and experimental morphology*, 49, pp.229–41.

T

Tabata, T. et al., 1995. Creating a Drosophila wing de novo, the role of engrailed, and the compartment border hypothesis. *Development (Cambridge, England)*, 121(10), pp.3359–69.

Takeda, K. et al., 2006. Apoptosis Signal-regulating Kinase (ASK) 2 Functions as a Mitogen-activated Protein Kinase Kinase Kinase in a Heteromeric Complex with ASK1. *Journal of Biological Chemistry*, 282(10), pp.7522–7531.

Takeda, K. et al., 2000. Apoptosis signal-regulating kinase 1 (ASK1) induces neuronal differentiation and survival of PC12 cells. *The Journal of biological chemistry*, 275(13), pp.9805–13.

Takeda, K. et al., 2008. Apoptosis Signal-Regulating Kinase 1 in Stress and Immune Response. *Annual Review of Pharmacology and Toxicology*, 48(1), pp.199–225.

Takeda, K. et al., 2004. Involvement of ASK1 in Ca2+-induced p38 MAP kinase activation. *EMBO reports*, 5(2), pp.161–166.

Taki, T.M. & Nickerson, P.A., 1985. Differentiation and proliferation of adrenocortical cells during the early stages of regeneration. *Laboratory investigation; a journal of technical methods and pathology*, 53(1), pp.91–100.

Tamori, Y., Suzuki, E. & Deng, W.-M., 2016. Epithelial Tumors Originate in Tumor Hotspots, a Tissue-Intrinsic Microenvironment. B. A. Edgar, ed. *PLoS biology*, 14(9), p.e1002537.

Tanaka, E.M. & Reddien, P.W., 2011. The cellular basis for animal regeneration. *Developmental cell*, 21(1), pp.172–85.

Taylor, G. et al., 2000. Involvement of follicular stem cells in forming not only the follicle but also the epidermis. *Cell*, 102(4), pp.451–61.

Theise, N.D. et al., 1999. The canals of Hering and hepatic stem cells in humans. *Hepatology (Baltimore, Md.)*, 30(6), pp.1425–33.

Thomas, T. et al., 2006. Expression of endoderm stem cell markers: evidence for the presence of adult stem cells in human thyroid glands. *Thyroid : official journal of the American Thyroid Association*, 16(6), pp.537–44.

Tobiume, K. et al., 2001. ASK1 is required for sustained activations of JNK/p38 MAP kinases and apoptosis. *EMBO reports*, 2(3), pp.222–228.

Tobiume, K. et al., 1997. Molecular cloning and characterization of the mouse apoptosis signal-regulating kinase 1. *Biochemical and biophysical research communications*, 239(3), pp.905–10.

Tobiume, K., Saitoh, M. & Ichijo, H., 2002. Activation of apoptosis signal-regulating kinase 1 by the stress-induced activating phosphorylation of pre-formed oligomer. *Journal of Cellular Physiology*, 191(1), pp.95–104.

Tonnesen, M.G. et al., 2000. Angiogenesis in Wound Healing. *Journal of Investigative Dermatology Symposium Proceedings*, 5(1), pp.40–46.

Torroja, C., Gorfinkiel, N. & Guerrero, I., 2005. Mechanisms of Hedgehog gradient formation and interpretation. *Journal of neurobiology*, 64(4), pp.334–56.

Tripura, C. et al., 2011. Regulation and activity of JNK signaling in the wing disc peripodial membrane during adult morphogenesis in Drosophila. *The International Journal of Developmental Biology*, 55(6), pp.583–590.

Tsai, Y.-C. & Sun, Y.H., 2004. Long-range effect of upd, a ligand for Jak/STAT pathway, on cell cycle in Drosophila eye development. *Genesis (New York, N.Y. : 2000)*, 39(2), pp.141–53.

Tu, S. & Johnson, S.L., 2011. Fate restriction in the growing and regenerating zebrafish fin. *Developmental cell*, 20(5), pp.725–32.

U

Uhlirova, M. & Bohmann, D., 2006. JNK- and Fos-regulated Mmp1 expression cooperates with Ras to induce invasive tumors in Drosophila. *The EMBO Journal*, 25(22), pp.5294–5304.

Uhlirova, M., Jasper, H. & Bohmann, D., 2005. Non-cell-autonomous induction of tissue overgrowth by JNK/Ras cooperation in a Drosophila tumor model. *Proceedings of the National Academy of Sciences of the United States of America*, 102(37), pp.13123–8.

Ursprung H., 1959. Fragmentation and radiation experiments to determine the determination and fate map of the Drosophila genital disc. *Roux's Arch. Entwickl.*, 151, pp.504–58.

V

Vallejo, D.M. et al., 2015. A brain circuit that synchronizes growth and maturation revealed through Dilp8 binding to Lgr3. *Science*, 350(6262), p.aac6767-aac6767.

Veal, E.A., Day, A.M. & Morgan, B.A., 2007. Hydrogen Peroxide Sensing and Signaling. *Molecular Cell*, 26(1), pp.1–14.

Venken, K.J.T. et al., 2011. MiMIC: a highly versatile transposon insertion resource for engineering Drosophila melanogaster genes. *Nature Methods*, 8(9), pp.737–743.

Verghese, S. & Su, T.T., 2016. Drosophila Wnt and STAT Define Apoptosis-Resistant Epithelial Cells for Tissue Regeneration after Irradiation. B. A. Edgar, ed. *PLoS biology*, 14(9), p.e1002536.

Vidal, S. et al., 2001. Mutations in the Drosophila dTAK1 gene reveal a conserved function for MAPKKKs in the control of rel/NF-kappaB-dependent innate immune responses. *Genes & development*, 15(15), pp.1900–12.

Vrailas-Mortimer, A. et al., 2011. A Muscle-Specific p38 MAPK/Mef2/MnSOD Pathway Regulates Stress, Motor Function, and Life Span in Drosophila. *Developmental Cell*, 21(4), pp.783–795.

W

Wang, L. et al., 2014. Pleiotropy of the Drosophila JAK pathway cytokine Unpaired 3 in development and aging. *Developmental biology*, 395(2), pp.218–31.

Wang, X.S. et al., 1996. Molecular cloning and characterization of a novel protein kinase with a catalytic domain homologous to mitogen-activated protein kinase kinase kinase. *The Journal of biological chemistry*, 271(49), pp.31607–11.

Wangler, M.F., Yamamoto, S. & Bellen, H.J., 2015. Fruit flies in biomedical research. *Genetics*, 199(3), pp.639–53.

Watanabe, T. et al., 2005. Apoptosis signal-regulating kinase 1 is involved not only in apoptosis but also in non-apoptotic cardiomyocyte death. *Biochemical and Biophysical Research Communications*, 333(2), pp.562–567.

Weber, U., Paricio, N. & Mlodzik, M., 2000. Jun mediates Frizzled-induced R3/R4 cell fate distinction and planar polarity determination in the Drosophila eye. *Development (Cambridge, England)*, 127(16), pp.3619–29.

Wells, B.S., Yoshida, E. & Johnston, L.A., 2006. Compensatory Proliferation in Drosophila Imaginal Discs Requires Dronc-Dependent p53 Activity. *Current Biology*, 16(16), pp.1606–1615.

Wenger, Y. et al., 2014. Injury-induced immune responses in Hydra. *Seminars in Immunology*, 26(4), pp.277–294.

Whalley, K., O'Neill, P. & Ferretti, P., 2006. Changes in response to spinal cord injury with development: vascularization, hemorrhage and apoptosis. *Neuroscience*, 137(3), pp.821–32.

Widmann, C. et al., 1999. Mitogen-activated protein kinase: conservation of a three-kinase module from yeast to human. *Physiological reviews*, 79(1), pp.143–80.

Williams-Boyce, P.K. & Daniel, J.C., 1986. Comparison of ear tissue regeneration in mammals. *Journal of anatomy*, 149, pp.55–63.

Williams, J.A., Paddock, S.W. & Carroll, S.B., 1993. Pattern formation in a secondary field: a hierarchy of regulatory genes subdivides the developing Drosophila wing disc into discrete subregions. *Development (Cambridge, England)*, 117(2), pp.571–84.

Wing, J.P. et al., 1998. Distinct cell killing properties of the Drosophila reaper, head involution defective, and grim genes. *Cell death and differentiation*, 5(11), pp.930–9.

Winterbourn, C.C., 2008. Reconciling the chemistry and biology of reactive oxygen species. *Nature chemical biology*, 4(5), pp.278–86.

Winterbourn, C.C. & Hampton, M.B., 2008. Thiol chemistry and specificity in redox signaling. *Free radical biology & medicine*, 45(5), pp.549–61.

Wittmann, C. et al., 2012. Hydrogen Peroxide in Inflammation: Messenger, Guide, and Assassin. *Advances in Hematology*, 2012, pp.1–6.

Wood, Z.A., Poole, L.B. & Karplus, P.A., 2003. Peroxiredoxin Evolution and the Regulation of Hydrogen Peroxide Signaling. *Science*, 300(5619), pp.650–653.

Worley, M.I., Setiawan, L. & Hariharan, I.K., 2012. Regeneration and Transdetermination in *Drosophila* Imaginal Discs. *Annual Review of Genetics*, 46(1), pp.289–310.

Worley, M.I., Setiawan, L. & Hariharan, I.K., 2013. TIE-DYE: a combinatorial marking system to visualize and genetically manipulate clones during development in Drosophila melanogaster. *Development (Cambridge, England)*, 140(15), pp.3275–84.

Wu, J. & Cohen, S.M., 2002. Repression of Teashirt marks the initiation of wing development. *Development (Cambridge, England)*, 129(10), pp.2411–8.

Wu, M., Pastor-Pareja, J.C. & Xu, T., 2010. Interaction between Ras(V12) and scribbled clones induces tumour growth and invasion. *Nature*, 463(7280), pp.545–8.

X

Xu, D. et al., Genetic control of programmed cell death (apoptosis) in Drosophila. *Fly*, 3(1), pp.78–90.

Xue, L. et al., 2007. Tumor suppressor CYLD regulates JNK-induced cell death in Drosophila. *Developmental cell*, 13(3), pp.446–54.

Y

Yagi, R., Mayer, F. & Basler, K., 2010. Refined LexA transactivators and their use in combination with the Drosophila Gal4 system. *Proc Natl Acad Sci U S A*, 107(37), pp.16166–16171.

Yamaguchi, O. et al., 2004. Cardiac-specific disruption of the c-raf-1 gene induces cardiac dysfunction and apoptosis. *The Journal of clinical investigation*, 114(7), pp.937–43.

Yamaguchi, O. et al., 2003. Targeted deletion of apoptosis signal-regulating kinase 1 attenuates left ventricular remodeling. *Proceedings of the National Academy of Sciences of the United States of America*, 100(26), pp.15883–8.

Yamamoto, S. et al., 2014. A drosophila genetic resource of mutants to study mechanisms underlying human genetic diseases. *Cell*, 159(1), pp.200–14.

Yan, R. et al., 1996. Identification of a Stat gene that functions in Drosophila development. *Cell*, 84(3), pp.421–30.

Yokoi, T. et al., 2006. Apoptosis signal-regulating kinase 1 mediates cellular senescence induced by high glucose in endothelial cells. *Diabetes*, 55(6), pp.1660–5.

Yokoyama, H., 2008. Initiation of limb regeneration: the critical steps for regenerative capacity. *Development, growth & differentiation*, 50(1), pp.13–22.

Yong, H.-Y., Koh, M.-S. & Moon, A., 2009. The p38 MAPK inhibitors for the treatment of inflammatory diseases and cancer. *Expert Opinion on Investigational Drugs*, 18(12), pp.1893–1905..

Yoo, S.J. et al., 2002. Hid, Rpr and Grim negatively regulate DIAP1 levels through distinct mechanisms. *Nature cell biology*, 4(6), pp.416–24.

Yoo, S.K. et al., 2012. Early redox, Src family kinase, and calcium signaling integrate wound responses and tissue regeneration in zebrafish. *The Journal of cell biology*, 199(2), pp.225–34.

Yoo, S.K. et al., 2011. Lyn is a redox sensor that mediates leukocyte wound attraction in vivo. *Nature*, 480(7375), pp.109–12.

Yoo, S.K. et al., 2016. Plexins function in epithelial repair in both Drosophila and zebrafish. *Nature communications*, 7, p.12282.

Z

Zarubin, T. & Han, J., 2005. Activation and signaling of the p38 MAP kinase pathway. *Cell research*, 15(1), pp.11–8.

Zecca, M., Basler, K. & Struhl, G., 1995. Sequential organizing activities of engrailed, hedgehog and decapentaplegic in the Drosophila wing. *Development (Cambridge, England)*, 121(8), pp.2265–78.

Zeidler, M.P. et al., 2004. Temperature-sensitive control of protein activity by conditionally splicing inteins. *Nature biotechnology*, 22(7), pp.871–6.

Zeidler, M.P., Bach, E.A. & Perrimon, N., 2000. The roles of the Drosophila JAK/STAT pathway. *Oncogene*, 19(21), pp.2598–606.

Zhang, L. et al., 2008. The stem cell niche of human livers: symmetry between development and regeneration. *Hepatology (Baltimore, Md.)*, 48(5), pp.1598–607.

Zhang, Q. et al., 2016. Reactive oxygen species generated from skeletal muscles are required for gecko tail regeneration. *Scientific reports*, 6, p.20752.

Zhu, M. et al., 2010. Activation of JNK signaling links lgl mutations to disruption of the cell polarity and epithelial organization in Drosophila imaginal discs. *Cell research*, 20(2), pp.242–5.

Zirin, J. & Perrimon, N., 2010. Drosophila as a model system to study autophagy. *Seminars in immunopathology*, 32(4), pp.363–72.

Zirin, J.D. & Mann, R.S., 2007. Nubbin and Teashirt mark barriers to clonal growth along the proximal-distal axis of the Drosophila wing. *Developmental biology*, 304(2), pp.745–58.

ANNEXES

Annex 1: Genotypes

Figure 27. A, G. wt**. C, D,E, F.** *ptc>rpr: UAS-rpr/+; ptc-Gal4/+; tubGal80^{TS}/+*

Figure 28. A. wt. **B, C, D, E.** *sal$^{E/Pv}$>rpr: UAS-rpr/+; sal$^{E/Pv}$-Gal4/+; tubGal80^{TS}/+*

F, G. *ptc>rpr: UAS-rpr/+; ptc-Gal4:tubGal80^{TS}/+*

Figure 29. A-D. *sal$^{E/Pv}$>rpr nub>GFP: w; nub-Gal4/UAS-GFP; sal$^{E/Pv}$-LHG:tubGal80^{TS}/lexO-rpr*

sal$^{E/Pv}$>rpr nub>Cat: w; nub-Gal4/UAS-Cat; sal$^{E/Pv}$-LHG:tubGal80^{TS}/lexO-rpr

sal$^{E/Pv}$>rpr nub>Sod: w; nub-Gal4/UAS-Sod; sal$^{E/Pv}$-LHG:tubGal80^{TS}/lexO-rpr

sal$^{E/Pv}$>rpr nub>Sod:Cat: w; nub-Gal4/UAS-Sod:Cat; sal$^{E/Pv}$-LHG:tubGal80^{TS}/lexO-rpr

E-H. *sal$^{E/Pv}$>rpr: w; ci-Gal4/UAS-GFP; sal$^{E/Pv}$-LHG:tubGal80^{TS}/lexO-rpr*

ci>RNAi DUOX: w; ci-Gal4/UAS-RNAi DUOX; sal$^{E/Pv}$-LHG:tubGal80^{TS}/lexO-GFP

sal$^{E/Pv}$>rpr ci>RNAi DUOX: w; ci-Gal4/UAS-RNAi DUOX; sal$^{E/Pv}$-LHG:tubGal80^{TS}/lexO-rpr

Figure 30. A. *ptc>rpr: UAS-rpr/+; ptc-Gal4:tubGal80^{TS}/TRE-DsRed.T4; puc-LacZ/+*

B, C. *w; TRE-DsRed.T4/+; puc-Gal4:UAS-GFP/+*

Figure 31. A. *ptc>rpr: UAS-rpr/+; ptc-Gal4:tubGal80^{TS}/TRE-DsRed.T4; puc-LacZ/+*

B. *ptc>rpr: UAS-rpr/+; ptc-Gal4:tubGal80^{TS}/+; puc-LacZ/+*

Figure 32. A. *ptc>rpr: UAS-rpr/+; ptc-Gal4:tubGal80^{TS}/TRE-DsRed.T4*

B. *sal$^{E/Pv}$>rpr: UAS-rpr/+; sal$^{E/Pv}$-Gal4/+; tubGal80^{TS}/+*

C, D. *sal$^{E/Pv}$>rpr: w; ci-Gal4/ lexO-rpr; sal$^{E/Pv}$-LHG:tubGal80^{TS}/+*

ci> UAS-bsk^{DN}: w; ci-Gal4/+; sal$^{E/Pv}$-LHG:tubGal80^{TS}/UAS-bsk^{DN}

sal$^{E/Pv}$>rpr ci> UAS-bsk^{DN}: w; ci-Gal4/ lexO-rpr; sal$^{E/Pv}$-LHG:tubGal80^{TS}/UAS-bsk^{DN}

Figure 33. A, B. *ptc>rpr: UAS-rpr/+ ; ptc-Gal4/+; tubGal80^{TS}/+.* **C, D.** *w; TRE-DsRed.T4*

Figure 34. A, B, C. wt. **D.** *w; ci-Gal4/UAS-Sod:Cat; $sal^{E/Pv}$-LHG:$tubGal80^{TS}$/lexO-rpr*

E, F. *ptc>rpr: UAS-rpr/+ ; ptc-Gal4/+; $tubGal80^{TS}$/+*

Figure 35. A, B, C. wt.

Figure 36. wt: *w; +; $sal^{E/Pv}$-LHG:$tubGal80^{TS}$/lexO-rpr* (control for *lexO-rpr* on the third chromosome) and *w; lexO-rpr/+; $sal^{E/Pv}$-LHG:$tubGal80^{TS}$/+* (control for *lexO-rpr* on the second chromosome).

$lic^{d13/+}$: lic^{d13}/+; +; $sal^{E/Pv}$-LHG:$tubGal80^{TS}$/lexO-rpr

$p38b^{d27/+}$: w; $p38b^{d27}$/+; $sal^{E/Pv}$-LHG:$tubGal80^{TS}$/lexO-rpr

$p38a^{1/+}$: w; lexO-rpr/+; $p38a^{1}$/sal^{EPv}-LHG:$tubGal80^{TS}$

$lic^{d13/+}p38b^{d27/+}$: lic^{d13}/+; $p38b^{d27}$/+; sal^{EPv}-LHG:$tubGal80^{TS}$/lexO-rpr

$dATF2^{PB/+}$: w; $Atf2^{PB}$/+; $sal^{E/Pv}$-LHG:$tubGal80^{TS}$/lexO-rpr

$dATF2^{PB-/-}$: w; $Atf2^{PB}$/$Atf2^{PB}$; $sal^{E/Pv}$-LHG:$tubGal80^{TS}$/lexO-rpr

$lic^{d13/+}$ $dATF2^{PB/+}$: lic^{d13}/+; $Atf2^{PB}$/+; $sal^{E/Pv}$-LHG:$tubGal80^{TS}$/lexO-rpr

$p38b^{d27/+}$ $dATF2^{PB/+}$: w; $p38b^{d27}$/$Atf2^{PB}$; $sal^{E/Pv}$-LHG:$tubGal80^{TS}$/lexO-rpr

$dATF2^{PB/+}p38a^{1/+}$: w; $Atf2^{PB}$/lexO-rpr; $p38a^{1}$/sal^{EPv}-LHG:$tubGal80^{TS}$

Figure 37. *$sal^{E/Pv}$>rpr: w; ci-Gal4/UAS-GFP; $sal^{E/Pv}$-LHG:$tubGal80^{TS}$/lexO-rpr*

ci>RNAi p38a: w; ci-Gal4/UAS-RNAi p38a; $sal^{E/Pv}$-LHG:$tubGal80^{TS}$/lexO-GFP

$sal^{E/Pv}$>rpr ci>RNAi p38a: w; ci-Gal4/UAS-RNAi p38a; $sal^{E/Pv}$-LHG:$tubGal80^{TS}$/lexO-rpr

ci>RNAi p38b: w; ci-Gal4/UAS-RNAi p38b; $sal^{E/Pv}$-LHG:$tubGal80^{TS}$/lexO-GFP

$sal^{E/Pv}$>rpr ci>RNAi p38b: w; ci-Gal4/UAS-RNAi p38b; $sal^{E/Pv}$-LHG:$tubGal80^{TS}$/lexO-rpr

ci>RNAi Atf2: w; ci-Gal4/UAS-RNAi Atf2; $sal^{E/Pv}$-LHG:$tubGal80^{TS}$/lexO-GFP

$sal^{E/Pv}$>rpr ci>RNAi Atf2: w; ci-Gal4/UAS-RNAi Atf2; $sal^{E/Pv}$-LHG:$tubGal80^{TS}$/lexO-rpr

ci>RNAi lic: w; ci-Gal4/UAS-RNAi lic; $sal^{E/Pv}$-LHG:$tubGal80^{TS}$/lexO-GFP

$sal^{E/Pv}$>rpr ci>RNAi lic: w; ci-Gal4/UAS-RNAi lic; $sal^{E/Pv}$-LHG:$tubGal80^{TS}$/lexO-rpr

Figure 38. A. *$sal^{E/Pv}$>rpr: UAS-rpr/+; $sal^{E/Pv}$-Gal4/+; $tubGal80^{TS}$/+*

B. *ptc>rpr: UAS-rpr/+; ptc-Gal4:$tubGal80^{TS}$/TRE-DsRed.T4*

Figure 39. A. *hep^{r75}: hep^{r75}/Y*. **B.** *en>RNAi lic: w; en-Gal4:UAS-GFP/UAS-RNAi lic*

Figure 40. A. *ptc>rpr hep^{r75}: hep^{r75}/Y; ptc-Gal4:tubGal80^{TS}/+; UAS-rpr/+*

B. *ptc>rpr: UAS-rpr/+; ptc-Gal4/+; tubGal80^{TS}/+*

Figure 41. wt*: w; TRE-DsRed.T4. p38a$^{-/-}$: w; TRE-DsRed.T4; p38a^{1}/p38a^{1}*

Figure 42. A, B. wt. **C, D.** *hep^{r75}: hep^{r75}/Y* **E, F, G, H** *ptc>rpr: UAS-rpr/+; ptc-Gal4/+; tubGal80^{TS}/+*

sal$^{E/Pv}$>rpr: UAS-rpr/+; sal-Gal4/+; tubGal80^{TS}/+

I, J. *upd-Gal4/+; UAS-myrtomato/10XSTAT92E-GFP*

Figure 43. A, B, C. *sal$^{E/Pv}$>rpr ci>GFP: w; ci-Gal4/lexO-rpr; sal$^{E/Pv}$-LHG:tubGal80^{TS}/UAS-GFP*

ci>dome^{DN} sal$^{E/Pv}$>GFP: w; ci-Gal4/lexO-rCD2::GFP; sal$^{E/Pv}$-LHG:tubGal80^{TS}/UAS-dome^{DN}

sal$^{E/Pv}$>rpr ci> dome^{DN}: w; ci-Gal4/lexO-rpr; sal$^{E/Pv}$-LHG:tubGal80^{TS}/UAS-dome^{DN}

sal$^{E/Pv}$>GFP ap>dome^{DN}: w; ap-Gal4/lexO-rCD2::GFP; sal$^{E/Pv}$-LHG:tubGal80^{TS}/UAS-dome^{DN}

sal$^{E/Pv}$>rpr ap> dome^{DN}: w; ap-Gal4/lexO-rpr; sal$^{E/Pv}$-LHG:tubGal80^{TS}/UAS-dome^{DN}

ci>Socs36E sal$^{E/Pv}$>GFP: w; ci-Gal4/lexO-rCD2::GFP; sal$^{E/Pv}$-LHG:tubGal80^{TS}/UAS-Socs36E

sal$^{E/Pv}$>rpr ci> Socs36E: w; ci-Gal4/lexO-rpr; sal$^{E/Pv}$-LHG:tubGal80^{TS}/UAS- Socs36E

D, E, F. wild type: *UAS-rpr/+; sal$^{E/Pv}$-Gal4/+; tubGal80^{TS}/+*

hop^{2}/+: UAS-rpr/hop^{2}; sal$^{E/Pv}$-Gal4/+; tubGal80^{TS}/+

hop^{27}/+: UAS-rpr/hop^{27}; sal$^{E/Pv}$-Gal4/+; tubGal80^{TS}/+

stat92e^{397}/+: UAS-rpr/+; sal$^{E/Pv}$-Gal4/+; tubGal80^{TS}/stat92e^{397}

stat92e^{06346}/+: UAS-rpr/+; sal$^{E/Pv}$-Gal4/+; tubGal80^{TS}/stat92e^{06346}

upd^{YM56}/+: UAS-rpr/upd^{YM55}; sal$^{E/Pv}$-Gal4/+; tubGal80^{TS}/+

Figure 44. A, B, C. *ci-Gal4 UAS-upd: w; ci-Gal4/UAS-upd; sal$^{E/Pv}$-LHG:tubGal80^{TS}/lexO-rCD2::GFP*

sal$^{E/Pv}$-LHG lexO-rpr: w; ci-Gal4/UAS-GFP; sal$^{E/Pv}$-LHG:tubGal80^{TS}/lexO-rpr

ci-Gal4 UAS-upd sal$^{E/Pv}$-LHG lexO-rpr: w; ci-Gal4/UAS-upd; sal$^{E/Pv}$-LHG:tubGal80^{TS}/lexO-rpr

Figure 45. A, B, C, D, E, F. wt: wild type. *p38a$^{-/-}$: w; +; p38a^{1}/p38a^{1}*

Figure 46. A, B, C. *ci-Gal4 UAS-upd: w; ci-Gal4/UAS-upd; sal$^{E/Pv}$-LHG:tubGal80^{TS}/lexO-rCD2::GFP*

sal$^{E/Pv}$-LHG lexO-rpr: w; ci-Gal4/UAS-GFP; sal$^{E/Pv}$-LHG:tubGal80^{TS}/lexO-rpr

ci-Gal4 UAS-upd sal$^{E/Pv}$-LHG lexO-rpr: w; ci-Gal4/UAS-upd; sal$^{E/Pv}$-LHG:tubGal80^{TS}/lexO-rpr

Figure 47. A. *sal$^{E/Pv}$>rpr: wUAS-rpr/+; sal$^{E/Pv}$-Gal4/+; tubGal80^{TS}/+*

sal$^{E/Pv}$>rpr ask1^{MB06489}/+: wUAS-rpr/+; sal$^{E/Pv}$-Gal4/+; tubGal80^{TS}/ask1^{MB06489}

sal$^{E/Pv}$>rpr ask1^{M102915}/+: wUAS-rpr/+; sal$^{E/Pv}$-Gal4/+; tubGal80^{TS}/ask1^{M102915}

B. *sal$^{E/Pv}$>rpr: w; ci-Gal4/LexO-rpr; sal$^{E/Pv}$-LHG:tubGal80^{TS}/UAS-GFP*

ci>RNAi Ask1: w; ci-Gal4/LexO-GFP; sal$^{E/Pv}$-LHG:tubGal80^{TS}/UAS-RNAi Ask1

sal$^{E/Pv}$>rpr ci>RNAi Ask1: w; ci-Gal4/LexO-rpr; sal$^{E/Pv}$-LHG:tubGal80^{TS}/UAS-RNAi Ask1

ap>RNAi Ask1: w; ap-Gal4/LexO-GFP; sal$^{E/Pv}$-LHG:tubGal80^{TS}/UAS-RNAi Ask1

sal$^{E/Pv}$>rpr ap>RNAi Ask1: w; ap-Gal4/LexO-rpr; sal$^{E/Pv}$-LHG:tubGal80^{TS}/UAS-RNAi Ask1

Figure 50. A, C, D, F. wt and injured*:* Canton S

B, E. *sal$^{E/Pv}$>rpr: wUAS-rpr/+; sal$^{E/Pv}$-Gal4/+; tubGal80^{TS}/+*

Figure 51. Canton S

Figure 52. A. *en> RNAi Ask1: w; en-Gal4/UAS-GFP; UAS-RNAi Ask1/+*

B, C. *sal$^{E/Pv}$>rpr ci>RNAi Ask1: w; ci-Gal4/LexO-rpr; sal$^{E/Pv}$-LHG:tubGal80^{TS}/UAS-RNAi Ask1*

Figure 53. A, C. *sal$^{E/Pv}$>rpr: w; +; sal$^{E/Pv}$-LHG:tubGal80^{TS}/LexO-rpr*

B, D, E. *sal$^{E/Pv}$>rpr ci>dp110^{DN}: w; ci-Gal4/UAS-dp110^{DN}; sal$^{E/Pv}$-LHG:tubGal80^{TS}/ LexO-rpr*

Figure 54. wt → *w^{118}; +; +. ap>dp110^{CAAX}: w; ap-Gal4/UAS-dp110^{CAAX}*

Figure 55. *sal$^{E/Pv}$>rpr: w; LexO-rpr/ +; sal$^{E/Pv}$-LHG:tubGal80^{TS}/+ (control for LexO-rpr in the second chromosome) and wUASrpr/+; sal$^{E/Pv}$-Gal4; tubGal80^{TS} (control for mutant backgrounds)*

ci>dp110^{DN}: w; ci-Gal4/UAS-dp110^{DN}; sal$^{E/Pv}$-LHG:tubGal80^{TS}/+

sal$^{E/Pv}$>rpr ci>dp110^{DN}: w; ci-Gal4/UAS-dp110^{DN}; sal$^{E/Pv}$-LHG:tubGal80^{TS}/ LexO-rpr

sal$^{E/Pv}$>rpr akt^{1}: wUAS-rpr/+; sal$^{E/Pv}$-Gal4; tubGal80^{TS}; akt^{1}/+

sal$^{E/Pv}$>rpr ask1^{MB06489}/+: wUAS-rpr/+; sal$^{E/Pv}$-Gal4; tubGal80^{TS}; akt^{1}/ask1^{MB06489}

sal$^{E/Pv}$>rpr ask1^{M102915}/+: wUAS-rpr/+; sal$^{E/Pv}$-Gal4; tubGal80^{TS}; akt^{1}/ask1^{M102915}

Figure 56. CTRL and NAC*: wUAS-rpr/+; sal$^{E/Pv}$-Gal4/+; tubGal80^{TS}/+*

Figure 57. A, D. CTRL*: w^{118}; +; +.* **B, E.** *ask1$^{-/-}$ → w; +; ask1^{MB06489}*

Figure 58. wt*: w^{118}; +; +. ask1$^{-/-}$: w; +; ask1^{MB06489}*

Figure 59. A, E. *sal$^{E/Pv}$>rpr: w; LexO-rpr/ +; sal$^{E/Pv}$-LHG:tubGal80^{TS}/+*

B, F. *sal$^{E/Pv}$>rpr ci>RNAi Ask1: w; ci-Gal4/LexO-rpr; sal$^{E/Pv}$-LHG:tubGal80^{TS}/UAS-RNAi Ask1*

C, G. *en>RNAi Ask1: w; en-Gal4/UAS-GFP; UAS-RNAi Ask1/+*

Figure 60. CTRL *sal$^{E/Pv}$>rpr: w; LexO-rpr/ +; sal$^{E/Pv}$-LHG:tubGal80^{TS}/+ (control for LexO-rpr in the second chromosome) and w; +; sal$^{E/Pv}$-LHG:tubGal80^{TS}/LexO-rpr (control for LexO-rpr in the third chromosome)*

ci>RNAi egr sal$^{E/Pv}$>rpr: w; ci-Gal4/UAS-RNAi egr; sal$^{E/Pv}$-LHG:tubGal80^{TS}/LexO-rpr

ap>RNAi egr sal$^{E/Pv}$>rpr: w; ap-Gal4/UAS-RNAi egr; sal$^{E/Pv}$-LHG:tubGal80^{TS}/LexO-rpr

ci>grnd^{extra} sal$^{E/Pv}$>rpr: w; ci-Gal4/LexO-rpr; sal$^{E/Pv}$-LHG:tubGal80^{TS}/UAS-grnd^{extra}

ap>grnd^{extra} sal$^{E/Pv}$>rpr: w; ap-Gal4/LexO-rpr; sal$^{E/Pv}$-LHG:tubGal80^{TS}/UAS-grnd^{extra}

egr^{3}/+ sal$^{E/Pv}$>rpr: w; egr^{3}/LexO-rpr; sal$^{E/Pv}$-LHG:tubGal80^{TS}/+

ci>RNAi wgn sal$^{E/Pv}$>rpr: w; ci-Gal4/LexO-rpr; sal$^{E/Pv}$-LHG:tubGal80^{TS}/UAS-RNAi wgn

ap>RNAi wgn sal$^{E/Pv}$>rpr: w; ap-Gal4/LexO-rpr; sal$^{E/Pv}$-LHG:tubGal80^{TS}/UAS-RNAi wgn

ci>RNAi grnd sal$^{E/Pv}$>rpr: w; ci-Gal4/UAS-RNAi grnd; sal$^{E/Pv}$-LHG:tubGal80^{TS}/LexO-rpr

ap>RNAi grnd sal$^{E/Pv}$>rpr: w; ap-Gal4/UAS-RNAi grnd; sal$^{E/Pv}$-LHG:tubGal80^{TS}/LexO-rpr

grnd^{minos} sal$^{E/Pv}$>rpr: w; grnd^{minos}; sal$^{E/Pv}$-LHG:tubGal80^{TS}/LexO-rpr

Figure 61. *ci>RNAi egr: w; ci-Gal4/UAS-RNAi egr; sal$^{E/Pv}$-LHG:tubGal80^{TS}/+*

ap>RNAi egr: w; ap-Gal4/UAS-RNAi egr; sal$^{E/Pv}$-LHG:tubGal80^{TS}/+

ci> grnd^{extra}: w; ci-Gal4/+; sal$^{E/Pv}$-LHG:tubGal80^{TS}/UAS-grnd^{extra}

ap> grnd^{extra}: w; ap-Gal4/+; sal$^{E/Pv}$-LHG:tubGal80^{TS}/UAS-grnd^{extra}

ci>RNAi wgn: w; ci-Gal4/+; sal$^{E/Pv}$-LHG:tubGal80^{TS}/UAS-RNAi wgn

ap>RNAi wgn: w; ap-Gal4/+; sal$^{E/Pv}$-LHG:tubGal80^{TS}/UAS-RNAi wgn

ci>RNAi grnd: w; ci-Gal4/UAS-RNAi grnd; sal$^{E/Pv}$-LHG:tubGal80^{TS}/+

ap>RNAi grnd: w; ap-Gal4/UAS-RNAi grnd; sal$^{E/Pv}$-LHG:tubGal80^{TS}/+

sal$^{E/Pv}$>rpr: w; LexO-rpr/ +; sal$^{E/Pv}$-LHG:tubGal80^{TS}/+ (control for LexO-rpr in the second chromosome) and w; +; sal$^{E/Pv}$-LHG:tubGal80^{TS}/LexO-rpr (control for LexO-rpr in the third chromosome)

ci>RNAi egr sal$^{E/Pv}$>rpr: w; ci-Gal4/UAS-RNAi egr; sal$^{E/Pv}$-LHG:tubGal80^{TS}/LexO-rpr

ap>RNAi egr sal$^{E/Pv}$>rpr: w; ap-Gal4/UAS-RNAi egr; sal$^{E/Pv}$-LHG:tubGal80^{TS}/LexO-rpr

ci>grnd^{extra} sal$^{E/Pv}$>rpr: w; ci-Gal4/LexO-rpr; sal$^{E/Pv}$-LHG:tubGal80^{TS}/UAS-grnd^{extra}

ap>grnd^{extra} sal$^{E/Pv}$>rpr: w; ap-Gal4/LexO-rpr; sal$^{E/Pv}$-LHG:tubGal80^{TS}/UAS-grnd^{extra}

egr^{3}/+ sal$^{E/Pv}$>rpr: w; egr^{3}/LexO-rpr; sal$^{E/Pv}$-LHG:tubGal80^{TS}/+

ci>RNAi wgn sal$^{E/Pv}$>rpr: w; ci-Gal4/LexO-rpr; sal$^{E/Pv}$-LHG:tubGal80^{TS}/UAS-RNAi wgn

ap>RNAi wgn sal$^{E/Pv}$>rpr: w; ap-Gal4/LexO-rpr; sal$^{E/Pv}$-LHG:tubGal80^{TS}/UAS-RNAi wgn

ci>RNAi grnd sal$^{E/Pv}$>rpr: w; ci-Gal4/UAS-RNAi grnd; sal$^{E/Pv}$-LHG:tubGal80^{TS}/LexO-rpr

ap>RNAi grnd sal$^{E/Pv}$>rpr: w; ap-Gal4/UAS-RNAi grnd; sal$^{E/Pv}$-LHG:tubGal80^{TS}/LexO-rpr

grnd^{minos} sal$^{E/Pv}$>rpr: w; grnd^{minos}; sal$^{E/Pv}$-LHG:tubGal80^{TS}/LexO-rpr

Figure 62. *sal$^{E/Pv}$>RNAi wgn: w; sal$^{E/Pv}$-Gal4/+; UAS-RNAi wgn/+*

sal$^{E/Pv}$>ecto-egr: w; sal$^{E/Pv}$-Gal4/UAS-ecto-eiger

sal$^{E/Pv}$> ecto-egr, RNAi wgn: w; sal$^{E/Pv}$-Gal4/ UAS-ecto-eiger; UAS-RNAi wgn/+

Figure 63. A. *sal$^{E/Pv}$>rpr: w; LexO-rpr/ +; sal$^{E/Pv}$-LHG:tubGal80^{TS}/+*

B. *ci>RNAi egr sal$^{E/Pv}$>rpr: w; ci-Gal4/UAS-RNAi egr; sal$^{E/Pv}$-LHG:tubGal80^{TS}/LexO-rpr*

C. *ci>RNAi wgn sal$^{E/Pv}$>rpr: w; ci-Gal4/LexO-rpr; sal$^{E/Pv}$-LHG:tubGal80^{TS}/UAS-RNAi wgn*

D, E. *enGal4> RNAi wgn: w; en-Gal4/TRE.DsRedT4; UAS-RNAi wgn/+*

F. *CTRL: w^{118}; +; +.* **G.** *egr^{3}: w; egr^{3} /egr^{3}.* **H.** *wgn^{KO}: wgn^{KO}/+*

Figure 64. A-C. *sal$^{E/Pv}$>rpr ci>RNAi wgn: w; ci-Gal4/LexO-rpr; sal$^{E/Pv}$-LHG:tubGal80^{TS}/UAS-RNAi wgn*

D, E. *enGal4> RNAi wgn: w; en-Gal4/+; UAS-RNAi wgn/+*

Figure 66. A. wt disc. **B, C.** *sal$^{E/Pv}$>rpr: w; +; sal$^{E/Pv}$-LHG:tubGal80^{TS}/LexO-rpr*

Figure 67. *hml (A)>rpr: wUASrpr/+; hmlGal4/+*

hml (B)>rpr: wUASrpr/+; +; hmlGal4/+

hml^{MB01940}>rpr: wUASrpr/+; +; hml^{MB01940}/+

sal$^{E/Pv}$>rpr: wUASrpr/+; sal$^{E/Pv}$-Gal4/+; tubGal80^{TS}/+

hml (A), sal$^{E/Pv}$ >rpr: wUASrpr/+; hmlGal4/sal$^{E/Pv}$-Gal4; tubGal80^{TS}/+

hml (B), sal$^{E/Pv}$ >rpr: wUASrpr/+; sal$^{E/Pv}$-Gal4/+; hmlGal4/ tubGal80^{TS}

hml^{MB01940}>rpr: wUASrpr/+; sal$^{E/Pv}$-Gal4/+; hml^{MB01940}/ tubGal80^{TS}

Figure 68. *ptc>rpr: UAS-rpr/+; ptc-Gal4/+; tubGal80^{TS}/+*

Figure 69. *sal$^{E/Pv}$>rpr: w; LexO-rpr/ +; sal$^{E/Pv}$-LHG:tubGal80^{TS}/+*

ci>RNAi inx1: w; ci-Gal4/+; sal$^{E/Pv}$-LHG:tubGal80^{TS}/UAS-RNAi inx1

ci>inx1 sal$^{E/Pv}$>rpr: w; ci-Gal4/LexO-rpr; sal$^{E/Pv}$-LHG:tubGal80^{TS}/UAS-RNAi inx1

ci>RNAi inx2: w; ci-Gal4/+; sal$^{E/Pv}$-LHG:tubGal80^{TS}/UAS-RNAi inx2

ci>inx2 sal$^{E/Pv}$>rpr: w; ci-Gal4/LexO-rpr; sal$^{E/Pv}$-LHG:tubGal80^{TS}/UAS-RNAi inx2

ci>RNAi aqp: w; ci-Gal4/+; sal$^{E/Pv}$-LHG:tubGal80^{TS}/UAS-RNAi aqp

ci>aqp sal$^{E/Pv}$>rpr: w; ci-Gal4/LexO-rpr; sal$^{E/Pv}$-LHG:tubGal80^{TS}/UAS-RNAi aqp

Figure 70. *sal$^{E/Pv}$>rpr: wUASrpr/+; sal$^{E/Pv}$-Gal4/+; tubGal80^{TS}/+*

sal$^{E/Pv}$>rpr; pnt^{d88}/+: wUASrpr/+; sal$^{E/Pv}$-Gal4/+; tubGal80^{TS}/pnt^{d88}

sal$^{E/Pv}$>rpr; ras^{c40b}/+: wUASrpr/+; sal$^{E/Pv}$-Gal4/+; tubGal80^{TS}/ras^{c40b}

sal$^{E/Pv}$>rpr; rl^{1}/+: wUASrpr/+; sal$^{E/Pv}$-Gal4/rl^{1}; tubGal80^{TS}/+

sal$^{E/Pv}$>rpr; top^{1}/+: wUASrpr/+; sal$^{E/Pv}$-Gal4/top^{1}; tubGal80^{TS}/+

Annex 2: Manuscript

ROS-Induced JNK and p38 Signaling Is Required for Unpaired Cytokine Activation during *Drosophila* Regeneration.

Santabárbara-Ruiz P, López-Santillán M, Martínez-Rodríguez I, Binagui-Casas A, Pérez L, Milán M, Corominas M and Serras F.

(2015) PLoS Genetics 11(10): e1005595.

PLOS | GENETICS

RESEARCH ARTICLE

ROS-Induced JNK and p38 Signaling Is Required for Unpaired Cytokine Activation during *Drosophila* Regeneration

Paula Santabárbara-Ruiz[1], Mireya López-Santillán[1], Irene Martínez-Rodríguez[1], Anahí Binagui-Casas[1¤], Lídia Pérez[2], Marco Milán[2,3], Montserrat Corominas[1], Florenci Serras[1]*

1 Departament de Genètica, Facultat de Biologia and Institut de Biomedicina de la Universitat de Barcelona (IBUB), Universitat de Barcelona, Barcelona, Spain, **2** Institute for Research in Biomedicine (IRB Barcelona), Barcelona, Spain, **3** ICREA, Catalan Institution for Research and Advanced Studies, Barcelona, Spain

¤ Current address: MRC Centre for Regenerative Medicine, The University of Edinburgh, Edinburgh, United Kingdom
* fserras@ub.edu

Citation: Santabárbara-Ruiz P, López-Santillán M, Martínez-Rodríguez I, Binagui-Casas A, Pérez L, Milán M, et al. (2015) ROS-Induced JNK and p38 Signaling Is Required for Unpaired Cytokine Activation during *Drosophila* Regeneration. PLoS Genet 11(10): e1005595. doi:10.1371/journal.pgen.1005595

Editor: Gregory P. Copenhaver, The University of North Carolina at Chapel Hill, UNITED STATES

Received: April 12, 2015

Accepted: September 18, 2015

Published: October 23, 2015

Data Availability Statement: All relevant data are within the paper and its Supporting Information files.

Funding: This project was funded by grants BFU2009-09781, CSD2007-00008, and BFU2012-36888, Ministerio de Economía y Competitividad, Spain (http://www.mineco.gob.es/portal/site/mineco/) to the FS and MC labs and by grant BFU2010-21123, PCIN-2013-048 and CSD2007-00008 to the MM lab. The funders had no role in study design, data collection and analysis, decision to publish, or preparation of the manuscript.

Abstract

Upon apoptotic stimuli, epithelial cells compensate the gaps left by dead cells by activating proliferation. This has led to the proposal that dying cells signal to surrounding living cells to maintain homeostasis. Although the nature of these signals is not clear, reactive oxygen species (ROS) could act as a signaling mechanism as they can trigger pro-inflammatory responses to protect epithelia from environmental insults. Whether ROS emerge from dead cells and what is the genetic response triggered by ROS is pivotal to understand regeneration of *Drosophila* imaginal discs. We genetically induced cell death in wing imaginal discs, monitored the production of ROS and analyzed the signals required for repair. We found that cell death generates a burst of ROS that propagate to the nearby surviving cells. Propagated ROS activate p38 and induce tolerable levels of JNK. The activation of JNK and p38 results in the expression of the cytokines Unpaired (Upd), which triggers the JAK/STAT signaling pathway required for regeneration. Our findings demonstrate that this ROS/JNK/p38/Upd stress responsive module restores tissue homeostasis. This module is not only activated after cell death induction but also after physical damage and reveals one of the earliest responses for imaginal disc regeneration.

Author Summary

Regenerative biology pursues to unveil the genetic networks triggered by tissue damage. Regeneration can occur after damage by cell death or by injury. We used the imaginal disc of *Drosophila* in which we genetically activated apoptosis or physically removed some parts and monitored the capacity to repair the damage. We found that dying cells generate a burst of reactive oxygen species (ROS) necessary to activate JNK and p38 signaling pathways in the surrounding living cells. The action of these pathways is necessary for the

Competing Interests: The authors have declared that no competing interests exist.

activation of the cytokines Unpaired (Upd). Eventually, Upd will turn on the JAK/STAT signaling pathway to induce regenerative growth. Thus, we present here a module of signals that depends on oxidative stress and that, through the p38-JNK interplay, will activate cytokine-dependent regeneration.

Introduction

Tissues and organs need to function reliably regardless of adverse environmental conditions. Injuries, disease, infection and environmental insults are stressors causing cell damage that can be repaired via homeostatic machinery. Thus, optimal health is largely dependent upon tissue homeostasis, which involves cell replacement and tissue repair. Although many signaling pathways have been proposed to respond to environmental insults, the early activation of those signals is poorly understood.

Response to damage can involve oxidative stress and, subsequently, the stimulation of stress-activated protein kinases. The production of reactive oxygen species (ROS) by various redox metabolic reactions, which has generally been considered to be deleterious, is now emerging as an active participant in cell signaling events [1,2]. ROS are byproducts of aerobic metabolism that include superoxide O_2^-, peroxide H_2O_2 and hydroxyl radicals OH·. ROS, and in particular H_2O_2 are required for inflammatory cell recruitment [3,4]. Amphibian and zebrafish injuries produce the ROS necessary to promote proliferation and regeneration [5–8]. In mammalian cells, ROS are known to act as second messengers to activate diverse redox-sensitive signaling transduction cascades, including the stress-activated MAP kinases p38 and the Jun-N Terminal kinase (JNK) [9–11]. ROS-mediated p38 activation occurs during the inflammatory response in rats [12] and during the loss of self-renewal and differentiation in glioma-initiating cells [13]. It has also been found that p38 and JNK are differentially required during repair. In endothelial cells, TNF-α stimulates repair through the positive action of JNK and negative regulation of p38 [14], whereas in corneal repair, p38, and not JNK, is required for epithelial migration [15]. In *Drosophila* both MAPK have been associated with stress responses [16]. *Drosophila* p38 pathway responds to different environmental stimuli and stressors [17,18]. Moreover, increasing ROS beyond basal level triggers precocious differentiation of *Drosophila* hematopoietic progenitors through JNK signaling [19].

The JNK signaling pathway has emerged as an early response to cell death and physical damage and appears to play a critical role in compensatory proliferation, regeneration and wound healing [20–28]. Moreover, upon apoptotic stimulus p53 and JNK are activated by the caspase Dronc and function upstream of pro-apoptotic genes, creating an amplifying loop that ensures cell death [29–33]. One of the early known responses to cell death is the transcriptional activation of the phosphatase *puckered* (*puc*), a downstream effector of the JNK pathway and a powerful negative regulator of the same pathway. Interestingly *puc* has been found in surviving cells of nearby tissue after cell death [23,27] and after physical injury [22,34]. JNK activation of the cytokines *unpaired* (*upd*), a family of cytokines linked to the human interleukin-6, is necessary for hyperproliferation in *Drosophila* tumors and for wound healing [34–36]. Thus, we hypothesize here that the activation of JNK, which is amplified in dying cells, is in some way propagated to nearby surviving tissue where beneficial low levels of JNK promote *upd* expression.

Apoptotic cells have been observed in the early regeneration of different animals and are thought to provide signals that regulate wound healing and regeneration [37–39]. As apoptosis has been associated with oxidative stress and cytokines act as a functional link between

oxidative stress and compensatory proliferation in mammals [40], we decided to investigate whether ROS occur upstream from the stress-activated protein kinases p38 and JNK and cytokines during tissue repair. We took advantage of the regeneration capacity of *Drosophila* imaginal disc epithelium (reviewed in [41,42]) to address these questions. Imaginal discs are larval epithelial sacs that possess a robust ability for homeostatic cell renewal to overcome the effect of stressors. We report here that, either by inflicting a physical lesion or after inducing cell death, imaginal disc cells produce ROS that are linked to the activation of p38 and JNK stress MAP kinases. In addition, JNK and p38 activity in the living tissue triggers transcription of the cytokine *unpaired* (*upd*), which acts as a ligand of the JAK/STAT signaling pathway and promotes regeneration of the missing part.

Results

ROS are produced after tissue damage

To monitor ROS after tissue damage we used CellROX Green, a cell-permeant fluorogenic probe that is non-fluorescent in the reduced state and exhibits bright fluorescence upon oxidation. We found high levels of CellROX Green near the wound edges of physically cut wing imaginal discs. Only a few of the CellROX Green positive cells were TO-PRO-3 positive cells (dying cells), indicating that most ROS-producing cells were alive (Fig 1A). We examined the production and propagation of ROS over time. Few minutes after cut (0–5') some cells at the wound edges were CellROX Green positive, indicating that the oxidative burst is rapidly occurring after damage (Figs 1B and 1C and S1). Ex vivo imaging showed that fluorescence propagates to the neighboring cells during the first 30' after damage (Figs 1B and S1).

We next monitored ROS production after controlled induction of cell death (also known as genetic ablation), which can be used as a type of insult to study cellular responses. Apoptosis was induced using *patched* (*ptc*)-*Gal4* to drive expression of the pro-apoptotic gene *reaper* (*rpr*) under the control of a UAS (henceforth *ptc>rpr*); the Gal4/UAS system was controlled by the temperature-sensitive form of Gal80 ($Gal80^{TS}$), which inhibits Gal4 and enables examination of regeneration after cell death [23,24]. As previously described, *ptc>rpr* discs show a stripe of apoptotic cells that eventually extrudes basally and is replaced apically by living cells (Fig 1D) [23]. CellROX Green was strongly incorporated into the *ptc>rpr* apoptotic cells (TO-PRO-3 positive) (Fig 1E). Strikingly, living cells adjacent to the apoptotic zone also showed ROS, albeit at much lower levels than in dead cells (Fig 1E and 1F). Similar observations were obtained using 2',7'-dichlorodihydrofluorescein diacetate (H2DCFDA) which upon oxidation is converted to the highly fluorescent DCF. Indeed, cut or *rpr*-ablated discs, showed high levels of fluorescence on the wound edges, in the apoptotic cells and also in the living cells near the apoptotic (S1B, S1C and S1D Fig).

Thus, these results showed that both physical injury and genetically induced apoptosis are insults that result in the production of ROS.

ROS are required for tissue repair

Oxidative burst following death or damage could propagate from dying to living cells in subtoxic doses and initiate repair. To explore this issue, we decided to deplete ROS production and examine adult wings after cell death. We first checked whether antioxidants (vitamin C, Trolox or N-acetyl cysteine [NAC]) are capable of blocking ROS production. We incubated cut discs in Schneider's medium containing antioxidants, and found strong reduction of CellROX Green fluorescence (S2 Fig).

Next, we studied the effects of ROS scavenging on regeneration. We used a Gal4 construct under the control of a wing-specific enhancer ($sal^{E/Pv}$-*Gal4*), which allows analysis in adult

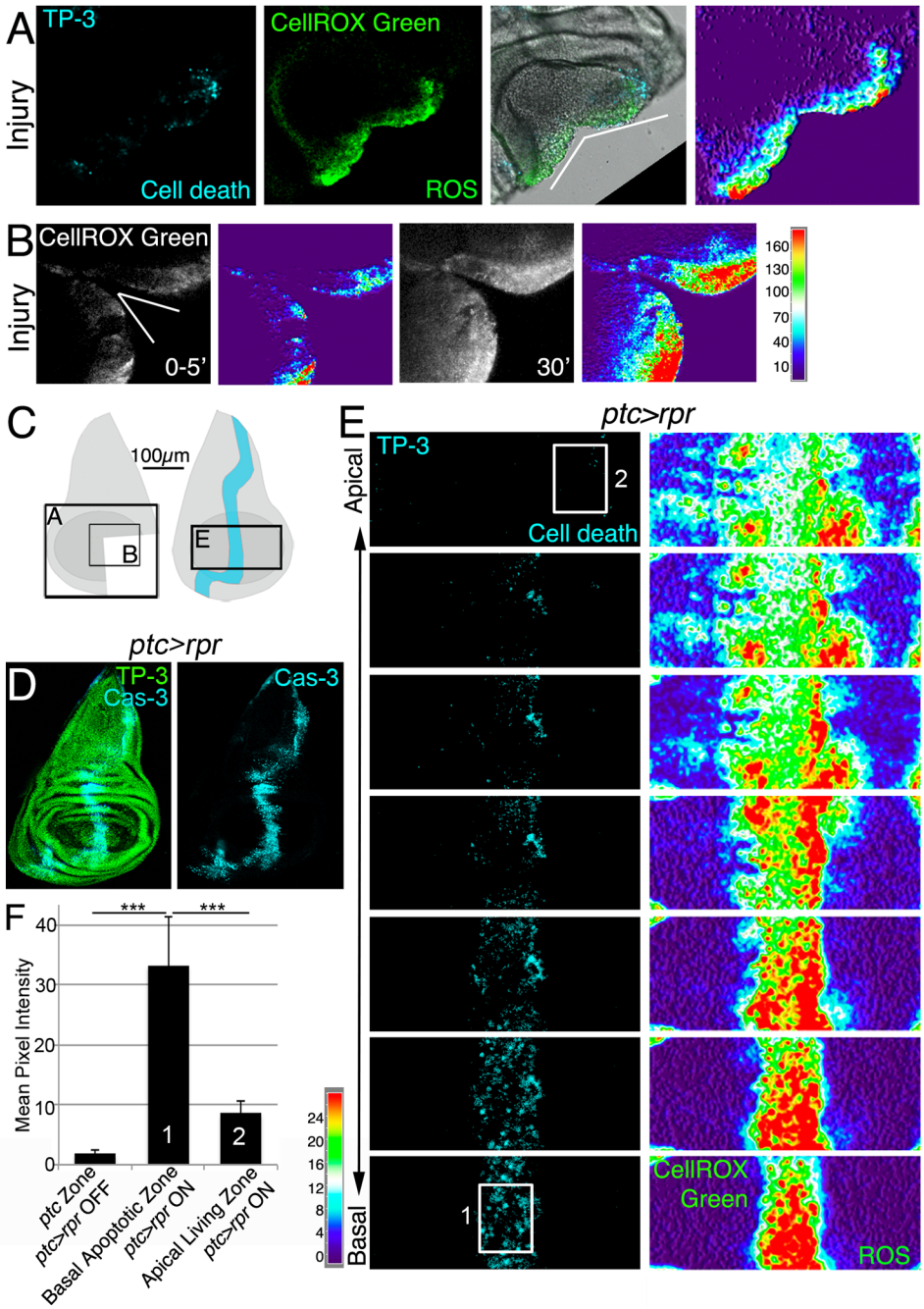

Fig 1. ROS produced after physical injury and after cell death. (A) Cut disc cultured ex vivo (white wedge indicates cut edges) and thermal LUT of CellROX Green. (B) Cut disc cultured ex vivo, imaged at just after cut (0–5') and 30' later. Thermal scale indicates pixel intensity. (C) Sketch of wing imaginal discs with the area (black square) shown in A, B and E. (D) Fixed disc stained for nuclei to show disc contour (TP-3: TO-PRO-3) and caspase-3 after *ptc>rpr* activation for 11h at 29°C. (E) *ptc>rpr* disc cultured ex vivo; basal images at the bottom, apical at the top. Left, cell death (TO-PRO-3). Right, thermal LUT taken from the ROS channel (CellROX Green) of the same preparation. Note that most dead cells (TO-PRO-3 positive) show high ROS (red in thermal image) whereas living cells (TO-PRO-3 negative) had low ROS (green-cyan in thermal image). (F) Mean pixel intensity (grey value) of the indicated zones in control discs without cell death (*ptc>rpr* OFF) and discs with cell death (*ptc>rpr* ON). The pixel intensity in the *ptc* domain in the absence of cell death (*ptc>rpr* OFF) was 1.76 ± 0.55 (SD; from 48 regions of interest [ROI] in n = 5 discs). The mean pixel intensity for the apoptotic region (basal; *ptc>rpr* ON) was 33.14±8.18 (SD), measured in 27 ROI on confocal images taken from n = 6 discs. Living cells adjacent to the apoptotic zone showed a mean grey value of 8.51±2.12

(SD; 15 ROI from 6 discs taken from cells near the *ptc* domain). White rectangles in E: example ROI for Basal Apoptotic Zone (1) and Apical Living Zone (2). The ROI's for the *ptc* Zone, in discs in which *ptc>rpr* is OFF, were placed as (1). ***$P<0.001$. Thermal scale indicates sample values from raw images.

doi:10.1371/journal.pgen.1005595.g001

wings while not affecting the rest of the organism, to activate *UAS-rpr* (henceforth $sal^{E/Pv}>rpr$). To deplete intracellular ROS, $sal^{E/Pv}>rpr$ larvae were fed with food supplemented with antioxidants (Fig 2A). ROS scavengers in $sal^{E/Pv}>rpr$ controls kept at 17°C to prevent cell death did not show any alteration of wing morphology (S2B Fig). Conversely, a $sal^{E/Pv}>rpr$ control group without scavengers moved to 29°C for 11 h showed complete wing regeneration (Fig 2B). However, the $sal^{E/Pv}>rpr$ experimental group with ROS scavengers and induced cell death showed incomplete regeneration in about 50% of the cases (Fig 2B and 2C). We considered incomplete regeneration when some veins or intervein sectors were missing. To discard that these effects could be caused by differences in survival or developmental delay, we checked whether proliferation is impaired after ROS depletion. We counted the number of mitoses after cell death induction in discs from NAC-fed larvae and found a significant decrease compared to discs from larvae fed in the absence of antioxidants (Fig 2D). The number of mitoses in controls fed with or without antioxidants and kept at 17°C to block cell death did not vary (Fig 2D).

In addition, we used enzymatic manipulation of ROS. Superoxide dismutase (Sod) catalyzes the dismutation of superoxide anion into oxygen and hydrogen peroxide. In the presence of hydrogen peroxide, Catalase (Cat) catalyzes its breakdown into water and oxygen. Thus, overexpression of Sod or Cat will remove their respective ROS substrates, whereas simultaneous activation of Sod and Cat will enhance the depletion of both O_2^- and H_2O_2. *UAS-Sod*, *UAS-Cat* or *UAS-Sod*:*UAS-Cat* were ectopically expressed under the *nub-Gal4* driver, which operates throughout the wing pouch (Fig 2E). To induce cell death, we used an independent transactivator based on the LexA/lexO binary system. We generated a $sal^{E/Pv}$*-LHG* transgene, which includes a Gal80 suppressible form of LexA [43], to conditionally express *lexO-rpr* in the $sal^{E/Pv}$ domain. This combination permits control of the temporary expression of two binary systems ($sal^{E/Pv}$*-LHG lexO-rpr* and *nub-Gal4 UAS*-transgene) by $tubGal80^{TS}$ (Fig 2E). This design has the advantage of simultaneously activating two wing-specific transgenes (*nub-Gal4* and $sal^{E/Pv}$*-LHG*) in overlapping domains, therefore hindering early ROS. After $sal^{E/Pv}$*-LHG lexO-rpr* genetic ablation and *nub-Gal4 UAS*-transgene expression we allowed the larvae to develop to adulthood and found a drop in the number of regenerated wings (Figs 2F and 2G and S2C and S2D). Together, these results indicate that chemical and enzymatic ROS scavengers interfere with regeneration.

ROS control JNK activity

To determine whether ROS act on JNK during wing disc repair, we first monitored the activity of this pathway in wing discs after cell death. We used two different reporters to monitor JNK activity: *puc-lacZ*, which marks *puc*-expressing cells [44], and the *TRE-DsRed.T4* reporter, which monitors the JNK substrate *AP1* transcription factor (hereafter *TRE-red* reporter) (Fig 3A and S3A Fig) [45]. In *ptc>rpr* discs, we found high levels of *TRE-red* reporter in the basal apoptotic zone and, to a lesser extent, in the apical living cells (Fig 3A and 3B). In contrast, *puc-lacZ* positive cells were found in the apical zone, as described previously [23], and rarely in the apoptotic zone. Some *puc* positive cells incorporated EdU, supporting that JNK is also induced in living cells (Fig 3C).

As NAC is an excellent source of sulfhydryl SH- groups and efficiently promotes scavenging of free radicals [46], it was the most suitable antioxidant to determine the relationship between

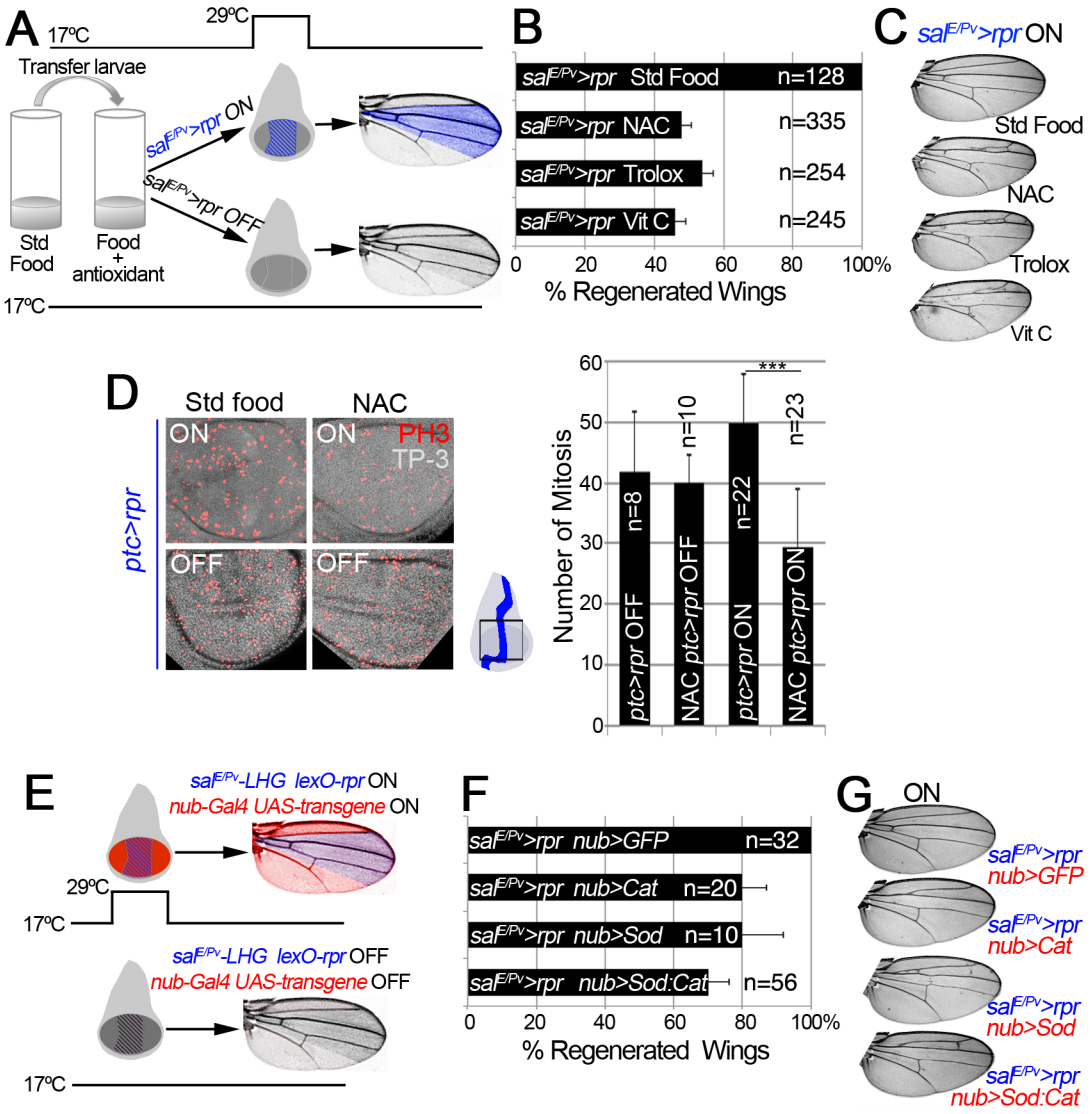

Fig 2. ROS are required for tissue repair. (A) Design for chemical antioxidant intake and cell death induction. At 17°C and 24 h before cell death induction, larvae were transferred to a vial with standard food supplemented with antioxidant. Cell death (*sal$^{E/Pv}$>rpr* ON) was induced by shifting temperature to 29°C for 11 h (blue stripes in the disc). Larvae were transferred to 17°C where they regenerated and emerged into adults, in which wings were scored. Blue color in the wing: area emerged from *sal$^{E/Pv}$*. Controls *sal$^{E/Pv}$>rpr* OFF were kept at 17°C to avoid cell death. (B) Percentage of regenerated wings after cell death (*sal$^{E/Pv}$>rpr* ON) in the absence of antioxidant (Std Food), or in the presence of antioxidants (NAC, Trolox or Vitamin C). (C) Examples of *sal$^{E/Pv}$>rpr* ON wings with the indicated food supplement. In controls without antioxidants (Std Food), the complete wing recovered. For each antioxidant an example of incomplete regeneration after cell death induction is shown. (D) Mitosis number in *ptc>rpr* discs from larvae fed with and without NAC and with or without *rpr*-ablation (ON versus OFF). *Ptc>rpr* OFF: 41.86 ± 9.84 (S.D.); NAC *ptc>rpr* OFF: 39.9 ± 4.68 (S.D.); *ptc>rpr* ON: 49.73 ± 8.18 (S.D.); NAC *ptc>rpr* ON: 29.52 ± 9.41 (S.D.) (E) Design for ectopic expression of enzymatic antioxidant transgenes and simultaneous cell death induction when shifted to 29°C for 11 h. The Gal4/UAS (red) activate Cat, Sod or Cat+Sod transgenes. Blue striped area: *sal$^{E/Pv}$-LHG lexO-rpr*. Adult wings were scored for complete regeneration of the missing zone. Red coloration indicates zone influenced by the enzymatic antioxidant; purple: zone influenced by enzymatic antioxidant and cell death. *sal$^{E/Pv}$-LHG* and *nub-Gal4* are under the control of *tubGal80^{TS}*. (F) Percentage of regenerated wings in Cat, Sod or Cat and Sod ectopically expressed transgenes. (G) Wings from individuals after cell death and transgene activation (ON). For Cat, Sod or Sod:Cat and example of incomplete regeneration is shown. TP-3: TO-PRO-3. ***P<0.001

doi:10.1371/journal.pgen.1005595.g002

ROS and JNK in stressed imaginal discs. To test NAC effects on JNK, we used the *TRE-red* reporter because is more rapidly and extensively expressed than *puc-lacZ* (Figs 3A and S3B) and because its activity is blocked in JNK mutants [45] or after chemical JNK inhibitors (S3C Fig). We found that the mean pixel intensity of the *TRE-red* reporter in *ptc>rpr* wing discs

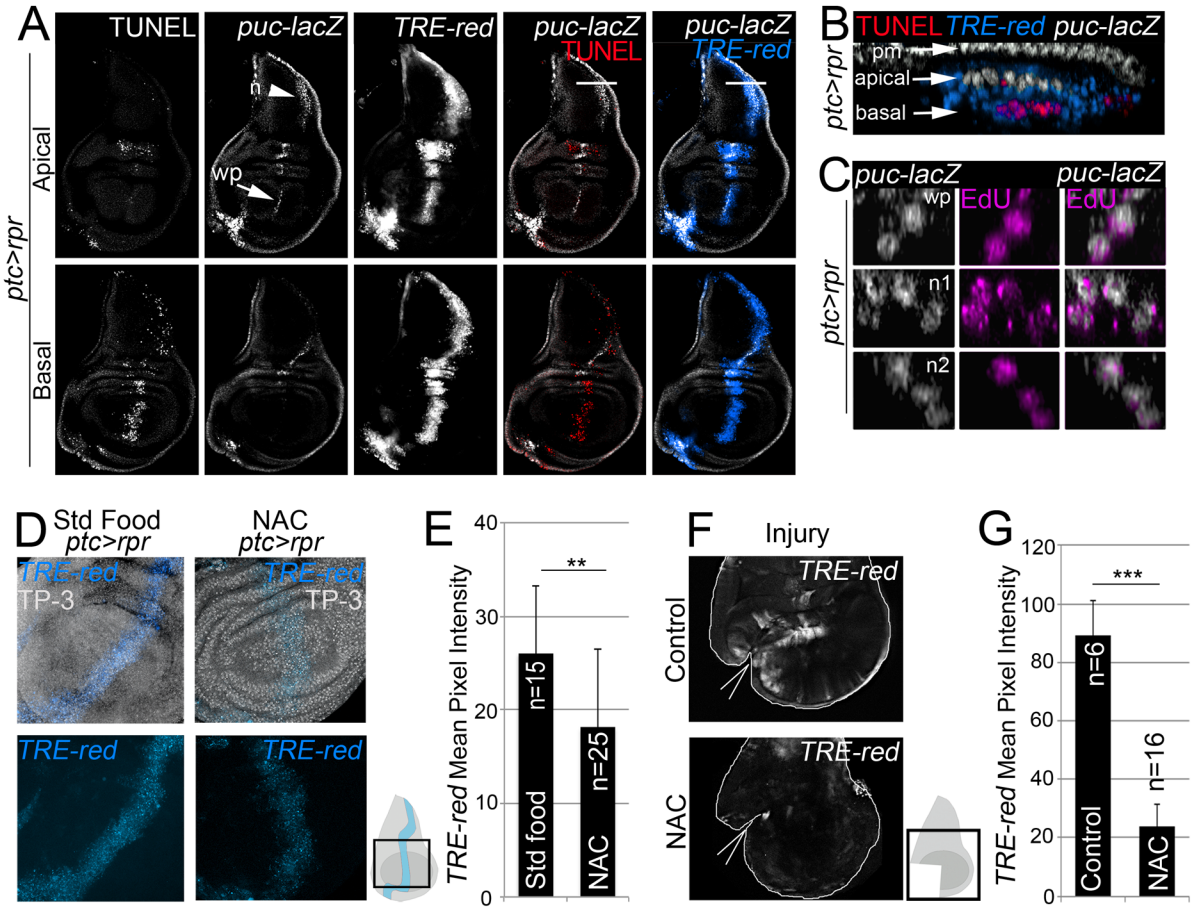

Fig 3. ROS control JNK activity. (A) Test of JNK reporters. All images in A correspond to the same disc after *ptc>rpr* induction. Top row: apical sections. Bottom row: basal sections. Note that *puc* is more abundant in apical than basal sections, particularly in the notum (n; arrowhead) and wing pouch (wp; arrow). Cell death (TUNEL) and high *TRE-red* are more abundant in basal sections. (B) Zoom of a digital cross section of the zone marked with a white line in A. Endogenous *puc-lacZ* is found in the outer layer of peripodial membrane cells (pm). *Puc-lacZ* cells in the disc columnar epithelium are apical (white), most apoptotic cells are basal (red), and *TRE-red* positive cells are apical and basal (blue). (C) Three digital cross section in an apical *puc-lacZ* zone of the wing pouch (wp) and notum (n1, n2). Each example contains three to four cells with co-localization of ß-galactosidase and EdU. (D) *TRE-red* reporter in *ptc>rpr* discs of larvae fed with standard food or NAC-supplemented food (NAC). TP-3: TO-PRO-3. (E) Mean pixel intensities of *TRE-red* reporter in *ptc>rpr* discs with standard or NAC food. The pixel intensity for standard food was 26.06 ± 7.22 (S.D.; n = 15) and for NAC 18.12 ± 8.32 (S.D.; n = 25). (F) *TRE-red* reporter expression in physically injured discs, cultured for 7 h ex vivo in Schneider's culture medium with or without NAC. Outline: disc contour. Wedges: cut. (G) Mean pixel intensities of *TRE-red* reporter in ex vivo cultured discs with or without NAC. The pixel intensity for standard culture was 88.98 ± 22.25 (S.D.; n = 6) and for NAC 23.98 ± 10.26 (S.D.; n = 16). ***P*<0.01, ****P*<0.001.

doi:10.1371/journal.pgen.1005595.g003

from animals grown in NAC-supplemented food was lower than in the same zone of individuals fed with standard food (Fig 3D and 3E). Moreover, discs cultured ex vivo in which NAC was added into the medium resulted in a drop of *TRE-red* activity after physical injury (Fig 3F and 3G). These observations indicate that activation of JNK is ROS dependent.

ROS stimulates p38 phosphorylation

Another potential response to ROS increase is the activation of the p38 signaling cascade [10,17,18]. Active p-38 signaling can be monitored using anti-phosphorylated p38 (P-p38). We found that discs fixed and incubated with anti-P-p38 a few minutes after physical injury showed P-p38 staining around the wound. P-p38 localization was variable and depended on the severity of the injury. In contrast, intact discs immediately stained after fixing did not show P-p38 (Fig 4A). However, discs cultured for 3 to 8 hours with or without injury showed P-p38

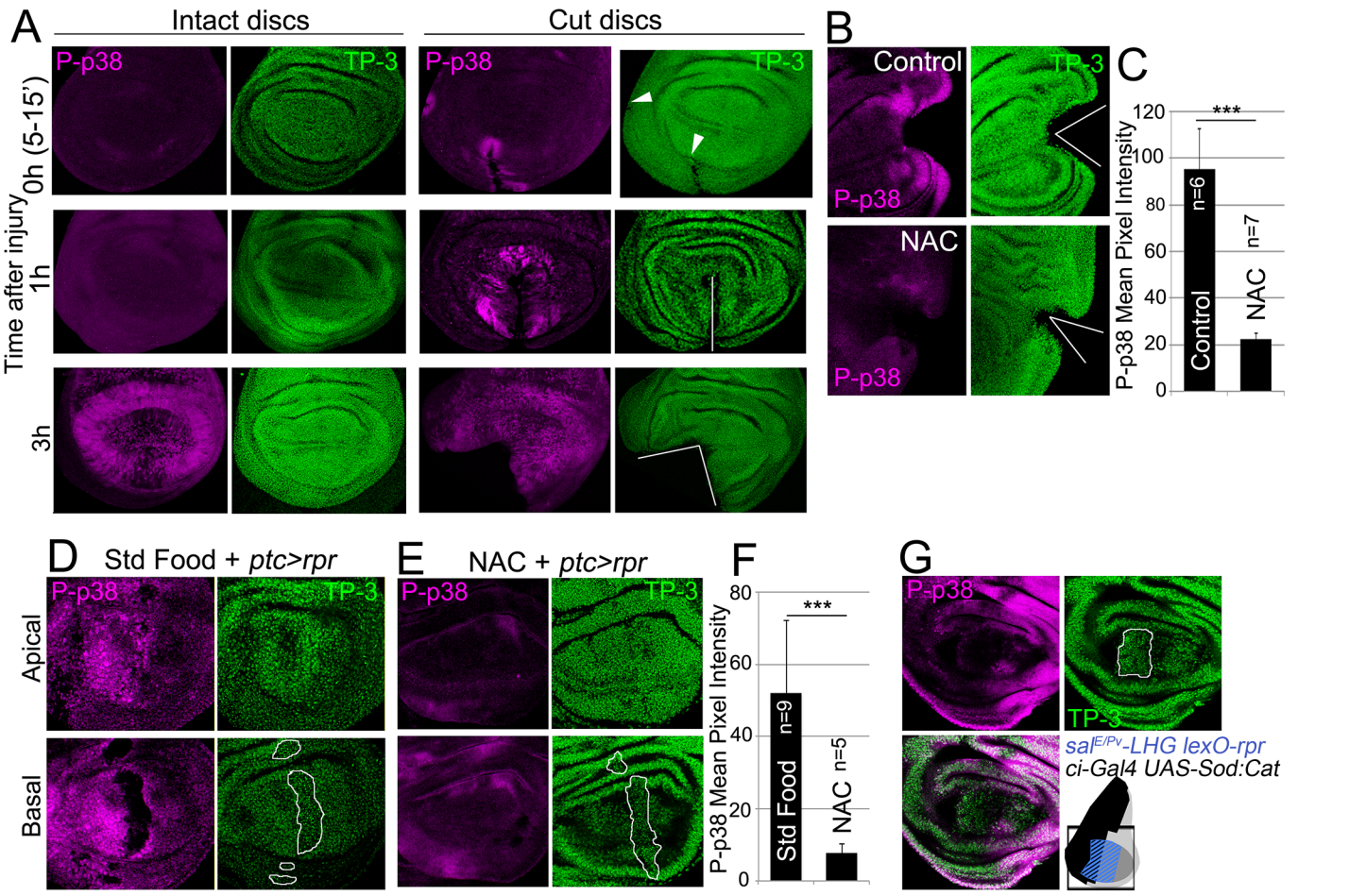

Fig 4. ROS stimulate p38 phosphorylation. (A) P-p38 staining of intact (uncut, controls) and cut discs cultured for the indicated times after injury. White lines: wound edges; white arrowhead: small incision. (B) Discs cultured with or without NAC, cut and stained for P-p38. (C) Mean pixel intensities of P-p38 fluorescence from cut discs cultured with standard medium (95.29 ± 17.52; S.D.) or NAC-supplemented (22.45±2.56; S.D.). (D) Apical and basal images of P-p38 after *ptc>rpr* induction. (E) Apical and basal images of *ptc>rpr* after NAC supplementation showing reduction of P-p38 localization. (F) Mean pixel intensities of P-p38 fluorescent labeling from *ptc>rpr* discs fed with standard (52.17±19.96; S.D.) or NAC-supplemented food (7,85 ± 2,42; S.D.). (G) Genetic ROS scavenging using *ci>Sod:Cat*, activated in the anterior compartment (*ci*, black in the sketch). Sal^{EPv}*>rpr* cell death (blue in the sketch) in the same disc results in inhibition of P-p38 only in anterior compartment. TP-3: TO-PRO-3 nuclei staining. Outlined white in D, E and G: apoptotic zone. ***P<0.001.

doi:10.1371/journal.pgen.1005595.g004

staining throughout the disc. This general staining is likely due to the stress generated by culturing, and contrasts with the fast local P-p38 response around the damaged zone. We next wondered whether the boost in ROS that propagates to the surviving tissue triggers p38 activation. We observed that the early P-p38 staining was blocked in discs cut and cultured ex vivo in medium containing NAC (Fig 4B and 4C).

We also analyzed p38 activation after inducing cell death and found P-p38 only in living cells but never in the basal apoptotic zone (Fig 4D). In the absence of cell death, no P-p38 was detected. Blocking of ROS production with NAC resulted in a significant drop in P-p38-labeled cells (Fig 4D and 4E). In addition, we used the double transcriptional trans-activator system consisting of the $sal^{E/Pv}$*-LHG lexO-rpr* to induce apoptosis and simultaneously interfere with ROS production by inducing *UAS-Sod*:*UAS-Cat* in the anterior (*ci-Gal4*) compartment (Fig 4G). The results showed a strong reduction of P-p38 in the anterior (*ci-Gal4 UAS-Sod*:*UAS-Cat*) compartment in comparison to the posterior.

To test whether an independent source of ROS could activate P-p38 in discs, we fed larvae for 2h with food supplemented with 1% H_2O_2 and checked for P-p38. Intact discs (no cut, no cell death) from these larvae resulted in high levels of P-p38 as well as high CellROX Green fluorescence (S4 Fig).

Together, these observations show that chemical (NAC) or genetic (*UAS-Sod:UAS-Cat)* ROS scavengers inhibit P-p38 and therefore indicate that oxidative stress is required for p38 activation.

p38 signaling is required for tissue repair

We next scored wing regeneration after $sal^{E/Pv}$>*rpr* induction of cell death in different mutant backgrounds of the p38 pathway. As most of the alleles are lethal or semilethal in homozygosis [47], we tested them in heterozygosis. Alleles of two *Drosophila* p38 genes, *p38a* and *p38b*, were used in this work. We found that heterozygous $p38b^{d27}$ animals regenerated entire wings (Fig 5A). However, a severe effect was observed with $p38a^{1}$ as the resulting wings lacked some sectors and presented notches in the margin. *Drosophila* p38 signaling is activated by MKK3/licorne (*lic*)-mediated phosphorylation [48]. Heterozygous lic^{d13} showed all wing sectors albeit wings were smaller than controls. However, double heterozygotes for lic^{d13} and $p38b^{d27}$ were unable to regenerate some wing sectors. We also tested $Atf2^{PB}$, a hypomorphic allele of the ATF2 transcription factor downstream of p38 [49], either in homozygosis or in double heterozygous combinations (lic^{d13} $Atf2^{PB}$ or $p38b^{d27}$ $Atf2^{PB}$). We found defects in size and pattern after $sal^{E/Pv}$>*rpr* induction. Regeneration was severely impaired in double heterozygotes for $p38a^{1}$ (MAPK) and $Atf2^{PB}$ (Fig 5A).

We also blocked the pathway with UAS-RNAi constructs for *lic*, *p38b*, *p38a* and *Atf2* and analyzed the adult wings. These transgenes were activated in the anterior compartment (ci>RNAi) and cell death was induced in the $sal^{E/Pv}$ domain ($sal^{E/Pv}$*-LHG lexO-rpr)*. We found a reduction of individuals capable to fully regenerate wings for those RNAi's (S5A Fig).

To gain further insight into the requirement for p38, we chemically blocked the pathway using the imidazole drug SB202190, a specific cell permeable p38 MAP kinase inhibitor that has been reported to do not interfere JNK or ERK kinases and is known to prevent phosphorylation of Atf2 in *Drosophila* S2 cells [50]. We first tested the specificity of the SB202190 on P-p38 in *rpr*-ablated discs and found significant differences between individuals fed with the drug and controls. In contrast, the differences on *TRE-red* reporter were not significant (S5C Fig). This indicates that SB202190 strongly blocked P-p38 and weakly the *TRE-red*. $Sal^{E/Pv}$>*rpr* larvae grown at 17°C to prevent cell death and fed with food containing SB202190 (0.12, 1.0 or 5.0 μM) emerged into normal adults (S5B Fig). However, $sal^{E/Pv}$>*rpr*-induced larvae fed with SB202190 developed wings lacking some sectors. The highest percentage of aberrant wings was found using 5 μM SB202190 (Fig 5B). This observation confirms that activation of p38 is required for wing repair.

p38 and JNK act independently

To assess the relationship between JNK and p38, we tested p38 activation in wounded null hemizygous JNKK *hemipterous* (hep^{r75}) discs. P-p38 was localized near the wound after physical injury (Fig 6A). This contrasts with the decrease in P-p38 when the MAPK kinase *lic*, which is the p38 activating kinase, was interfered with RNAi in injured discs (S6A Fig).

Moreover, P-p38 staining was localized in hep^{r75} discs after *ptc*>*rpr* induction, as in the wild type (Fig 6B, compare with Fig 4), indicating that JNK and p38 act independently. In addition, we fed animals with the JNK Inhibitor IX, which abolishes *TRE-red* reporter expression

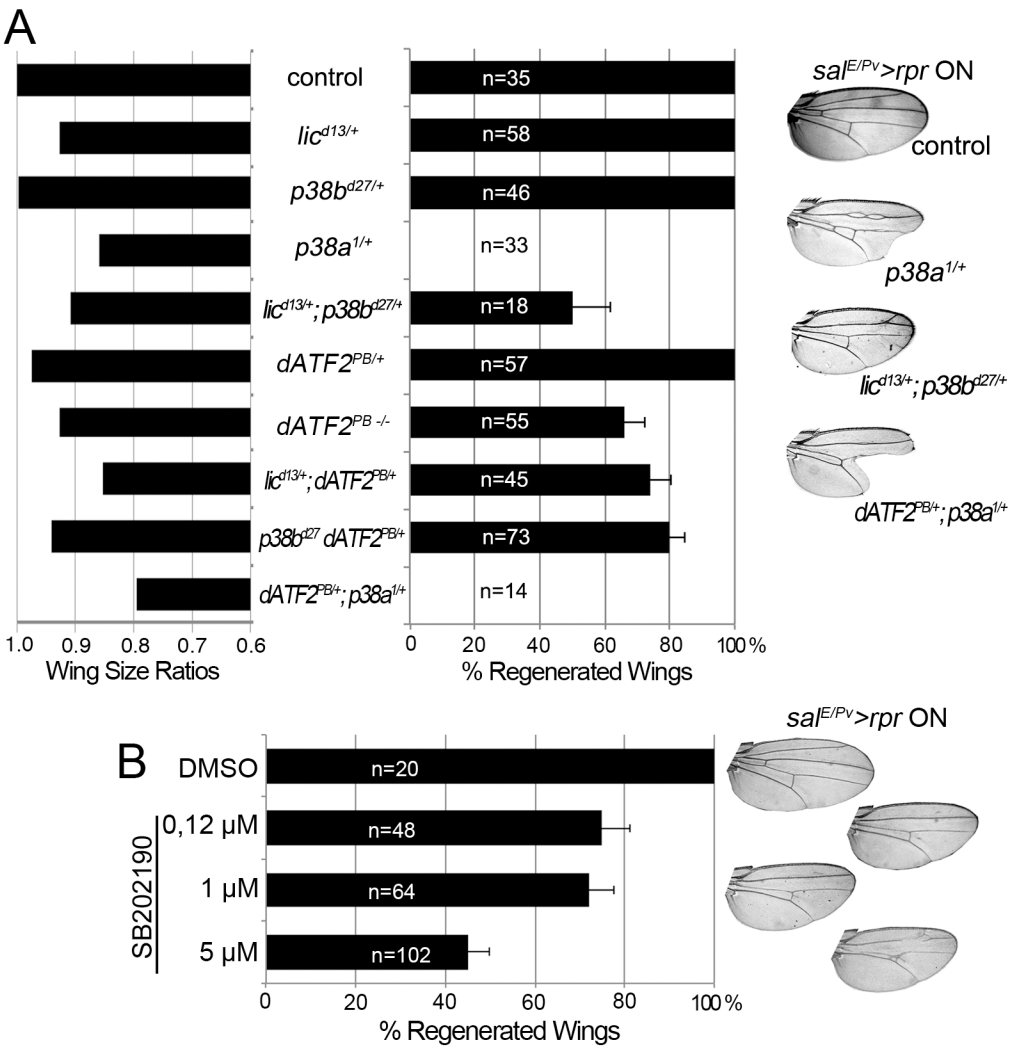

Fig 5. p38 inhibition impairs tissue repair. (A) Adult wing parameters in p38 signaling mutant backgrounds after genetic ablation. Left: ratios of the wing areas between experimental groups (*rpr* induction $sal^{E/Pv}$>*rpr* ON) and control (no *rpr* induction $sal^{E/Pv}$>*rpr* OFF). Right: percentage of fully regenerated wings. Far right: examples of wings with full regeneration (control) and incomplete regeneration (indicated genotypes) after $sal^{E/Pv}$>*rpr*. (B) Percentage of fully regenerated wings after SB202190 intake in $sal^{E/Pv}$>*rpr* flies. Right: wing fully regenerated (top) and examples of incomplete regeneration for each SB202190 concentration.

doi:10.1371/journal.pgen.1005595.g005

and inhibits regeneration (S3C and S3D Fig), and found that P-p38 after *rpr*-ablation was not affected (S6B Fig).

To confirm that JNK and p38 act independently, we blocked the *p38* pathway and checked for *TRE-red* reporter activity. As the $p38a^{1}$ allele in heterozygosis strongly affects regeneration (Fig 5), we used this null allele in homozygosis and tested *TRE-red* activity after physical injury. Our results showed that *TRE-red* is induced at the wound edges of $p38a^{1-/-}$ mutant discs (Fig 6C and 6D). Together, these results demonstrate that p38 and JNK stress responses act independently in damaged imaginal discs.

Upd expression is triggered by ROS

The evidence that JNK is active in the living tissue located near damaged zones arises from the expression of *puc* and *TRE-red* reporters (Fig 3A and 3B), and also because inhibition of JNK

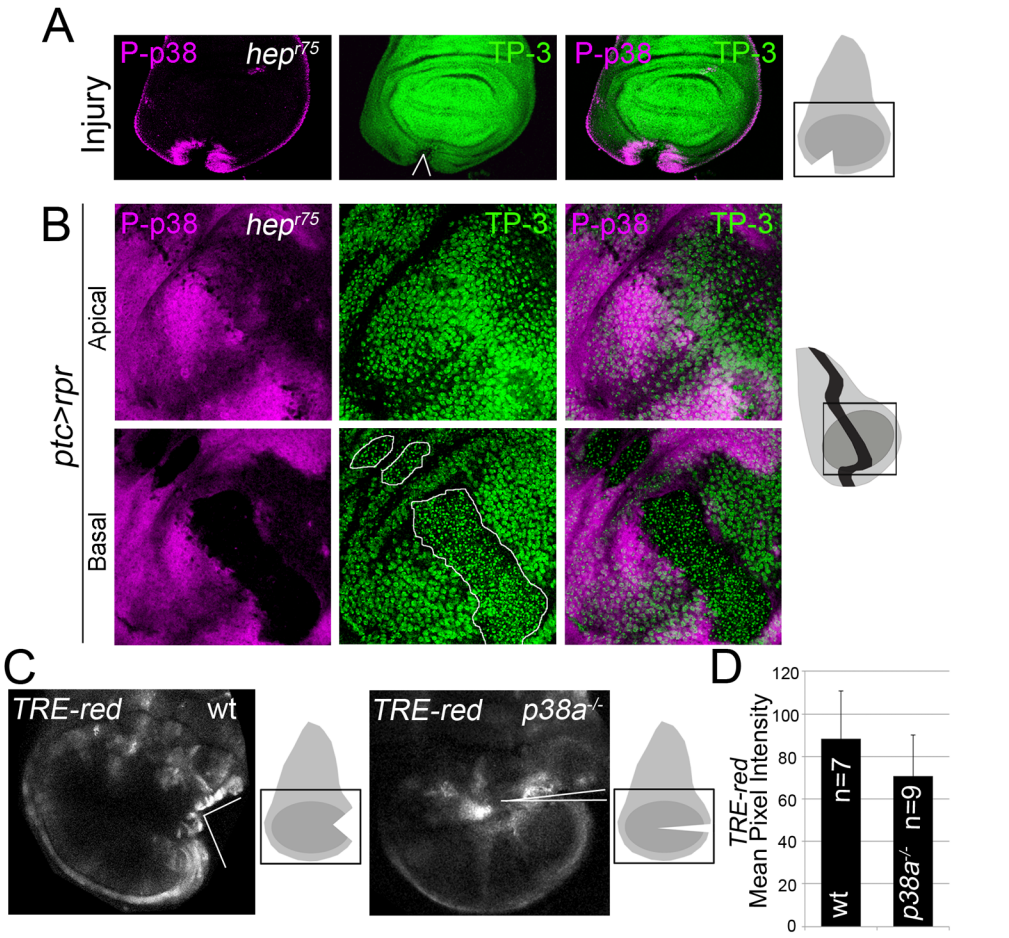

Fig 6. p38 and JNK are activated independently. (A) *Hep*^{r75} hemizygous disc cut (wedge) and stained with P-p38. Sketch of wing discs with square indicate location of images. (B) *Hep*^{r75} hemizygous disc after *ptc>rpr* induction and stained for P-p38. Dead domain is outlined white. TP-3; TO-PRO-3. (C) Wild type and *p38a*$^{1-/-}$ discs, cultured for 7h showing *TRE-red* activation close to the cut edges. (D) Mean pixel intensity for *TRE-red* measured in discs with physical injury in wild type (88.24 ± 22.58; S.D.) and *p38a*$^{1-/-}$ (70.80 ± 19.14; S.D.). P = 0.33 n.s.

doi:10.1371/journal.pgen.1005595.g006

results in defects in repair [21,23,25,26,51]. Moreover, JNK activation promotes *upd* expression in different contexts [28,52]. We wondered whether those low non-deleterious JNK levels are capable of triggering tissue repair through *upd* expression. Upd cytokines are ligands that associate with the receptor *domeless* (*dome*) to stimulate the kinase activity of the receptor associated protein kinase *hopscotch* (*hop*), which in turn phosphorylates dimers of the transcription factor STAT92E [53]. We found *upd* and *upd3* expression near the wound after both physical injury and cell death (Fig 7A, 7B, 7F and 7G). This injury-induced *upd* expression was blocked in JNKK *hep*^{r75} mutants (Fig 7C and 7D) and by JNK Inhibitor IX (S3C Fig), which is consistent with previous observations [28,35].

To study the requirement for JAK/STAT for regeneration, we used the *sal*$^{E/Pv}$*-LHG lexO-rpr* to induce apoptosis and simultaneously interfered with the receptor *dome* using the dominant negative form *UAS-dome*^{DN} driven by *ci-Gal4*. These wings lacked most of the tissue where cell death was induced and *dome* was blocked (Fig 7J and 7K), indicating that JAK/STAT signaling is needed for tissue recovery. Moreover, heterozygous alleles for the JAK/STAT pathway resulted in partial disruption of adult wing recovery after cell death (S7 Fig).

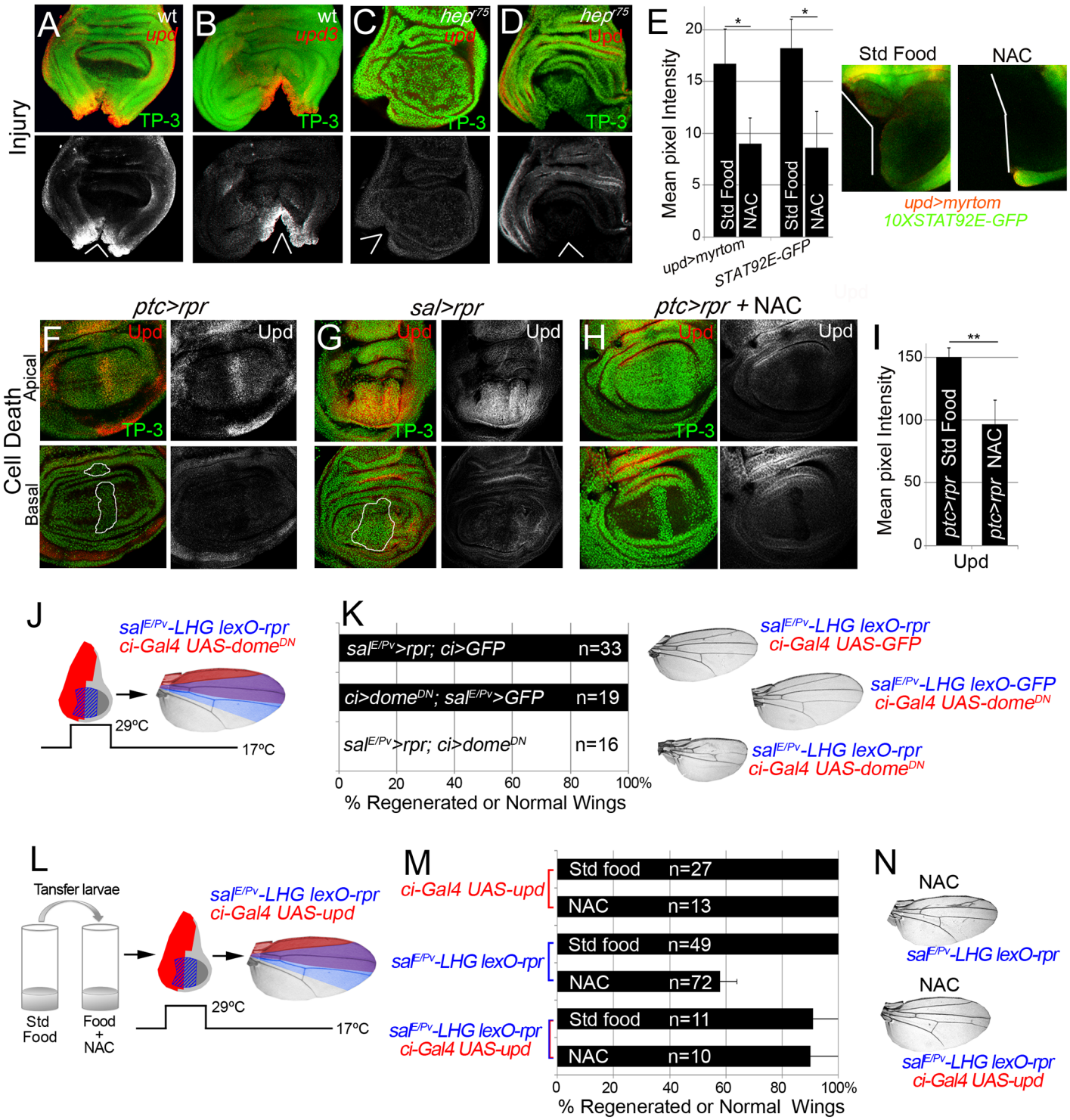

Fig 7. Cytokine signaling is controlled by ROS and JNK. (A, B) In situ hybridization of *upd* (A) and *upd3* (B) in wild type (wt) discs and JNKK hep^{r75} hemizygotes (C) after injury. (D) hep^{r75} hemizygote stained with anti-Upd after injury. (E) Mean pixel intensities of *upd* reporter (*upd>myrtom* Std food: 16.68 ± 3.22 and NAC: 9.01 ± 3.41, S.D.) and STAT92E reporter (*10xSTAT92E-GFP* Std food: 18.24 ± 2.73 and NAC: 8.63 ± 4.07, S.D.) after standard or NAC-supplemented food. White wedges indicate zone of injury. (F, G) Upd (anti-Upd) is mainly expressed in living cells and not in dead cells after *ptc>rpr* or *sal>rpr*. (H) Upd expression declines after NAC intake. TP-3: TP-PRO-3 nuclei staining. (I) Mean pixel intensities of Upd stained *ptc>rpr* discs with or without NAC feeding (150.29 ± 7.11 and 96.69 ± 18.97, S.D.). (J) Inhibition of the JAK/STAT signaling within $dome^{DN}$ impairs wing regeneration. Genetic design (J) using double transactivator system (as in Fig 2) to induce death (blue) and activate $dome^{DN}$ (red). (K) Percentage of regenerated wings for controls (*rpr* or $dome^{DN}$ expression only) and experimental (*rpr* and $dome^{DN}$ dual expression). Note that $dome^{DN}$ wings were not able to regenerate (*rpr* and $dome^{DN}$ dual

expression), whereas *dome*^{DN} wings in the absence of cell death are normal. Examples of wings (left) of controls and experimental. (L) Experimental design for testing the rescue of NAC effects by ectopic activation of *upd*. (M) NAC effect on repair ability was rescued by *upd* overexpression. Quantification of the percentage of wings that regenerate after NAC feeding for the indicated genotypes. (N) Examples of wings from NAC-feeding with *rpr*-ablation defects (upper) and with rescue after *rpr*-ablation and *upd* activation (lower). *P<0.05 **P<0.01.

doi:10.1371/journal.pgen.1005595.g007

We next analyzed if JAK/STAT signaling requires ROS in this context. Two different reporters (*10XSTAT92E-GFP* and *upd-Gal4 UAS-myrtomato*) were used in physically injured discs and showed reduced expression after NAC feeding (Fig 7E). In addition, *ptc>rpr* induced discs from NAC fed larvae showed a reduction of *upd* expression (Fig 7H and 7I). Thus, this expression is ROS dependent after both physical injury and cell death. We speculated that if ROS operate upstream *upd*, the impairment of regeneration resulting from NAC feeding should be rescued by activating Upd. To this aim, we used the double transactivation system to induce cell death in NAC-fed individuals and concomitantly activate *upd* expression (Fig 7L). Analysis of the resulting wings showed that *upd* ectopic expression rescued the NAC inhibition phenotype (Fig 7M and 7N). These observations demonstrate that ROS function upstream of JAK/STAT during repair.

We wondered whether p38 is also required for *upd* expression in damaged discs. Expression of *upd* or *upd3* was severely reduced in *p38a*$^{1-/-}$ wound edges (Figs 8A–8C and S8). This suggests that in addition to JNK, p38 is essential for *upd* expression upon stress. Finally, we argued that if p38 is required for repair through *upd*, its ectopic expression should rescue the impaired regeneration after inhibition of p38. We, again, used the double transactivation system to induce cell death in SB202190-fed individuals, to block p38 phosphorylation and alongside activate *upd* expression (Fig 8D). Indeed, we found that the number of wings that regenerated after p38 inhibition increased (Fig 8E and 8F). Altogether these results position Upd cytokines downstream from the ROS/p38/JNK module.

Discussion

In this work, we demonstrate a stress-responsive module activated upon cell death or physical damage. This module consists of ROS dependent stimulation of non-deleterious levels of JNK and p38 MAP kinases necessary for the expression of Upd and JAK/STAT signaling which drives regeneration. Non-lethal levels of JNK may have multiple functions, among them cytoskeleton organization [44,54], healing and initiation of regenerative growth [21,23–26,51,55,56]. Thus, this early responsive module is crucial to maintain tissue in a healthy condition, trigger tissue repair and restore homeostasis.

In an apoptotic context, Rpr dimerizes and, through direct binding, brings the *Drosophila* inhibitor of apoptosis protein-1 (DIAP1) to mitochondria, concomitantly promoting DIAP1 auto-ubiquitination and destruction [57,58]. Rpr action on the mitochondria results in alteration of cytochrome C driven by caspases [59] and in mitochondrial disruption [60]. The ROS dyes used here detect a wide range of ROS, and therefore we cannot discriminate between membrane oxidases or mitochondrial origin. However, since Rpr acts on mitochondria, mitochondrial alterations could cause the burst of ROS in apoptotic cells. Of note, we observed that high ROS levels are associated with high levels of JNK in apoptotic cells. It has been proposed that ROS can mediate the activation of JNK [61] by quenching the MAP kinase phosphatases [62]. Conversely, low levels of ROS detected in nearby surviving tissue correlate with low non-deleterious levels of JNK and activation of MAP kinase phosphatases. Thus, *puc* MAP kinase phosphatase could protect the living cells close to the damage from the noxious effects of high JNK. Indeed, living cells near the wound retain low levels of JNK, not sufficient to kill but necessary for tissue recovery.

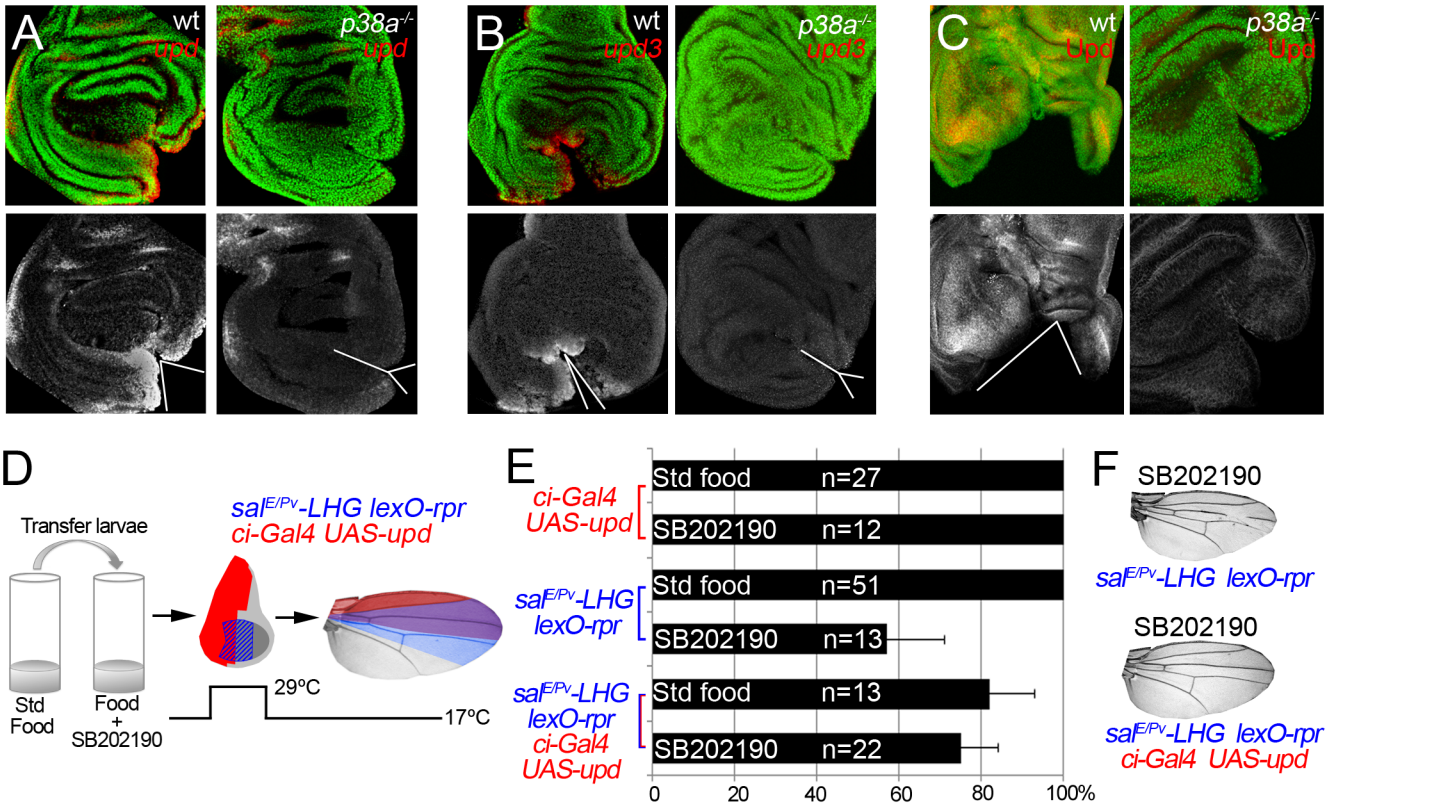

Fig 8. p38 controls *upd* expression. (A) In situ hybridization of *upd* in wild type (wt) and $p38a^{1-/-}$ cut discs. (B) In situ hybridization of *upd3* in wild type (wt) and $p38a^{1-/-}$ cut discs. (C) Immunostaining with anti-Upd in wild type (wt) and $p38a^{1-/-}$ cut discs. White lines and wedges indicate the position of the cut (D) Experimental design for testing the rescue of SB202190 effects by ectopic activation of *upd*. (E) SB202190 effect on repair ability was rescued by *upd* overexpression. Quantification of the percentage of wings that regenerate after SB202190 feeding for the indicated genotypes. (F) Examples of wings from SB202190-feeding with *rpr*-ablation defects (upper) and with rescue after *rpr*-ablation and *upd* activation (lower).

doi:10.1371/journal.pgen.1005595.g008

Additionally, the caspase Dronc, which acts downstream from Rpr, has functions beyond apoptosis [63]. Dronc is involved in the activation of JNK and p53, which activate the pro-apoptotic genes, creating an amplification loop that ensures apoptosis [27,29–31,64]. The JNK/p53 driven apoptosis stimulates proliferation of the nearby tissues [29–31,65]. Although still unclear, it has been proposed that apoptotic cells can release the products of mitogenic genes such as *wingless* (*wg*) and *decapentaplegic* (*dpp*) [33,66,67][31,68]. Alternatively, we show here that ROS operate as signals responding to insults (apoptosis, mechanical stress) that turn on the homeostatic machinery to compensate the epithelial damage. This fits with a scenario in which ROS are able to either diffuse from cell to cell or perhaps to propagate their production to several rows of cells. Indeed, ROS have been proven to cross cell membranes, to spread through gap junctions [69–71] and to enter into the cell through specific membrane aquaporin channels [71,72]. Therefore, ROS behave as an efficient paracrine signal that ultimately will result in Upd activation.

In addition to JNK, ROS are stressors involved in p38 activation [73]. ROS may activate the p38 pathway through the oxidative modification of intracellular kinases such as redox-sensitive activating protein-1 ASK1 [74]. We showed here that not only JNK but also p38 is required for regeneration. Moreover, the $p38a^{1}$ allele seems to particularly affect *upd* expression and regeneration. This concurs with the finding that *Drosophila* p38a is more susceptible to environmental stressors, such as oxidative stress [18]. However, other p38 kinases could contribute to

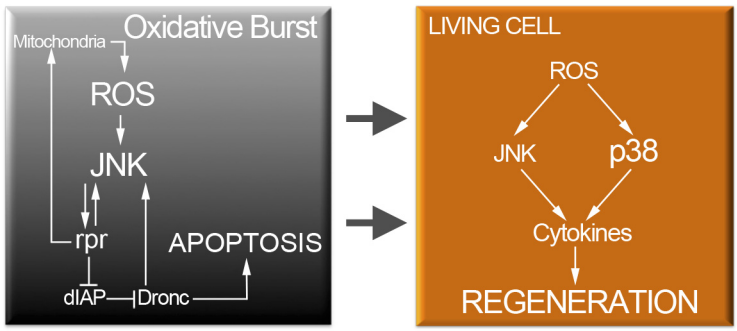

Fig 9. Cell protection module activated by injury or cell death. Oxidative stress in dying cells is likely of mitochondrial origin and results in highly toxic JNK. However, low levels of ROS propagate to adjacent surviving cells (arrows). Non-deleterious ROS will activate moderate levels of JNK and p38 only in surviving cells. P38 and JNK are required for cytokine activation and tissue repair.

doi:10.1371/journal.pgen.1005595.g009

tissue regeneration. Indeed, heterozygous alleles of the p38 activating kinase *lic*, which normally do not show patterning defects after *rpr*-mediated ablation, can result in incomplete regeneration when a dose of *p38b* is missing (Fig 5A). Moreover, RNAi of *p38b* also can show defective regeneration individuals (S2 Fig). In addition, we cannot discard that *p38c*, which has been recently found involved in intestinal immune homeostasis [75], may also function in imaginal disc regeneration.

We have found that both hep^{r75} and $p38a^{1}$ inhibit *upd* expression. But hep^{r75} mutants, which block JNK signaling, do not affect p38 phosphorylation and viceversa, $p38a^{1}$ mutants, which block at least the p38a branch of the p38 kinase, do not interfere with the *TRE-red* reporter expression. This suggests that ROS activate p38 and JNK independently and that both MAP kinases act on *upd* expression to drive tissue repair. Thus, ROS signaling operates through these two MAP kinase pathways that in turn will converge to stimulate the transcriptional expression of the cytokines (Fig 9).

JNK and p38 are not only activated after cell death but also after physical injury. Beneficial ROS production is an ubiquitous reaction associated with inflammatory responses to wounding [4,6,76]. Recent findings show that ROS produced in dynamic epithelia operate as a tuning mechanism for reorganization of epithelia [77]. Therefore, it could be that changes in mechanical stress generated during wounding and epithelial disruption (mechanical stretching) results in ROS production. Some dead cells were also found after physical injury. Thus, a partial contribution of dead cells in addition to the stress due to epithelial disruption can account for the oxidative burst generated after physical injury.

In summary, an early boost of oxidative stress is required to activate p38 and JNK in apoptotic cells or near the wound. Moreover, *upd* is turned on downstream JNK and p38. Thus, downstream of the stress response module, cytokines operate to control tissue growth during regeneration.

Materials and Methods

Drosophila strains

The *Drosophila melanogaster* strains used were *ptc-Gal4* [78], $tubGal80^{TS}$ [79], *UAS-rpr* [80], *ci-Gal4* [81], *nub-Gal4* [82] *sal-Gal4* and $sal^{E/Pv}$-*Gal4* [83], $p38b^{d27}$, lic^{d13} [47], $dATF2^{PB}$ [49], $p38a^{1}$, [17], *LexO-rCD2::GFP* [43], *TRE-DsRed.T4* [45] as *AP1* reporter, *puc-lacZ* [44], $puc^{E69\text{-}A}$-*Gal4* [84], *UAS-upd* [85], *upd-Gal4* (from D. Harrison), *10XSTAT92E-GFP* [86], *en-Gal4*, *UAS-GFP*, *UAS-myrtomato*, *UAS-Sod.A* (*sod1*), *UAS-Cat.A*, $UAS\text{-}dome^{DN}$, *hop2*, hop^{27},

stat92e^{06346} (Bloomington Stock center), *stat92e*^{397} [87], and *hep*^{r75} [88]. Transgenic *Drosophila shRNAi* lines were obtained from the Vienna Drosophila RNAi Center (VDRC). Canton S was used as the wild type control.

Imaginal disc culture and physical injury

Wing discs were dissected from third instar larvae in Schneider's insect medium (Sigma-Aldrich) and a small fragment was removed with tungsten needles. Discs were cultured in Schneider's insect medium supplemented with 2% heat activated fetal calf serum, 2.5% fly extract and 5 μg/ml insulin, for different periods of time (from 1 to 10 hours) at 25°C. Ex vivo images were taken using a Leica SPE confocal microscope and processed with Fiji software.

Generation of LexA/lexO strains for genetic ablation

The *sal*$^{E/Pv}$*-LHG* construct was created cutting the wing specific enhancer of *spalt*, *sal*$^{E/Pv}$ [83] from *pC4LacZ-Spalt PE* EcoRI/BamHI and cloning this fragment into the plasmid *attB-LHG* containing a *Gal80*-suppressible form of *LexA* transcriptional activator (*LHG*) [43]. *LHG* contains both the binding domain of *LexA* and the activator domain of *Gal4*, which is recognized by the inhibitor *Gal80*^{TS}.The *LexO-rpr* strain was obtained subcloning the pro-apoptotic gene *reaper* (*rpr*) from *pOT2-rpr* (IP02529) EcoRI/XhoI in the *pLOTattB* plasmid [89] carrying the *lexA* operator *LexO*. Transgenic flies were performed with standard protocols.

Genetic ablation and dual Gal4/LexA transactivator system

Cell death was genetically induced as previously described [23,90]. We used two different drivers to induce cell death. The first, *ptc-Gal4* which is expressed in a narrow stripe in the center of the disc. This strain was used to induce cell death in imaginal discs (*UAS-rpr*), because the dead domain can be easily discerned from the neighboring living domain. The second, *sal*$^{E/Pv}$*-Gal4* strain, which consists of *sal* wing enhancer with expression confined to the wing [83] has been used in this work to score adult wing parameters.

The UAS line used to promote cell death was *UAS-rpr*, and the system was controlled by the thermo sensitive repressor *tubGal80*^{TS}. We also used the *sal*$^{E/Pv}$*-LHG* and *LexO-rpr* strains for genetic ablation using the same design as for *Gal4/UAS*.

Embryos were kept at 17°C until the 8th day/192 h after egg laying (equivalent to 96 hours at 25°C) to prevent *rpr* expression. They were subsequently moved to 29°C for 11 hours and then back to 17°C until adulthood. Controls without *rpr* expression were always treated in parallel.

In dual transactivation experiments, we used the *sal*$^{E/Pv}$*-LHG LexO-rpr* to ablate the *sal*$^{E/Pv}$ domain, whereas *Gal4* was used to express different transgenes under the control of *nub-Gal4* or *ci-Gal4*.

In the experiments on antioxidants (Fig 2) and *upd* (Figs 7 and 8) overexpression, larvae were transferred to NAC- (100 μg/ml) or SB202190- (5 μM) supplemented food 24 h before cell death induction.

ROS detection ex vivo

All experiments for ROS detection were done in living conditions. To detect the presence of ROS we used CellROX Green Reagent (Life Technologies), which is an indicator of oxidative stress in living cells. For both genetic ablation and physical injury experiments, third instar discs were dissected in Schneider´s medium immediately after cell death or injury and incubated for 15 minutes in medium containing 5 μM CellROX Green Reagent, followed by three

washes. Samples were protected from light throughout. Then they were mounted using culture medium supplemented with 1 μM TO-PRO-3 (Life Technologies) nucleic acid stain. As TO-PRO-3 only enters dead cells, we used it to distinguish dead cells from living cells in the ex vivo experiments. Images were taken using a Leica SPE and SPII confocal microscope. Grey values of regions of interest (ROI) were measured using Fiji software. ROIs were established at the wound edges of injured discs (examples in S2 Fig), or in rectangles as indicated in Fig 1E. Pixel intensities were collected and analyzed from raw images taken under the same laser confocal conditions. Thermal LUT images were rendered from slices taken from the confocal using the Interactive 3D Surface Plot tool of the Fiji software (ImageJ). We also used the cell-permeant 2',7'-dichlorodihydrofluorescein diacetate (H2DCFDA 5μM, Life Technologies) which upon oxidation is converted to the highly fluorescent 2',7'-dichlorofluorescein (DCF).

To visualize the ROS images in Fig 1 after genetic ablation, the whole stacks were subject to the Enhance Contrast tool at 0.4 pixel saturation in whole stack normalization. For physical injury images, thermal LUT images were obtained from raw stacks.

ROS scavenging

To prevent ROS production, we used two protocols. The first was mainly used for *rpr*-ablation discs. It consisted in that antioxidants were supplemented into standard fly food. As antioxidants we used vitamin C (250 μg/ml), Trolox (an analog of vitamin E; 20 μg/ml) and N-acetyl cysteine (NAC) (100 μg/ml), all from Sigma-Aldrich. To score adult wings, larvae were transferred from vials containing standard food to vials containing food with the desired antioxidant concentration. Antioxidant treatment was administered at 168 h of development at 17°C (equivalent to 84 h AEL at 25°C). After 24 hours, experimental larvae were moved to 29°C for 11 hours to promote *rpr* apoptosis. Meanwhile one control consisted of larvae maintained at 17°C and another control consisted of larvae transferred to a vial with standard food and moved to 29°C for the same period as in the experimental group. After *rpr* induction temperature was returned to 17°C to allow tissue recovery. This protocol was applied for Figs 2A–2D, 3D, 3E, 4E, 4F and 7E.

The second was used for ex vivo cultured discs. Wing imaginal discs were incubated for 30 minutes in Schneider's insect medium supplemented with NAC 100 μg/ml. Then, they were transferred to Schneider's containing CellROX Green (S2 Fig). NAC incubated discs were used for monitoring *TRE-red* (Fig 3F and 3G) or for P-p38 antibody staining (Fig 4B and 4C). In S2 Fig medium was supplemented with NAC, Trolox or Vit C.

Chemical inhibition of p38 and JNK pathway

The imidazole drug SB202190 (Sigma-Aldrich) was added to standard fly food to prevent p38 activation. We used three different concentrations (0.12 μM, 1 μM and 5 μM), and DMSO as the control. To inhibit chemically JNK we used the JNK Inhibitor IX (5 μM, Selleckchem) which is a thienylnaphthamide compound that is a selective and potent inhibitor of the ATP binding site of JNK. The timing and protocol followed to inhibit both pathways was the same as that to scavenge ROS.

Oxidative stress induction

Third instar larvae were transferred to vials containing 1% H_2O_2, 1,3% low melting agarose and 5% sucrose. To avoid loss of oxidative capacity, H_2O_2 was added at a temperature under 45°C. Larvae were fed for 2h in this medium prior dissection and fixation of the discs. Controls without H_2O_2 were done in parallel.

Test for regenerated adult wings and statistics

For testing the capacity to regenerate we used adult wings emerged from $sal^{E/Pv}$>*rpr* individuals, in which patterning defects can be easily scored. Flies were fixed in glycerol:ethanol (1:2) for 24 h. Wings were dissected on water and then washed with ethanol. Then they were mounted on 6:5 lactic acid:ethanol and analyzed and imaged under a microscope.

Definition of regenerated/non-regenerated wings: when veins or interveins were missing, we considered them as defective in their capacity to restore the normal pattern. Therefore, the % of regenerated wings (Figs 2, 5, 7, 8, S2, S3, S5 and S7) was calculated after the number of wings with the complete set of veins and interveins. For each sample of "regenerated wings" we scored the percentage of individuals that belong to the "regenerated wings" class and calculated the standard error of sample proportion based on binomial distribution (regenerate complete wing or not) SE = $\sqrt{p}$ (1-p)/n, where p is the proportion of successes in the population.

Ratios between wing areas (Fig 5) were used as an indication of the size achieved after cell death for each genetic background, and consisted of a comparison between wing size with and without *rpr* induction.

Immunochemistry and fluorescence in situ hybridization (FISH)

Immunostaining and FISH were performed using standard protocols. Primary antibodies used in this work were P-p38 (rabbit 1:50, Cell Signaling Technology), phospho-Histone-H3 (rabbit 1:1000, Millipore), ß-galactosidase (rabbit 1:1000, ICN Biomedicals), Upd (rabbit 1:800, gift from D. Harrison) and cleaved caspase-3 (rabbit 1:100, Cappel).

Fluorescently labeled secondary antibodies were from Life Technologies and Jackson Immunochemicals. Discs were mounted in SlowFade (Life Technologies) supplemented with 1 μM TO-PRO-3 (Life Technologies) to label nuclei. Note that in fixed tissues all nuclei are TO-PRO-3 labeled, whereas in ex-vivo culture only nuclei of dead or dying cells are TO-PRO-3 labeled.

The number of mitosis after analyzing the stacks of confocal images was calculated using Fiji software (Cell counter plug-in). Mitosis were counted for the entire anterior compartment of the wing pouch for each disc.

For apoptotic cell detection, we used both anti cleaved caspase 3 or TUNEL assay. For TUNEL we used the fluorescently labeled dUTP ChromaTide BODIPY FL-14-dUTP (Life Technologies) and incorporated using terminal deoxynucleotidyl transferase (Roche).

EdU was incorporated using the Click-iT EdU Imaging Kit (Life Technologies). Wing discs were dissected after cell death induction and incubated in Schneider's insect medium supplemented with 1 mg/ml EdU for 5 minutes. Following EdU incorporation, discs were fixed and immunostained.

Riboprobes for *upd and upd3* were synthesized using cDNA clones from DGRC AT1366 and FI03911.

Genotypes

Fig 1

A, B. Wild type

D, E, F. *ptc>rpr: UAS-rpr/+; ptc-Gal4/+; $tubGal80^{TS}$/+*

Fig 2

A, B, C. *$sal^{E/Pv}$>rpr: UAS-rpr/+; $sal^{E/Pv}$-Gal4/+; $tubGal80^{TS}$/+*

D. *ptc>rpr: UAS-rpr/+; ptc-Gal4:$tubGal80^{TS}$/+*

E, F, G. *$sal^{E/Pv}$>rpr nub>GFP: w; nub-Gal4/UAS-GFP; $sal^{E/Pv}$-LHG:$tubGal80^{TS}$/lexO-rpr*

$sal^{E/Pv}$>rpr nub>Cat: w; nub-Gal4/UAS-Cat; $sal^{E/Pv}$-LHG:$tubGal80^{TS}$/lexO-rpr

$sal^{E/Pv}$>rpr nub>Sod: w; nub-Gal4/UAS-Sod; $sal^{E/Pv}$-LHG:$tubGal80^{TS}$/lexO-rpr

$sal^{E/Pv}$>rpr nub>Sod:Cat: w; nub-Gal4/UAS-Sod:Cat; $sal^{E/Pv}$-LHG:tubGal80^{TS}/lexO-rpr

Fig 3

A, B. *ptc>rpr: UAS-rpr/+; ptc-Gal4:tubGal80^{TS}/TRE-DsRed.T4; puc-LacZ/+*

C. *ptc>rpr: UAS-rpr/+; ptc-Gal4:tubGal80^{TS}/+; puc-LacZ/+*

D, E. *ptc>rpr: UAS-rpr/+; ptc-Gal4:tubGal80^{TS}/TRE-DsRed.T4*

F, G. *w; TRE-DsRed.T4*

Fig 4

A, B, C. Wild type.

D, E, F. *ptc>rpr: UAS-rpr/+; ptc-Gal4/+; tubGal80^{TS}/+*

G. *w; ci-Gal4/UAS-Sod:Cat; $sal^{E/Pv}$-LHG:tubGal80^{TS}/lexO-rpr*

Fig 5

A. Control: *w; +; $sal^{E/Pv}$-LHG:tubGal80^{TS}/lexO-rpr* (control for *lexO-rpr* on the third chromosome) and *w; lexO-rpr/+; $sal^{E/Pv}$-LHG:tubGal80^{TS}/+* (control for *lexO-rpr* on the second chromosome)

$lic^{d13/+}$: lic^{d13}/+; +; $sal^{E/Pv}$-LHG:tubGal80^{TS}/lexO-rpr

$p38b^{d27/+}$: w; $p38b^{d27}$/+; $sal^{E/Pv}$-LHG:tubGal80^{TS}/lexO-rpr

$p38a^{1/+}$: w; lexO-rpr/+; $p38a^{1}$/sal^{EPv}-LHG:tubGal80^{TS}

$lic^{d13/+}p38b^{d27/+}$: lic^{d13}/+; $p38b^{d27}$/+; sal^{EPv}-LHG:tubGal80^{TS}/lexO-rpr

$dATF2^{PB/+}$: w; $Atf2^{PB}$/+; $sal^{E/Pv}$-LHG:tubGal80^{TS}/lexO-rpr

$dATF2^{PB-/-}$: w; $Atf2^{PB}$/$Atf2^{PB}$; $sal^{E/Pv}$-LHG:tubGal80^{TS}/lexO-rpr

$lic^{d13/+}$ $dATF2^{PB/+}$: lic^{d13}/+; $Atf2^{PB}$/+; $sal^{E/Pv}$-LHG:tubGal80^{TS}/lexO-rpr

$p38b^{d27/+}$ $dATF2^{PB/+}$: w; $p38b^{d27}$/$Atf2^{PB}$; $sal^{E/Pv}$-LHG:tubGal80^{TS}/lexO-rpr

$dATF2^{PB/+}p38a^{1/+}$: w; $Atf2^{PB}$/lexO-rpr; $p38a^{1}$/sal^{EPv}-LHG:tubGal80^{TS}

B. *$sal^{E/Pv}$>rpr: UAS-rpr/+; $sal^{E/Pv}$-Gal4/+; tubGal80^{TS}/+*

Fig 6

A. *hep^{r75}: hep^{r75}/Y*

B. *ptc>rpr hep^{r75}: hep^{r75}/Y; ptc-Gal4:tubGal80^{TS}/+; UAS-rpr/+*

C. wt: *w; TRE-DsRed.T4*

$p38a^{-/-}$: w; TRE-DsRed.T4; $p38a^{1}$/$p38a^{1}$

Fig 7

A, B. Wild type.

C, D. *hep^{r75}: hep^{r75}/Y*

E. *upd-Gal4/+; UAS-myrtomato/10XSTAT92E-GFP*

F, G, H, I. *ptc>rpr: UAS-rpr/+; ptc-Gal4/+; tubGal80^{TS}/+*

$sal^{E/Pv}$>rpr: UAS-rpr/+; sal-Gal4/+; tubGal80^{TS}/+

J, K. *$sal^{E/Pv}$>rpr ci>GFP: w; ci-Gal4/lexO-rpr; $sal^{E/Pv}$-LHG:tubGal80^{TS}/UAS-GFP*

ci>$dome^{DN}$ $sal^{E/Pv}$>GFP: w; ci-Gal4/lexO-rCD2::GFP; $sal^{E/Pv}$-LHG:tubGal80^{TS}/UAS-$dome^{DN}$

$sal^{E/Pv}$>rpr ci> $dome^{DN}$: w; ci-Gal4/lexO-rpr; $sal^{E/Pv}$-LHG:tubGal80^{TS}/UAS-$dome^{DN}$

L, M, N. *ci-Gal4 UAS-upd: w; ci-Gal4/UAS-upd; $sal^{E/Pv}$-LHG:tubGal80^{TS}/lexO-rCD2::GFP*

$sal^{E/Pv}$-LHG lexO-rpr: w; ci-Gal4/UAS-GFP; $sal^{E/Pv}$-LHG:tubGal80^{TS}/lexO-rpr

ci-Gal4 UAS-upd $sal^{E/Pv}$-LHG lexO-rpr: w; ci-Gal4/UAS-upd; $sal^{E/Pv}$-LHG:tubGal80^{TS}/lexO-rpr

Fig 8

A, B, C. Wild type.

$p38a^{-/-}$: w; +; $p38a^{1}$/$p38a^{1}$

D, E, F. *ci-Gal4 UAS-upd: w; ci-Gal4/UAS-upd; $sal^{E/Pv}$-LHG:tubGal80^{TS}/lexO-rCD2::GFP*

$sal^{E/Pv}$-LHG lexO-rpr: w; ci-Gal4/UAS-GFP; $sal^{E/Pv}$-LHG:tubGal80^{TS}/lexO-rpr

ci-Gal4 UAS-upd $sal^{E/Pv}$-LHG lexO-rpr: w; ci-Gal4/UAS-upd; $sal^{E/Pv}$-LHG:$tubGal80^{TS}$/lexO-rpr

S1 Fig

A, C, D. Wild type.

B. *ptc>rpr: UAS-rpr/+; ptc-Gal4:$tubGal80^{TS}$/+*

S2 Fig

A. wt

B. *$sal^{E/Pv}$>rpr: UAS-rpr/+; $sal^{E/Pv}$-Gal4/+; $tubGal80^{TS}$/+*

C. *$sal^{E/Pv}$>rpr nub>GFP: w; nub-Gal4/UAS-GFP; $sal^{E/Pv}$-LHG:$tubGal80^{TS}$/lexO-rpr*

$sal^{E/Pv}$>rpr nub>Cat: w; nub-Gal4/UAS-Cat; $sal^{E/Pv}$-LHG:$tubGal80^{TS}$/lexO-rpr

$sal^{E/Pv}$>rpr nub>Sod: w; nub-Gal4/UAS-Sod; $sal^{E/Pv}$-LHG:$tubGal80^{TS}$/lexO-rpr

$sal^{E/Pv}$>rpr nub>Sod:Cat: w; nub-Gal4/UAS-Sod:Cat; $sal^{E/Pv}$-LHG:$tubGal80^{TS}$/lexO-rpr

D. *$sal^{E/Pv}$>rpr nub>GFP: w; nub-Gal4/UAS-GFP; $sal^{E/Pv}$-LHG:$tubGal80^{TS}$/lexO-rpr*

$sal^{E/Pv}$>rpr nub>Cat: w; nub-Gal4/UAS-Cat; $sal^{E/Pv}$-LHG:$tubGal80^{TS}$/lexO-rpr

nub>Cat: w; nub-Gal4/UAS-Cat; $sal^{E/Pv}$-LHG:$tubGal80^{TS}$/lexO-GFP

$sal^{E/Pv}$>rpr nub>Sod: w; nub-Gal4/UAS-Sod; $sal^{E/Pv}$-LHG:$tubGal80^{TS}$/lexO-rpr

nub>Sod: w; nub-Gal4/UAS-Sod; $sal^{E/Pv}$-LHG:$tubGal80^{TS}$/lexO-GFP

$sal^{E/Pv}$>rpr nub>Sod:Cat: w; nub-Gal4/UAS-Sod:Cat; $sal^{E/Pv}$-LHG:$tubGal80^{TS}$/lexO-rpr

nub>Sod:Cat: w; nub-Gal4/UAS-Sod:Cat; $sal^{E/Pv}$-LHG:$tubGal80^{TS}$/lexO-GFP

S3 Fig

A. Wild type.

B. *w; TRE-DsRed.T4/+; puc-Gal4:UAS-GFP/+*

C. *ptc>rpr: UAS-rpr/+; ptc-Gal4:$tubGal80^{TS}$/TRE-DsRed.T4*

D. *$sal^{E/Pv}$>rpr: UAS-rpr/+; $sal^{E/Pv}$-Gal4/+; $tubGal80^{TS}$/+*

S4 Fig

Wild type

S5 Fig

A. *$sal^{E/Pv}$>rpr: w; ci-Gal4/UAS-GFP; $sal^{E/Pv}$-LHG:$tubGal80^{TS}$/lexO-rpr*

ci>RNAi p38a: w; ci-Gal4/UAS-RNAi p38a; $sal^{E/Pv}$-LHG:$tubGal80^{TS}$/lexO-GFP

$sal^{E/Pv}$>rpr ci>RNAi p38a: w; ci-Gal4/UAS-RNAi p38a; $sal^{E/Pv}$-LHG:$tubGal80^{TS}$/lexO-rpr

ci>RNAi p38b: w; ci-Gal4/UAS-RNAi p38b; $sal^{E/Pv}$-LHG:$tubGal80^{TS}$/lexO-GFP

$sal^{E/Pv}$>rpr ci>RNAi p38b: w; ci-Gal4/UAS-RNAi p38b; $sal^{E/Pv}$-LHG:$tubGal80^{TS}$/lexO-rpr

ci>RNAi Atf2: w; ci-Gal4/UAS-RNAi Atf2; $sal^{E/Pv}$-LHG:$tubGal80^{TS}$/lexO-GFP

$sal^{E/Pv}$>rpr ci>RNAi Atf2: w; ci-Gal4/UAS-RNAi Atf2; $sal^{E/Pv}$-LHG:$tubGal80^{TS}$/lexO-rpr

ci>RNAi lic: w; ci-Gal4/UAS-RNAi lic; $sal^{E/Pv}$-LHG:$tubGal80^{TS}$/lexO-GFP

$sal^{E/Pv}$>rpr ci>RNAi lic: w; ci-Gal4/UAS-RNAi lic; $sal^{E/Pv}$-LHG:$tubGal80^{TS}$/lexO-rpr

B. *$sal^{E/Pv}$>rpr: UAS-rpr/+; $sal^{E/Pv}$-Gal4/+; $tubGal80^{TS}$/+*

C. *$sal^{E/Pv}$>rpr: UAS-rpr/+; $sal^{E/Pv}$-Gal4/+; $tubGal80^{TS}$/+*

ptc>rpr: UAS-rpr/+; ptc-Gal4:$tubGal80^{TS}$/TRE-DsRed.T4

S6 Fig

en>RNAi lic: w; en-Gal4:UAS-GFP/UAS-RNAi lic

S7 Fig

Control: *UAS-rpr/+; $sal^{E/Pv}$-Gal4/+; $tubGal80^{TS}$/+*

$hop^{2/+}$: UAS-rpr/hop^{2}; $sal^{E/Pv}$-Gal4/+; $tubGal80^{TS}$/+

$hop^{27/+}$: UAS-rpr/hop^{27}; $sal^{E/Pv}$-Gal4/+; $tubGal80^{TS}$/+

$stat92e^{397/+}$: UAS-rpr/+; $sal^{E/Pv}$-Gal4/+; $tubGal80^{TS}$/$stat92e^{397}$

$stat92e^{06346/+}$: UAS-rpr/+; $sal^{E/Pv}$-Gal4/+; $tubGal80^{TS}$/$stat92e^{06346}$

S8 Fig

Wild type.
p38a$^{-/-}$: w; +; p38a^{1}/p38a^{1}

Supporting Information

S1 Fig. Additional data on ROS activation after damage. (A) Propagation of ROS labeled with CellROX Green towards the adjacent tissue during the first 15' after injury. Thermal scale corresponds to the same as in Fig 1B. White line indicates cut edge. (B) ROS detected with H2DCFDA after *ptc>rpr*. ROS are found in dead cells and in adjacent living cells. TP-3: TO-PRO-3. (C, D) ROS detected with H2DCFDA after physical injury (white wedge).
(TIF)

S2 Fig. Additional controls for Fig 2. (A) Ex vivo analysis of cut imaginal discs cultured in Schneider's medium, incubated with NAC, Trolox or VitC. Top row shows images of control discs (no antioxidant). Lower row shows images of discs incubated with the indicated antioxidant. Dotted lines indicate zones used as ROI for pixel intensity measurements (below). White wedges indicate the position of the cut. $^{*}P<0.05$ $^{**}P<0.01$. (B) Examples of control wings kept at 17°C (*sal^{EPv}>rpr OFF*) that grew in food supplemented with antioxidant. All cases, showed normal set of interveins and veins. (C) Examples of control wings kept at 17°C (*sal^{EPv}>rpr OFF*) that grew from the indicated genotypes. (D) Controls for transgenes of Fig 2F. Activation of transgenes (*nub>Cat; nub>Sod; nub>Sod:Cat*) in the absence of cell death results in normal wings.
(TIF)

S3 Fig. Test of JNK reporters and additional data for Fig 3. (A) Endogenous expression of the *TRE-red* and *puc-lacZ* reporters. Note that both reporters are expressed only at the tip of the notum (n: notum; wp: wing pouch). (B) *TRE-red* and *puc>GFP* expression after physical injury. Note that *TRE-red* expression is activated earlier and more extensive than *puc>GFP*. White wedges indicate the position of the cut. Dotted line indicates the edges of the disc. (C) The JNK Inhibitor IX eliminates *TRE-red* activity and *upd* expression. Top row: *rpr*–ablated disc from larvae fed with standard food stained for nuclei (TP3: TO-PRO-3), *TRE-red* reporter, and anti-Upd. Bottom row: *rpr*–ablated disc from larvae supplemented with JNK Inhibitor IX. (D) JNK Inhibitor IX inhibits regeneration. Quantification of regenerated *sal^{EPv}>rpr* wings after feeding with standard food or JNK Inhibitor IX supplemented.
(TIF)

S4 Fig. Additional data for Fig 4. To test whether P-p38 is activated after an independent mechanism of oxidative stress in the absence of damage, larvae were fed with 1% H_2O_2 for 2 h before processed for imaging. (A) Live imaging showing high ROS in the entire disc. (B) Fixed disc stained with P-p38.
(TIF)

S5 Fig. Additional data for Fig 5. (A) Inhibition of p38 with RNAi constructs prevents tissue repair. Ectopic expression of p38 RNAis under the control of *ci-Gal4* and simultaneous cell death induction with *sal$^{E/Pv}$-LHG LexO-rpr* when shifted to 29°C for 11 h. Adult wing size was measured after ectopic expression of the indicated RNAi transgenes (red). The experiments with *rpr*-ablation are indicated in blue. (B) Examples of control wings of Fig 5B, in which no *rpr*-ablation was induced (kept at 17°C) for the indicated concentrations of the p38 inhibitor SB202190. (C) Test for the reliability of the SB202190. Discs were dissected from *rpr*-ablated larvae that were fed with 5 μM SB202190, fixed and imaged. SB202190 intake reduces P-p38 activation after cell death as measured from the Mean Pixel Intensity in comparison to DMSO

fed larvae. *TRE-red* in individuals fed with 5 μM SB202190 is active. Right: Mean Pixel Intensities for both experiments. For p38: control 48.77 ± 30.82 (S.D.); SB202190 10.52 ± 8.09 (S.D.). For *TRE-red*: control 136.46 ± 44.5 (S.D.); SB202190 93.5 ± 23.19 (S.D.). $^{***}P<0.001$ for the P-p38 and P = 0,15 n.s. for *TRE-red*.
(TIF)

S6 Fig. Additional data for Fig 6. (A) RNA interference of MKK *lic* inhibits p38 phosphorilation after injury. The *UAS-RNAi lic* was activated in the posterior compartment together with *UAS-GFP* (white). Two injuries were inflected with tungsten needles, one in the anterior and one in the posterior compartment. The cuts were performed in Schneider's medium, and fixation for immunostaining 20' after injury. P-p38 activation was localized in the anterior compartment and almost absent around the posterior cut. (B) Blocking JNK with JNK Inhibitor IX does not affect P-p38 after *rpr*-ablation. The domain of dead cells is outlined in white.
(TIF)

S7 Fig. Loss of JAK/STAT impedes repair after *rpr*-ablation. Percentages of regenerated wings for the indicated genetic background after $sal^{E/Pv}$>*rpr* ablation. Right wings: $sal^{E/Pv}$>rpr OFF column: wings of those genetic backgrounds without cell death (kept at 17°C). All wings raised in those conditions contain the normal set of veins and interveins. $sal^{E/Pv}$>*rpr* ON column: top (wt) is an example of fully regenerated wing. The rest of wings are examples of non-regenerated or incomplete regeneration in the heterozygous condition indicated.
(TIF)

S8 Fig. Additional data for Fig 8. Quantification of in situ hybridizations of *upd* mRNA (A) and *upd3* mRNA (B) and antibody localization for Upd (C). Regions of interest were determined around the wound edges (as in S2 Fig) of wild type discs (wt) and $p38a^{1-/-}$ mutants. Images in Fig 8A–8C are examples of the quantification shown here. $^{***}P<0.001$ $^{**}P<0.01$. Bars indicate standard deviation.
(TIF)

Acknowledgments

We thank R. Yagi and K. Basler for providing us with the vectors for the LexA/lexO system. We thank H. Stocker for stocks and discussion. We also thank H. Bellen, A. Nebreda, E. Vizcaya, M. Salicrú, M. Giralt and F. Villaroya, for discussion and suggestions. We also thank the Confocal Unit of the CCiT-UB and in particular M. Bosch. We are also grateful to N. Ferreira and E. Alcañiz for their help in the early stages of this work.

Author Contributions

Conceived and designed the experiments: FS MC PSR. Performed the experiments: PSR MLS ABC LP FS IMR. Analyzed the data: FS PSR MC. Contributed reagents/materials/analysis tools: PSR IMR MLS ABC LP MM MC FS. Wrote the paper: FS PSR MC.

References

1. Finkel T. Signal transduction by reactive oxygen species. J Cell Biol. 2011; 194: 7–15. doi: 10.1083/jcb.201102095 PMID: 21746850
2. Bigarella CL, Liang R, Ghaffari S. Stem cells and the impact of ROS signaling. Development. 2014; 141: 4206–4218. doi: 10.1242/dev.107086 PMID: 25371358
3. Moreira S, Stramer B, Evans I, Wood W, Martin P. Prioritization of competing damage and developmental signals by migrating macrophages in the Drosophila embryo. Curr Biol. 2010; 20: 464–70. doi: 10.1016/j.cub.2010.01.047 PMID: 20188558

4. Niethammer P, Grabher C, Look AT, Mitchison TJ. A tissue-scale gradient of hydrogen peroxide mediates rapid wound detection in zebrafish. Nature. 2009; 459: 996–9. doi: 10.1038/nature08119 PMID: 19494811
5. Gauron C, Rampon C, Bouzaffour M, Ipendey E, Teillon J, Volovitch M, et al. Sustained production of ROS triggers compensatory proliferation and is required for regeneration to proceed. Sci Rep. 2013; 3: 2084. doi: 10.1038/srep02084 PMID: 23803955
6. Love NR, Chen Y, Ishibashi S, Kritsiligkou P, Lea R, Koh Y, et al. Amputation-induced reactive oxygen species are required for successful Xenopus tadpole tail regeneration. Nat Cell Biol. 2013; 15: 222–8. doi: 10.1038/ncb2659 PMID: 23314862
7. Seyfried J, Wüllner U. Inhibition of thioredoxin reductase induces apoptosis in neuronal cell lines: role of glutathione and the MKK4/JNK pathway. Biochem Biophys Res Commun. 2007; 359: 759–64. PMID: 17559804
8. Shi Y, Nikulenkov F, Zawacka-Pankau J, Li H, Gabdoulline R, Xu J, et al. ROS-dependent activation of JNK converts p53 into an efficient inhibitor of oncogenes leading to robust apoptosis. Cell Death Differ. Macmillan Publishers Limited; 2014; 21: 612–23. doi: 10.1038/cdd.2013.186 PMID: 24413150
9. Droge W. Free Radicals in the Physiological Control of Cell Function. Physiol Rev. 2002; 82: 47–95. PMID: 11773609
10. McCubrey JA, Lahair MM, Franklin RA. Reactive oxygen species-induced activation of the MAP kinase signaling pathways. Antioxid Redox Signal. 2006; 8: 1775–89. PMID: 16987031
11. Jiang F, Zhang Y, Dusting GJ. NADPH oxidase-mediated redox signaling: roles in cellular stress response, stress tolerance, and tissue repair. Pharmacol Rev. 2011; 63: 218–42. doi: 10.1124/pr.110.002980 PMID: 21228261
12. Jia Y-T, Wei W, Ma B, Xu Y, Liu W-J, Wang Y, et al. Activation of p38 MAPK by reactive oxygen species is essential in a rat model of stress-induced gastric mucosal injury. J Immunol. American Association of Immunologists; 2007; 179: 7808–19.
13. Sato A, Okada M, Shibuya K, Watanabe E, Seino S, Narita Y, et al. Pivotal role for ROS activation of p38 MAPK in the control of differentiation and tumor-initiating capacity of glioma-initiating cells. Stem Cell Res. 2014; 12: 119–31. doi: 10.1016/j.scr.2013.09.012 PMID: 24185179
14. Kanaji N, Nelson A, Wang X, Sato T, Nakanishi M, Gunji Y, et al. Differential roles of JNK, ERK1/2, and p38 mitogen-activated protein kinases on endothelial cell tissue repair functions in response to tumor necrosis factor-α. J Vasc Res. 2013; 50: 145–56. doi: 10.1159/000345525 PMID: 23258237
15. Sharma G-D, He J, Bazan HEP. p38 and ERK1/2 coordinate cellular migration and proliferation in epithelial wound healing: evidence of cross-talk activation between MAP kinase cascades. J Biol Chem. 2003; 278: 21989–97. PMID: 12663671
16. Karkali K, Panayotou G. The Drosophila DUSP puckered is phosphorylated by JNK and p38 in response to arsenite-induced oxidative stress. Biochem Biophys Res Commun. 2012; 418: 301–6. doi: 10.1016/j.bbrc.2012.01.015 PMID: 22266315
17. Seisenbacher G, Hafen E, Stocker H. MK2-dependent p38b signalling protects Drosophila hindgut enterocytes against JNK-induced apoptosis under chronic stress. PLoS Genet. 2011; 7: e1002168. doi: 10.1371/journal.pgen.1002168 PMID: 21829386
18. Craig CR, Fink JL, Yagi Y, Ip YT, Cagan RL. A Drosophila p38 orthologue is required for environmental stress responses. EMBO Rep. 2004; 5: 1058–63. PMID: 15514678
19. Owusu-Ansah E, Banerjee U. Reactive oxygen species prime Drosophila haematopoietic progenitors for differentiation. Nature. 2009; 461: 537–41. doi: 10.1038/nature08313 PMID: 19727075
20. Ryoo HD, Gorenc T, Steller H. Apoptotic cells can induce compensatory cell proliferation through the JNK and the Wingless signaling pathways. Dev Cell. 2004; 7: 491–501. PMID: 15469838
21. Bosch M, Serras F, Martin-Blanco E, Baguna J. JNK signaling pathway required for wound healing in regenerating Drosophila wing imaginal discs. Dev Biol. 2005; 280: 73–86. PMID: 15766749
22. Bosch M, Baguna J, Serras F. Origin and proliferation of blastema cells during regeneration of Drosophila wing imaginal discs. Int J Dev Biol. 2008; 52: 1043–1050. doi: 10.1387/ijdb.082608mb PMID: 18956337
23. Bergantiños C, Corominas M, Serras F. Cell death-induced regeneration in wing imaginal discs requires JNK signalling. Development. 2010; 137: 1169–1179. doi: 10.1242/dev.045559 PMID: 20215351
24. Smith-Bolton RK, Worley MI, Kanda H, Hariharan IK. Regenerative growth in Drosophila imaginal discs is regulated by Wingless and Myc. Dev Cell. 2009; 16: 797–809. doi: 10.1016/j.devcel.2009.04.015 PMID: 19531351

25. Mattila J, Omelyanchuk L, Kyttala S, Turunen H, Nokkala S. Role of Jun N-terminal Kinase (JNK) signaling in the wound healing and regeneration of a Drosophila melanogaster wing imaginal disc. Int J Dev Biol. 2005; 49: 391–399. PMID: 15968584

26. Lee N, Maurange C, Ringrose L, Paro R. Suppression of Polycomb group proteins by JNK signalling induces transdetermination in Drosophila imaginal discs. Nature. 2005; 438: 234–237. PMID: 16281037

27. Fan Y, Wang S, Hernandez J, Yenigun VB, Hertlein G, Fogarty CE, et al. Genetic models of apoptosis-induced proliferation decipher activation of JNK and identify a requirement of EGFR signaling for tissue regenerative responses in Drosophila. PLoS Genet. Public Library of Science; 2014; 10: e1004131. doi: 10.1371/journal.pgen.1004131 PMID: 24497843

28. Pastor-Pareja JC, Wu M, Xu T. An innate immune response of blood cells to tumors and tissue damage in Drosophila. Dis Model Mech. 2008; 1: 144–154. doi: 10.1242/dmm.000950 PMID: 19048077

29. Shlevkov E, Morata G. A dp53/JNK-dependant feedback amplification loop is essential for the apoptotic response to stress in Drosophila. Cell Death Differ. 2012; 19: 451–60. doi: 10.1038/cdd.2011.113 PMID: 21886179

30. Kondo S, Senoo-Matsuda N, Hiromi Y, Miura M. DRONC coordinates cell death and compensatory proliferation. Mol Cell Biol. 2006; 26: 7258–7268. PMID: 16980627

31. Wells BS, Yoshida E, Johnston LA. Compensatory proliferation in Drosophila imaginal discs requires Dronc-dependent p53 activity. Curr Biol. 2006; 16: 1606–1615. PMID: 16920621

32. Perez-Garijo A, Martin FA, Morata G. Caspase inhibition during apoptosis causes abnormal signalling and developmental aberrations in Drosophila. Development. 2004; 131: 5591–5598. PMID: 15496444

33. Perez-Garijo A, Shlevkov E, Morata G. The role of Dpp and Wg in compensatory proliferation and in the formation of hyperplastic overgrowths caused by apoptotic cells in the Drosophila wing disc. Development. 2009; 136: 1169–1177. doi: 10.1242/dev.034017 PMID: 19244279

34. Wu M, Pastor-Pareja JC, Xu T. Interaction between Ras(V12) and scribbled clones induces tumour growth and invasion. Nature. 2010; 463: 545–548. doi: 10.1038/nature08702 PMID: 20072127

35. Álvarez-Fernández C, Tamirisa S, Prada F, Chernomoretz A, Podhajcer O, Blanco E, et al. Identification and functional analysis of healing regulators in Drosophila. PLoS Genet. 2015; 11: e1004965. doi: 10.1371/journal.pgen.1004965 PMID: 25647511

36. Jiang H, Patel PH, Kohlmaier A, Grenley MO, McEwen DG, Edgar BA. Cytokine/Jak/Stat signaling mediates regeneration and homeostasis in the Drosophila midgut. Cell. 2009; 137: 1343–55. doi: 10.1016/j.cell.2009.05.014 PMID: 19563763

37. Fuchs Y, Steller H. Programmed cell death in animal development and disease. Cell. 2011; 147: 742–58. doi: 10.1016/j.cell.2011.10.033 PMID: 22078876

38. King RS, Newmark PA. The cell biology of regeneration. J Cell Biol. 2012; 196: 553–62. doi: 10.1083/jcb.201105099 PMID: 22391035

39. Vriz S, Reiter S, Galliot B. Cell death: a program to regenerate. Curr Top Dev Biol. 2014; 108: 121–51. doi: 10.1016/B978-0-12-391498-9.00002-4 PMID: 24512708

40. Nishina T, Komazawa-Sakon S, Yanaka S, Piao X, Zheng D-M, Piao J-H, et al. Interleukin-11 links oxidative stress and compensatory proliferation. Sci Signal. 2012; 5: ra5. doi: 10.1126/scisignal.2002056 PMID: 22253262

41. Worley MI, Setiawan L, Hariharan IK. Regeneration and transdetermination in Drosophila imaginal discs. Annu Rev Genet. 2012; 46: 289–310. doi: 10.1146/annurev-genet-110711-155637 PMID: 22934642

42. Bergantiños C, Vilana X, Corominas M, Serras F. Imaginal discs: Renaissance of a model for regenerative biology. Bioessays. 2010; 32: 207–217. doi: 10.1002/bies.200900105 PMID: 20127699

43. Yagi R, Mayer F, Basler K. Refined LexA transactivators and their use in combination with the Drosophila Gal4 system. Proc Natl Acad Sci U S A. 2010; 107: 16166–16171. doi: 10.1073/pnas.1005957107 PMID: 20805468

44. Martin-Blanco E, Gampel A, Ring J, Virdee K, Kirov N, Tolkovsky AM, et al. puckered encodes a phosphatase that mediates a feedback loop regulating JNK activity during dorsal closure in Drosophila. Genes Dev. 1998; 12: 557–570. PMID: 9472024

45. Chatterjee N, Bohmann D. A versatile ΦC31 based reporter system for measuring AP-1 and Nrf2 signaling in Drosophila and in tissue culture. Jennings B, editor. PLoS One. Public Library of Science; 2012; 7: e34063. doi: 10.1371/journal.pone.0034063 PMID: 22509270

46. Kelly GS. Clinical applications of N-acetylcysteine. Altern Med Rev. 1998; 3: 114–127. PMID: 9577247

47. Cully M, Genevet A, Warne P, Treins C, Liu T, Bastien J, et al. A role for p38 stress-activated protein kinase in regulation of cell growth via TORC1. Mol Cell Biol. 2010; 30: 481–95. doi: 10.1128/MCB.00688-09 PMID: 19917724

48. Suzanne M, Irie K, Glise B, Agnès F, Mori E, Matsumoto K, et al. The Drosophila p38 MAPK pathway is required during oogenesis for egg asymmetric development. Genes Dev. 1999; 13: 1464–74. PMID: 10364162

49. Seong K-H, Li D, Shimizu H, Nakamura R, Ishii S. Inheritance of stress-induced, ATF-2-dependent epigenetic change. Cell. 2011; 145: 1049–61. doi: 10.1016/j.cell.2011.05.029 PMID: 21703449

50. Frantz B, Klatt T, Pang M, Parsons J, Rolando A, Williams H, et al. The activation state of p38 mitogen-activated protein kinase determines the efficiency of ATP competition for pyridinylimidazole inhibitor binding. Biochemistry. 1998; 37: 13846–53. PMID: 9753474

51. Galko MJ, Krasnow MA. Cellular and genetic analysis of wound healing in Drosophila larvae. PLoS Biol. 2004; 2: E239. PMID: 15269788

52. Bunker BD, Nellimoottil TT, Boileau RM, Classen AK, Bilder D. The transcriptional response to tumorigenic polarity loss in Drosophila. Elife. 2015; 4. doi: 10.7554/eLife.03189 PMID: 25719210

53. Amoyel M, Anderson AM, Bach EA. JAK/STAT pathway dysregulation in tumors: a Drosophila perspective. Semin Cell Dev Biol. 2014; 28: 96–103. doi: 10.1016/j.semcdb.2014.03.023 PMID: 24685611

54. Dobens LL, Martin-Blanco E, Martinez-Arias A, Kafatos FC, Raftery LA. Drosophila puckered regulates Fos/Jun levels during follicle cell morphogenesis. Development. 2001; 128: 1845–1856. PMID: 11311164

55. Lesch C, Jo J, Wu Y, Fish GS, Galko MJ. A targeted UAS-RNAi screen in Drosophila larvae identifies wound closure genes regulating distinct cellular processes. Genetics. 2010; 186: 943–57. doi: 10.1534/genetics.110.121822 PMID: 20813879

56. Ramet M, Lanot R, Zachary D, Manfruelli P. JNK signaling pathway is required for efficient wound healing in Drosophila. Dev Biol. 2002; 241: 145–156. PMID: 11784101

57. Freel CD, Richardson DA, Thomenius MJ, Gan EC, Horn SR, Olson MR, et al. Mitochondrial localization of Reaper to promote inhibitors of apoptosis protein degradation conferred by GH3 domain-lipid interactions. J Biol Chem. 2008; 283: 367–79. PMID: 17998202

58. Sandu C, Ryoo HD, Steller H. Drosophila IAP antagonists form multimeric complexes to promote cell death. J Cell Biol. 2010; 190: 1039–52. doi: 10.1083/jcb.201004086 PMID: 20837774

59. Varkey J, Chen P, Jemmerson R, Abrams JM. Altered cytochrome c display precedes apoptotic cell death in Drosophila. J Cell Biol. 1999; 144: 701–10. PMID: 10037791

60. Abdelwahid E, Yokokura T, Krieser RJ, Balasundaram S, Fowle WH, White K. Mitochondrial disruption in Drosophila apoptosis. Dev Cell. 2007; 12: 793–806. PMID: 17488629

61. Lo YY, Wong JM, Cruz TF. Reactive oxygen species mediate cytokine activation of c-Jun NH2-terminal kinases. J Biol Chem. 1996; 271: 15703–7. PMID: 8663189

62. Ilmarinen P, Moilanen E, Kankaanranta H. Mitochondria in the center of human eosinophil apoptosis and survival. Int J Mol Sci. Multidisciplinary Digital Publishing Institute; 2014; 15: 3952–69. doi: 10.3390/ijms15033952 PMID: 24603536

63. Huh JR, Guo M, Hay BA. Compensatory proliferation induced by cell death in the Drosophila wing disc requires activity of the apical cell death caspase Dronc in a nonapoptotic role. Curr Biol. 2004; 14: 1262–1266. PMID: 15268856

64. Dichtel-Danjoy M-L, Ma D, Dourlen P, Chatelain G, Napoletano F, Robin M, et al. Drosophila p53 isoforms differentially regulate apoptosis and apoptosis-induced proliferation. Cell Death Differ. 2013; 20: 108–16. doi: 10.1038/cdd.2012.100 PMID: 22898807

65. Wells BS, Johnston LA. Maintenance of imaginal disc plasticity and regenerative potential in Drosophila by p53. Dev Biol. Elsevier Inc; 2012; 361: 263–276. doi: 10.1016/j.ydbio.2011.10.012 PMID: 22036477

66. Ryoo HD, Gorenc T, Steller H. Apoptotic cells can induce compensatory cell proliferation through the JNK and the Wingless signaling pathways. Dev Cell. 2004; 7: 491–501. PMID: 15469838

67. Fan Y, Bergmann A. Distinct mechanisms of apoptosis-induced compensatory proliferation in proliferating and differentiating tissues in the Drosophila eye. Dev Cell. 2008; 14: 399–410. doi: 10.1016/j.devcel.2008.01.003 PMID: 18331718

68. Herrera SC, Martin R, Morata G. Tissue homeostasis in the wing disc of Drosophila melanogaster: immediate response to massive damage during development. PLoS Genet. 2013; 9: e1003446. doi: 10.1371/journal.pgen.1003446 PMID: 23633961

69. Autsavapromporn N, de Toledo SM, Little JB, Jay-Gerin J- P, Harris AL, Azzam EI. The role of gap junction communication and oxidative stress in the propagation of toxic effects among high-dose α-particle-irradiated human cells. Radiat Res. 2011; 175: 347–57. doi: 10.1667/RR2372.1 PMID: 21388278

70. Feine I, Pinkas I, Salomon Y, Scherz A. Local oxidative stress expansion through endothelial cells—a key role for gap junction intercellular communication. Ushio-Fukai M, editor. PLoS One. Public Library of Science; 2012; 7: e41633. doi: 10.1371/journal.pone.0041633 PMID: 22911831

71. Bienert GP, Schjoerring JK, Jahn TP. Membrane transport of hydrogen peroxide. Biochim Biophys Acta. 2006; 1758: 994–1003. PMID: 16566894

72. Bienert GP, Møller ALB, Kristiansen KA, Schulz A, Møller IM, Schjoerring JK, et al. Specific aquaporins facilitate the diffusion of hydrogen peroxide across membranes. J Biol Chem. 2007; 282: 1183–92. PMID: 17105724

73. Son Y, Kim S, Chung H-T, Pae H-O. Reactive oxygen species in the activation of MAP kinases. Methods Enzymol. 2013; 528: 27–48. doi: 10.1016/B978-0-12-405881-1.00002-1 PMID: 23849857

74. Tobiume K, Matsuzawa A, Takahashi T, Nishitoh H, Morita K, Takeda K, et al. ASK1 is required for sustained activations of JNK/p38 MAP kinases and apoptosis. EMBO Rep. 2001; 2: 222–8. PMID: 11266364

75. Chakrabarti S, Poidevin M, Lemaitre B. The Drosophila MAPK p38c regulates oxidative stress and lipid homeostasis in the intestine. PLoS Genet. Public Library of Science; 2014; 10: e1004659. doi: 10.1371/journal.pgen.1004659 PMID: 25254641

76. Razzell W, Evans IR, Martin P, Wood W. Calcium Flashes Orchestrate the Wound Inflammatory Response through DUOX Activation and Hydrogen Peroxide Release. Curr Biol. 2013; 23: 424–429. doi: 10.1016/j.cub.2013.01.058 PMID: 23394834

77. Muliyil S, Narasimha M. Mitochondrial ROS regulates cytoskeletal and mitochondrial remodeling to tune cell and tissue dynamics in a model for wound healing. Dev Cell. 2014; 28: 239–52. doi: 10.1016/j.devcel.2013.12.019 PMID: 24486154

78. Hinz U, Giebel B, Campos-Ortega JA. The basic-helix-loop-helix domain of Drosophila lethal of scute protein is sufficient for proneural function and activates neurogenic genes. Cell. 1994; 76: 77–87. PMID: 8287481

79. McGuire SE, Le PT, Osborn AJ, Matsumoto K, Davis RL. Spatiotemporal rescue of memory dysfunction in Drosophila. Science (80-). 2003; 302: 1765–1768.

80. Wing JP, Zhou L, Schwartz LM, Nambu JR. Distinct cell killing properties of the Drosophila reaper, head involution defective, and grim genes. Cell Death Differ. 1998; 5: 930–939. PMID: 9846179

81. Martin FA, Morata G. Compartments and the control of growth in the Drosophila wing imaginal disc. Development. 2006; 133: 4421–4426. PMID: 17035294

82. Baena-Lopez LA, García-Bellido A. Control of growth and positional information by the graded vestigial expression pattern in the wing of Drosophila melanogaster. Proc Natl Acad Sci U S A. 2006; 103: 13734–9. PMID: 16950871

83. Barrio R, de Celis JF. Regulation of spalt expression in the Drosophila wing blade in response to the Decapentaplegic signaling pathway. Proc Natl Acad Sci U S A. 2004; 101: 6021–6026. PMID: 15079076

84. Pastor-Pareja JC, Grawe F, Martin-Blanco E, Garcia-Bellido A. Invasive cell behavior during Drosophila imaginal disc eversion is mediated by the JNK signaling cascade. Dev Cell. 2004; 7: 387–399. PMID: 15363413

85. Harrison DA, Binari R, Nahreini TS, Gilman M, Perrimon N. Activation of a Drosophila Janus kinase (JAK) causes hematopoietic neoplasia and developmental defects. Embo J. 1995; 14: 2857–2865. PMID: 7796812

86. Bach EA, Ekas LA, Ayala-Camargo A, Flaherty MS, Lee H, Perrimon N, et al. GFP reporters detect the activation of the Drosophila JAK/STAT pathway in vivo. Gene Expr Patterns. 2007; 7: 323–331. PMID: 17008134

87. Hou XS, Melnick MB, Perrimon N. Marelle acts downstream of the Drosophila HOP/JAK kinase and encodes a protein similar to the mammalian STATs. Cell. 1996; 84: 411–419. PMID: 8608595

88. Glise B, Bourbon H, Noselli S. hemipterous encodes a novel Drosophila MAP kinase kinase, required for epithelial cell sheet movement. Cell. 1995; 83: 451–461. PMID: 8521475

89. Lai S-L, Lee T. Genetic mosaic with dual binary transcriptional systems in Drosophila. Nat Neurosci. 2006; 9: 703–9. PMID: 16582903

90. Repiso A, Bergantinos C, Serras F. Cell fate respecification and cell division orientation drive intercalary regeneration in Drosophila wing discs. Development. 2013; 140: 3541–3551. doi: 10.1242/dev.095760 PMID: 23903186

S1 Figure

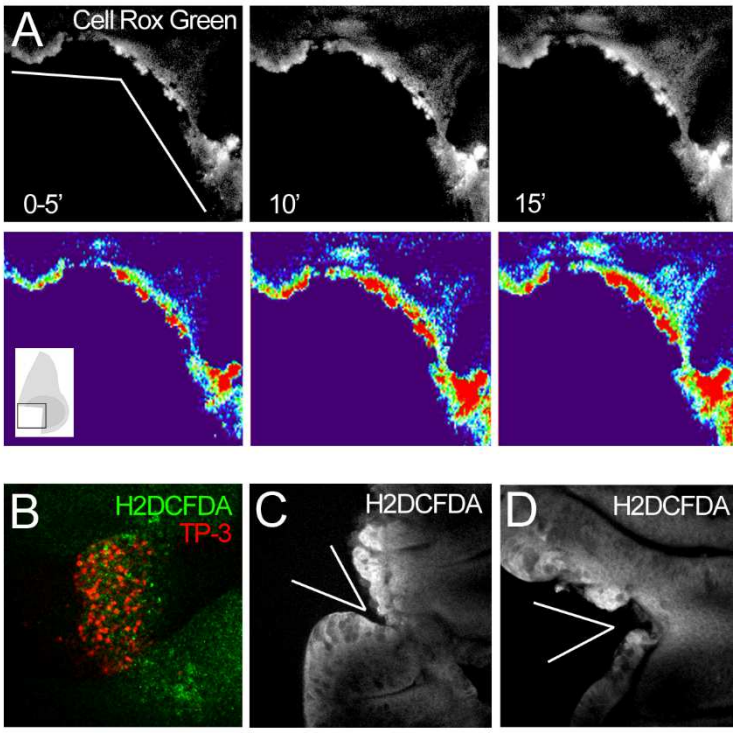

S2 Figure

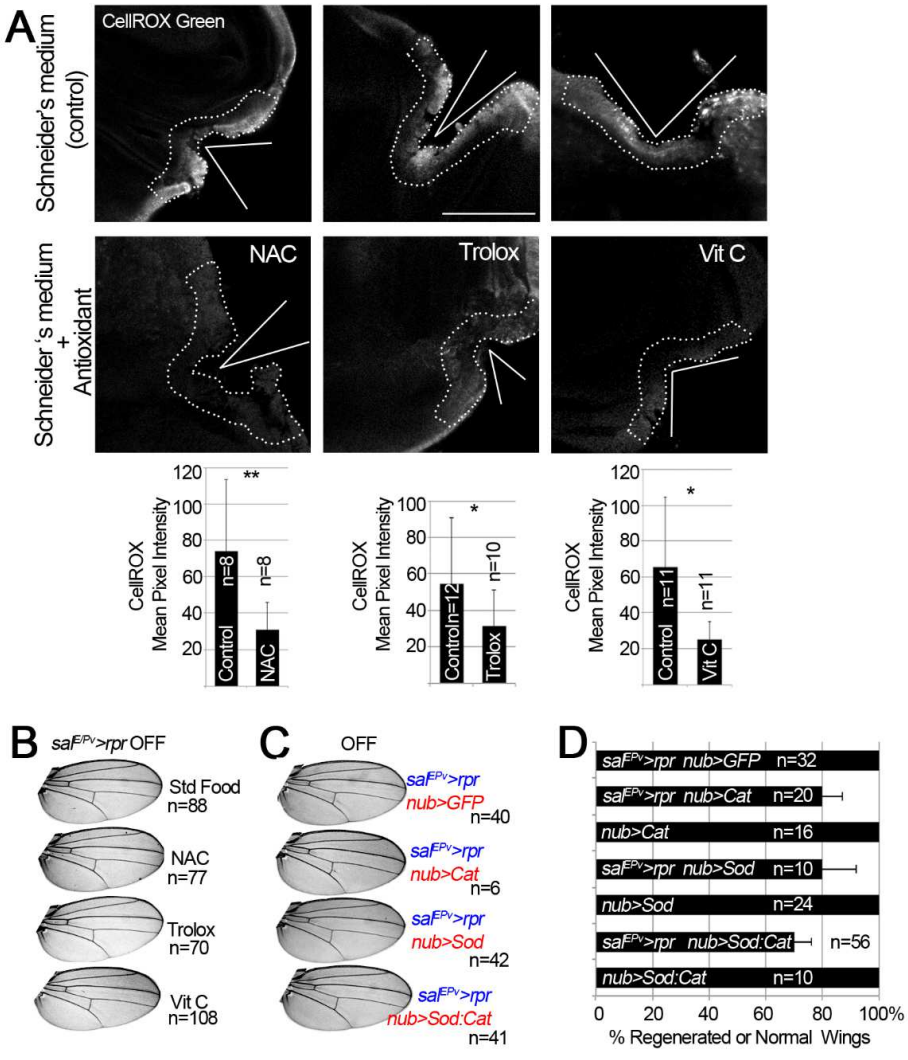

S3 Figure

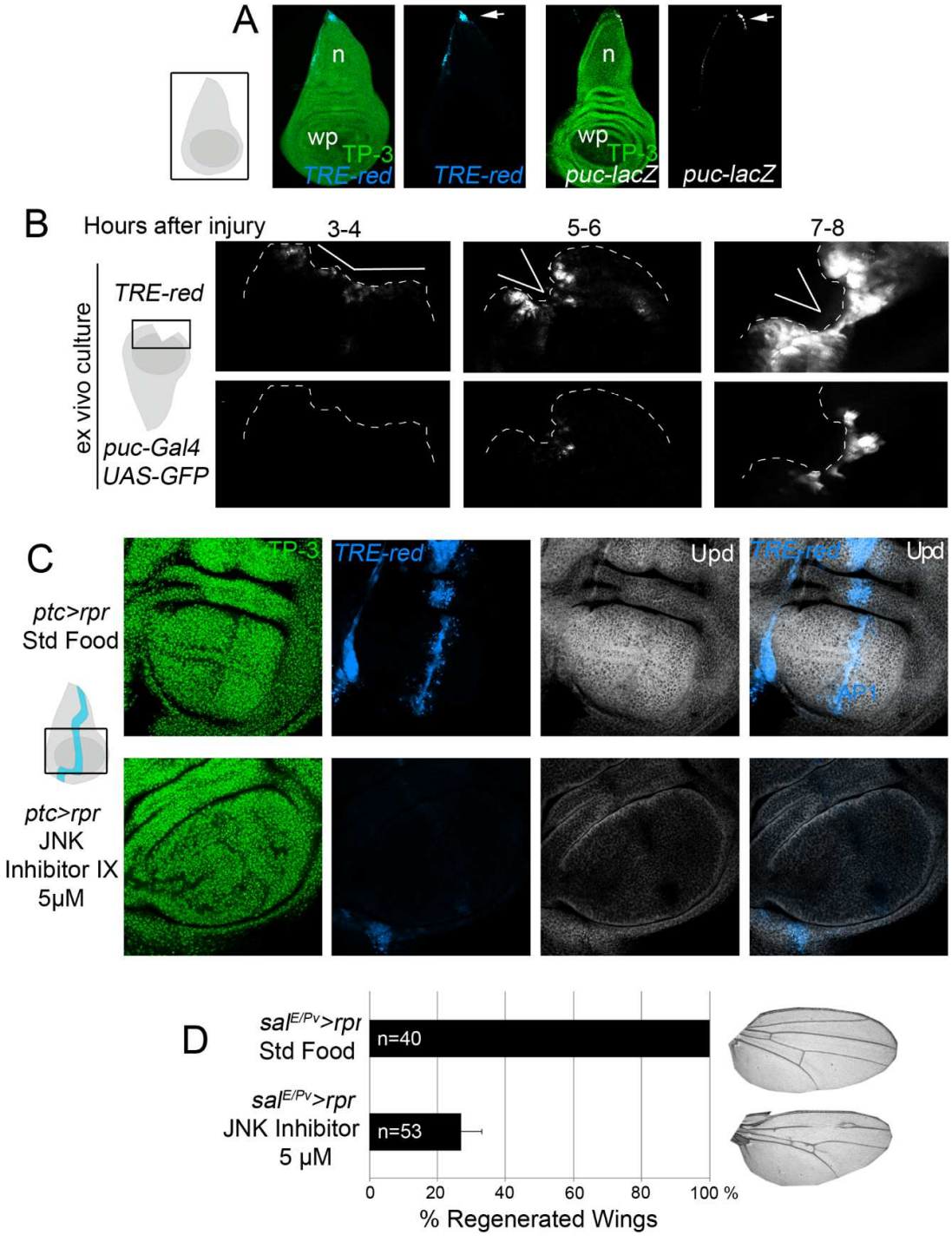
A
n
wp
TP-3
TRE-red
TRE-red
n
wp
TP-3
puc-lacZ
puc-lacZ
B
Hours after injury
3-4
5-6
7-8
ex vivo culture
TRE-red
puc-Gal4
UAS-GFP
C
ptc>rpr
Std Food
TP-3
TRE-red
Upd
TRE-red
Upd
AP1
ptc>rpr
JNK
Inhibitor IX
5μM
D
sal^E/Pv>rpr
Std Food
n=40
sal^E/Pv>rpr
JNK Inhibitor
5 μM
n=53
0
20
40
60
80
100 %
% Regenerated Wings

S4 Figure

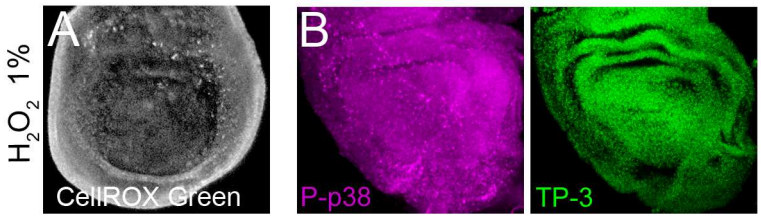

S5 Figure

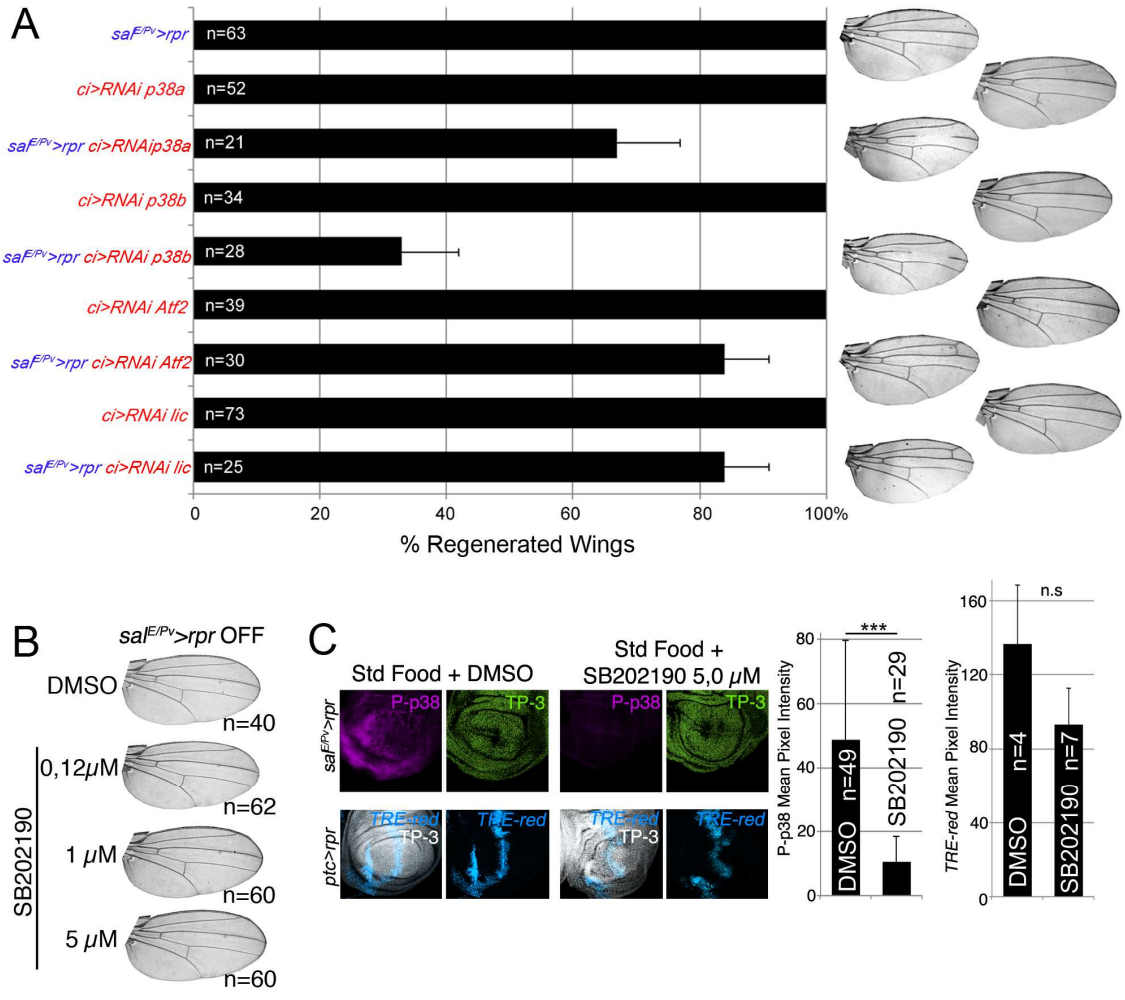

S6 Figure

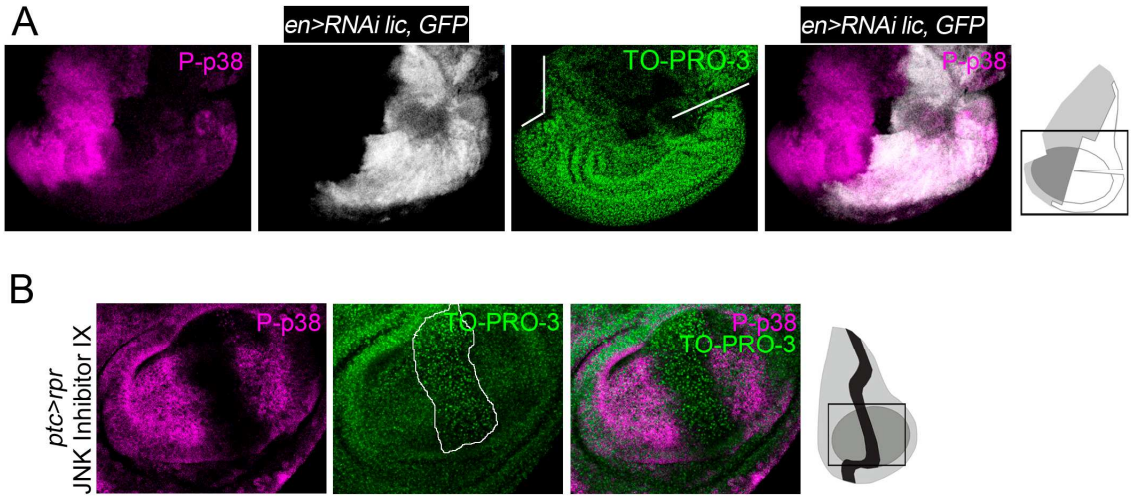

S7 Figure

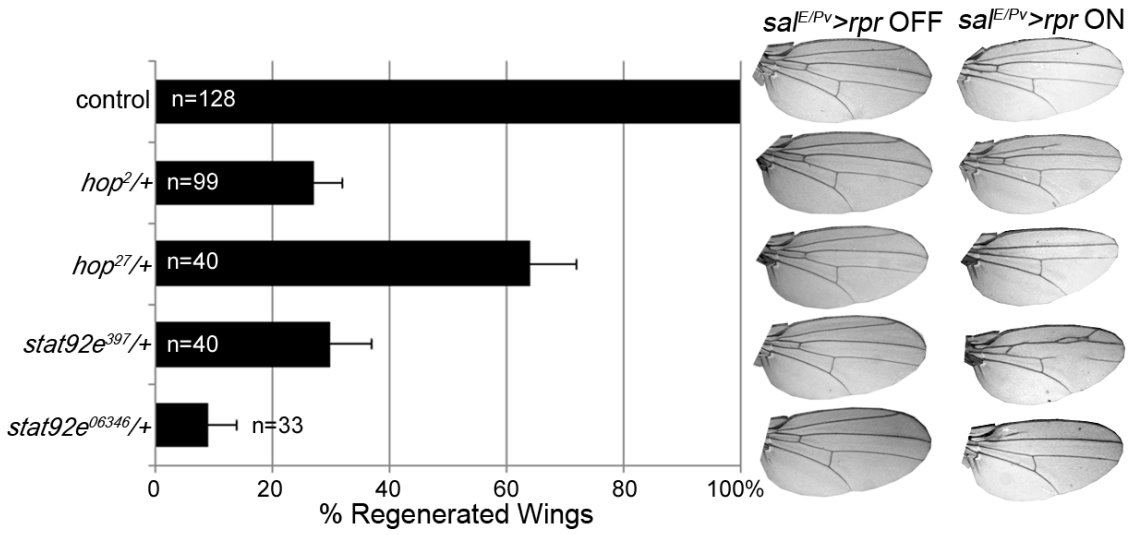

S8 Figure